TECHNICAL REPORT NO. 63-54

# WICHITA MOUNTAINS SEISMOLOGICAL OBSERVATORY
# REPORT ON PHASE V

THE GEOTECHNICAL CORPORATION
3401 Shiloh Road
Garland, Texas

1 June

## CONTENTS


| | | Page |
|---|---|---|
| 1. | INTRODUCTION | 1 |
| | 1.1 Authority | 1 |
| | 1.2 Purpose of WMSO | 1 |
| | 1.3 History of WMSO | 1 |
| | 1.4 Work of Phase V | 2 |
| 2. | SUMMARY | 3 |
| | 2.1 Operation of WMSO | 3 |
| | 2.2 Evaluation of Standard Instrumentation | 3 |
| | 2.3 Routine Analysis | 3 |
| | 2.4 Evaluation and Special Studies | 4 |
| | 2.5 Special Tests | 4 |
| 3. | OPERATION OF WMSO | 5 |
| | 3.1 General | 5 |
| | 3.2 Basic Operation | 5 |
| | 3.2.1 Personnel Organization | 5 |
| | 3.2.2 Operating Parameters of the Routine Seismographs at WMSO | 7 |
| | 3.3 Changes and/or Additions to the Standard Instrumentation at WMSO | 7 |
| | 3.4 Modifications of Physical Facilities at WMSO | 12 |
| | 3.5 Data Channels Recorded at WMSO | 17 |
| | 3.6 Installation and Operation of the 10-Kilometer Linear Array | 17 |
| | 3.7 Reactivation of the "H" Array | 21 |
| | 3.8 Installation of 13-Element Array at WMSO | 23 |
| 4. | EVALUATION OF STANDARD INSTRUMENTATION AT WMSO | 23 |
| | 4.1 Short-Period Seismographs, Triangular Array | 23 |
| | 4.1.1 Variations in Response Characteristics | 24 |
| | 4.1.2 Stability of Frequency Response | 24 |
| | 4.1.3 Stability of Magnification at 1 cps | 25 |
| | 4.1.4 Electrical Noise | 25 |

CONTENTS (Continued)


| | | Page |
|---|---|---|
| 4.1.5 | Short-Period Phototube Amplifiers | 27 |
| 4.1.6 | Reliability of Short-Period Seismographs | 27 |
| 4.1.7 | Summations of Short-Period Seismographs | 29 |
| 4.2 | Short-Period Vaults, Triangular Array | 32 |
| 4.3 | Long-Period Seismographs | 33 |
| 4.3.1 | Stability of Frequency Response | 33 |
| 4.3.2 | Stability of Magnification at 0.04 cps | 33 |
| 4.3.3 | Phase Response of Long-Period Seismographs | 33 |
| 4.3.4 | Electrical Noise | 35 |
| 4.3.5 | Effects of Pressure Change on the Sprengnether Long-Period Seismometers | 37 |
| 4.3.6 | Operational Changes of the Sprengnether Long-Period System | 37 |
| 4.4 | Broad-Band Seismographs | 38 |
| 4.4.1 | Stability of Frequency Response | 38 |
| 4.4.2 | Stability of Magnification at 1.0 cps | 38 |
| 4.4.3 | Reliability of the Broad-Band Seismographs | 38 |
| 4.5 | Intermediate-Band Seismographs | 39 |
| 4.5.1 | Stability of Frequency Response | 39 |
| 4.5.2 | Stability of Magnification at 1.0 cps | 39 |
| 4.5.3 | Reliability of the Intermediate-Band Seismographs | 39 |
| 4.6 | Lightning Protection | 40 |
| 4.6.1 | History of Lightning Protection Systems Tested at WMSO | 40 |
| 4.6.2 | Preliminary Evaluation of Present Lightning Protection System at WMSO | 41 |
| 4.6.3 | Summary of Lightning Damage at WMSO During Phase V Compared to Damage During Other Phases | 41 |
| 4.7 | Data Control and Recording | 44 |
| 4.7.1 | Data Control | 44 |
| 4.7.2 | Recording | 44 |
| 4.8 | Calibration | 45 |
| 4.8.1 | Stability of Calibration Actuators | 45 |

CONTENTS (Continued)


4.8.2 Calibration Control Unit Problems and Remedies
4.8.3 Reliability of Calibration Circuits
4.9 Timing
4.9.1 Primary Timing
4.9.2 Secondary Timing
4.10 Power Circuits
4.10.1 Commercial Power
4.10.2 Emergency Power
4.10.3 Power Failure of 25 December 1962
4.10.4 Frequency-Regulated Power

5. ROUTINE ANALYSIS AND ANALYSIS EVALUATION
5.1 Introduction
5.2 Procedures
5.2.1 Preliminary Analysis
5.2.2 Checking of Analysis
5.2.3 Daily Report to USC&GS
5.2.4 Final Analysis - Epicenter and Phase Association
5.2.5 Report on Registration of Earthquakes

6. EVALUATION AND SPECIAL STUDIES
6.1 Earthquake Detection Capability of WMSO
6.1.1 Earthquakes Detected and Recorded During Phase V
6.1.2 Epicentral Areas From Which WMSO Commonly Records Earthquake Signals
6.1.3 Magnitude Study
6.1.4 WMSO Detection Capabilities Compared to the Detection Capabilities of Observatories with Less Extensive Instrumentation
6.1.5 Relative Phase Detection Capability of the Individual WMSO Systems
6.2 Quarry Blast Study
6.3 Array Characteristics
6.4 Comparison of the "H" and Triangular Arrays at WMSO

CONTENTS (Continued)


| | Page |
|---|---|
| 6.4.1 Relative Cancellation of 2-cps Microseisms | |
| 6.4.2 Relative Capabilities of the "H" and Triangular Arrays at WMSO to Detect Low-Level Signals | 107 |
| 6.4.3 Conclusions | 107 |
| 6.5 Comparison of Linear and Triangular Arrays | 114 |
| 7. SPECIAL TESTS | 114 |
| 7.1 Long-Period Tripartite | 114 |
| 7.2 Seismic Data Filter, Geotech Model 11760 | |
| 7.3 Broad-Band Flat Velocity Response | 138 |
| 7.4 SIE Unmanned Seismograph | 139 |
| 8. VISITORS AT WMSO | |
| 9. BIBLIOGRAPHY | 145 |
| APPENDIX 1 - Statement of Work | |
| APPENDIX 2 - Mailing List for WMSO Earthquake Bulletin | |
| APPENDIX 3 - Microseismic Noise Curves | |

## ILLUSTRATIONS


| Figure | | Page |
|---|---|---|
| 1 | Flow diagram of WMSO operations | 6 |
| 2 | Personnel organization for Phase V of Project VT/036 | 8 |
| 3 | Response characteristics of seismographs at WMSO | 11 |
| 4 | Floor plan of the central-recording building at WMSO prior to the addition of the trailer annex and the modification of the operating room | 13 |
| 5 | Floor plan of the central-recording building at WMSO after annexation of the trailer but before modification of the operating room | 14 |
| 6 | Floor plan of the central-recording building and trailer annex at WMSO after modification of the operating room | 15 |
| 7 | Data control consoles in the operation room at WMSO after modification of the operation room (new console shown on left) | 16 |
| 8 | Orientation of linear and triangular arrays at WMSO | 19 |
| 9 | Orientation of triangular array, H array, and planned 13-element array at WMSO | 22 |
| 10 | Mean frequency response of the ten-short period JM seismographs of the triangular array at WMSO during Phase V. Dotted lines indicate one standard deviation confidence limits. | 25 |
| 11 | Phase response of short-period JM seismographs Z2 and Z3 | 26 |
| 12 | Noise level diagram for a typical JM seismograph in the triangular array | 28 |

## ILLUSTRATIONS (Continued)


| Figure | | Pag |
|---|---|---|
| 13 | Directivity pattern for the summation of 10 short-period seismographs in the triangular array for several wavelengths ($\lambda$) | 30 |
| 14 | Short-period Develocorder record illustrating the effectiveness of the $\Sigma$1, 3, 5, 6 during periods of high wind. Wind velocity approximately 45-50 mph. | 31 |
| 15 | Profile view of vault for short-period vertical JM seismometers for triangular array at WMSO | 32 |
| 16 | Wind noise as a function of wind velocity for all seismographs of the triangular array at WMSO | 34 |
| 17 | Average frequency response of the Sprengnether long-period seismographs at WMSO during Phase V | 35 |
| 18 | Phase response of the Sprengnether long-period seismographs at WMSO during Phase V | 36 |
| 19 | Frequency of occurrence of electrical storms at WMSO during Phase V | 42 |
| 20 | Playback of the recording of the output of the Time Encoder, Geotech Model 13159, from the Minneapolis-Honeywell magnetic-tape recorder at WMSO. Time recorded is: day of year 009, hour 18:00Z, minutes 30. | 48 |
| 21 | Sample WMSO preliminary analysis sheet | 51 |
| 22 | Sample page of WMSO's daily report to USC&GS | 51 |
| 23 | Sample page from WMSO's monthly Report on the Registration of Earthquakes | 54 |

ILLUSTRATIONS (Continued)

Figure


24 Polar plot of epicenters from which P and P' arrivals were recorded in February, June, and September 1962, showing azimuth and distance from WMSO.

25 Polar plot of epicenters from which S arrivals were recorded in February, June, and September 1962, showing azimuth and distance from WMSO

26 Polar plot of epicenters from which surface wave arrivals were recorded in February, June, and September 1962, showing azimuth and distance from WMSO

27 Polar plot of epicenters from which the indicated P-phase combinations were recorded in February, June, and September 1962, showing azimuth and distance from WMSO

28 $m_p$ versus distance ($\Delta$) for earthquakes located by USC&GS and detected at WMSO 1 March-30 November 1962 - $m_p$ calculated from WMSO seismograms

29 $M_{H20}$ versus distance ($\Delta$) for earthquakes located by USC&GS and detected at WMSO 1 March-31 May and 10 September-30 November 1962 - $M_{H20}$ calculated from WMSO seismograms

30 Theoretical threshold of detection curves for WMSO for $m_p$ and $M_{H20}$ for earthquakes with a focal depth of 33 kilometers occurring at varying distances from WMSO

31 $M_{Hmax}$ as a function of $M_{H20}$ for 102 earthquakes recorded at WMSO 1 March-31 May 1962

## ILLUSTRATIONS (Continued)


| Figure | | Pa |
|---|---|---|
| 32 | $M_{Hmax}$-$M_{H20}$ versus the ratio between the periods at which the measurements for each were made for 108 events recorded at WMSO 1 March-31 May 1962 | 6 |
| 33 | Plot of the period at which the maximum amplitude-to-period ratio occurred in the horizontal component of the surface group as measured on the long-period seismograms versus epicentral distance for 108 events recorded at WMSO 1 March-31 May 1962 | 6 |
| 34 | $M_{Zmax}$ as a function of $M_{Hmax}$ for 95 events recorded on the long period seismograms at WMSO 1 March-31 May 1962 | 6 |
| 35 | $m_p$ as a function of M as reported by USC&GS for events recorded at WMSO 1 March-31 October 1962 | 7 |
| 36 | $m_p$ as a function of $M_{H20}$ for 124 earthquakes recorded at WMSO 1 March-31 May and 10 September-30 November 1962. Focal depths of events $\leq$ 80 kilometers. | 7 |
| 37 | $m_p$ as a function of $M_{Hmax}$ for 64 earthquakes recorded at WMSO 1 March-31 May 1962. Focal depth of events $\leq$ 80 kilometers. | 7 |
| 38 | $m_p$ calculated from long-period data as a function of $M_{H20}$ for 13 earthquakes recorded at WMSO 1 March-31 May and 10 September-30 November 1962 | 7 |
| 39 | $m_p$ calculated from long-period data as a function of $m_p$ calculated from short-period data for 33 earthquakes recorded at WMSO 1 March-31 May and 10 September-30 November 1962 | 7 |

## ILLUSTRATIONS (Continued)


| Figure | | Page |
|---|---|---|
| 40 | $m_p$ calculated from short-period data as a function of $m_p$ calculated from broad-band data for 39 earthquakes recorded at WMSO 1 March-31 May 1962 | 75 |
| 41 | $m_s$ calculated from broad-band data as a function of $m_s$ calculated from long-period data for 16 earthquakes recorded at WMSO 1 March-31 May 1962. | 76 |
| 42 | $m_{pp}$ as a function of $m_p$ calculated from short-period data for 73 earthquakes recorded at WMSO 1 March-31 May 1962 | 77 |
| 43 | $m_p$ versus $m_s$, both calculated from short-period data for 28 earthquakes recorded at WMSO 1 March-31 May 1962 | 78 |
| 44 | $m_p$ calculated from short-period data versus $m_s$ calculated from long-period data for 46 earthquakes recorded at WMSO 1 March-31 May 1962 | 79 |
| 45 | Geographic distribution of the slopes of the least-square lines ($P_{LW}$) obtained from the relationships between $m_p$ computed from LRSM station short-period data and $m_p$ computed from WMSO short-period data, 1 April-30 November 1962 | 82 |
| 46 | Geographic distribution of the intercepts of the least-square lines on the LRSM station axes ($L_O$) obtained from the relationships between $m_p$ computed from LRSM station short-period data and WMSO short-period data, 1 April-30 November 1962 | 82 |
| 47 | Method of masking WMSO seismograms to stimulate the seismograms of other observatories (System A illustrated) | 83 |
| 48 | Block diagram of equipment used to record quarry blasts | 93 |

## ILLUSTRATIONS (Continued)


| Figure | | Page |
|---|---|---|
| 49 | Polar plot showing locations of quarries relative to WMSO | 95 |
| 50 | Ground displacement at WMSO as a function of weight of explosives for 48 blasts detonated by a single quarry | 98 |
| 51 | Directional response of the H array | 101 |
| 52 | Directional response of the triangular array | 102 |
| 53 | Directional response of the linear array | 103 |
| 54 | Directional response of the Star-of-David array | 104 |
| 55 | Observed response of a single-array element (Z6) and calculated responses of the summations of each of the four arrays to a typical teleseismic signal with a period of 1.0 second and an apparent surface velocity of 12 kilometers per second | 105 |
| 56a<br>56b | Short-period Develocorder record of a typical low-level signal (arrow) detected by the analyst only on the triangular array at WMSO. Corresponding time interval for H array shown in 56a | 108<br>109 |
| 57a<br>57b | Short-period Develocorder record of a typical low-level signal (arrow) detected by the analyst only on the triangular array at WMSO. Corresponding time interval for H array shown in 57a | 110<br>111 |
| 58a<br>58b | Short-period Develocorder record of a typical low-level signal (arrow) detected by the analysts on both arrays, but more clearly on the triangular array at WMSO. Corresponding time interval for H array shown in 58a | 112<br>113 |

## ILLUSTRATIONS (Continued)


| Figure | | Page |
|---|---|---|
| 59 | Short-period Develocorder record illustrating the response of the linear array to a signal that is nearly in-line with the array. Azimuth from WMSO 42°, $\Delta$ = 86° | 115 |
| 60 | Short-period Develocorder record illustrating the response of the linear array to a signal that is nearly in-line with the array. Azimuth from WMSO 39°, $\Delta$ = 49° | 116 |
| 61 | Short-period Develocorder record illustrating the response of the linear array to a signal that is nearly broadside to the array. Azimuth from WMSO 143°, $\Delta$ = 36.5° | 117 |
| 62 | Record of test Develocorder recording the Geotech long-period tripartite, illustrating the effects of atmospheric pressure change on the seismometers (unsealed) | 119 |
| 63 | Test Develocorder record showing response to pressure change and P-wave signal on the Geotech long-period seismometers of the tripartite (sealed and unsealed) | 120 |
| 64 | Record from test Develocorder recording the Geotech long-period tripartite, illustrating the response of the seismometers to atmospheric pressure change | 121 |
| 65 | Test Develocorder record illustrating the relative effectiveness of the two methods of sealing the period-adjusting rod hole in the seismometer cover | 122 |
| 66 | Test Develocorder record illustrating the effects of thermo-electric noise on the tripartite seismograms with the protector in the circuit when the protector door was opened in direct sunlight | 123 |
| 67 | Test Develocorder record illustrating the effect of the notch filter in attenuating 6-second microseisms | 125 |

ILLUSTRATIONS (Continued)


| Figure | | Page |
|---|---|---|
| 68 | Comparison of the frequency response curves of the Seismic Data Filters, Geotech Model 11760, and Krohn-Hite Model 330A, as operated at WMSO prior to 8 November 1962 | 127 |
| 69 | Frequency response of Seismic Data Filter, Model 11760, operating in the range 0.8 cps, 18 db/octave to 5.0 cps, 24 db/octave | 128 |
| 70 | Short-period Develocorder record illustrating enhancement of a teleseismic signal and cancellation of microseisms in the 6-second period range by the Seismic Data Filter, Model 11760, operating in the range 0.8 cps, 18 db/octave to 5.0 cps, 24 db/octave | 129 |
| 71 | Short-period Develocorder record illustrating the enhancement of a teleseismic signal and the cancellation of microseisms in the 6-second period range by the Seismic Data Filter, Model 11760, operating in the range 0.8 cps, 18 db/octave to 5.0 cps, 24 db/octave | 130 |
| 72 | Frequency response of Seismic Data Filter, Model 11760, operating at a bandpass range of 0.8 cps, 12 db/octave to 5.0 cps, 6 db/octave | 131 |
| 73 | Short-period Develocorder record illustrating the value of the filtered Σ1-10 trace as a flag trace. Note earlier start of event (arrow) indicated by filtered trace. Seismic Data Filter, Model 11760, operating in the bandpass range 0.8 cps, 12 db/octave to 5.0 cps, 6 db/octave | 132 |

ILLUSTRATIONS (Continued)

Figure


74 Short-period Develocorder record illustrating the value of the Geotech seismic data filter in the cancellation of microseisms in the 6-second period range. Seismic Data Filter, Model 11760, operating in the bandpass range 0.8 cps, 12 db/octave to 5.0 cps, 6 db/octave

75 Frequency response of Seismic Data Filter, Model 11760, operating in the bandpass range of 0.8 cps, 12 db/octave to 3.0 cps, 6 db/octave

76 Short-period Develocorder record illustrating the cancellation of low-frequency microseisms and the enhancement of a low-level teleseismic signal which is partially masked by these microseisms (arrow) by the Seismic Data Filter, Model 11760, operating in the bandpass range 0.8 cps, 12 db/octave to 3.0 cps, 6 db/octave

77 Short-period Develocorder record illustrating the attenuation of high-amplitude microseisms in the period range of 5 to 9 seconds by the Seismic Data Filter, Model 11760, operating in the bandpass range 0.8 cps, 12 db/octave to 3.0 cps, 6 db/octave

78 Short-period Develocorder record illustrating the value of the Σ1-10 filtered seismogram as a flag trace. Note the arrival of a teleseismic event well defined on the filtered trace. Seismic Data Filter, Model 11760, operating in the bandpass range 0.8 cps, 12 db/octave to 3.0 cps, 6 db/octave

79 Frequency response of the $JM_{20}$

80 Test Develocorder record illustrating the limited detection capability of the SIE unmanned seismograph for relatively longer period P waves of teleseisms

## ILLUSTRATIONS (Continued)


| Figure | | Page |
|---|---|---|
| 81 | Test Develocorder record illustrating the difference between the response of the SIE unmanned seismograph and the JM20 seismograph to a typical near-regional signal | 143 |


## TABLES


| Table | | Page |
|---|---|---|
| 1 | Operating Parameters and Tolerances for the WMSO Seismographs | 9 |
| 2 | Calibration Norms and Operating Tolerances for Frequency Responses of Seismographs at WMSO | 10 |
| 3 | Data Channel Assignments During Phase V | 18 |
| 4 | Locations and Elevations of Each of the Seismometers of the Linear Array | 20 |
| 5 | Outages due to Electrical Storms | 43 |
| 6 | Earthquakes Detected by WMSO and Earthquakes Reported by USC&GS During Phase V | 55 |
| 7 | Comparison of LRSM Magnitudes ($m_L$) to WMSO Magnitudes ($m_W$) | 80 |
| 8 | Data samples Selected and "Detection Credits" Awarded Each System | 87 |

TABLES (Continued)


| Table | | Page |
|---|---|---|
| 9 | WMSO Detection Capabilities Compared to the Detection Capabilities of Observatories with Less Extensive Instrumentation | 88 |
| 10 | Past and Present Recording Rates for Recording Seismometric Data on 16-millimeter Develocorder Film at WMSO | 89 |
| 11 | WMSO's Relative Detection Capability as Determined During Phase V Compared to Phase II | 89 |
| 12 | Number of Times the Indicated Phases were Detected by Each Seismograph, Showing Relative Detection Capability | 91 |
| 13 | Overall Relative Phase Detection Capability for Each WMSO System, by Phase | 92 |
| 14 | Individual WMSO System Capability | 92 |
| 15 | Locations of Quarries in the WMSO Area | 96 |
| 16 | Origin Times Recorded and Travel Times Computed by WMSO from Quarry Blasts | 97 |
| 17 | Relative Detection Capability of the H and Triangular Arrays for Low-Level Signals | 107 |
| 18 | Evaluation of the Detection Capabilities of JM 20 versus SIE, JM 20 versus Triangular (Δ) Array, and SIE versus Triangular (Δ) Array | 141 |
| 19 | Man-Days Spent at WMSO by Visitors | 144 |

# WICHITA MOUNTAINS SEISMOLOGICAL OBSERVATORY
# REPORT ON PHASE V

## 1. INTRODUCTION

This is a report of the operation of the Wichita Mountains Seismological Observatory (WMSO) from 1 March 1962 through 28 February 1963.

### 1.1 AUTHORITY

Authority for the operation of WMSO from 1 March 1962 through 28 February 1963 was contained in Contract AF 33(600)-41318, Project VT/036, Phase V, dated 28 May 1962. The Air Force Technical Applications Center (AFTAC) has technical supervision of the contract as a part of Project VELA UNIFORM, which is under the overall direction of the Advanced Research Projects Agency (ARPA).

### 1.2 PURPOSE OF WMSO

The work at WMSO has been threefold. First, WMSO routinely records and analyzes seismometric data daily, and maintains and evaluates the standard instrumentation of the observatory. Second, WMSO is utilized as a field laboratory to field test and evaluate new instruments and techniques to determine their value for use in an observatory. Third, the seismometric data recorded at WMSO are studied in an effort to improve and refine interpretive techniques, and to learn more about earthquake mechanisms and the mechanisms of propagation of seismic waves through the earth.

### 1.3 HISTORY OF WMSO

During Phase I of Contract 41318, WMSO was designed, constructed, and equipped with seismic instruments that have characteristics recommended by the 1958 Geneva Conference of Experts to Study Methods of Detecting Violations

of a Possible Agreement on the Suspension of Nuclear Tests. The general parameters of the equipment recommended by the 1958 Geneva Conference of Experts are quoted, and the standard instrumentation of WMSO is described in Information Bulletin No. 2 of the Wichita Mountains Seismological Observatory, published on 1 January 1963. The work done during Phase I of the contract is described in Geotech Technical Report No. 61-1, published on 10 January 1961.

Phase II of Contract 41318 included the recording and evaluation of seismometric data at WMSO, and modifications and/or additions to the standard instrumentation in an effort to improve the detection capabilities of the observatory. Phase II, which began immediately upon completion of Phase I and covered the period from 1 October 1960 through 28 February 1961, is described in Geotech Technical Report No. 61-2 published on 25 May 1961.

The work of Phase III of the contract was an extension of Phase II for a period of 1 year, from 1 March 1961 through 28 February 1962, and is described in Geotech Technical Report No. 62-8 published on 15 May 1962. Phase IV of the contract (Technical Reports Nos. 61-6, 62-2, 62-3, 62-4, and 62-7) covered the selection of recommended site locations for five additional seismological observatories.

## 1.4 WORK OF PHASE V

The work of Phase V was primarily a continuation of the work done under Phases II and III of Contract 41318, and can be subdivided into three categories, as follows:

a. Continued operation of WMSO;

b. Evaluation of standard and experimental detection equipment in order to provide a more efficient observatory;

c. Routine and special analysis of resultant seismometric data.

The detailed work statement is included in this report as appendix 1.

## 2. SUMMARY

### 2.1 OPERATION OF WMSO

The following modifications were made to the facilities at WMSO:

a. A window air-conditioning unit was installed as an emergency unit;

b. A trailer was annexed to the central-recording building.

A 10-kilometer, 11-element, linear array was installed and operated during a portion of Phase V.

For comparison with and better evaluation of the triangular array, the "H" array of ten Benioff seismometers was reactivated and operated for three months during Phase V.

Work was begun for the addition of three elements to the triangular array late in Phase V.

### 2.2 EVALUATION OF STANDARD INSTRUMENTATION

Shortly after the beginning of Phase V, transformer-type signal isolators were installed in the short-period and intermediate-band seismographs; this made the modification of certain operational procedures necessary. The stability measurements made during Phase V are a better indication of overall operational stability and reliability than of actual instrument stability.

Stability of magnification and frequency response are given for all seismograph systems, based on routine operational data.

An improved lightning protection system for the triangular array was installed at WMSO.

### 2.3 ROUTINE ANALYSIS

No major changes in routine analysis were made during Phase V.

## 2.4 EVALUATION AND SPECIAL STUDIES

Magnitudes were calculated independently for data recorded on several of the WMSO systems as well as for each of several phases. For the purpose of calculating magnitudes (M) from surface waves, measurements may be made at any period greater than 17 seconds at which the amplitude-to-period ratio is maximum, and measurements may be made of the vertical component as well as of the horizontal component. P-wave magnitudes calculated from the Long-Range Seismic Measurements (LRSM) Program data were compared to P-wave magnitudes calculated from WMSO data. A possible station correction factor relative to WMSO is developed for each LRSM station considered.

The earthquake detection capability of WMSO was compared to the detection capabilities of simulated observatories with less extensive instrumentation.

The directional response of each of four arrays at WMSO to a sinusoidal signal and to a typical teleseismic signal of similar period was calculated.

The triangular array was compared to the "H" array and found to be superior, both with respect to detection capability and to cancellation of 2-cps microseismic noise.

## 2.5 SPECIAL TESTS

The response of the long-period vertical seismometers of the tripartite to pressure change was substantially reduced by improved sealing of the seismometer cases. The effect of 6-second notch filters was investigated.

The Seismic Data Filter, Geotech Model 11760, was tested and evaluated. The filter was found to be an asset to analysis and was subsequently added to the standard instrumentation of the observatory.

A JM seismometer with a 20-cps galvanometer in the PTA (JM 20) was compared to the SIE unmanned seismograph to determine their relative detection capabilities.

# 3. OPERATION OF WMSO

## 3.1 GENERAL

During Phase V, WMSO was operated and data were recorded on a continuous basis. Personnel were on duty at the station daily. On weekdays, the observatory was manned an average of 10 hours a day. On weekends and holidays, a skeleton crew was employed; however, additional assistance was on call at all times in case of an emergency.

As the result of findings and recommendations made during Phase III and certain developments of Phase V, some changes and additions were made to the instrumentation at WMSO, after approval had been received from the Project Officer.

Flexibility of the analysis capabilities of WMSO was increased by the addition of a Minneapolis-Honeywell 14-channel FM magnetic-tape recorder. A 10-kilometer linear array of Johnson-Matheson (JM) short-period vertical seismographs was installed and operated (on a temporary basis) during a large portion of Phase V. The physical facilities at WMSO were modified in order to make additional working space available. Initial arrival times from earthquakes were reported to the USC&GS daily, and a monthly earthquake bulletin was published in which earthquake phase-arrival times recorded at WMSO are tabulated. In addition, analysis studies were conducted using WMSO data. Observatory facilities, technical assistance, and the accumulated data were made available to other participants in the VELA-UNIFORM Program.

## 3.2 BASIC OPERATION

### 3.2.1 Personnel Organization

Figure 1 is a flow diagram of the tasks involved in the operations performed by personnel at WMSO and/or by WMSO support personnel in Dallas. In general, personnel at WMSO are completely responsible for the operation and maintenance of equipment and items 2, 4, 5, and 8 of the analysis and evaluation portions of the operation. Responsibility for items 1 and 3 of the analysis and evaluation portion is divided between WMSO and Dallas, and personnel in Dallas are responsible for items 6 and 7.

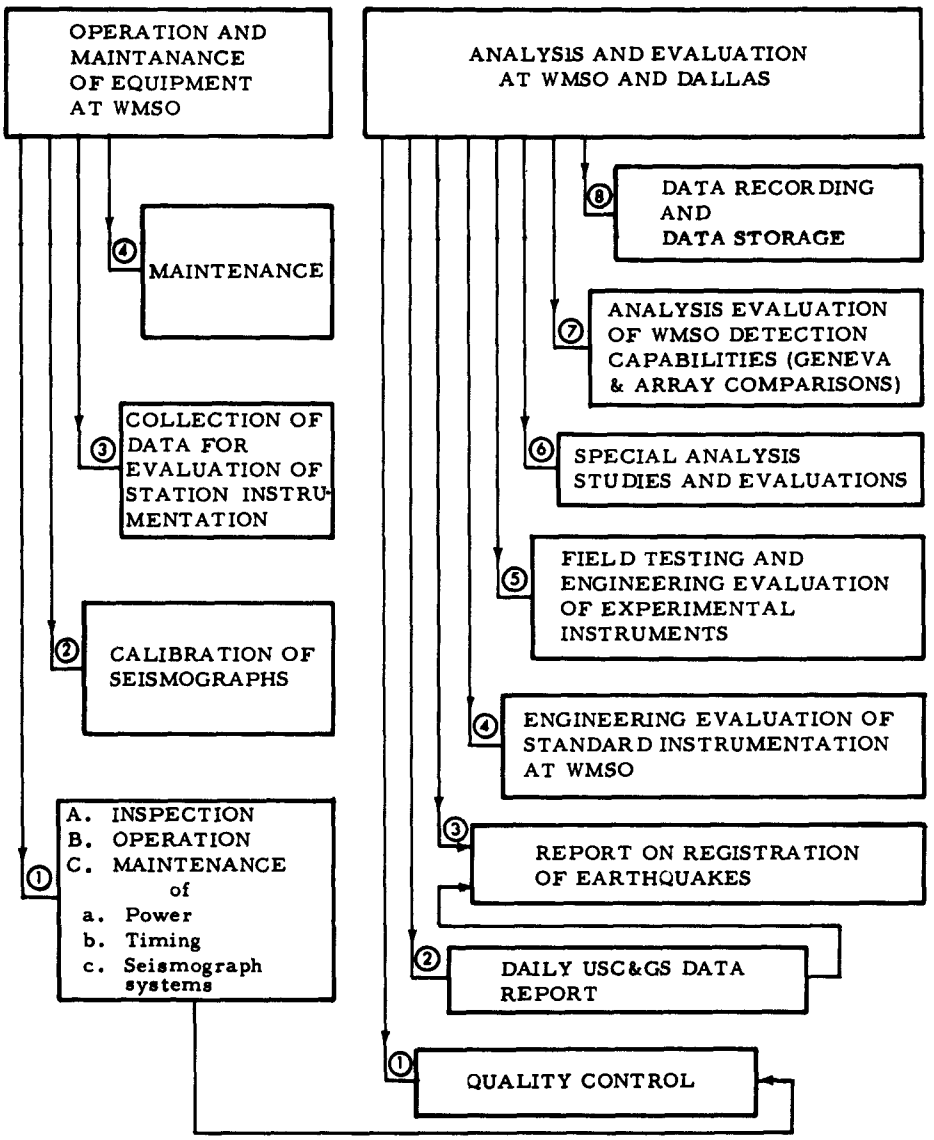


Figure 1. Flow diagram of WMSO operations

Figure 2 is a chart of the organization of personnel assigned to project VT/036 during Phase V.

### 3.2.2 Operating Parameters of the Routine Seismographs at WMSO

The operating parameters and the tolerances for allowable deviations from these parameters are tabulated in table 1. These parameters are checked and reset when the routine frequency responses exceed the tolerances stated in table 2. The response characteristics of WMSO seismographs are shown in figure 3.

## 3.3 CHANGES AND/OR ADDITIONS TO THE STANDARD INSTRUMENTATION AT WMSO

The following changes and/or additions were made to the standard instrumentation at WMSO. Each is discussed in detail in a later section of this report.

a. A 14-channel Minneapolis-Honeywell magnetic-tape recorder became operational near the end of March 1962.

b. Improved lightning protection was installed for the triangular array beginning in mid-July.

c. The available commercial power was increased on 14 August 1962.

d. The free periods and damping of the Sprengnether long-period seismometers were modified on 28 and 29 August 1962.

e. The suspension system of the Sprengnether long-period vertical seismometer was modified on 28 August 1962.

f. The Sprengnether long-period horizontal seismometers, the three-component intermediate-band seismometers, and the three-component broad-band seismometers were moved to the tank farm (figure 9) during December 1962.

g. A Time Encoder, Geotech Model 13159, was installed on 18 December 1962.

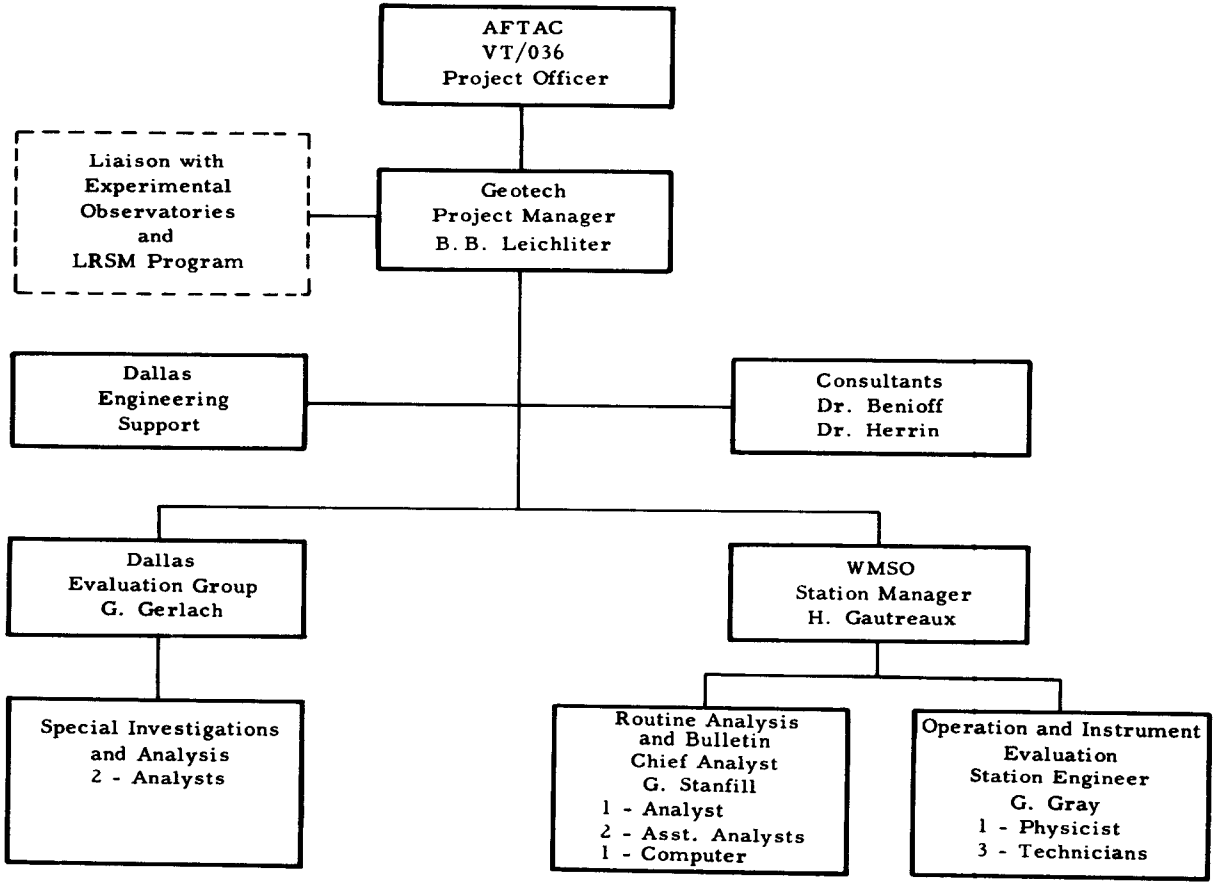


Figure 2. Personnel organization for Phase V of Project VT/036

Table 1. Operating Parameters and Tolerances for the WMSO Seismographs

| Seismograph | Operating parameters and tolerances | | | | | | | | | | Filter bandpass at 3-db cutoff (sec) | Filter cutoff rate at SP side (db/oct) |
|---|---|---|---|---|---|---|---|---|---|---|---|---|
| | $T_s$ | | $\lambda_s$ | | $T_g$ | | $\lambda_g$ | | $\sigma^2$ | | | |
| SP Vertical Johnson-Matheson | 1.25 | ±2% | 0.51 | ±5% | 0.33 | ±5% | 0.65 | ±5% | 0.03 | | 0.1-100 | 12 |
| SP Vertical Benioff | 1.0 | ±5% | 1.0 | ±5% | 0.2 | ±5% | 1.0 | ±5% | 0.01 | | 0.1-100 | 12 |
| SP Horizontal Benioff | 1.0 | ±5% | 1.0 | ±5% | 0.2 | ±5% | 1.0 | ±5% | 0.01 | | 0.1-100 | 12 |
| UA SP Vertical Benioff | 1.0 | ±5% | 0.8 | | 0.0625 | ±5% | | | 0.2 | | | |
| IB Vertical Melton | 2.5 | ±5% | 0.65 | ±5% | 0.64 | ±5% | 1.5 | ±5% | 0.002 | | 0.05-100 | 12 |
| IB Horizontal Sprengnether | 2.5 | ±5% | 0.65 | ±5% | 0.64 | ±5% | 1.5 | ±5% | 0.0005 | | 0.05-100 | 12 |
| BB Vertical Press-Ewing | 12.5 | ±5% | 0.4 | ±5% | 0.64 | ±5% | 9.0 | ±5% | 0.0002 | | 0.05-100 | 12 |
| BB Horizontal Sprengnether | 12.5 | ±5% | 0.4 | ±5% | 0.64 | ±5% | 9.0 | ±5% | 0.0004 | | 0.05-100 | 12 |
| LP Vertical Sprengnether | 25.0<br>20.0 | ±5%<br>±5%[a] | 1.0<br>0.7 | ±5%<br>±5%[a] | 30.0 | ±5% | 1.0 | ±5% | 0.004 | | 25-1000 | 12 |
| LP Horizontal Sprengnether | 25.0<br>20.0 | ±5%<br>±5%[a] | 1.0<br>0.7 | ±5%<br>±5%[a] | 30.0 | ±5% | 1.0 | ±5% | 0.004 | | 25-1000 | 12 |

[a]After 1 September 1962

Key to abbreviations:

SP - Short-period
UA - Unamplified (earth-powered)
IB - Intermediate-band
BB - Broad-band
LP - Long-period
$T_s$ - Free period of seismometer (seconds)
$\lambda_s$ - Damping constant of seismometer
$T_g$ - Free period of galvanometer (seconds)
$\lambda_g$ - Damping constant of galvanometer
$\sigma^2$ - Coupling coefficient

Table 2. Calibration Norms and Operating Tolerances for Frequency Responses of Seismographs at WMSO

| f (cps) | T (secs) | Relative amplitude | Amplitude tolerance (%) |
|---|---|---|---|
| **Short-period Horizontal** | | | |
| 0.2 | 5 | 0.01 | ± 15 |
| 0.5 | 2 | 0.15 | 10 |
| 0.8 | 1.25 | 0.56 | 5 |
| 1.0 | 1.0 | 1.0 | 0 |
| 1.5 | 0.67 | 2.15 | 5 |
| 2.0 | 0.5 | 2.8 | 5 |
| 3.0 | 0.33 | 3.2 | 10 |
| 4.0 | 0.25 | 3.0 | 15 |
| 5.0 | 0.2 | 2.4 | 20 |
| **Intermediate-Band** | | | |
| 0.1 | 10 | 0.0090 | ± 20 |
| 0.2 | 5 | 0.068 | 15 |
| 0.3 | 3.3 | 0.25 | 10 |
| 0.4 | 2.5 | 0.46 | 5 |
| 0.5 | 2.0 | 0.64 | 5 |
| 0.7 | 1.43 | 0.86 | 5 |
| 1.0 | 1.0 | 1.00 | 0 |
| 1.5 | 0.67 | 1.04 | 5 |
| 2.0 | 0.5 | 1.00 | 5 |
| 3.0 | 0.33 | 0.89 | 10 |
| 5.0 | 0.2 | 0.66 | 10 |
| **Long-period Sprengnether Prior to 1 September 1962** | | | |
| 0.1 | 10 | 0.22 | ± 20 |
| 0.0667 | 15 | 0.53 | 10 |
| 0.05 | 20 | 0.83 | 5 |
| 0.04 | 25 | 1.0 | 0 |
| 0.03 | 33 | 0.82 | 5 |
| 0.025 | 40 | 0.55 | 10 |
| 0.02 | 50 | 0.33 | 15 |
| 0.015 | 66.7 | 0.17 | 15 |
| 0.01 | 100 | 0.06 | 20 |

| f (cps) | T (secs) | Relative amplitude | Amplitude tolerance (%) |
|---|---|---|---|
| **Short-period Johnson-Matheson** | | | |
| 0.2 | 5 | 0.012 | ± 15 |
| 0.5 | 2 | .195 | 10 |
| 0.8 | 1.25 | 0.685 | 5 |
| 1.0 | 1.0 | 1.0 | 0 |
| 1.5 | 0.67 | 1.52 | 5 |
| 2.0 | 0.5 | 1.9 | 5 |
| 3.0 | 0.33 | 2.12 | 10 |
| 4.0 | 0.25 | 2.0 | 15 |
| 5.0 | 0.2 | 1.45 | 20 |
| **Broad-Band** | | | |
| 0.0667 | 15 | .5 | ± 15 |
| 0.08 | 12.5 | .775 | 10 |
| 0.1 | 10 | 0.95 | 5 |
| 0.2 | 5 | 1 | 5 |
| 0.4 | 2.5 | 1 | 5 |
| 0.8 | 1.25 | 1 | 0 |
| 1.6 | 0.625 | 1 | 5 |
| 3.2 | 0.312 | 1 | 10 |
| 6.4 | 0.156 | 0.98 | 15 |

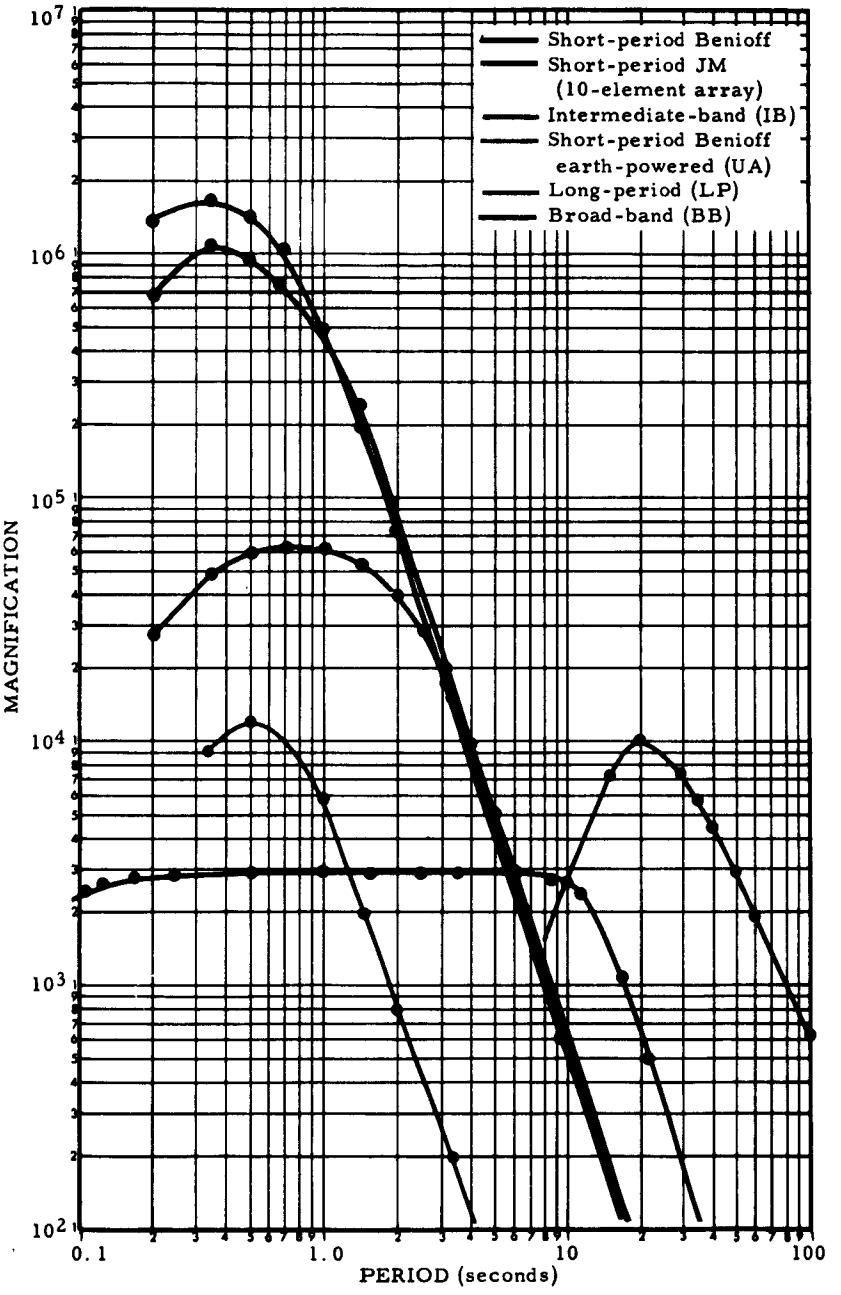


Figure 3. Response characteristics of seismographs at WMSO

h. A Seismic Data Filter, Geotech Model 11760, became part of the standard instrumentation in late December 1962.

i. Modification of the Calibration Control Unit, Geotech Model 2520, was completed near the end of Phase V.

## 3.4 MODIFICATION OF PHYSICAL FACILITIES AT WMSO

Twice during Phase V, the central air-conditioning unit at WMSO failed. On the night of 9 July, a bearing burned out and replacement parts did not arrive until the afternoon of 13 July. During this period, the temperature in the observatory reached 108 degrees, but no electronic failures were experienced due to the excessive heat.

On 1 August, during the second failure of the central air-conditioning unit, which lasted for eight days, several transistors and the power supply in the primary Timing System, Model 5400, were damaged as the result of operating under conditions of excessive heat. During this period, the ambient temperature exceeded 100 degrees. Difficulty was also encountered in obtaining good quality film records because of the high temperatures that the processing chemicals and films reached in the Develocorders while the air-conditioning unit was inoperative.

A 23,000-BTU window air-conditioning unit was installed on 6 August to serve as an auxiliary unit in the event of failure of the central air-conditioning unit. Although this unit is not adequate to cool the entire central-recording building, it will serve as a stand-by unit to maintain the temperature within the operations room to a safe level for the operation of the electronic equipment.

During Phase V, it became necessary to expand the facilities at WMSO in order to efficiently conduct the operation of WMSO. In addition to the instrumentation required for the routine operation of the station, several newly developed instruments became the responsibility of WMSO personnel for field testing. Additional instruments are scheduled to be assigned to WMSO for field testing in the near future. Figure 4 is the floor plan of the central-recording building at WMSO prior to the modification of the facilities.

A trailer unit, 10 feet by 55 feet, was leased and was installed adjacent to the south door of the central-recording building; joined to the central-recording

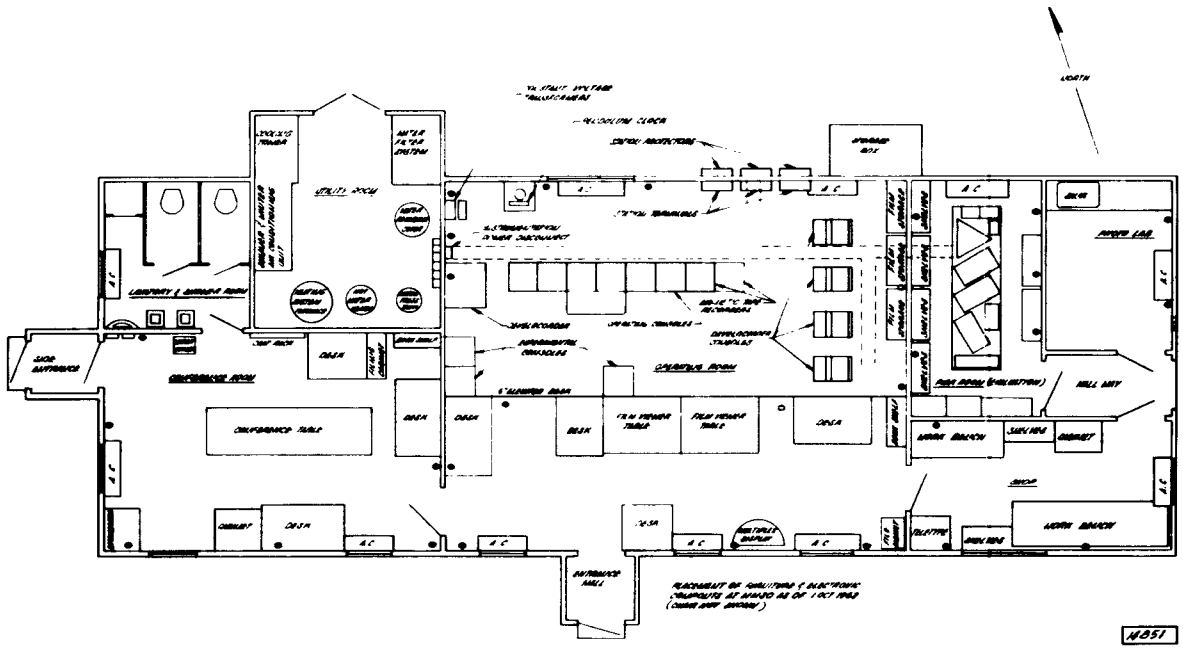

Figure 4. Floor plan of the central-recording building at WMSO prior to the addition of the trailer annex and the modification of the operating room

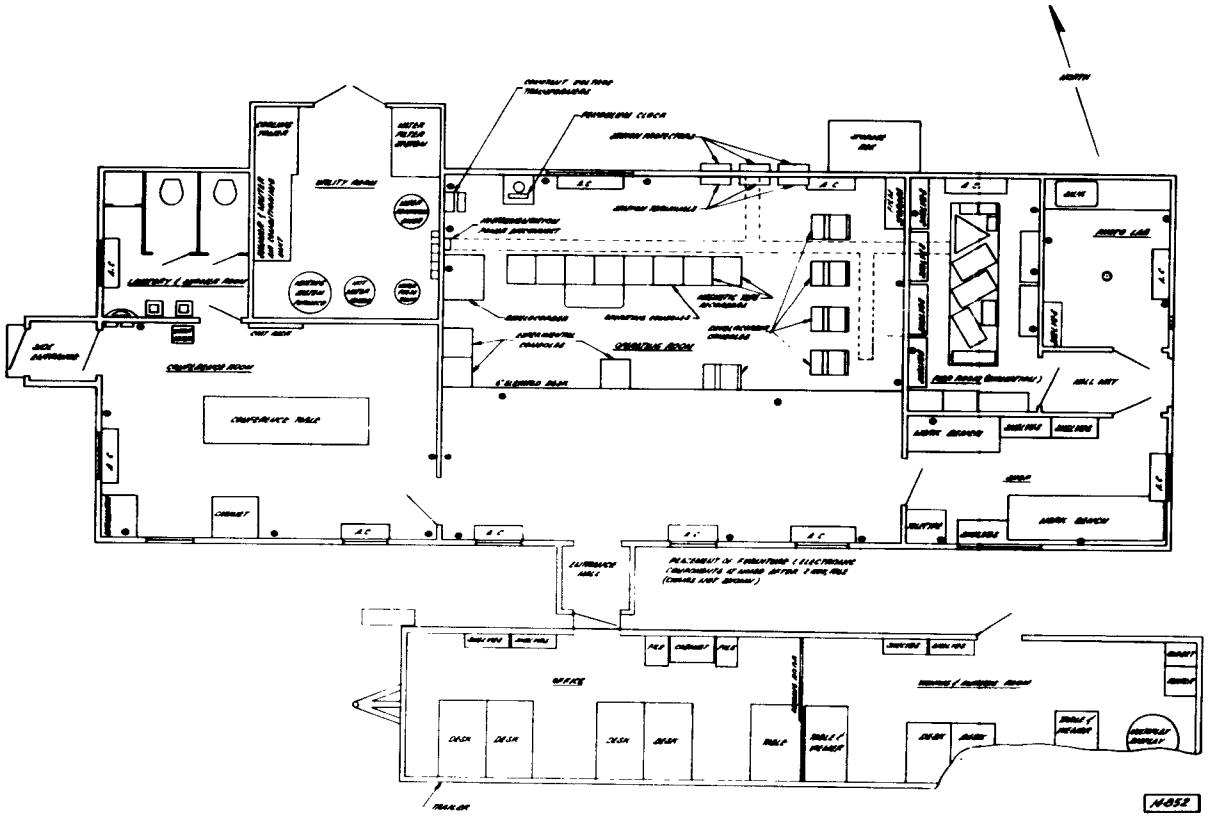

Figure 5. Floor plan of the central-recording building at WMSO after annexation of the trailer but before modification of the operating room

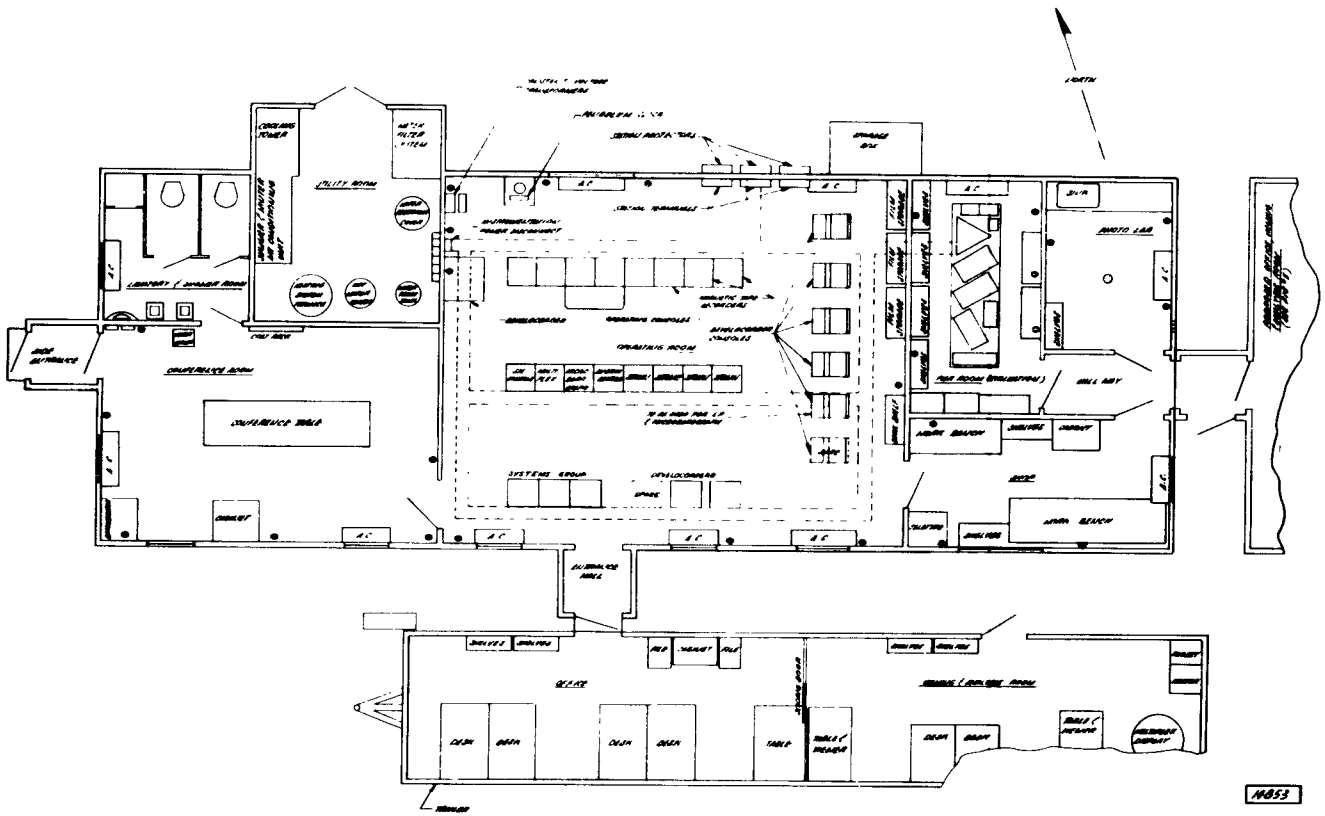

Figure 6. Floor plan of the central-recording building and trailer annex at WMSO after modification of the operating room

building by an all-weather passageway. The trailer was anchored to the bedrock on all sides in order to stabilize it during periods of high wind.

The purpose of adding the trailer unit was to provide a quiet office and viewing area, isolated from the traffic and noise of the operations room, and to increas the available instrument space in the operations room. Installation of the trailer annex was completed by 2 November. Figure 5 is the floor plan of the central-recording building after the office and viewing equipment was moved into the trailer annex.

Work on the modification of the operations room was completed on 19 December (figure 6). Since the completion of the remodeling of the operations room, four console racks and two Develocorders have been added to the equipment. The photograph (figure 7) shows a portion of the operations room since additional equipment has been added.

Figure 7. Data control consoles in the operation room at WMSO after modification of the operation room (new console shown on left)

## 3.5 DATA CHANNELS RECORDED AT WMSO

Table 3 shows the data channels that were recorded at WMSO during Phase V.

## 3.6 INSTALLATION AND OPERATION OF THE 10-KILOMETER LINEAR ARRAY

On 8 May 1962, the Project Officer requested that a study be made to determine the feasibility of installing and operating a 10-kilometer linear array of short-period seismographs at WMSO on a temporary basis. The array was to be oriented at an azimuth of 252 degrees. There was not sufficient area available on the artillery range for the entire array without infringing on maneuver zones or impact areas. The northwest leg of the 3-kilometer triangular array (vaults 4T, 5T, 6P, and 7T, figure 8) is oriented at approximately 252 degrees, and the extension of this leg of the array northeast and southwest offered the most feasible solution to the problem.

The results of the study were reported to the Project Officer by telephone on 9 May, along with an estimate of the time required to install the array and to begin recording on magnetic tape. Verbal approval to install the linear array was received from the Project Officer on 10 May and was later confirmed by letter. Major Frank Pilotte, of AFTAC, was assigned the responsibility for the task of reduction and analysis of linear-array data.

Mr. Julian A. Howard, Manager of the Wichita Mountains Wildlife Refuge, agreed to a survey of sites for the additional seismometers prior to the receipt of approval of our request to install equipment on the Wildlife Refuge. Figure 8 shows the location of the seismometers of the linear array. The elevation and location of each of the 11 seismometers are given in table 4.

Seismometers L4, L5, L6, and L7 are common to both the triangular and linear arrays, and are permanent locations. Three of the four seismometers common to both arrays are housed in sealed tank vaults which are coupled to the granite bedrock by concrete. The seismometer at L7 is in a concrete "walk-in" type vault.

The remaining 7 seismometers (L0-L3 and L8-L10) are temporary installations. At each of these locations, the overburden was removed in order to expose the granite bedrock. One sack of concrete mix was poured on the rock to form a level pier, approximately 2 feet in diameter, on which the

## Table 3. Data Channel Assignments during Phase V

### DEVELOCORDER

| Chan | No. 1[a] | Mag @ 1 cps | No. 2 | Magnification | No. 3[b] 1 July-8 Oct 62 After 7 Feb 63 | No. 3[b] 8 Oct 62 To 21 Jan 63 | Mag @ 1 cps | No. 4 | Mag @ 1 cps |
|---|---|---|---|---|---|---|---|---|---|
| 1 | WWV | | WWV | | WWV | WWV | | WWV | |
| 2 | JM Z1 | 500K | BB V | 4K @ 1 cps | LO | Benioff Z1 | 500K | Σ1-4 | 500K |
| 3 | Z2 | 500K | BB HN | 4K @ 1 cps | L1 | Z2 | 500K | Σ4-7 | 500K |
| 4 | Z3 | 500K | BB HE | 4K @ 1 cps | L2 | Z3 | 500K | Σ7-1 | 500K |
| 5 | Z4 | 500K | Spr LP V | 10K @ 25 sec | L3 | Z4 | 500K | EP HG | 60K |
| 6 | Z5 | 500K | Spr LP HN | 10K @ 25 sec | L4 | Z5 | 500K | EP LG | 5K |
| 7 | Z6 | 500K | Spr LP HE | 10K @ 25 sec | L5 | Z6 | 500K | IB | 60K |
| 8 | Z7 | 500K | 1/10 Spr LP V | 1K @ 25 sec | L6 | Z7 | 500K | IB HN | 60K |
| 9 | Z8 | 500K | 1/10 Spr LP HN | 1K @ 25 sec | L7 | Z8 | 500K | IB HE | 60K |
| 10 | Z9 | 500K | 1/10 Spr LP HE | 1K @ 25 sec | L8 | Z9 | 500K | Σ1-10 | 1000K |
| 11 | Z10 | 500K | Geo LP V | 10K @ 25 sec | L9 | Z10 | 500K | Test | |
| 12 | Σ1-10 | 1000K | Geo LP HN | 10K @ 25 sec | L10 | Σ1-10 | 500K | Test | |
| 13 | Σ1-10F | 2000K | Geo LP HE | 10K @ 25 sec | Test | Test | | Test | |
| 14 | HN | 500K | Σ1-10 | 270K @ 1 cps | Test | Test | | JM 20 | 500K |
| 15 | HE | 500K | M SP | | Test | Test | | SIE | 60K |
| 16 | 1/10/Z5 | 50K | A | | ST | Test | | Test | |

### MAGNETIC-TAPE RECORDERS

| Chan | Ampex: 1 July to 8 Oct 62 After 7 Feb 63 | Ampex: Prior to July 62 and 8 Oct 62 to 21 Jan 63 | Minneapolis-Honeywell |
|---|---|---|---|
| 1 | ST | ST | ST |
| 2 | LO | JM Z6 | JM Z1 |
| 3 | L1 | BB V | Z2 |
| 4 | L2 | SP HN | Z3 |
| 5 | L3 | JM 20 | Z4 |
| 6 | L4 | SP HE | Z5 |
| 7 | Comp | Comp | Comp |
| 8 | L5 | IB V | Z6 |
| 9 | L6 | Spr LP V | Z6 (low gain) |
| 10 | L7 | IB HN | Z7 |
| 11 | L8 | Spr LP HN | Z8 |
| 12 | L9 | IB HE | Z9 |
| 13 | L10 | Spr LP HE | Z10 |
| 14 | Voice & WWV | Voice & WWV | Voice & WWV |

### KEY

Z - Short-period vertical
Σ - Summation
F - Filtered
H - Horizontal
N - North-South
E - East-West
BB - Broad-band
V - Vertical
Spr - Sprengnether
LP - Long-period
Geo - Geotech
M - Microbarograph
SP - Short-period
A - Anemometer
L - Linear
ST - Station time
EP - Earth-powered
HG - High-gain
LG - Low-gain
IB - Intermediate-band
JM20 - Johnson-Matheson with 20-cps Galvo
Comp - Compensation

Single-pen Helicorder monitors or records short-period data.

Three-pen Helicorder monitors or records long-period data.

Develocorder No. 5 is being used to record 10 channels of data from a cable study program under Contract AF 33(657)-7060. One channel is used for WWV and one for VLF radio time. Other projects under the same contract will use the other channels within the next month.

Develocorder No. 6 is being used to record 6 channels of data. Three channels are used for the long-period tripartite, one for a microbarograph (LP), one for a microbarograph (SP), and one for station time.

[a]Data switched between Develocorder No. 1 and No. 3 in order to record data continuously.

[b]Except during indicated periods, Develocorders No. 1 and No. 3 recorded identical data on alternate days.

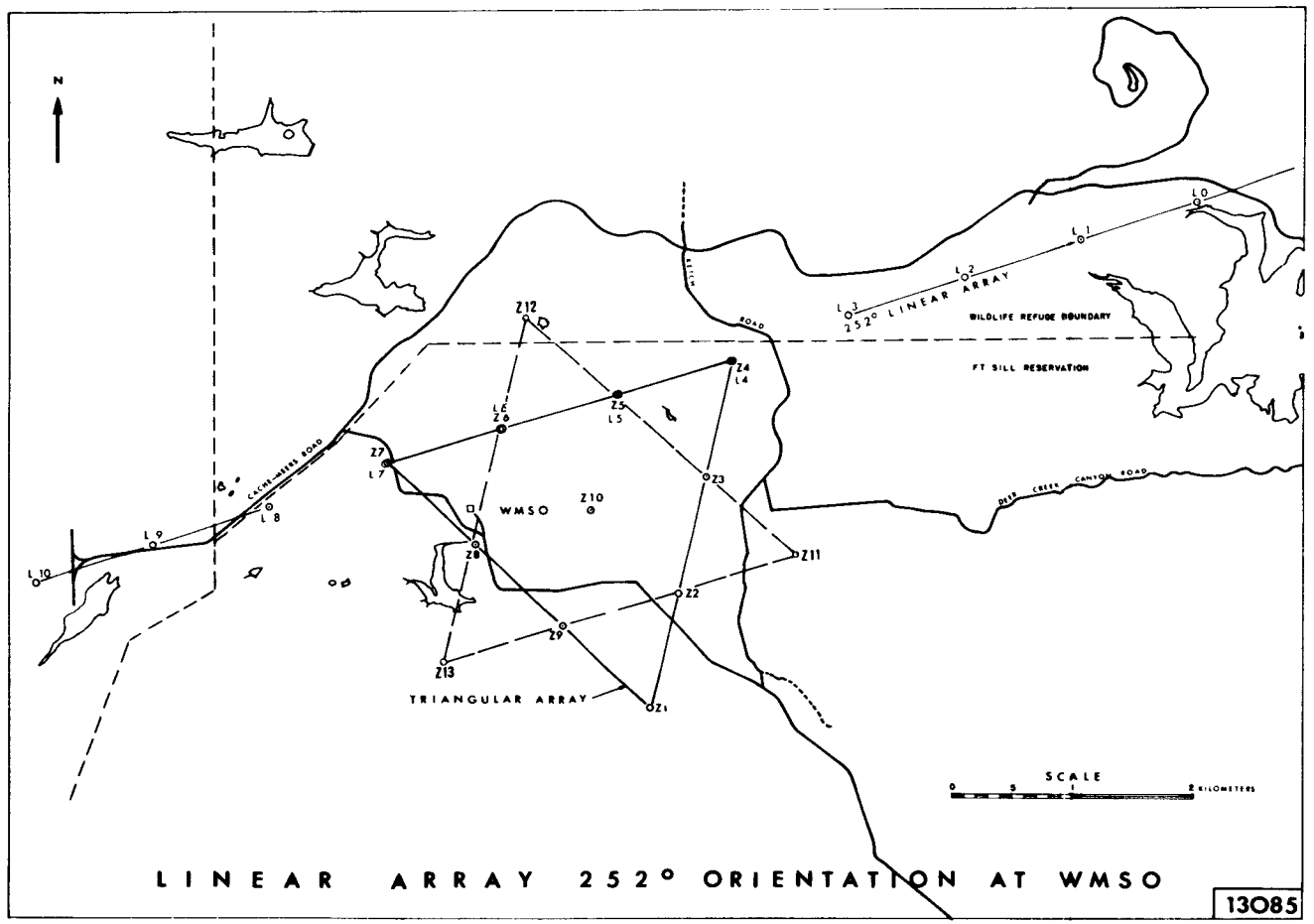


Figure 8. Orientation of linear and triangular arrays at WMSO

seismometer was located. After the free period, seismometer damping, and calibrations had been checked, the seismometers were covered with a plastic sheet and approximately 2 feet of earth.

A top priority was assigned to the installation of the linear array, second only to the maintenance of normal operations of the observatory, in an effort to complete the installation within one week as requested by the Project Officer.

By 15 May, 9 of the 11 seismometers were operational; however, all of the available spiral-four cable had been used. Several reels of surplus spiral-four cable were borrowed from the Signal Depot at Fort Sill in order to complete the installation of the other two seismometers. On 18 May, all 11 elements of the linear array were being recorded on the Ampex magnetic-tape recorder.

The linear array was operated until 8 October, at which time it was discontinued at the request of the Project Officer. Data from the linear array were recorded on both 16-millimeter film and magnetic tape. Table 3 lists the data-channel assignments for the linear array during Phase V. Approximately 23 1/2 hours of data were recorded on each recorder daily during the operating period. All data and operating logs pertaining to the linear array were shipped to the VELA-UNIFORM Data Analysis and Technique Development Center in Alexandria, Virginia.

Table 4. Locations and Elevations of Each of the Seismometers of the Linear Array

| Seismometer | Actual location (relative to surveyed point figure 8) | Elevation |
|---|---|---|
| L0* | 40' north | 1408.0 |
| L1* | 15' north | 1432.5 |
| L2* | 90' east | 1447.1 |
| L3* | 125' west | 1518.2 |
| L4** | 175' north | 1610.9 |
| L5** | 50' north | 1587.3 |
| L6** | 50' south | 1656.5 |
| L7** | 175' south | 1585.8 |
| L8* | 140' east | 1516.6 |
| L9* | 125' south | 1499.6 |
| L10* | at surveyed point | 1485.1 |

* Temporary seismometer locations
** Used in both triangular and linear array; permanent seismometer locations

After the operation of the linear array was completed, the JM seismometers used in the linear array that were not common to the triangular array, and the 21 miles of spiral-four cable that was located on the Wildlife Refuge were gathered by 8 November.

In mid-January 1963, the Project Officer requested that we investigate the possibility of reinstalling the linear array. A permit was obtained through Mr. Julian Howard, Manager of the Wildlife Refuge, to reinstall those seismometers that had been located on the Refuge. Confirmation of the request to reactivate the linear array at WMSO was received from the Project Officer on 25 January.

Reinstallation of the JM seismometers, the lightning protectors, and the stringing of cable for the linear array was completed on 30 January. Calibration of the linear-array seismographs began on 31 January. The damping was set, calibration completed, gains equalized, and recording of the linear array began at 00:00Z on 7 February. Data are again being sent to DATDC in Alexandria, Virginia; the first shipment was made on 27 February.

An evaluation of the operation of the linear array and a comparison of its performance with the performance of the triangular array is presented in section 6.5 of this report.

## 3.7 REACTIVATION OF THE "H" ARRAY

Simultaneous operation of the old H array (figure 9) and the new triangular array began on 7 May, but was temporarily suspended on 10 May at the request of the Project Officer, in order to make PTA's and adequate recording facilities available for the operation of the 10-kilometer linear array.

Immediately after the completion of the operation of the 10-kilometer linear array on 8 October, the Benioff seismometers of the old H array were checked and serviced prior to the resumption of the operation of the H array. Test recording of the H array began on 12 October and final calibration was completed by 29 October. Recording of the summation of the 10 vertical Benioff seismographs of the old array began on 20 November. The operation of the H array was discontinued on 21 January 1963, by which time sufficient data had been recorded to make a comparison of the two arrays. The results of this comparison are presented in section 6.4 of this report.

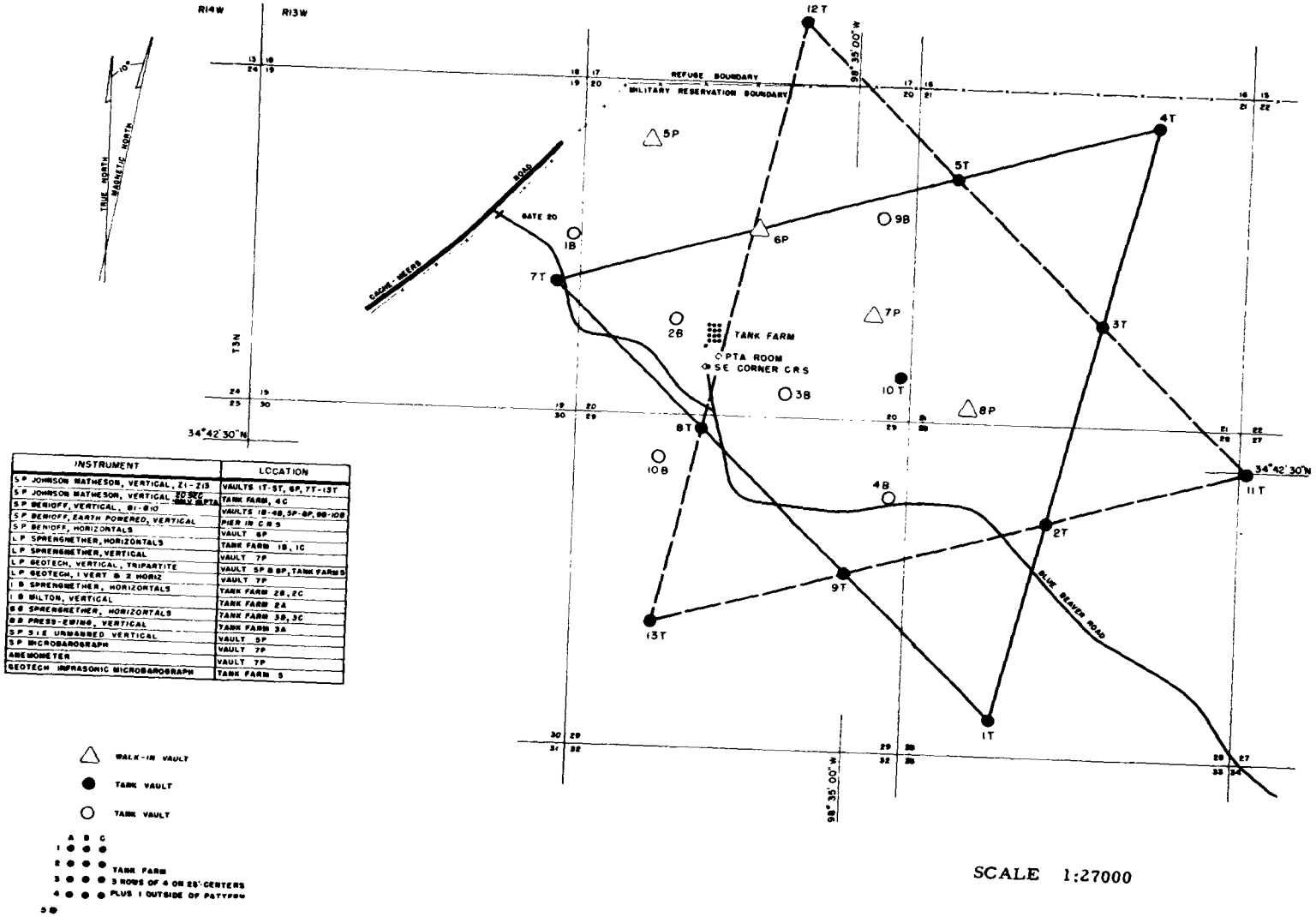


| INSTRUMENT | LOCATION |
|---|---|
| SP JOHNSON MATHESON, VERTICAL, Z1-Z13 | VAULTS 1T-5T, 6P, 7T-13T |
| SP JOHNSON MATHESON, VERTICAL, 20 SEC | TANK FARM, 4C |
| SP BENIOFF, VERTICAL, B1-B10 | VAULTS 1B-4B, 5P-8P, 9B-10B |
| SP BENIOFF, EARTH POWERED, VERTICAL | PIER IN C R S |
| SP BENIOFF, HORIZONTALS | VAULT 8P |
| LP SPRENGNETHER, HORIZONTALS | TANK FARM 1B, 1C |
| LP SPRENGNETHER, VERTICAL | VAULT 7P |
| LP GEOTECH, VERTICAL, TRIPARTITE | VAULT 5P & 8P, TANK FARM B |
| LP GEOTECH, 1 VERT & 2 HORIZ | VAULT 7P |
| 1 B SPRENGNETHER, HORIZONTALS | TANK FARM 2B, 2C |
| 1 B MILTON, VERTICAL | TANK FARM 2A |
| 6 B SPRENGNETHER, HORIZONTALS | TANK FARM 3B, 3C |
| 8 D PRESS-EWING, VERTICAL | TANK FARM 3A |
| SP SIE UNMANNED VERTICAL | VAULT 5P |
| SP MICROBAROGRAPH | VAULT 7P |
| ANEMOMETER | VAULT 7P |
| GEOTECH INFRASONIC MICROBAROGRAPH | TANK FARM B |

Figure 9. Orientation of triangular array, H array, and planned 13-element array at WMSO

### 3.8 INSTALLATION OF 13-ELEMENT ARRAY AT WMSO

All possible advance preparations were made for the addition of three JM vertical seismometers to the present 10-element triangular array at WMSO. The sites for Z11 and Z13, located at 11T and 13T, respectively (figure 9), were readied by blasting the necessary holes for the installation of the tank vaults. The location of the site for Z12 (figure 9) is on the Wichita Mountains Wildlife Refuge; installation of the tank vault will be started when approval of our request for use of the site is received from the Bureau of Land Management at Santa Fe, New Mexico.

## 4. EVALUATION OF STANDARD INSTRUMENTATION AT WMSO

The installation of a triangular array using Johnson-Matheson seismometers was a major change in standard instrumentation which occurred at the end of Phase III. Shortly after the beginning of Phase V, transformer-type signal isolators were installed in the short-period and intermediate-band channels. Equalization of each individual seismograph to the summation imposed the necessity of maintaining equal voltage gains on the outputs of the short-period PTA's which required periodic changes in the coupling between the seismometers and galvanometers. The changes in coupling, together with the resetting of the seismometer damping which was required after each change, reduced the precision of instrumental stability measurements, as compared with the stability measurements made during Phases II and III. The precision of measurement was, however, adequate for a good indication of overall operational stability.

### 4.1 SHORT-PERIOD SEISMOGRAPHS, TRIANGULAR ARRAY

Johnson-Matheson (JM) seismometers are used in the triangular array. The output of each JM seismometer is loosely coupled to a 3-cps galvanometer (located in a phototube amplifier), the galvanometer is adjusted to 0.65 of critical damping. Seismometer natural frequency and damping are 0.8 cps and 0.51 of critical, respectively.

### 4.1.1 Variations in Response Characteristics

Because of the method of recording on magnetic tape and of summing the outputs of the phototube amplifiers (PTA's), it is essential that signal levels at the outputs of the PTA's be maintained at a nearly constant value; the only method of accomplishing this, at the present time, is to vary the coupling between seismometer and galvanometer by means of a trim potentiometer on the line-termination module. A change in the setting of the trim potentiometer is accompanied by a small change in damping of the seismometer. The seismometer damping must then be remeasured and, if necessary, reset. In the routine application of these procedures, the seismometer damping is normally reset to within a tolerance of ± 2 percent. The standard deviation of the frequency responses of the 10 seismographs from the mean frequency response over the period range of 4.0 to 0.2 second was computed for each of 7 sets of 10 frequency responses measured during Phase V. The minimum standard deviation is 4.1 percent of the mean for the set of frequency responses taken 30 October 1962; the maximum standard deviation is 5.3 percent of the mean for the frequency responses taken 27 December 1962. The average of the standard deviation values for all 7 sets of frequency responses is 4.66 percent. Figure 10 is a graph of the mean of all the frequency responses with the variation of individual seismograph frequency responses indicated by one standard deviation confidence limits.

The phase responses of two of the short-period JM seismographs were measured (figure 11). One of the seismographs selected for the phase measurements (Z3) had a frequency response that was very near the average frequency response of the 10 seismographs. The other seismograph was selected because it had frequency-response characteristics which indicated that its phase response would differ from the average phase response to a greater degree than any of the other seismographs.

### 4.1.2 Stability of Frequency Response

The stability of the frequency responses of the 10 seismographs of the triangular array is more of an indication of the accuracy to which seismometer damping, galvanometer free period, and galvanometer damping were reset than an indication of instrumental stability, because periodic gain adjustments and occasional galvanometer and seismometer repairs were required during Phase V. For each of the 10 seismographs, the mean of the 7 frequency responses which were measured during Phase V was computed for the period range of 4.0 to 0.2 second, and the average of the 10 mean frequency responses

was computed. The average deviation of the means from the average frequency response was 2.6 percent of the average frequency response.

4.1.3 Stability of Magnification at 1 cps

The variation in the magnification at 1.0 cps was computed for one of the short-period seismographs (Z6) and for the summation of the 10 seismographs. All routine calibrations in July, August, November, and December 1962, and January 1963 were used. The average deviation of the magnification values from the mean is 0.76 percent of the mean for Z6 and 3.86 percent of the mean for the summation of the 10 seismographs.

4.1.4 Electrical Noise

Electrical noise in the JM short-period seismographs was measured by blocking the seismometer pendulums and recording the output of the PTA's at increased gain. The average microseismic signal to electrical-noise ratio is about 70 db. A graph showing the average electrical noise as a function of period compared to the

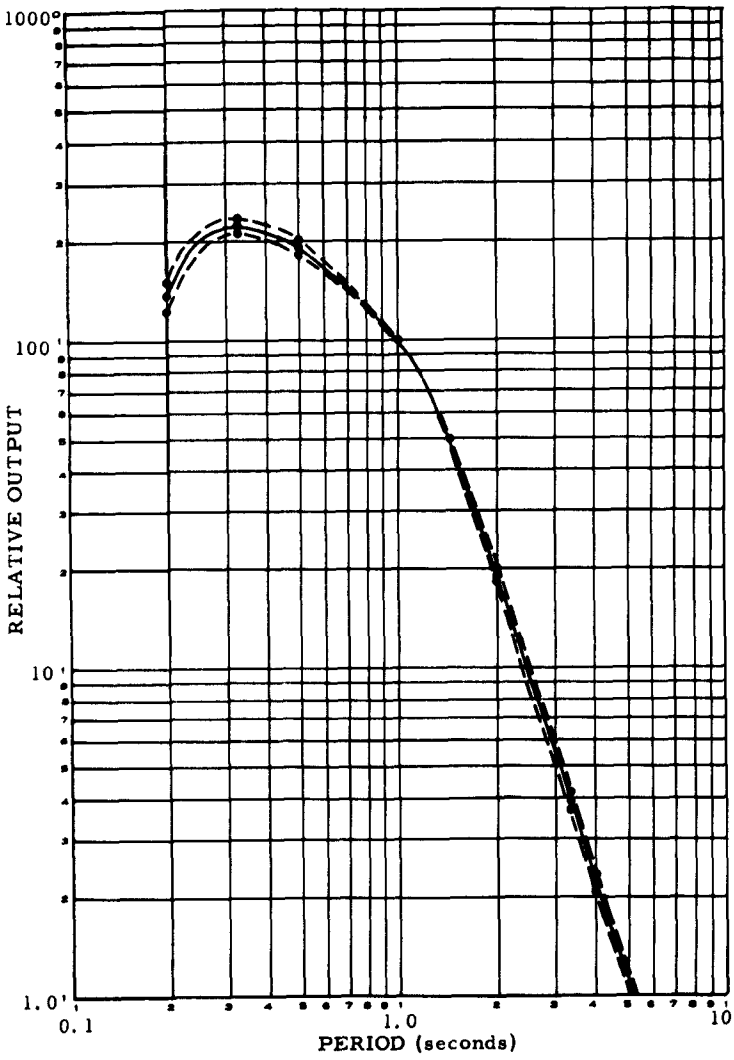


Figure 10. Mean frequency response of the ten short-period JM seismographs of the triangular array at WMSO during Phase V. Dotted lines indicate one standard deviation confidence limits.

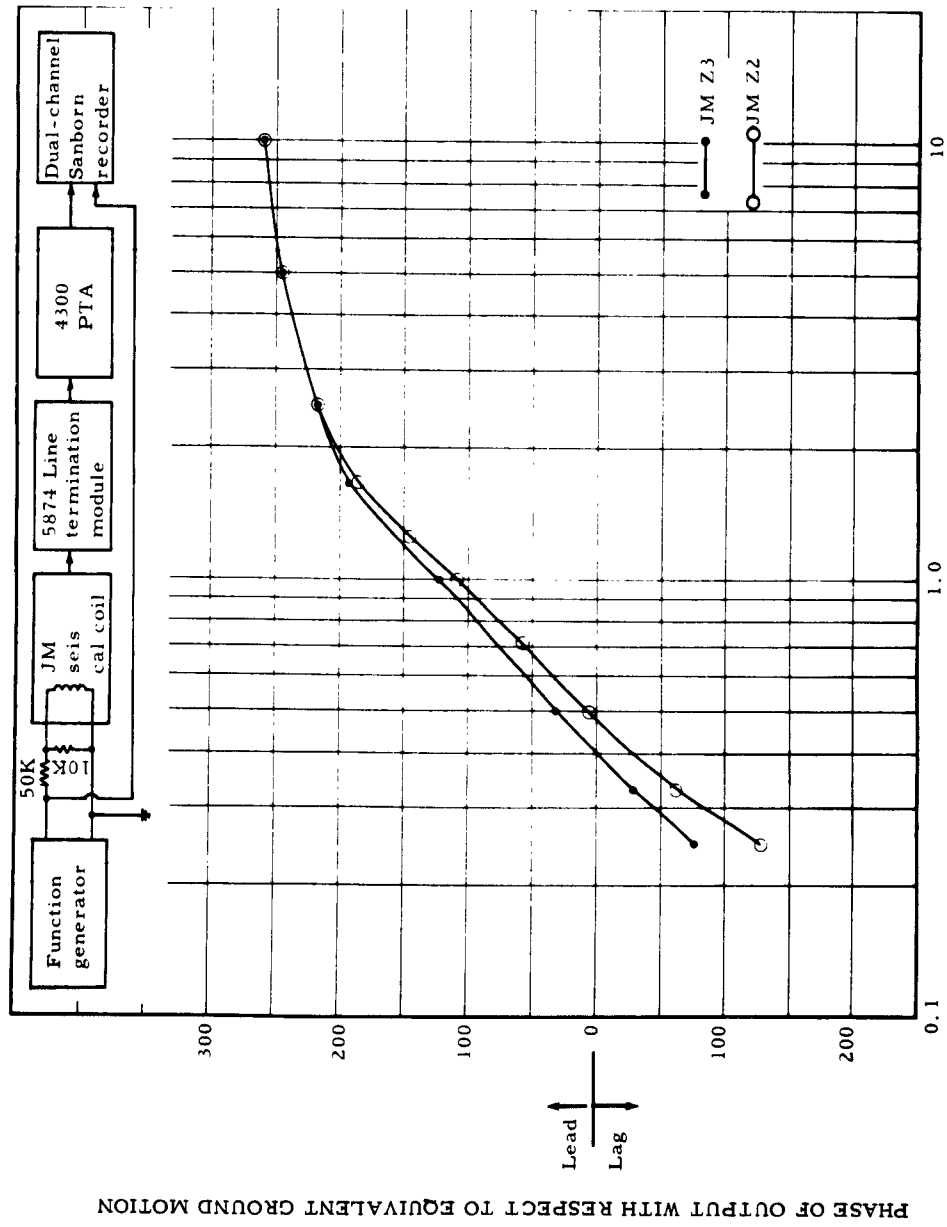


Figure 11. Phase response of short-period JM seismographs Z2 and Z3

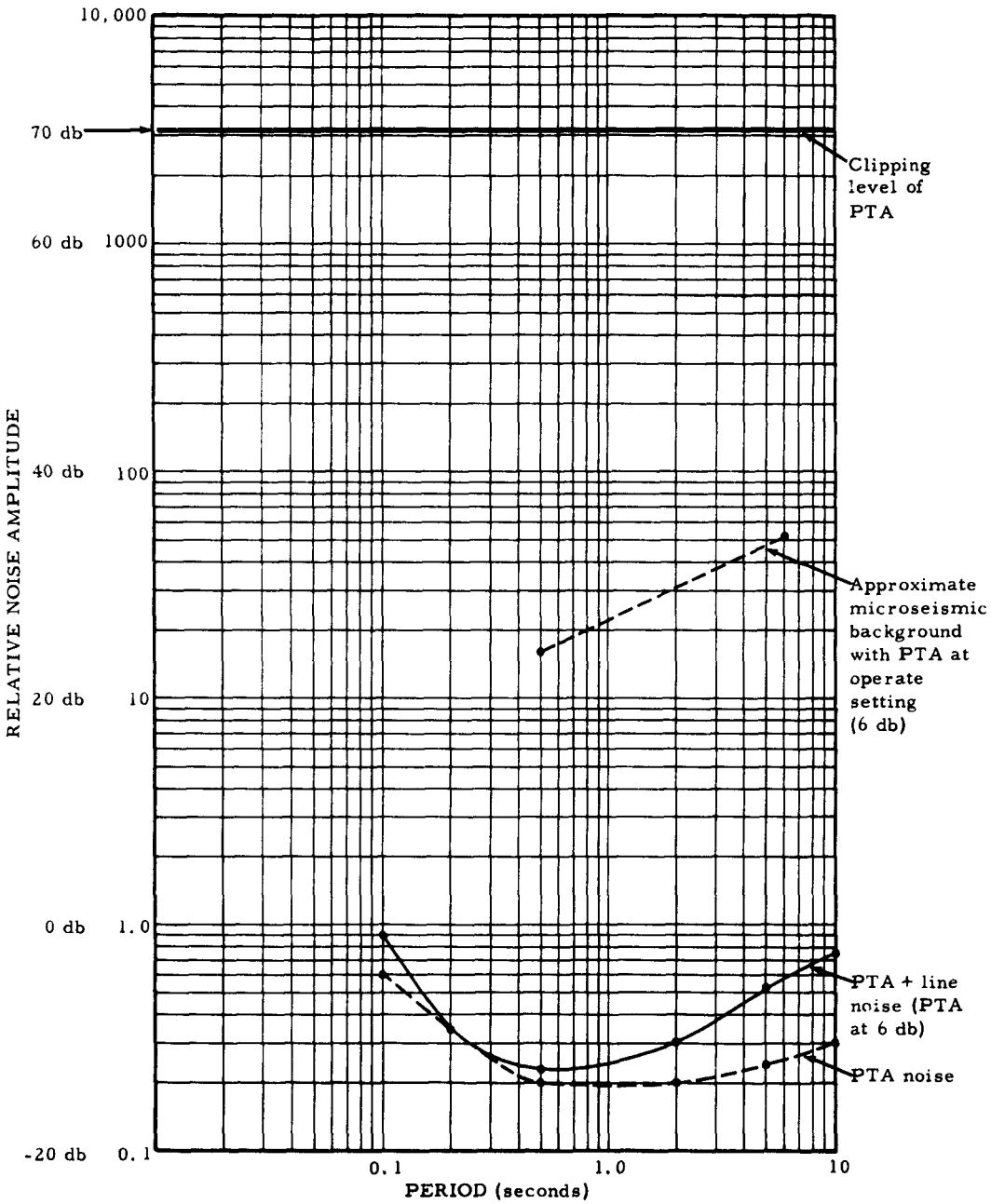


Figure 12. Noise level diagram for a typical JM seismograph in the triangular array

### 4.1.7 Summations of Short-Period Seismographs

The summation of the 10 vertical seismographs is relatively nondirectional for wavelengths, the horizontal components of which are greater than approximately 6 kilometers (figure 13). The method used to sum the outputs of the seismographs was changed shortly after the beginning of Phase V by the installation of transformer-type Signal Isolators, Geotech Model 6722A.

Before the installation of the signal isolators, summing had been done by adjustable resistive networks. The signal isolators provide more efficient utilization of the output power available from the PTA's but impose the requirement that the individual seismograph gains must be equalized ahead of the PTA's. Equalizing gains by this method requires relatively long outages to readjust the seismometer damping. The theoretical increase in signal-to-noise ratio obtained by summing remains constant within 1 percent for individual gain inequalities of up to 25 percent, assuming random noise; therefore, equalization of individual seismograph contributions to the summations was done at infrequent intervals. The magnifications of the individual seismographs and the magnifications of the summation seismographs were equalized at more frequent intervals by means of control modules when they deviated more than 10 percent from the nominal value.

The summations of the seismographs of the individual sides of the triangular array have directional properties in addition to short-period noise cancellation properties. In order to utilize the directivity of the summations of the individual sides of the triangular array, the contribution of each individual seismograph to the summations must be more nearly equalized than is necessary to obtain good short-period noise cancellation only. Magnification of each summation seismograph must also be closely controlled in order to use the directivity of the summations for effective determination of bearing angles of incident P waves. There is preliminary evidence that, even under the best conditions, variations in individual-vault coupling may produce amplitude variations that would make it difficult to utilize the summation traces to determine bearing angles of P waves using only measurements of relative amplitudes of the traces.

An additional summation trace, added on 7 January 1963, is composed of four short-period seismographs which are among the quietest during high wind. This summation trace is a valuable aid to analysis during windy periods. An example of its effectiveness is shown in figure 14.

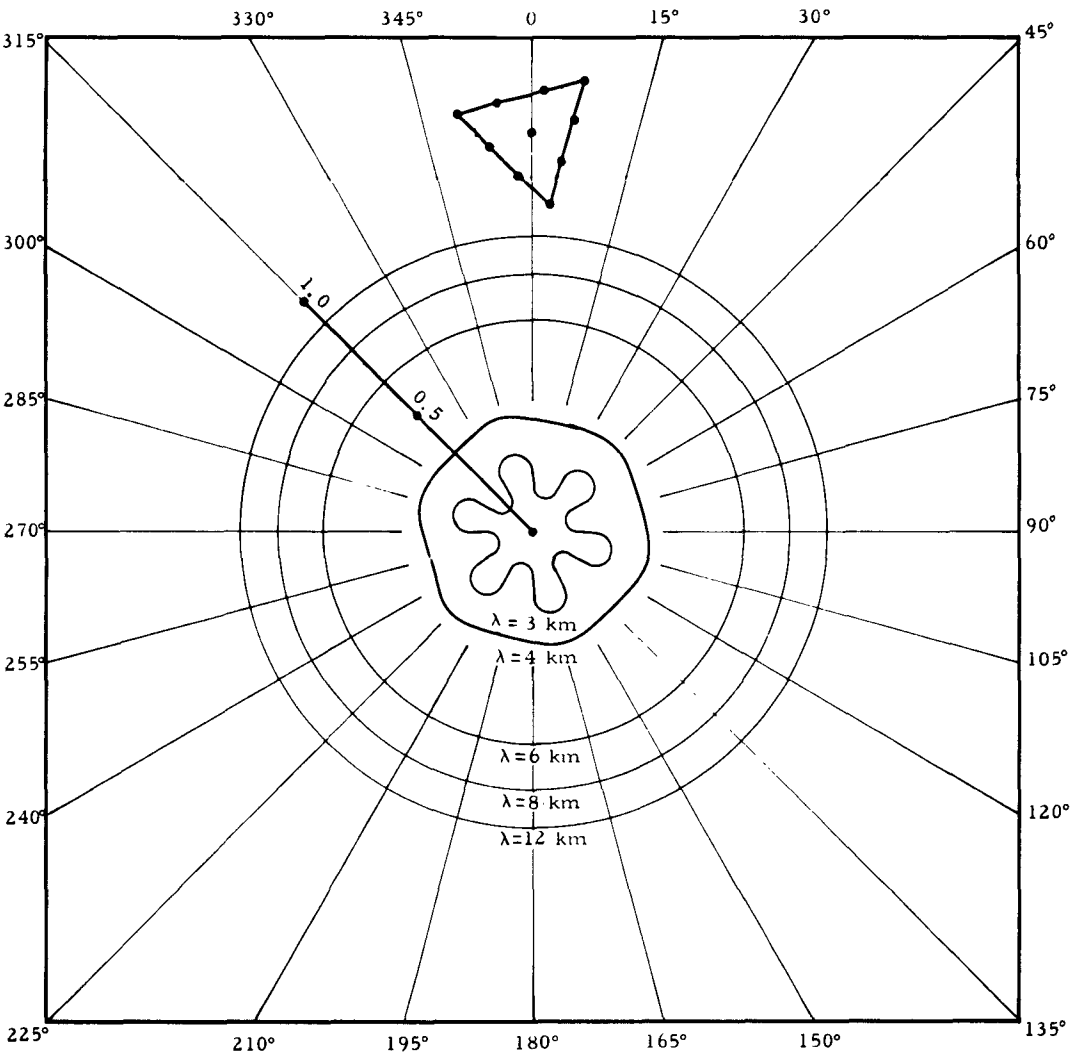


Figure 13. Directivity pattern for the summation of 10 short-period seismographs in the triangular array for several wavelengths (λ)

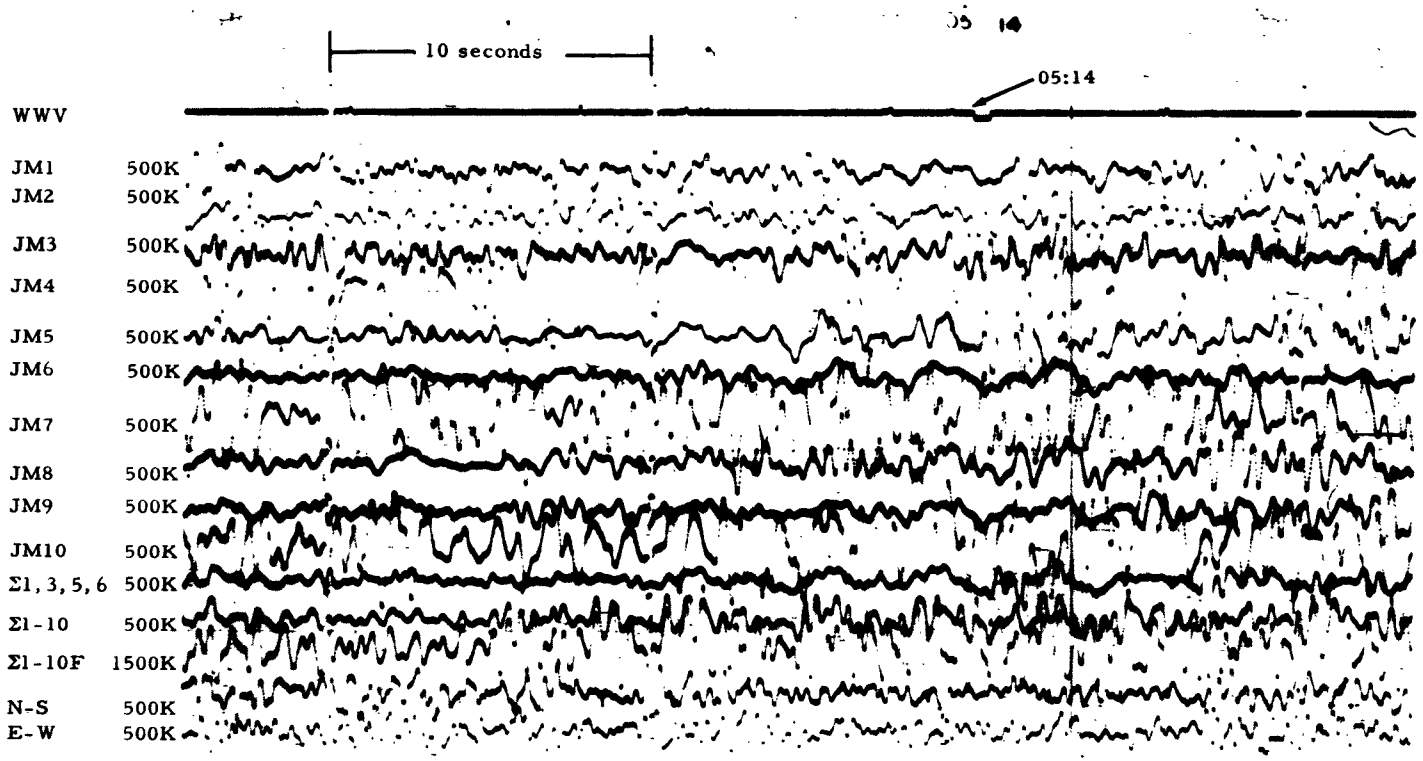


Figure 14. Short-period Develocorder record illustrating the effectiveness of the Σ1, 3, 5, 6 during periods of high wind. Wind velocity approximately 45-50 mph.

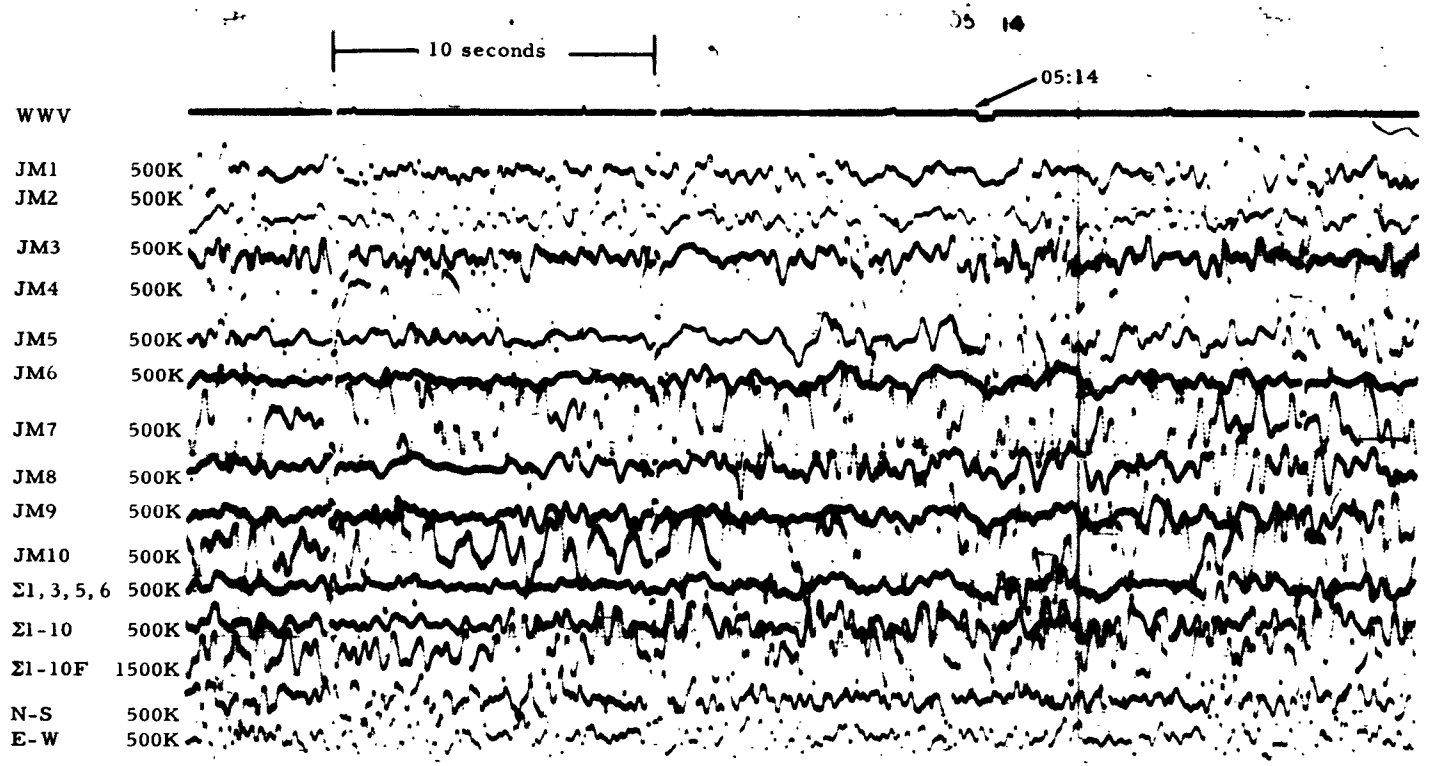


Figure 14. Short-period Develocorder record illustrating the effectiveness of the Σ1, 3, 5, 6 during periods of high wind. Wind velocity approximately 45-50 mph.

## 4.2 SHORT-PERIOD VAULTS, TRIANGULAR ARRAY

All vaults of the triangular array except vault 6P are metal tank vaults, cemented into holes in bedrock which were excavated using explosives. A diagram of a typical tank vault installation for the triangular array is shown in figure 15. Vault 6P is a large concrete vault, and contains several other instruments in addition to the JM vertical seismometer. Vault 6P is the only vault in the triangular array that is common to the old H array of 10 Benioff vertical seismographs. The location of each vault in the triangular array and in the H array is shown in figure 9.

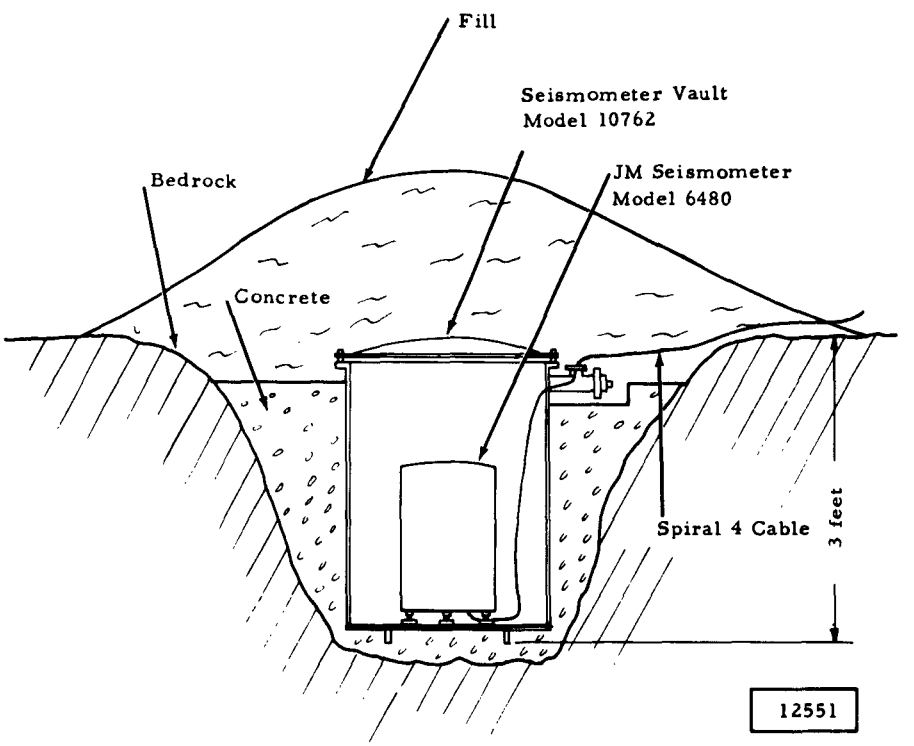


Figure 15. Profile view of vault for short-period vertical JM seismometers for triangular array at WMSO

The response of the seismograph in each vault of the triangular array to wind generated noise is shown in figure 16. The summations, $\Sigma 1, 3, 5, 6$, and $\Sigma 1\text{-}10$, are included in the plot of peak trace amplitude as a function of peak wind velocities.

## 4.3 LONG-PERIOD SEISMOGRAPHS

Operating parameters of the Sprengnether long-period seismographs were changed on 28 and 29 August 1962. At the same time, other modifications were made which were designed to decrease the variation of free period with mass position of the vertical seismometer. The free periods of the seismometers were changed from 25 to 20 seconds, and the damping factors were changed from critical to 0.7 critical.

### 4.3.1 Stability of Frequency Response

The average frequency responses of the Sprengnether long-period seismographs, before and after the changes in free period and damping parameters, are shown in figure 17. The average deviations of the individual frequency responses from the mean responses were 5.5 percent of the mean for the vertical and 4.4 percent for the horizontal seismographs during the first half of Phase V (before the change in parameters). The corresponding values during the last half of Phase V (after the change in parameters) were 7.0 percent for the vertical and 5.6 percent for the horizontal seismographs.

### 4.3.2 Stability of Magnification at 0.04 cps

Data from the routine calibration of the Sprengnether long-period seismographs were used in the computation of the magnification stability data at 0.04 cps. The average deviations of the magnification values from the means were 11.4 percent of the mean and 13.2 percent of the mean for the vertical and horizontal seismographs, respectively.

### 4.3.3 Phase Response of Long-Period Seismographs

The phase responses of the long-period seismographs with the free period and damping parameters used at WMSO during Phase V are shown in figure 18. The phase responses of the galvanometer and filter (both in Phototube Amplifier, Geotech Model 1452) were measured and combined with the computed phase response of the long-period seismometers in each case.

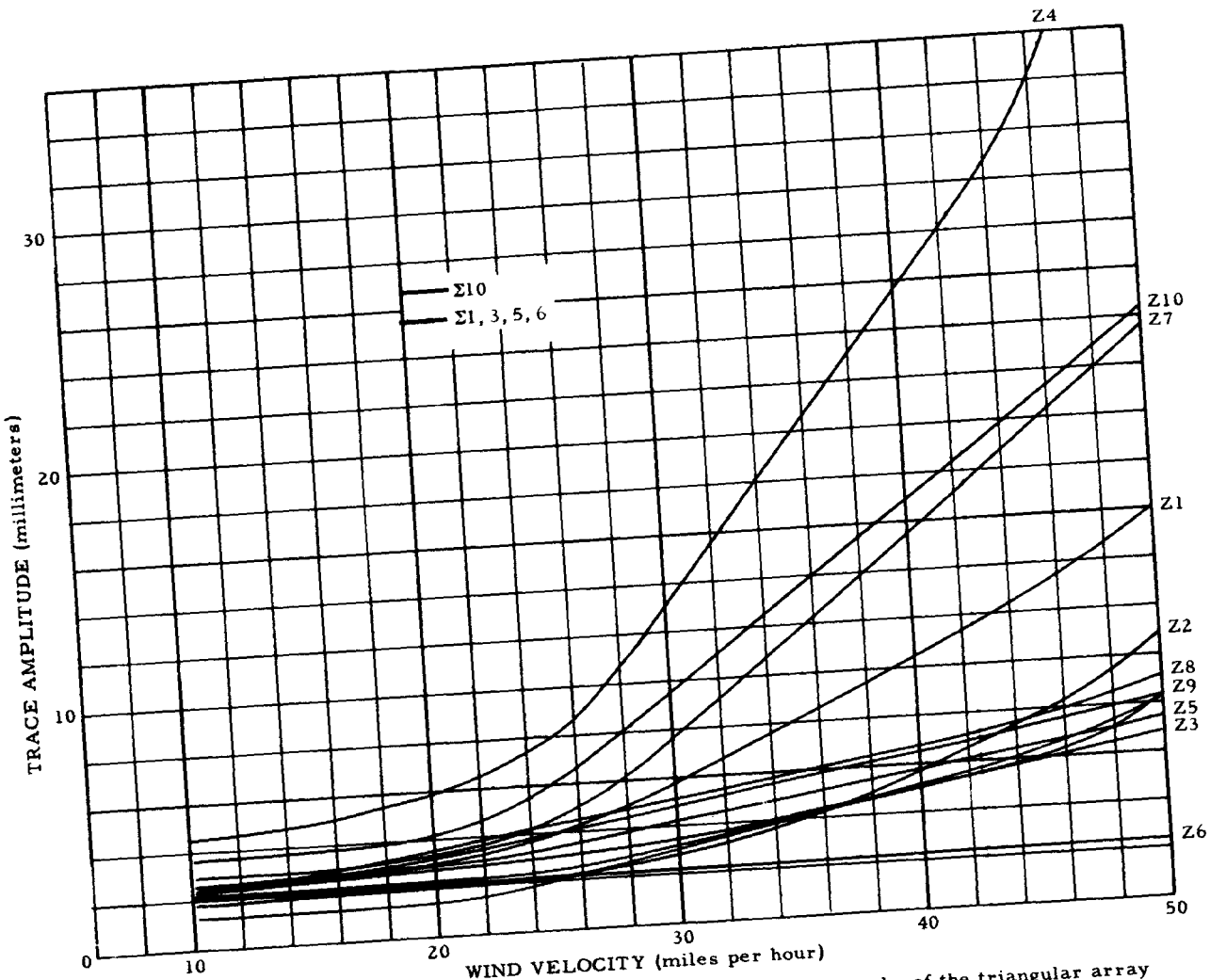


Figure 16. Wind noise as a function of wind velocity for all seismographs of the triangular array at WMSO

### 4.3.4 Electrical Noise

#### 4.3.4.1 Line Noise

Line noise on the three-component Sprengnether seismographs was not normally present at a sufficiently high level to be a problem during Phase V. The average amplitude of the line noise in the Sprengnether long-period system, measured by replacing the seismometer with a 500-ohm resistor, is approximately 40 millimicrons peak-to-peak at 25-second period, referred to equivalent seismometer input. The line noise amplitude tends to increase with increasing free period of the galvanometer in the PTA's, and was investigated in an experimental long-period system which uses 100-second galvanometers. Sources of line noise in the experimental system and methods of reducing this noise are discussed in section 7.1, "Long-Period Tripartite."

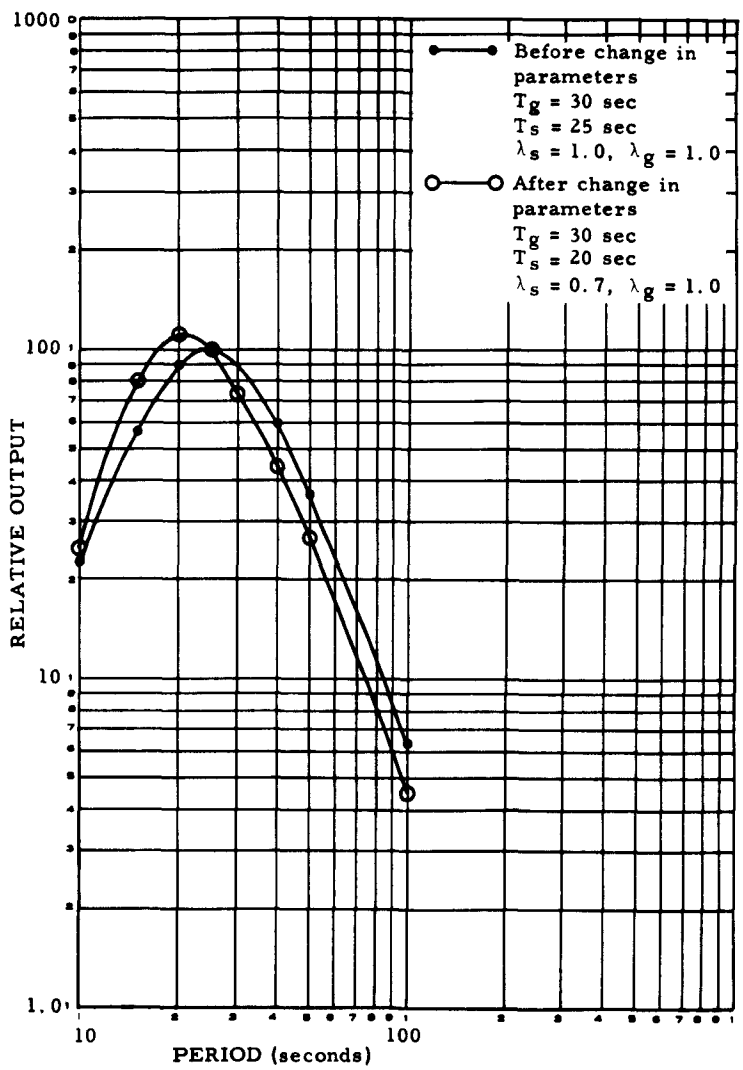


Figure 17. Average frequency response of the Sprengnether long-period seismographs at WMSO during Phase V

#### 4.3.4.2 Amplifier Noise

Long-period PTA noise was measured by recording the PTA output while

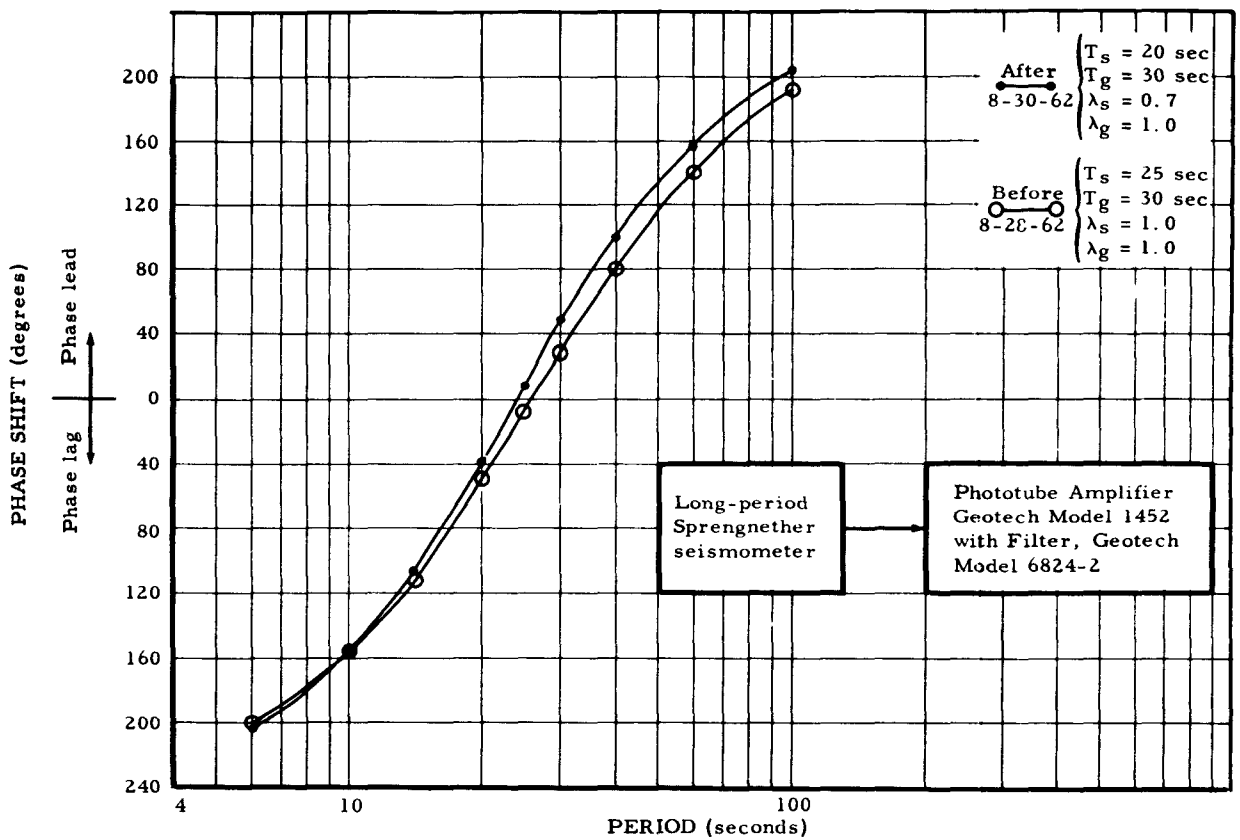


Figure 18. Phase response of the Sprengnether long-period seismographs at WMSO during Phase V. Phase shift of PTA with filter was measured; phase shift of seismometer was computed.

the input was terminated with a resistor of a value equal to the data line resistance. The average amplitude of the electrical noise originating in the amplifier is approximately 7 millimicrons peak-to-peak at about 25-second period referred to equivalent seismometer input.

### 4.3.5 Effects of Pressure Change on the Sprengnether Long-Period Seismometers

A series of tests was conducted during Phase V at WMSO, during which the response of the three-component system of Sprengnether long-period seismometers to atmospheric pressure change was evaluated. The following are conclusions, based on data obtained as a result of these tests:

a. The predominant effect of localized pressure change on the Sprengnether long-period vertical seismometer is best explained by a change in the buoyant force acting on the seismometer mass which results from the change in density of the surrounding air associated with a change in pressure.

b. Because the Sprengnether long-period vertical seismometer is not in a sealed case or sealed vault, the average noise due to localized pressure change exceeds the average background seismic noise when the average wind velocity exceeds 5 miles per hour.

c. The Sprengnether long-period horizontal seismometers respond to localized pressure change with a 90-degree phase shift as compared to the response of the vertical instrument. At a period of about 35 seconds, the horizontals respond with approximately one-tenth of the peak amplitude observed on the vertical seismogram. A possible explanation of the response of the horizontal seismometers to pressure change is that the coil and magnet assemblies act as pistons in partially closed cylinders.

### 4.3.6 Operational Changes of the Sprengnether Long-Period System

Several important operational changes were made to the Sprengnether long-period system during Phase V. The changes are listed below.

a. The free period of the seismometers was changed from 25 to 20 seconds, and the seismometer damping was changed from critical to 0.7 critical on 28 and 29 August.

b. Thin wire hinges were installed at each end of the spring on the vertical seismometer on 28 August.

c. All three seismometers were insulated with styrofoam inside and outside the seismometer covers and under the bases on 29 August.

d. The horizontal seismometers were moved from vault 7P to tank vaults at the tank farm. The move was completed on 13 December.

## 4.4 BROAD-BAND SEISMOGRAPHS

### 4.4.1 Stability of Frequency Response

During the first 10 months of Phase V, before the broad-band seismometers were moved to the tank farm from vault 8P, 5 frequency responses were measured from the three-component broad-band seismographs. Of the 5 frequency responses, 2 were run over the period range 20 to 0.156 second, and 3 were run over the period range 8.0 to 1.0 second, the primary period range of interest for the broad-band system. The average deviation of each complete response from the mean response over the period range of 20 to 0.31 second was 4.3 percent of the mean for the vertical, and 2.9 percent of the mean for the horizontals. The 3 frequency responses which were run over a smaller range of periods (8.0 to 1.0 second) had average deviations from the respective means of less than 2.0 percent.

### 4.4.2 Stability of Magnification at 1.0 cps

One hundred eighteen routine calibrations of the broad-band seismographs measured during Phase V were used for computation of the magnification stability at 1.0 cps. The average deviations of the magnifications from the mean magnification were 5.6 percent of the mean for the vertical and 7.5 percent of the mean for the horizontal seismographs.

### 4.4.3 Reliability of the Broad-Band Seismographs

The broad-band vertical and one of the broad-band horizontal seismographs were operated from the beginning of Phase V until 21 December with no malfunctions other than fuses blown by lightning or recorder outages. The other horizontal seismometer required adjustment of the coil and magnet

b. Thin wire hinges were installed at each end of the spring on the vertical seismometer on 28 August.

c. All three seismometers were insulated with styrofoam inside and outside the seismometer covers and under the bases on 29 August.

d. The horizontal seismometers were moved from vault 7P to tank vaults at the tank farm. The move was completed on 13 December.

## 4.4 BROAD-BAND SEISMOGRAPHS

### 4.4.1 Stability of Frequency Response

During the first 10 months of Phase V, before the broad-band seismometers were moved to the tank farm from vault 8P, 5 frequency responses were measured from the three-component broad-band seismographs. Of the 5 frequency responses, 2 were run over the period range 20 to 0.156 second, and 3 were run over the period range 8.0 to 1.0 second, the primary period range of interest for the broad-band system. The average deviation of each complete response from the mean response over the period range of 20 to 0.31 second was 4.3 percent of the mean for the vertical, and 2.9 percent of the mean for the horizontals. The 3 frequency responses which were run over a smaller range of periods (8.0 to 1.0 second) had average deviations from the respective means of less than 2.0 percent.

### 4.4.2 Stability of Magnification at 1.0 cps

One hundred eighteen routine calibrations of the broad-band seismographs measured during Phase V were used for computation of the magnification stability at 1.0 cps. The average deviations of the magnifications from the mean magnification were 5.6 percent of the mean for the vertical and 7.5 percent of the mean for the horizontal seismographs.

### 4.4.3 Reliability of the Broad-Band Seismographs

The broad-band vertical and one of the broad-band horizontal seismographs were operated from the beginning of Phase V until 21 December with no malfunctions other than fuses blown by lightning or recorder outages. The other horizontal seismometer required adjustment of the coil and magnet

assemblies twice to eliminate friction. The three broad-band seismometers were moved from vault 8P to tank vaults at the tank farm on 21 December.

After installation in the tank vaults, difficulty was experienced with noise on all three components during periods of large temperature variation. In addition, the instability of the temperature in the tank vault affected the mass position stability of the vertical seismometer. The mass had to be recentered on several occasions after large temperature changes caused it to drift against a stop. Vermiculite insulation was placed around and over the tank during the first week of January 1963. Subsequently, improvement in the temperature stability of the vertical seismometer has been observed.

## 4.5 INTERMEDIATE-BAND SEISMOGRAPHS

### 4.5.1 Stability of Frequency Response

The average deviation from the mean response of four frequency responses taken during Phase V was 2.5 percent of the mean for the intermediate-band vertical seismograph. The corresponding average deviation for the horizontal seismographs was 3.9 percent of the mean.

### 4.5.2 Stability of Magnification at 1.0 cps

Routine calibration data were used to determine the average deviation of magnification values from the mean magnifications. The average deviations were 2.3 percent of the mean and 4.3 percent of the mean for the vertical and horizontal seismographs, respectively.

### 4.5.3 Reliability of the Intermediate-Band Seismographs

No outages occurred on intermediate-band seismographs during Phase V other than those due to lightning damage or recorder malfunction. The intermediate-band seismometers were moved to the tank farm from vault 6P on 18 December. No recentering of the seismometer pendulums has been necessary since initial installation in the tank vaults.

## 4.6 LIGHTNING PROTECTION

### 4.6.1 History of Lightning Protection Systems Tested at WMSO

The lightning protectors that were originally installed at WMSO were Vault Protector, Geotech Model 8399, Vault Terminal, Geotech Model 8318, and Station Protector, Geotech Model 7148, installed at respective ends of the calibration lines and data lines. Back-to-back silicon diodes in the Line Termination Modules, Geotech Model 5874, connected across the PTA inputs, were used to provide additional protection for the galvanometers. This diode arrangement has not been changed since the observatory was originally installed. The diodes are of great value in protecting the galvanometers. The protection of the seismometers provided by the other protectors seemed to be adequate; however, considerable trouble was experienced with open circuits in the models 8399 and 7148 protectors. The fuse-holder assemblies in these units were redesigned and substituted for the original protectors in mid-November 1961. The frequency with which open circuits occurred in the fuse holders was greatly reduced. The redesigned protectors are the same as the original protectors except that the pressure contacts between connected parts of the fuse holders were eliminated. Each channel of these protectors incorporates a 0.005-inch carbon gap from each side of the circuit to ground.

These protectors were satisfactory for the Benioff seismometers, but after installation of the JM seismometers, several seismometers were damaged during lightning storms. The minimum gap between the JM coil and the magnet pole pieces can be less than that at the carbon blocks, especially since small metal particles may sometimes partially bridge the gap in the seismometer.

In order to improve the lightning protection system for the JM seismometers, the following investigations were made:

a. Two silicon diodes of opposite polarity were connected from each of the signal circuits to ground so that, when the potential of the signal circuit exceeded approximately 0.6 volt above or below ground, the diodes would conduct the transients to ground. Use of these units resulted in spiking on the signal traces due to differences between the static potentials on the line and the ground at the diodes.

b. Zener diodes, Thyrecters (zener-type devices), and silicon-controlled rectifiers with firing circuits were connected in a manner similar to that outlined in paragraph a. These units failed when lightning caused high-voltage transients. They did not cause spiking; however, they failed to provide adequate protection for the seismometers.

c. Tests were made to determine the voltage level of the transients caused by electrical storms. Amplitudes greater than 1600 volts were measured across carbon gaps which were theoretically limited to about 750 volts.

d. A passive protection system that required isolation of the transducer from ground was devised. Glass plates were placed between the feet of the seismometers and the vault floors. The seismometer cases at four of the vaults were then connected to each of the signal conductors by a pair of back-to-back diodes. Five ampere fuses and 0.004-inch carbon gaps were used in the protectors. At the other six vaults, the seismometer cases were insulated from ground but no diodes were used. The shields of the data and calibration cables, and the ground side of the carbon gaps in the protectors were connected to the grounded tanks and not connected to the seismometers.

### 4.6.2 Preliminary Evaluation of Present Lightning Protection System at WMSO

Lightning damaged JM seismometers in the triangular array three times during May and June 1962 before glass plates were installed beneath the seismometer feet. There has been no lightning damage to seismometers since glass plates have been used to isolate them from ground. However, lightning storms have been less severe and less frequent since the glass plates were installed. There is a strong indication, however, that merely ungrounding the seismometer provides a greater degree of protection from lightning damage than the other methods that have been utilized. The 10-kilometer linear array (section 3.6) utilizes 7 JM seismometers not housed in tank vaults and directly buried in the earth. Of these 7 seismometers of the linear array, one has been damaged by lightning since the other JM seismometers were put on glass plates.

### 4.6.3 Summary of Lightning Damage at WMSO during Phase V Compared to Damage During other Phases

During Phase V, 43 lightning storms occurred at WMSO; 38 lightning storms occurred during Phase III. The distribution of storms during the year was similar for both phases. Figure 19 is a graph of the frequency of occurrence

of electrical storms at WMSO during Phase V. No tabulation of the actual minor damage (blown fuses, etc.) due to lightning was made during Phase III, and lightning caused no major damage to instruments during Phase III. Outages caused by electrical storms during Phase V are tabulated in table 5. The increased incidence of seismometer damage during Phase V is primarily due to the following:

a. Improved protection for the JM seismometers was not developed until after the period of storms of greatest severity was over.

b. The lightning storms which occurred during Phase V were of greater apparent intensity than those that occurred during Phase III.

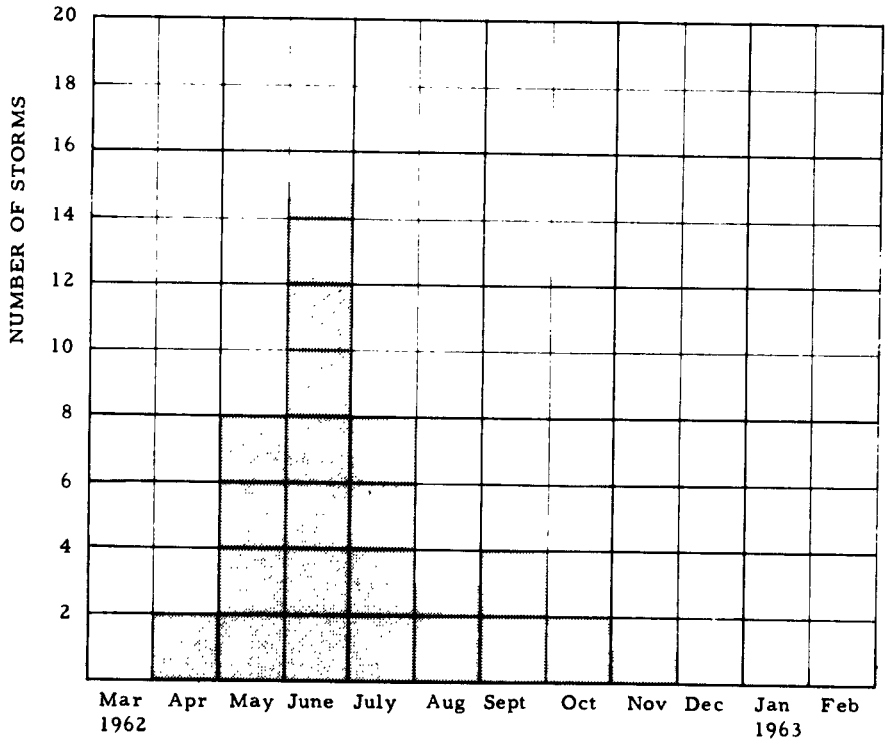


Figure 19. Frequency of occurrence of electrical storms at WMSO during Phase V

Table 5. Outages due to Electrical Storms

| Component | 1962 M | A | M | J | J | A | S | O | N | D | 1963 J | F |
|---|---|---|---|---|---|---|---|---|---|---|---|---|
| Z1 | | 1 | 6 | 6 | 1 | 1 | 1 | 2 | | | | |
| Z2 | | 1 | | 4 | 1 | 1 | | 2 | | | | |
| Z3 | | 1 | 1 | 4 | 3 | 1 | | 2 | | | | |
| Z4 & L4 | | 2 | 3 | 3 | | 1 | 2 | 1 | | | | |
| Z5 & L5 | | 1 | 4 | 3 | | 1 | 1 | | | | | |
| Z6 & L6 | | | 2 | 2 | | 1 | 1 | 2 | | | | |
| Z7 & L7 | | 1 | 6 | 8s | 4 | 1 | | | | | | |
| Z8 | | | 2 | 2s | | 1 | | | | | | |
| Z9 | | 2 | 2 | 6 | 3 | 1 | 1 | 1 | | | | |
| Z10 | | 2 | 4 | 2 | | 1 | | 1 | | | | |
| SP N-S | | | 1 | 3 | | 1 | | 1 | | | | |
| SP E-W | No damage | | 1 | 3 | | 1 | | 1 | No damage | | | |
| LPV Spr | | | | 1 | | 1 | | | No damage | | | |
| LP N-S Spr | | | | 1 | | 1 | | | No damage | | | |
| LP E-W Spr | | | 2 | 2 | | 1 | | | | | | |
| IBV | | | | 1 | | 1 | | | | | | |
| IB N-S | | | | 1 | | 1 | 1 | 1 | | | | |
| IB E-W | | | | 2 | | 1 | | | | | | |
| BBV | | | | 1 | | 1 | | 2 | | | | |
| BB N-S | | | 1 | 3 | 1 | 1 | | | | | | |
| BB E-W | | | | 2 | | 1 | | 2g | | | | |
| TR V1 | | | 1 | | | 1 | | | | | | |
| TR V2 | | | 1 | 2 | | 1 | | | | | | |
| TR V3 | | | | | | 1 | | | | | | |
| EP Benioff | | | | | | | | | | | | |

| Component | 1962 M | A | M | J | J | A | S | O | N | D | 1963 J | F |
|---|---|---|---|---|---|---|---|---|---|---|---|---|
| L0 | Operation began 18 May | | 4 | 5s | 2s | 3g | 1 | Operation stopped 08 Oct | | | | |
| L1 | | | 2 | 5s | 1 | 2 | | | | | | |
| L2 | | | 2 | 3s | | 2 | | | | | | |
| L3 | | | 1 | 4 | 2g | 2 | | | | | | |
| L8 | | | 1 | 7 | | 1 | | | | | | |
| L9 | | | 1 | 6 | 1 | 1 | | | | | | |
| L10 | | | 1 | 5 | | 1 | | | | | | |
| Benioff #1 | | | | | | | | 1 | | | | |
| Benioff #2 | | | | | | | | 1 | | | | |
| Benioff #3 | | | | | | | | 1 | | | | |
| Benioff #4 | | | | | | | | 1 | | | | |
| Benioff #5 | No damage | | | | | | | | No damage | | | |
| Benioff #6 | | | | | | | | | No damage | | | |
| Benioff #7 | | | | | | | | | No damage | | | |
| Benioff #8 | | | | | | | | | No damage | | | |
| Benioff #9 | | | | | | | | 1 | | | | |
| Benioff #10 | | | | | | | | 1 | | | | |
| M-H tape | Operated 07-14 May | | 1 | 2 | | 1 | | | | | | |
| Ampex tape | | | | 1 | | 1 | | | | | | |
| Microbarograph | | | | | 1 | 1 | | | | | | |
| LP tank Geotech | | | | | | 1 | 1 | 1 | | | | |
| LP #8 Geotech | | | | | | 1 | 1 | 1 | | | | |
| LP #5 Geotech | | | | | | 1 | 1 | 1 | | | | |
| JM 20 | | | | | | 1 | | 2 | | | | |

Operation began 10 Oct

s - seismometer damaged  g - galvanometer damaged

Power lost to PTA room during one storm in June

## 4.6 LIGHTNING PROTECTION

### 4.6.1 History of Lightning Protection Systems Tested at WMSO

The lightning protectors that were originally installed at WMSO were Vault Protector, Geotech Model 8399, Vault Terminal, Geotech Model 8318, and Station Protector, Geotech Model 7148, installed at respective ends of the calibration lines and data lines. Back-to-back silicon diodes in the Line Termination Modules, Geotech Model 5874, connected across the PTA inputs, were used to provide additional protection for the galvanometers. This diode arrangement has not been changed since the observatory was originally installed. The diodes are of great value in protecting the galvanometers. The protection of the seismometers provided by the other protectors seemed to be adequate; however, considerable trouble was experienced with open circuits in the models 8399 and 7148 protectors. The fuse-holder assemblies in these units were redesigned and substituted for the original protectors in mid-November 1961. The frequency with which open circuits occurred in the fuse holders was greatly reduced. The redesigned protectors are the same as the original protectors except that the pressure contacts between connected parts of the fuse holders were eliminated. Each channel of these protectors incorporates a 0.005-inch carbon gap from each side of the circuit to ground.

These protectors were satisfactory for the Benioff seismometers, but after installation of the JM seismometers, several seismometers were damaged during lightning storms. The minimum gap between the JM coil and the magnet pole pieces can be less than that at the carbon blocks, especially since small metal particles may sometimes partially bridge the gap in the seismometer.

In order to improve the lightning protection system for the JM seismometers, the following investigations were made:

a. Two silicon diodes of opposite polarity were connected from each of the signal circuits to ground so that, when the potential of the signal circuit exceeded approximately 0.6 volt above or below ground, the diodes would conduct the transients to ground. Use of these units resulted in spiking on the signal traces due to differences between the static potentials on the line and the ground at the diodes.

b. Zener diodes, Thyrecters (zener-type devices), and silicon-controlled rectifiers with firing circuits were connected in a manner similar to that outlined in paragraph a. These units failed when lightning caused high-voltage transients. They did not cause spiking; however, they failed to provide adequate protection for the seismometers.

c. Tests were made to determine the voltage level of the transients caused by electrical storms. Amplitudes greater than 1600 volts were measured across carbon gaps which were theoretically limited to about 750 volts.

d. A passive protection system that required isolation of the transducer from ground was devised. Glass plates were placed between the feet of the seismometers and the vault floors. The seismometer cases at four of the vaults were then connected to each of the signal conductors by a pair of back-to-back diodes. Five ampere fuses and 0.004-inch carbon gaps were used in the protectors. At the other six vaults, the seismometer cases were insulated from ground but no diodes were used. The shields of the data and calibration cables, and the ground side of the carbon gaps in the protectors were connected to the grounded tanks and not connected to the seismometers.

### 4.6.2 Preliminary Evaluation of Present Lightning Protection System at WMSO

Lightning damaged JM seismometers in the triangular array three times during May and June 1962 before glass plates were installed beneath the seismometer feet. There has been no lightning damage to seismometers since glass plates have been used to isolate them from ground. However, lightning storms have been less severe and less frequent since the glass plates were installed. There is a strong indication, however, that merely ungrounding the seismometer provides a greater degree of protection from lightning damage than the other methods that have been utilized. The 10-kilometer linear array (section 3.6) utilizes 7 JM seismometers not housed in tank vaults and directly buried in the earth. Of these 7 seismometers of the linear array, one has been damaged by lightning since the other JM seismometers were put on glass plates.

### 4.6.3 Summary of Lightning Damage at WMSO during Phase V Compared to Damage During other Phases

During Phase V, 43 lightning storms occurred at WMSO; 38 lightning storms occurred during Phase III. The distribution of storms during the year was similar for both phases. Figure 19 is a graph of the frequency of occurrence

of electrical storms at WMSO during Phase V. No tabulation of the actual minor damage (blown fuses, etc.) due to lightning was made during Phase III, and lightning caused no major damage to instruments during Phase III. Outages caused by electrical storms during Phase V are tabulated in table 5. The increased incidence of seismometer damage during Phase V is primarily due to the following:

a. Improved protection for the JM seismometers was not developed until after the period of storms of greatest severity was over.

b. The lightning storms which occurred during Phase V were of greater apparent intensity than those that occurred during Phase III.

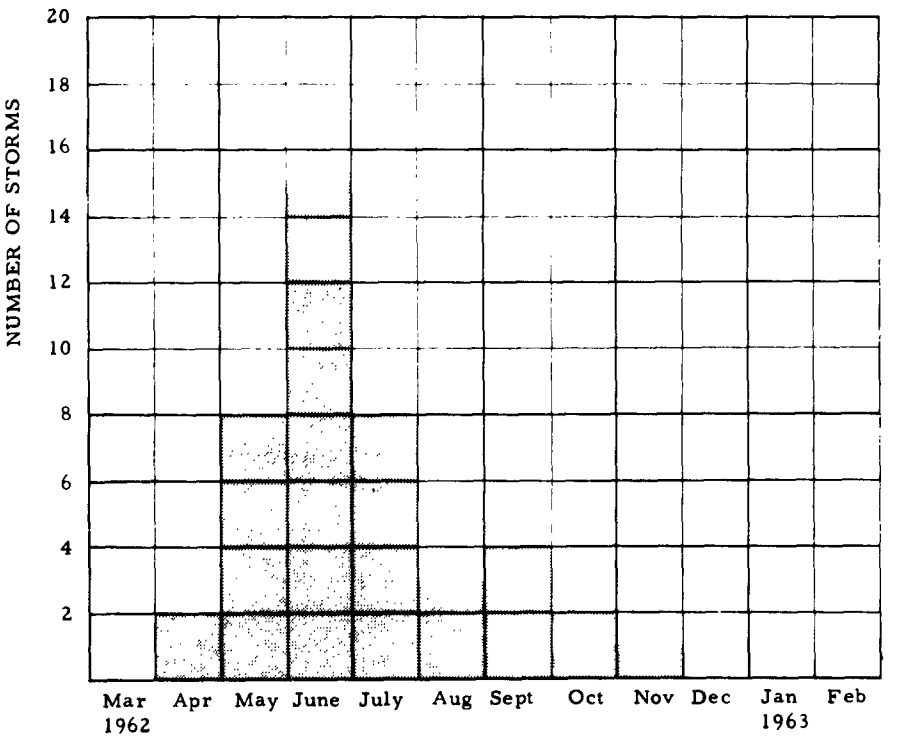


Figure 19. Frequency of occurrence of electrical storms at WMSO during Phase V

Table 5. Outages due to Electrical Storms

| Component | 1962 M | A | M | J | J | A | S | O | N | D | 1963 J | F |
|---|---|---|---|---|---|---|---|---|---|---|---|---|
| Z1 | | 1 | 6 | 6 | 1 | 1 | 1 | 2 | | | | |
| Z2 | | 1 | | 4 | 1 | 1 | | 2 | | | | |
| Z3 | | 1 | 1 | 4 | 3 | 1 | | 2 | | | | |
| Z4 & L4 | | 2 | 3 | 3 | | 1 | 2 | 1 | | | | |
| Z5 & L5 | | 1 | 4 | 3 | | 1 | 1 | | | | | |
| Z6 & L6 | | | 2 | 2 | | 1 | 1 | 2 | | | | |
| Z7 & L7 | | 1 | 6 | 8s | 4 | 1 | | | | | | |
| Z8 | | | 2 | 2s | | 1 | | | | | | |
| Z9 | | 2 | 2 | 6 | 3 | 1 | 1 | 1 | | | | |
| Z10 | | 2 | 4 | 2 | | 1 | | 1 | | | | |
| SP N-S | | | 1 | 3 | | 1 | | 1 | | | | |
| SP E-W | No damage | | 1 | 3 | | 1 | | 1 | No damage | | | |
| LPV Spr | | | | 1 | | 1 | | | No damage | | | |
| LP N-S Spr | | | | 1 | | 1 | | | No damage | | | |
| LP E-W Spr | | | 2 | 2 | | 1 | | | No damage | | | |
| IBV | | | | 1 | | 1 | | | | | | |
| IB N-S | | | | 1 | | 1 | 1 | 1 | | | | |
| IB E-W | | | | 2 | | 1 | | | | | | |
| BBV | | | | 1 | | 1 | | 2 | | | | |
| BB N-S | | | 1 | 3 | 1 | 1 | | | | | | |
| BB E-W | | | | 2 | | 1 | | 2g | | | | |
| TR V1 | | | 1 | | | 1 | | | | | | |
| TR V2 | | | 1 | 2 | | 1 | | | | | | |
| TR V3 | | | | | | 1 | | | | | | |
| EP Benioff | | | | | | | | | | | | |

| Component | 1962 M | A | M | J | J | A | S | O | N | D | 1963 J | F |
|---|---|---|---|---|---|---|---|---|---|---|---|---|
| L0 | | | 4 | 5s | 2s | 3g | 1 | | | | | |
| L1 | | | 2 | 5s | 1 | 2 | | | | | | |
| L2 | | | 2 | 3s | | 2 | | | | | | |
| L3 | | | 1 | 4 | 2g | 2 | | | | | | |
| L8 | | | 1 | 7 | | 1 | | | | | | |
| L9 | | | 1 | 6 | 1 | 1 | | | | | | |
| L10 | | | 1 | 5 | | 1 | | | | | | |
| Benioff #1 | | | | | | | | 1 | | | | |
| Benioff #2 | | | | | | | | 1 | | | | |
| Benioff #3 | | | | | | | | 1 | | | | |
| Benioff #4 | | | | | | | | 1 | | | | |
| Benioff #5 | No damage | | | | | | | | No damage | | | |
| Benioff #6 | | | | | | | | | No damage | | | |
| Benioff #7 | | | | | | | | | No damage | | | |
| Benioff #8 | | | | | | | | | No damage | | | |
| Benioff #9 | | | | | | | | 1 | | | | |
| Benioff #10 | | | | | | | | 1 | | | | |
| M-H tape | | | 1 | 2 | | 1 | | | | | | |
| Ampex tape | | | | 1 | | 1 | | | | | | |
| Microbarograph | | | | | 1 | 1 | | | | | | |
| LP tank Geotech | | | | | | 1 | 1 | 1 | | | | |
| LP #8 Geotech | | | | | | 1 | 1 | 1 | | | | |
| LP #5 Geotech | | | | | | 1 | 1 | 1 | | | | |
| JM 20 | | | | | | 1 | | 2 | | | | |

Operation began 18 May — Operated 07-14 May — Operation began 10 Oct — Operation stopped 08 Oct

s - seismometer damaged  g - galvanometer damaged

Power lost to PTA room during one storm in June

## 4.7 DATA CONTROL AND RECORDING

### 4.7.1 Data Control

Transformer-type signal isolators (Geotech Model 6722A) were used in the short-period, broad-band, and intermediate-band seismograph systems during all of Phase V. The advantages of the transformer-type signal isolators are as follows:

a. An input-to-output impedance ratio of 625 to 1.0 (10,000 ohms to 16 ohms) is obtained with an input-to-output voltage ratio of approximately 25 to 1.0. A resistive network with the same impedance ratio would have an input-to-output voltage ratio of 626 to 1.0. The output impedance determines the number of recording galvanometers which can be driven without interaction. The transformers provide 25 times more current to each recording galvanometer circuit than would a resistive impedance matching circuit for any given output impedance.

b. While the transformers have flat frequency response characteristics down to approximately 0.1 cps, they do not transmit direct current, and therefore, eliminate dc drift from the seismograms. This generally improves the appearance of the seismograms without affecting the frequency response of the seismographs over the frequency band of interest.

The signal isolators were found to be linear within the accuracy of measurement (about ±1.0 percent) for amplitudes ranging from 50 millimicrons at 1 cps to the clipping levels of the short-period PTA's. Comparison of traces recorded from the input and output of the signal isolators has revealed no discernible difference.

In general, the performance of the signal isolator has been reliable, and no operational difficulties have been encountered in its use. A desirable addition to the signal isolator would be gain-trim circuits for each individual channel input circuit. This would make equalization of gains in the summations a more straightforward procedure.

### 4.7.2 Recording

The routine assignments of data to the short-period Develocorders and the Ampex tape recorder were interrupted early in Phase V at the request of the Project Officer. Since this interruption, the short-period Develocorder which

is normally on standby operation has been used for special tests. The 10-kilometer linear array was recorded on the standby Develocorder and on the Ampex tape recorder from 18 May to 8 October 1962. The Ampex tape recorder was immediately returned to the routine assignments, but the standby Develocorder was used to record the H array of 10 Benioff seismometers. The 10 kilometer linear array was reinstalled in January 1963, and linear-array data were recorded on the Ampex tape recorder and the standby Develocorder beginning 7 February. Essentially continuous use of all Develocorders made it difficult to perform the preventive maintenance necessary to ensure complete reliability of operation. Excessive heat in the central-recording building during part of the summer, due to air-conditioner failures, further descreased the operating reliability of the Develocorders.

The two tape recorders at WMSO had few outages due to recorder malfunctions because preventive maintenance was effective.

Table 3 shows the channel assignments for the Develocorders and magnetic-tape recorders.

## 4.8 CALIBRATION

### 4.8.1 Stability of Calibration Actuators

There was no indication of any large changes in the motor constants of the calibration actuators of any of the seismometers except when some of the instruments were dismantled for repair, cleaning, or change of location. The stability of most of the calibration actuators could not be measured precisely, because the meters used to determine motor constants during the early part of Phase V were not available, or were out of calibration later, when motor constants were checked. In most cases, the error of measurement for comparison purposes was less than ±6 percent. More accurate data on the stability of the calibration actuators will be available later because a higher range has been added to the meter circuit of the model 2520 calibration control unit. With this X200 range, the calibration control can be used to measure the motor constants of the JM seismometer calibration actuators. Additional modifications on the low range of the meter circuit will permit more accurate measurement of low values of current. These modifications are discussed in greater detail in the following section.

### 4.8.2 Calibration Control Unit Problems and Remedies

The Calibration Control Unit, Geotech Model 2520, has performed reliably since the installation of WMSO. The meter damping is such that current values may be read at 1.0 cps; that is, the meter sensitivity is the same for current at 1.0 cps as for direct current. However, calibration recordings and linearity tests made near the end of Phase V indicated a 7 percent discrepancy in the delivered calibration current, depending on the setting of the meter range switch on the calibration control unit. Tests were made to determine the source of this discrepancy. At the X1 range switch position, the meter damping changed from the proper value to a value which produced a meter reading that was 8 percent higher than the actual current. At the same time, an increase in the impedance of the meter at 1.0 cps reduced the current flowing in the average calibration circuit just enough to prevent a chang' in the meter reading when the range switch was moved from a higher setting to the X1 position. The meter circuit was modified to provide the correct meter damping at all settings of the range switch. A provision was also made for switching a high resistance into the calibration circuit for use with the X1 and X5 switch positions to prevent change of calibration current when different line resistances are switched into the circuit. Additional tests on the modified calibration control unit indicated that readings were correct within 2 percent at all range switch positions.

The calibration control unit was also modified to provide a high meter range (X200) which could be used to make the current measurements needed to determine the motor constant of the JM seismometer calibration actuators. With the X200 meter range on the calibration control unit, no other external meter is needed.

### 4.8.3 Reliability of Calibration Circuits

The major source of trouble in the calibration circuits early in Phase V was intermittently faulty switches in the calibration switching unit. These switches were replaced with switches of another type in July 1962. Since the switches were replaced, the only malfunctions which have occurred in the calibration circuits were caused by lightning.

## 4.9 TIMING

### 4.9.1 Primary Timing

The primary timing system operated about 98 percent of the total time in Phase V. The principal cause of primary time outage was failure of the frequency-regulated power. The average time correction on the short-period recordings during Phase V was 42 milliseconds.

A Time Encoder, Geotech Model 13159, was installed on 18 December. The time encoder provides date and time information in binary code for the two magnetic-tape recorders. Figure 20 shows a playback of a recording of the output of the time encoder. No indication of unsatisfactory performance of the time encoder has been observed. It is, however, dependent on the continuity of voltage-regulated power as well as frequency-regulated power.

### 4.9.2 Secondary Timing

The secondary timing system (synchronome clock) had no malfunctions during Phase V. Average drift was about 200 milliseconds per day. Secondary timing was in use approximately 2 percent of the total time during Phase V.

## 4.10 POWER CIRCUITS

### 4.10.1 Commercial Power

Commercial power was available at WMSO 99.86 percent of the time during Phase V, with outage never exceeding four hours at any one time. Commercial power capability was increased at WMSO on 14 August from 25 to 40 kilovolt-amperes by the installation of larger transformers in the power line. The work was done without charge by the Cotton Electric Cooperative, the commercial power supplier.

### 4.10.2 Emergency Power

Emergency power, provided by 18 Nicad cells and a 500-volt-ampere rotary converter, was adequate for maintaining continuity of Develocorder recording during all commercial-power outages during Phase V.

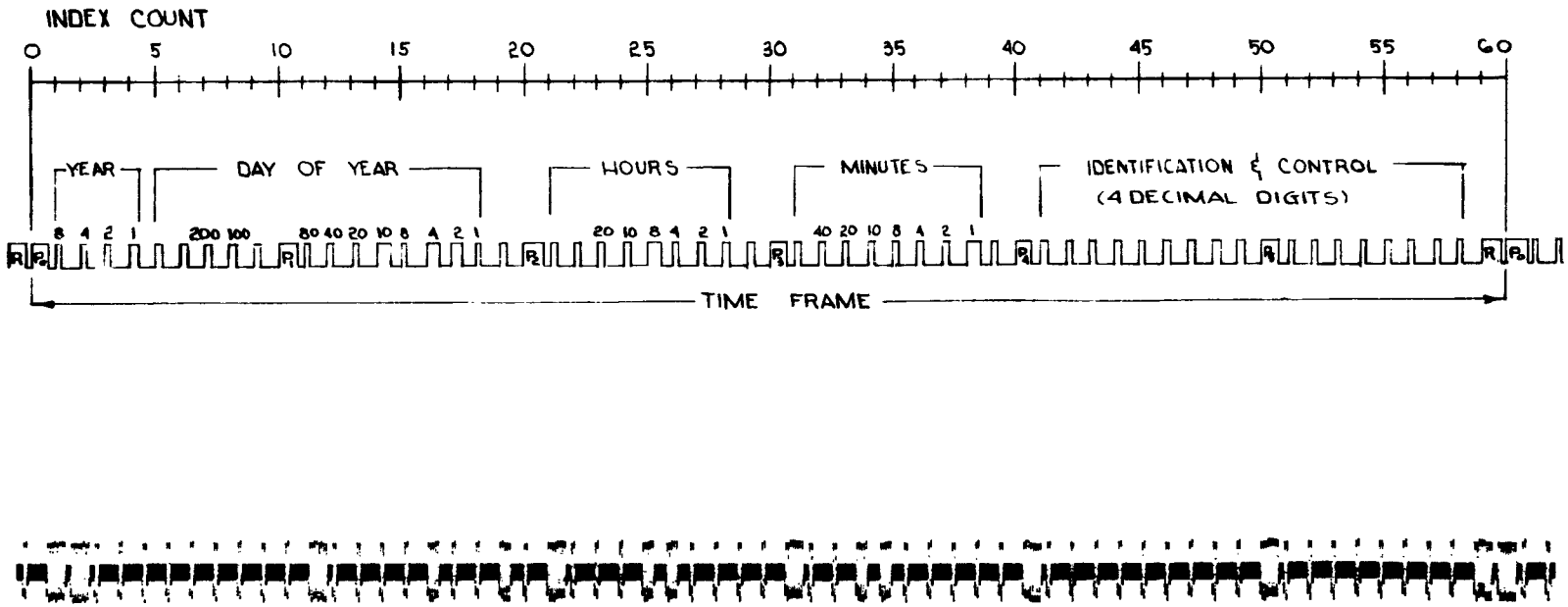


Figure 20. Playback of the recording of the output of the Time Encoder, Geotech Model 13159, from the Minneapolis-Honeywell magnetic-tape recorder at WMSO. Time recorded is: day of year 009, hour 18:00Z, minutes 30.

### 4.10.3 Power Failure of 25 December 1962

A power outage at WMSO on 25 December 1962 lasted approximately 6 hours and was caused by a short circuit in Develocorder No. 4. The initial short apparently occurred between the red wire in a power harness and the tip of the screw located in the lower-right corner of the lower front panel. This overheated the wire connected to pin A of J5 causing it to short to the adjacent grounded wire from pin C of J5. The ungrounded side of the voltage-regulated power was connected to pin A of J5 rather than to pin B, and therefore, was not protected by the fuse which is connected to pin B.

As a result of this short circuit, one of the armature wires of relay K2 in the Power Control Unit, Model 7679, burned in two. When emergency power was switched on, one of the fuses in the inverter-input circuit burned out. Then one of the 2N629 transistors in the frequency-regulated power amplifier burned out, apparently due to the dc voltage surges at the input.

The voltage-regulated power connections to all Develocorders were reversed to prevent a recurrence of this type of power failure.

### 4.10.4 Frequency-Regulated Power

Frequency-regulated power was obtained from a 60-volt-ampere Power Amplifier, Geotech Model 7894, driven by the 5400 timing system. The amplifier was required to operate with a heavier load than the specified maximum of 60 watts during a portion of Phase V. Frequency-regulated power was available about 96 percent of the time during Phase V. Approximately one-fourth of the outage time was due to air-conditioner failures during the summer. Steps are being taken to increase the amount of available frequency-regulated power, and also to improve the overall reliability of the timing system.

# 5. ROUTINE ANALYSIS AND ANALYSIS EVALUATION

## 5.1 INTRODUCTION

WMSO records seismometric data on a continuous basis. The accumulated data are routinely analyzed, the analysis checked, and a tabulation of initial arrival times of earthquake signals is transmitted to the United States Coast and Geodetic Survey (USC&GS) daily. Analysis data are finalized when the USC&GS' Preliminary Determination of Epicenter (PDE) cards are received and the monthly bulletin, Registration of Earthquakes at WMSO, is prepared from these finalized data. The data recorded at WMSO are also used in making system evaluations and in conducting special studies and research projects (e.g., magnitude study, section 6.1.3).

## 5.2 PROCEDURES

### 5.2.1 Preliminary Analysis

Seismograms recorded at WMSO are periodically studied during each 24-hour period. Preliminary analysis is done at the Develocorders, and is recorded on work sheets, as shown in figure 21. These sheets are used to compile data for use in statistical analyses such as ground motion and magnitude.

### 5.2.2 Checking of Analysis

The seismograms are reviewed by a second analyst who checks the arrival times recorded on the work sheets, and studies the seismograms for events which the first analyst might have overlooked. After verification of the preliminary analysis, the appropriate data are transmitted to the USC&GS.

### 5.2.3 Daily Report to USC&GS

Arrival times of events recorded at WMSO are reported daily to the Director of the United States Coast and Geodetic Survey in Washington, D. C. Prior to 30 October, an information copy of the report was also supplied to Headquarters, AFTAC/TD-1 in Washington, D. C., but this was discontinued at the request of the Project Officer. The report is transmitted by teletype via the GSA operator in Oklahoma City, Oklahoma, except on weekends and holidays, when it is transmitted via commercial telegraph.

Record No. 355 Date 21 Dec 62

| System | Phase | Time | Z | Z | N | E | Per. | Dir. | Type | Δ | Remarks |
|---|---|---|---|---|---|---|---|---|---|---|---|
| | | G.C.T. | mm X10 | mμ | mm X10 | mm X10 | | | | deg | |
| SP | eP | 00 07 05.3 | 06.0 | | | | 0.3 | NE | L | | |
| SP | eS | 08.6 | LG2.5 04.0 | | | | 0.7 | | | | |
| SP | eP | 01 03 40.5 | 17.0 | | | | 1.2 | NW | T | | |
| LP | ✓ | | | | | | | | | | |
| SP | e | 48.5 | LG5 04.5 | | | | 1.0 | | | | |
| SP | e | 05 43.7 | 15.0 | | | | 1.3 | | | | |
| SP | ePP | 06 50.8 | 12.0 | | | | 1.3 | PP | | 82° | Possibly OFF COAST OF HOKKAIDO, JAPAN |
| LP | ✓ | | | | | | | | | | |
| | e | 07 19.0 | 12.0 | | | | 1.3 | | | | |
| LPE | e | 13 46 | | | | 10.0 | 20.0 | | | | |
| SP | eP | C 1 15 14.6 | 03.5 | | | | 1.0 | | | | Possible PKKP D = 108° - 109° |
| SP | e | 38.4 | 09.0 | | | | 1.6 | SE | | | |
| SP | e | 16 00.2 | 06.0 | | | | 2.0 | | | | |
| LP | e | 58 | 12.0 | | | | 22.0 | | | | |

Form WMSO-2, 6 Dec 1960

Sheet 1 of 11

Figure 21. Sample WMSO preliminary analysis sheet

Data reported are phase, day, hour, minute, seconds, and tenth of second for each P phase. For locals and near-regionals of magnitude 4 or greater, both P and S arrivals are reported. The depth phase, pP, of teleseismic events is reported as AP when it can be reliably identified. An average of 12 arrival times were reported per message, during Phase V.

A sample page of the data report sent to USC&GS is shown in figure 22.

### 5.2.4 Final Analysis - Epicenter and Phase Association

The final analysis of recorded data depends on receipt of the USC&GS' PDE cards. By making use of the epicentral locations, origin times, and focal depths listed on the cards, many phase arrivals recorded at WMSO can be associated. Periods, amplitudes, and starting times are re-examined. The discrepancy between actual arrival times and predicted arrival times of identified phases is recorded at this time.

### 5.2.5 Report on Registration of Earthquakes

The finalized data on the work sheets are transcribed onto data forms for use in publishing WMSO's monthly Report on the Registration of Earthquakes. A sample of a typical page from the report is shown in figure 23.

Earthquake magnitudes have been computed and reported since June 1962 for all earthquakes located by the USC&GS, and for which sufficient data were recorded by WMSO.

OUTGOING MESSAGE - WMSO

FROM: Cache, Oklahoma 405-429-3706

To: Director Coast and Geodetic Survey
Washington, D.C.

SEISMO WMSO

EP 27 00 17 363

EP 04 29 019

EP 04 45 387

EP 04 48 331

EP 07 47 073

EP 11 10 043

EP 12 42 151

EP 16 05 171

EP 18 20 323

EP 19 31 113

EP 21 19 379

EP 23 09 388

EP 23 44 546

Analyst REAGOR Date time group 28 02 63 16557 Msg. No. 0058

Operator GARRETT

Released by STANFILL Checked by STANFILL

Form WMSO 16
Rev 1-10-63

Figure 22. Sample page of WMSO's daily report to USC&GS

| DATE | Syst. | Phase | Arrival Time G.C.T. h. | m. | s. | Ground Motion A | T | Dir. | Type | Magnitude m | M | Remarks |
|---|---|---|---|---|---|---|---|---|---|---|---|---|
| 1962 | | | | | | | | | | | | |
| 28 Oct | | iP | 22 | 57 | 17.8 c | 159 | 0.6 | | T | 5.5 | | Chiapas, Mexico |
| | | e | | | 45.3 | | 1.1 | | | | | 16.0 N 93.6 W |
| | | e | | 58 | 14.9 | | 1.2 | | | | | h about 110 km |
| | LPN | e | | | 36 | | 14.0 | | | | | O = 22 53 01.3 |
| | | eSur | 23 | 00 | 43.3 | | 1.0 | | | | | $\Delta = 19^{o}$ |
| | | e | | 01 | 11.6 | | 1.3 | | | | | Strong surface waves |
| | | e | | | 25.4 | | 1.1 | | | | | on all systems |
| | | ePcP | | | 40.6 | | 0.9 | | | | | |
| | LPN | eSur | | 02 | 14 | | | | | | | |
| 29 Oct | | eP | 00 | 25 | 57.9 | 44 | 0.9 | | T | 5.4 | | Off south coast of Panama |
| | | ePP | | 26 | 57.2 | | 1.3 | | | | | 7.1 N 82.6 W |
| | | e | | 27 | 46.2 | | 1.2 | | | | | h about 21 km |
| | | e | | 28 | 18.3 | | 1.3 | | | | | O = 00 10 39.7 |
| | | ePcP | | | 53.5 | | 0.8 | | | | | $\Delta = 31^{o}$ |
| | LPE | e | | 32 | 02 | | 11.0 | | | | | Medium surface waves |
| | E | ePcS | | | 37.2 | | 1.1 | | | | | on LP |
| | LPN | e | | 34 | 25 | | | | | | | |
| 29 Oct | | eP | 02 | 46 | 28.2 | 28 | 1.7 | | R | 5.1 | | Mag. 4 3/4-5 (PS) |
| | | e | | | 35.0 | | 1.5 | | | | | San Bernadino County, |
| | | e | | | 44.3 | | 1.6 | | | | | California |
| | | e | | 47 | 24.0 | | 1.7 | | | | | 34.3 N 117.0 W |
| | | e | | | 35.4 | | 1.3 | | | | | h about 33 km |
| | E | e | | 48 | 37.0 | | 1.7 | | | | | O = 02 42 56.1 |
| | | e | | | 45.4 | | 1.4 | | | | | $\Delta = 15^{o}$ |
| | E | e | | | 53.5 | | 1.7 | | | | | Strong surface waves on |
| | | e(S) | | 49 | 13.5 | | 1.7 | | | | | all systems |
| | | eSur | | 50 | 38.8 | 999 | | | | | | |
| 29 Oct | | eP | 07 | 36 | 27.6 | 2 | 1.0 | | T | | | |
| 29 Oct | | eP | 07 | 37 | 01.8 | 10 | 0.9 | NNW | T | | | Medium surface waves |
| | LPE | eSur | 08 | 17 | 51 | | | | | | | on LP |
| | LPN | eSur | | 24 | 06 | | | | | | | |
| 29 Oct | | eP | 09 | 42 | 15.6 | 29 | 1.4 | | T | 5.1 | | Central Chile |
| | | e | | | 26.1 | | 1.3 | | | | | 33.9 S 70.7 W |
| | | e | | | 33.6 | | 1.0 | | | | | h about 33 km |
| | | | | | | | | | | | | O = 09 30 48.2 |
| | | | | | | | | | | | | $\Delta = 73^{o}$ |



**Figure 23. Sample page from WMSO's monthly Report on the Registration of Earthquakes**

# 6. EVALUATION AND SPECIAL STUDIES

## 6.1 EARTHQUAKE DETECTION CAPABILITY OF WMSO

### 6.1.1 Earthquakes Detected and Recorded During Phase V

During Phase V, WMSO reported 4,488 arrival times to USC&GS. The various types of arrivals reported to USC&GS in the daily messages are as follows:

| Phase | | | |
|---|---|---|---|
| EP | IP | ES | pP |
| 4,388 | 73 | 3 | 24 |

The number of earthquakes detected by WMSO and earthquakes reported by USC&GS during Phase V are listed in table 6 by epicentral distance zones.

Table 6. Earthquakes Detected by WMSO and Earthquakes Reported by USC&GS During Phase V

| WMSO distance in degrees | Earthquakes reported by USC&GS detected by WMSO | Percentage of earthquakes reported by USC&GS detected by WMSO | Earthquakes reported by USC&GS not detected by WMSO | Percentage of earthquakes reported by USC&GS not detected by WMSO |
|---|---|---|---|---|
| 6-15 | 38 | 80.9 | 9 | 19.1 |
| 16-29 | 114 | 89.8 | 13 | 10.2 |
| 30-59 | 323 | 93.4 | 23 | 6.6 |
| 60-89 | 426 | 91.8 | 38 | 8.2 |
| 90-103 | 310 | 47.4 | 344 | 52.6 |
| 104-109 | 72 | 34.4 | 137 | 65.6 |
| 110-180 | 261 | 49.1 | 271 | 50.9 |
| Total | 1544 | 65.0 | 835 | 35.0 |

| | |
|---|---|
| Total events located and reported by USC&GS | 2,382 |
| Total events detected by WMSO, not located by USC&GS | 2,879 |
| Total events detected by WMSO | 5,513 |
| Total events detected by WMSO, excluding local and near-regional events | 4,475 |
| Total local and near-regional events | 1,038 |
| Total phases reported to USC&GS from WMSO preliminary analysis | 4,488 |

### 6.1.2 Epicentral Areas From Which WMSO Commonly Records Earthquake Signals

Figures 24 through 27 are polar plots of epicentral regions, relative to WMSO, from which WMSO commonly records the indicated phases of earthquake signals. Typical examples of events from these regions will be included in the "Atlas of Typical Signals and Noise" for which some data have been collected and which will be published at a later date.

### 6.1.3 Magnitude Study

#### 6.1.3.1 General

A study of earthquake magnitudes was undertaken at WMSO late in August 1962. The seismometric data recorded at WMSO during the 3-month period 1 March through 31 May were studied critically; and magnitudes were calculated for all events recorded at WMSO during this period, for which accurate epicentral data were available from the USC&GS' PDE cards. Data from as many of the following phases recorded for each located event were used in the calculation of magnitudes:

a. Body wave phases PZ, PPZ, and SH.

b. Surface phase components H20, Hmax, Z20, Zmax, which are defined as follows:

H20 - the maximum amplitude-to-period ratio for the vector sum of the horizontal components of surface wave motion within the period range 17 to 23 seconds.

Hmax - the maximum amplitude-to-period ratio for the vector sum of the horizontal components of surface wave motion at whatever period the maximum ratio occurred.

Z20 - the maximum amplitude-to-period ratio for the vertical component of surface wave motion within the period range 17 to 23 seconds.

Zmax - the maximum amplitude-to-period ratio for the vertical component of surface wave motion at whatever period the maximum ratio occurred.

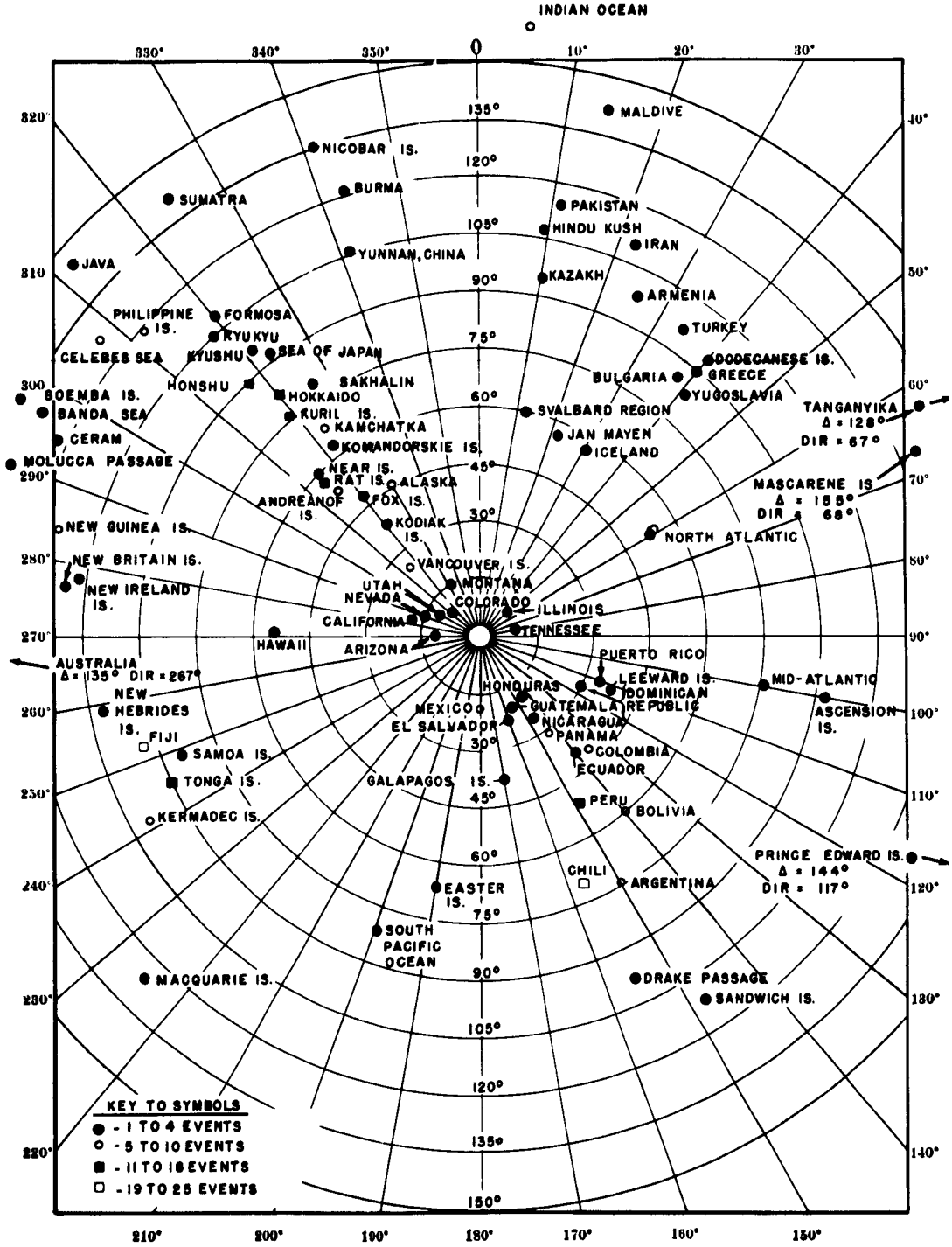


Figure 24. Polar plot of epicenters from which P and P' arrivals were recorded in February, June, and September 1962, showing azimuth and distance from WMSO.

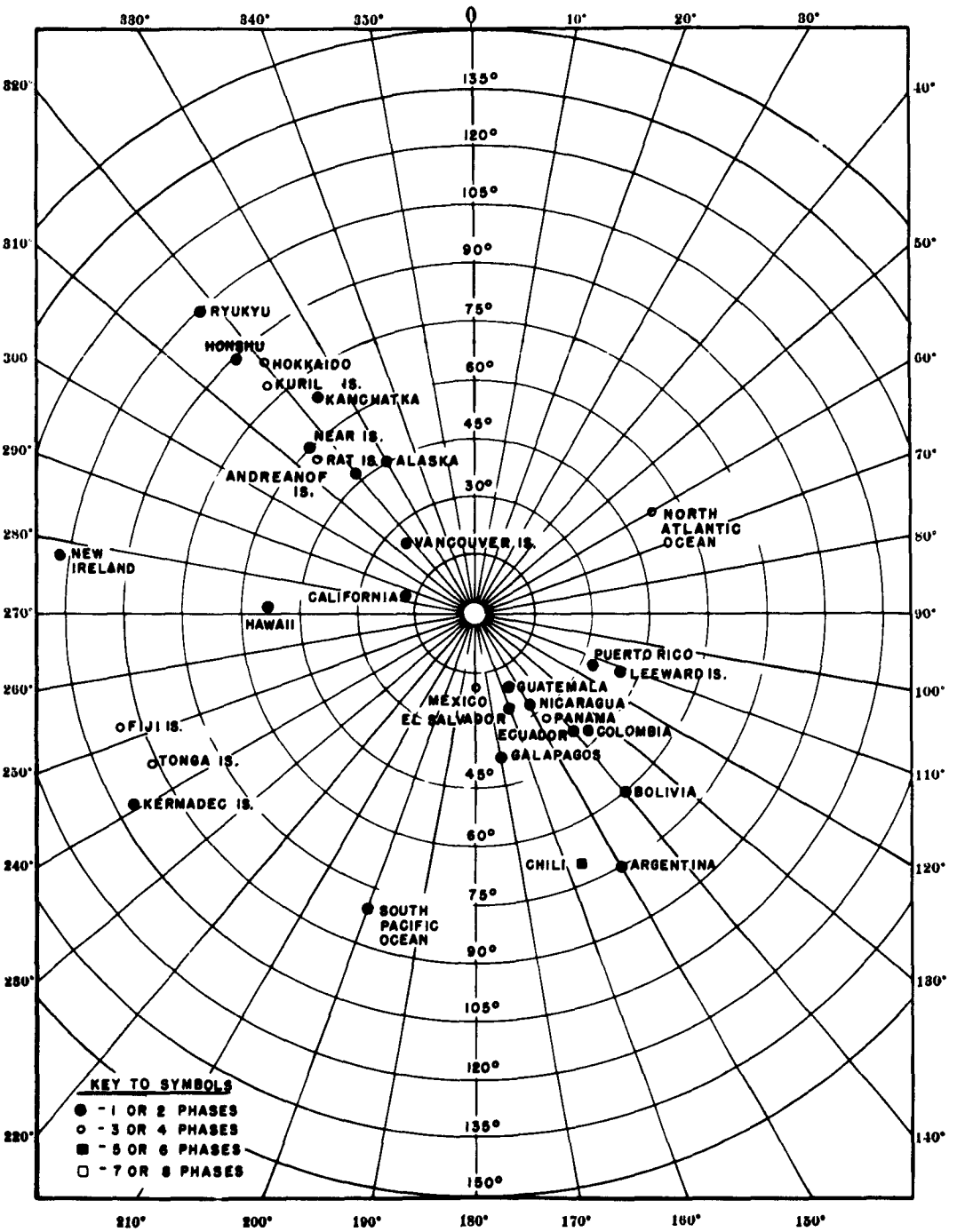


Figure 25. Polar plot of epicenters from which S arrivals were recorded in February, June, and September 1962, showing azimuth and distance from WMSO.

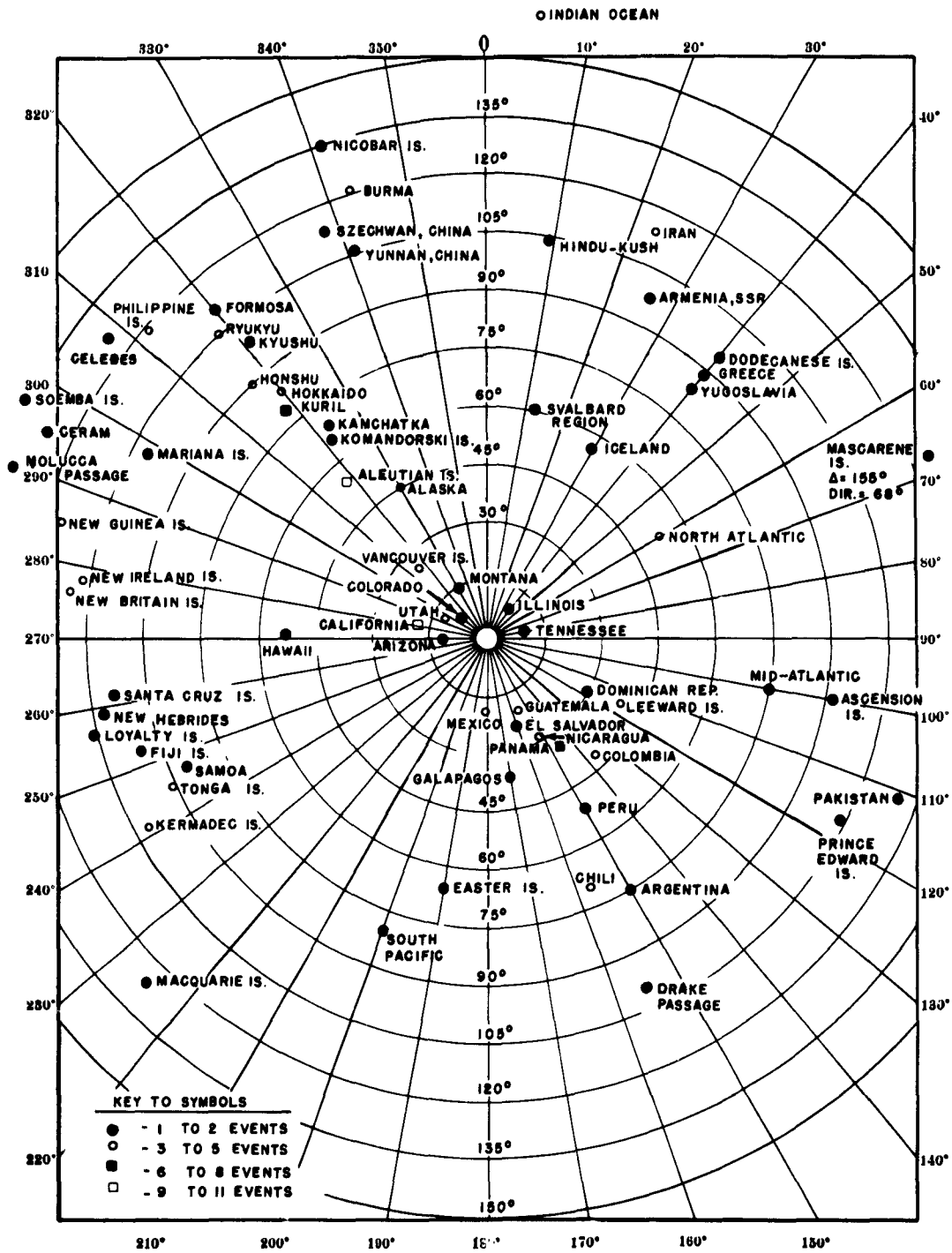


Figure 26. Polar plot of epicenters from which surface wave arrivals were recorded in February, June, and September 1962, showing azimuth and distance from WMSO.

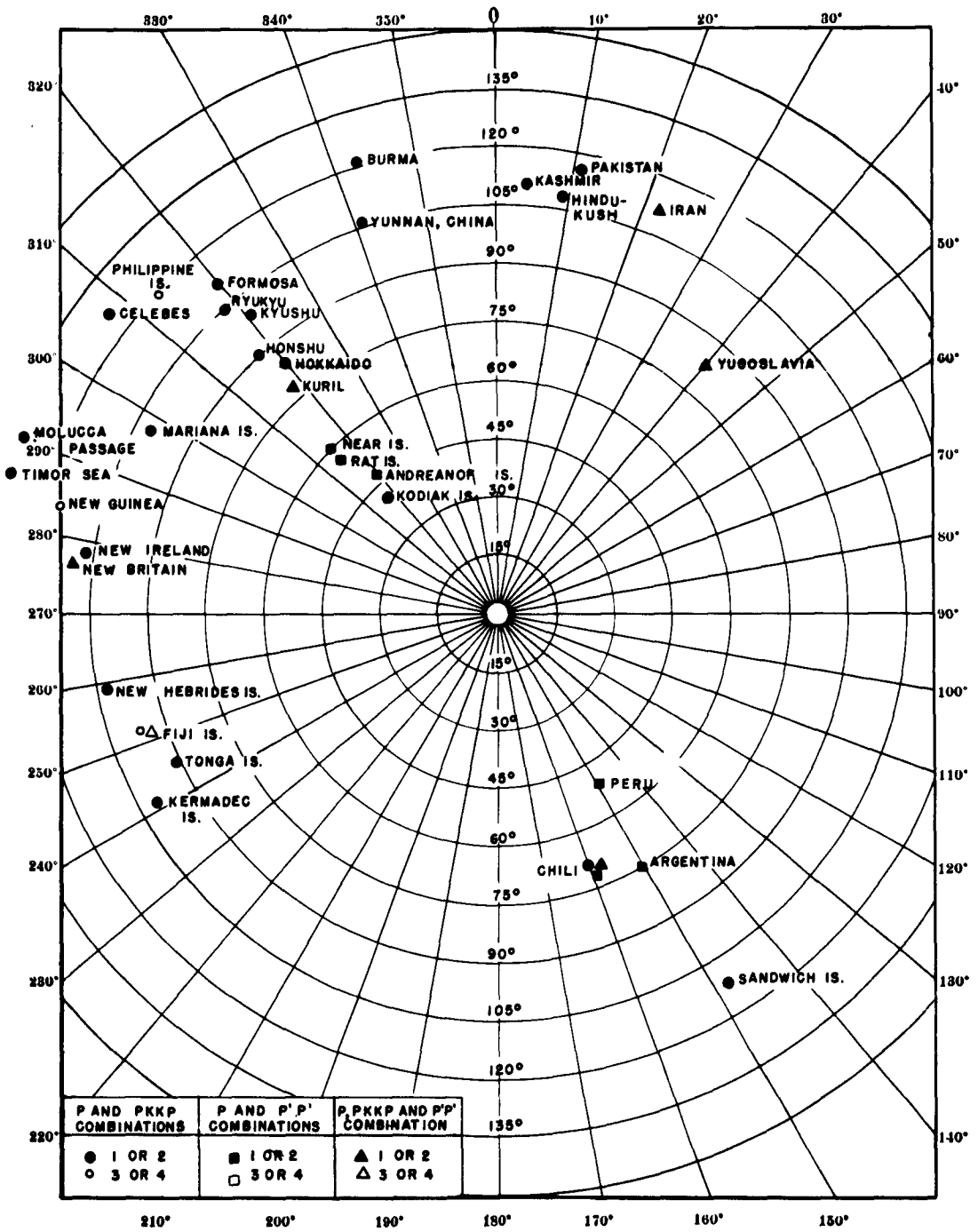


Figure 27. Polar plot of epicenters from which the indicated P-phase combinations were recorded in February, June, and September 1962, showing azimuth and distance from WMSO.

In calculating magnitudes from the surface phase components H20 and Z20, the period range within which data were chosen was restricted between 17 and 23 seconds, because in the data sample chosen the maximum amplitude-to-period ratio was found to occur in the 17- to 23-second period range for 66 percent of the earthquakes for which surface waves were recorded. Furthermore, this range of periods is consistent with the criterion, specified by Richter (1958), of using the maximum surface wave motion with period "near 20 seconds." Båth (1952) used the 17- to 23-second period range in the procedure he developed for calculating magnitudes from the vertical component of surface-wave motion.

Magnitudes were calculated independently for data recorded on several of the WMSO systems as well as for each of the various phases mentioned. The results of the magnitude calculations were compared in an effort to determine what systematic relationships exist between magnitudes calculated using data from the various phases and WMSO systems.

In this report, body-wave magnitudes are designated as "m" with a subscript indicating the phase from which data were measured (e.g., $m_p$ - P-wave magnitude, $m_{pp}$ - PP-wave magnitude). Magnitudes which were calculated using surface-wave data are designated "M" and subscripted to indicate the phase component from which data were measured. The relationships used in the calculation of m and M are as follows:

Body-wave magnitude

$$m = \log_{10} \frac{A}{T} + Q'(\Delta, h) + S$$

A = ground displacement of body phase pulse in millimicrons peak-to-peak

T = period of body phase pulse in seconds

$Q'(\Delta, h) = Q(\Delta, h) - 3.30$; $Q(\Delta, h)$ = calibrating function, dependent on epicentral distance ($\Delta$) and depth of focus (h) (Gutenberg and Richter, 1956).

S = station correction factor (not yet determined for WMSO; therefore, not used in the calculations).

Surface-wave magnitude

$$M = \log_{10} \frac{20A}{T} - \log B' + S$$

A = ground displacement of surface wave pulse in millimicrons peak-to-peak

T = period of surface wave pulse in seconds

$-\log B' = -\log B - 3.30$; $-\log B$ = calibrating function, dependent on epicentral distance (Gutenberg, 1945).

S = station correction factor (not yet determined for WMSO; therefore, not used in the calculations).

6.1.3.2 WMSO Detection "Threshold"

Both earthquake magnitude and epicentral distance from the observatory are factors which influence the ability of a station to detect an earthquake; therefore, an effort has been made to evaluate the detection capabilities of WMSO relative to these parameters.

P-wave magnitudes were calculated for all events for which P-phase data were recorded at WMSO from 1 March through 30 November, and for which accurate epicentral data were available from the USC&GS' PDE cards. These events are plotted in terms of WMSO magnitude, $m_p$, and epicentral distance from WMSO in figure 28. In addition, $M_{H20}$ was calculated for events recorded at WMSO between 1 March and 31 May and between 1 September and 30 November; these data are presented in figure 29.

Theoretical detection curves for $m_p$ and $M_{H20}$ are shown in figure 30. The lower curve of each set indicates a detection threshold based on an assumed 0.5 probability of detection. The 0.5 probability is based on a ratio of A to T of 2.0 and 7.5 millimicrons per second for $m_p$ and $M_{H20}$, respectively, produced by earthquakes 33 kilometers deep at varying distances from WMSO. The upper curve of each set indicates an assumed 0.98 probability of detection. The 0.98 probability of detection is based on a ratio of A to T of 6.0 and 22.5 millimicrons per second for $m_p$ and $M_{H20}$, respectively. These assumed 0.5 and 0.98 probabilities are estimates based on experience and the average noise

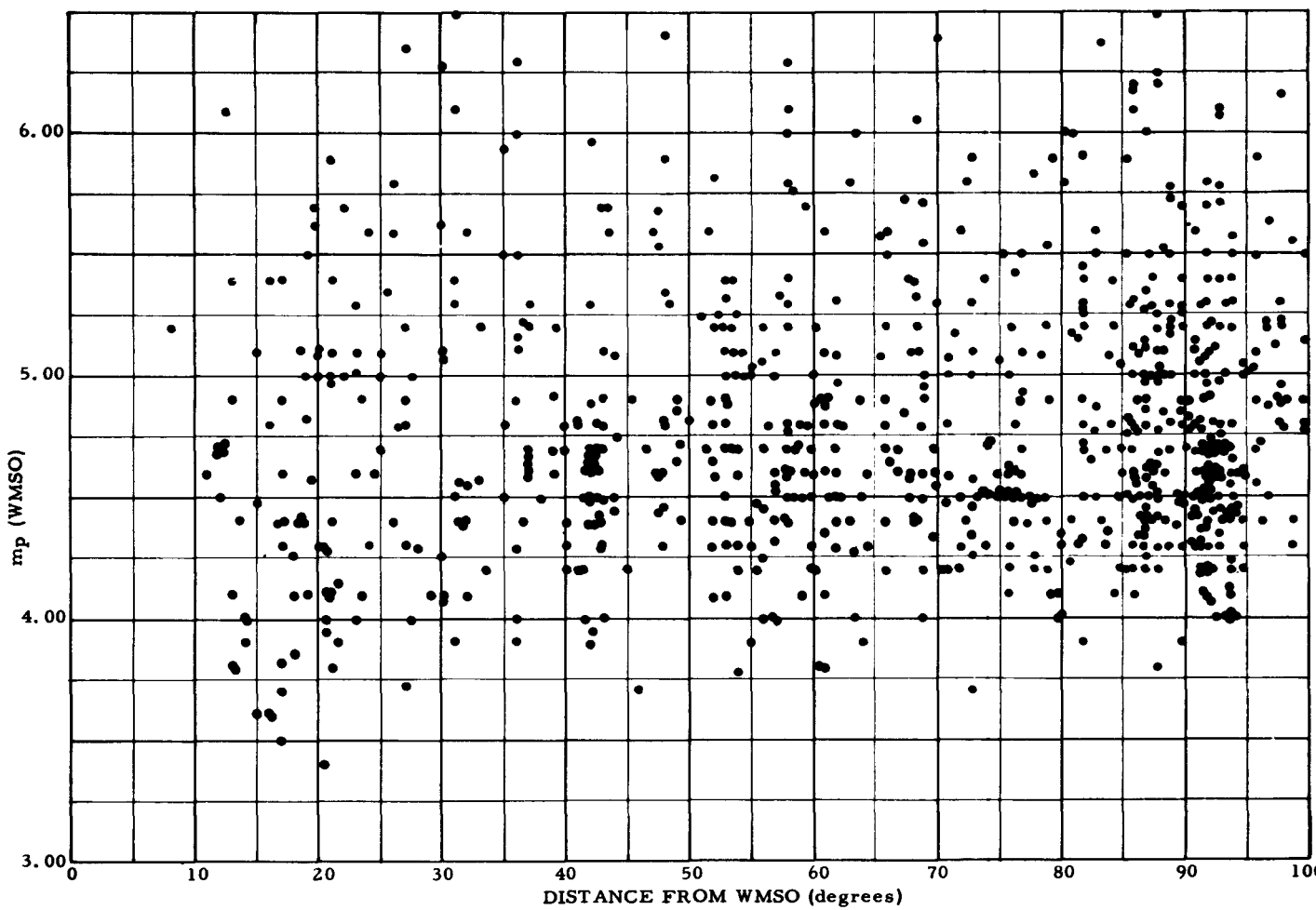


Figure 28. $m_p$ versus distance ($\Delta$) for earthquakes located by USC&GS and detected at WMSO 1 March-30 November 1962 - $m_p$ calculated from WMSO seismograms

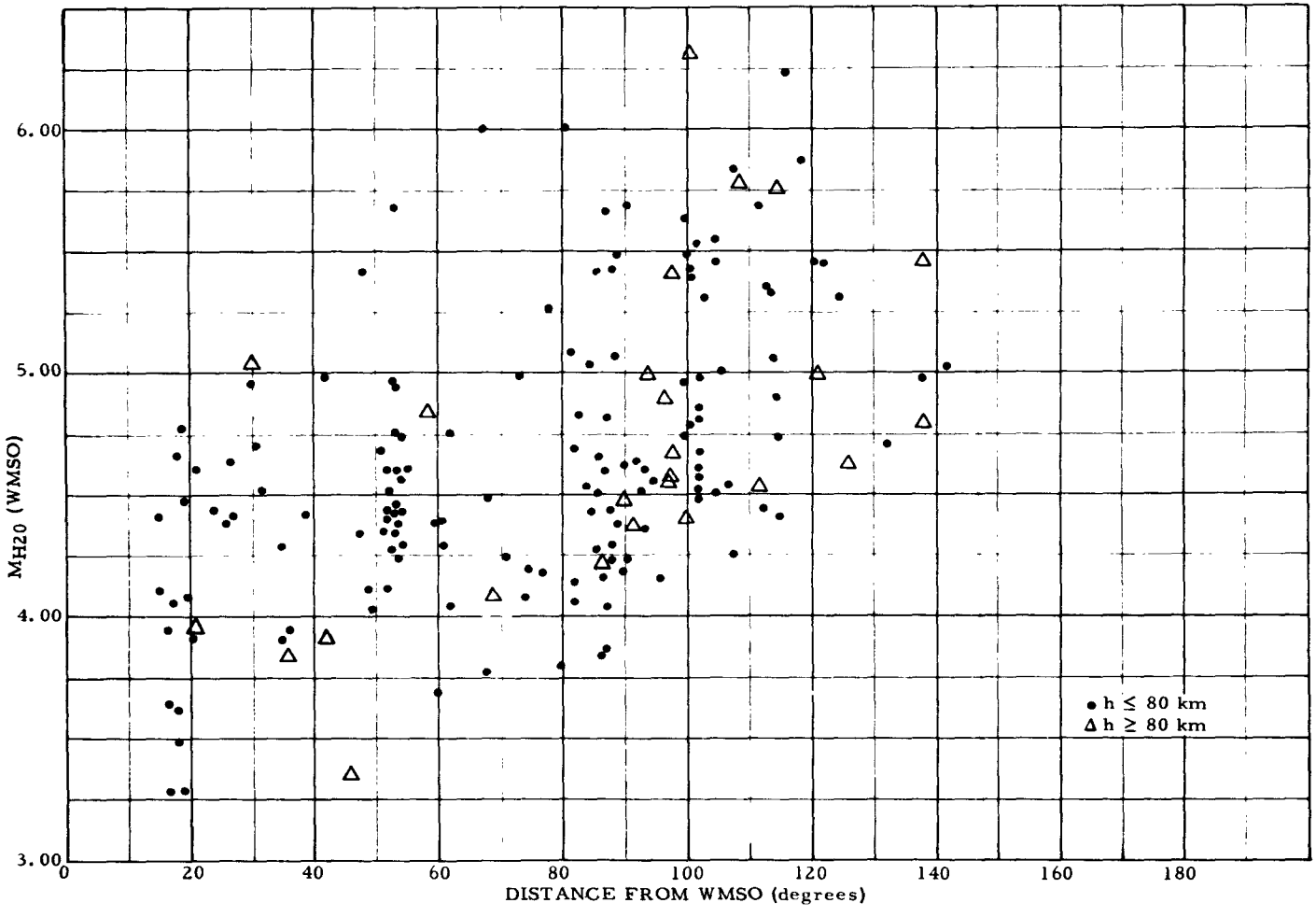


Figure 29. $M_{H20}$ versus distance (Δ) for earthquakes located by USC&GS and detected at WMSO 1 March-31 May and 10 September-30 November 1962 - $M_{H20}$ calculated from WMSO seismograms

levels observed on WMSO seismograms. Of approximately 1380 regional and teleseismic events detected by WMSO for which USC&GS reported no epicentr information during this period, more than half would fall between the two theoretical detection probability curves. The validity of the correction factor Q' (Δ, h), and - log B', can be neither confirmed nor repudiated by comparing the data presented in figures 28 and 29 with the theoretical curves, because

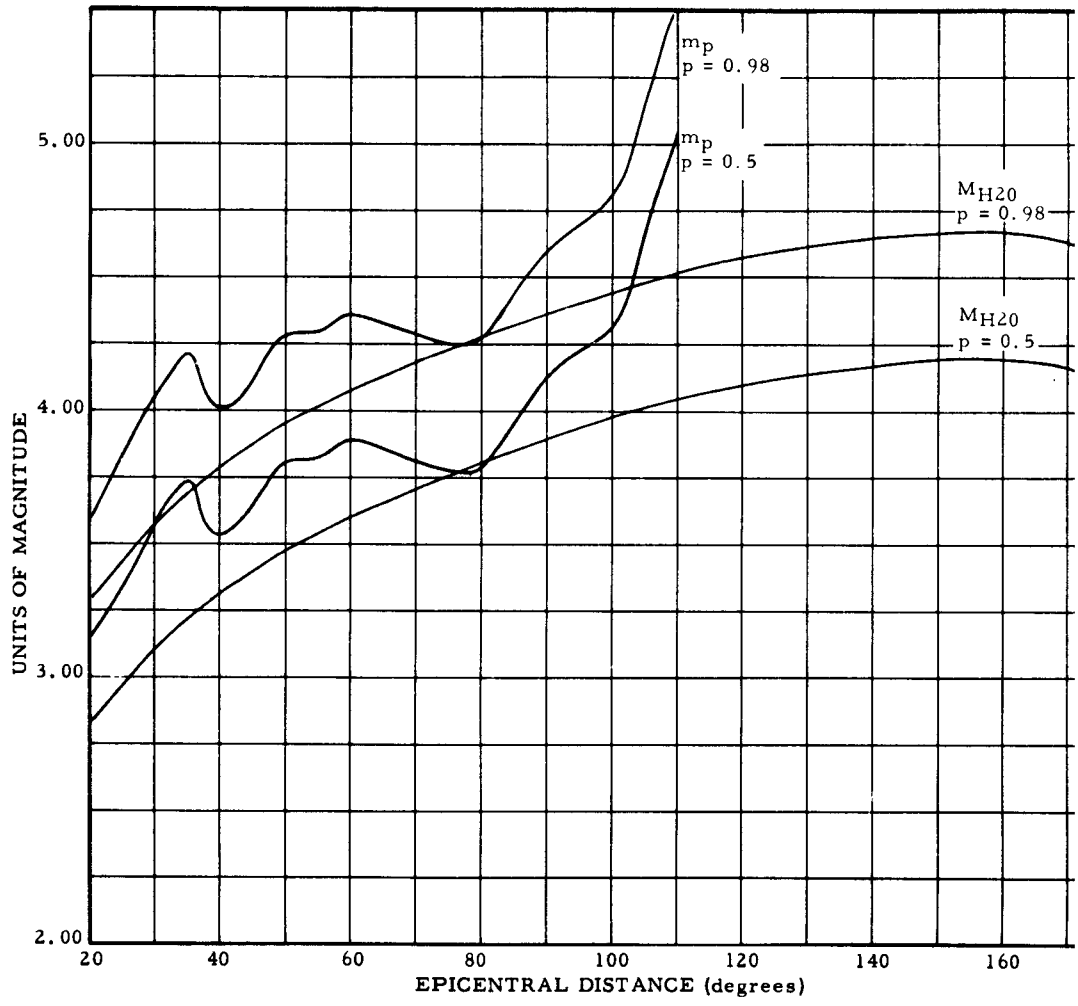


Figure 30. Theoretical threshold of detection curves for WMSO for $m_p$ and $M_{H20}$ for earthq with a focal depth of 33 kilometers occurring at varying distances from WMSO

magnitudes for both actual and theoretical earthquakes apply only to WMSO. With the increased availability of magnitudes based on data recorded at other observatories, it should be possible to check the validity of the correction factors by comparing these values with WMSO's theoretical detection probability curves and with magnitudes calculated using WMSO data. In addition, the values of $\frac{A}{T}$ for 0.5 and 0.98 probability of detection will be more precisely established.

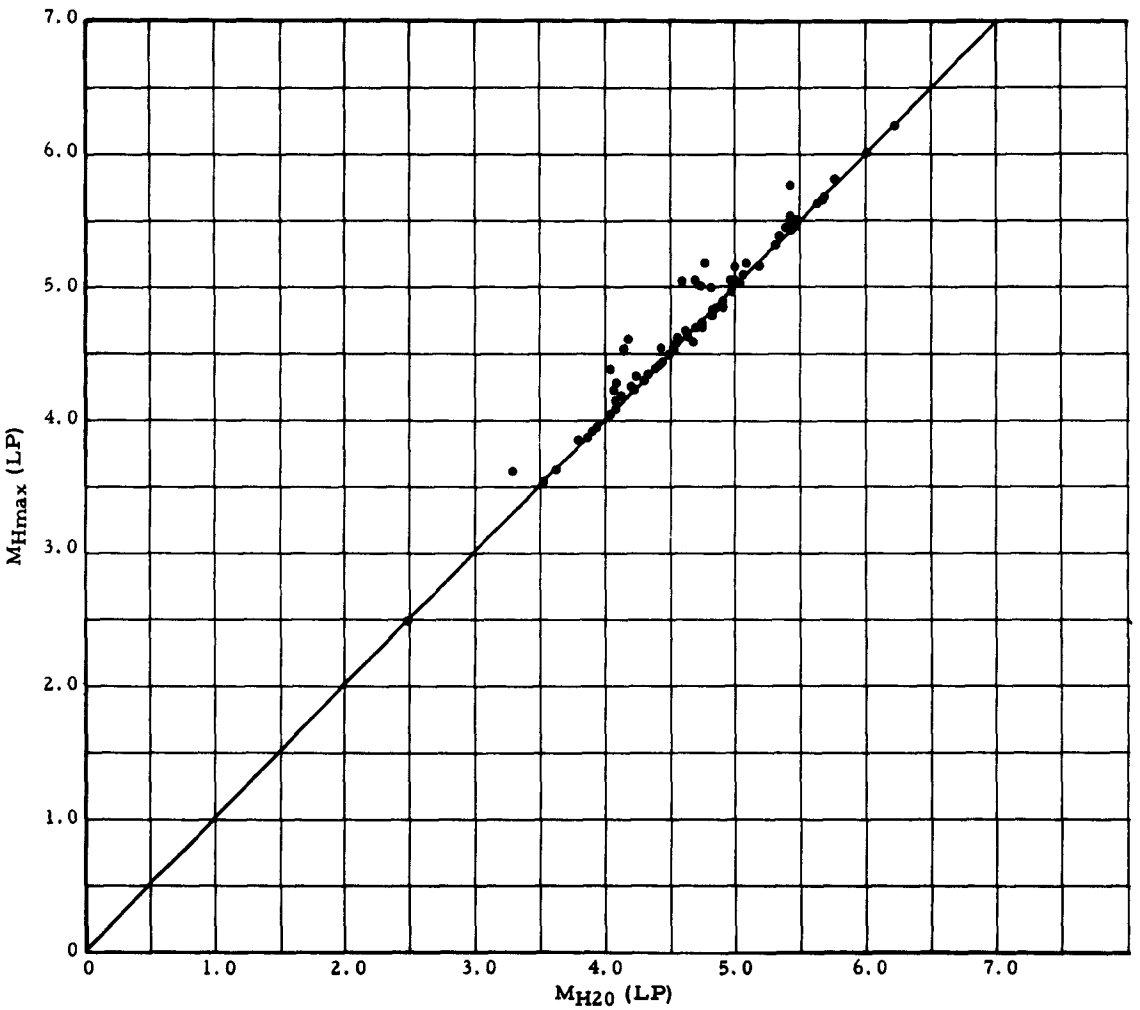


Figure 31. $M_{Hmax}$ as a function of $M_{H20}$ for 102 earthquakes recorded at WMSO 1 March-31 May 1962

Magnitudes $M_{H20}$ and $M_{Hmax}$ for the same events were compared. In addition, an effort was made to determine whether the period at which the maximum amplitude-to-period ratio occurred on the long-period seismographs varied with epicentral distance from WMSO.

Figure 31 is a plot of the relationship between $M_{H20}$ and $M_{Hmax}$.

Figure 32 relates the difference between horizontal surface-wave magnitudes computed from the maximum amplitude-to-period ratio at whatever period the maximum occurred ($M_{Hmax}$) and the maximum amplitude-to-period ratio in the period range 17-23 seconds ($M_{H20}$) to the ratio of the periods at which the two measurements were made.

In 66 percent of the cases, the maximum amplitude-to-period ratio occurred within the period range 17-23 seconds. The difference between $M_{Hmax}$ and $M_{H20}$ exceeded 0.2 magnitude unit in only 10 percent of the cases, including periods greater than 40 seconds. On the basis of these data, we conclude the differences between $M_{Hmax}$ and $M_{H20}$ computed using the relation $M = \log_{10} \frac{20A}{T} - \log B' + S$ is not significant if $M_{Hmax}$ is based on measurements at periods greater than 17 seconds.

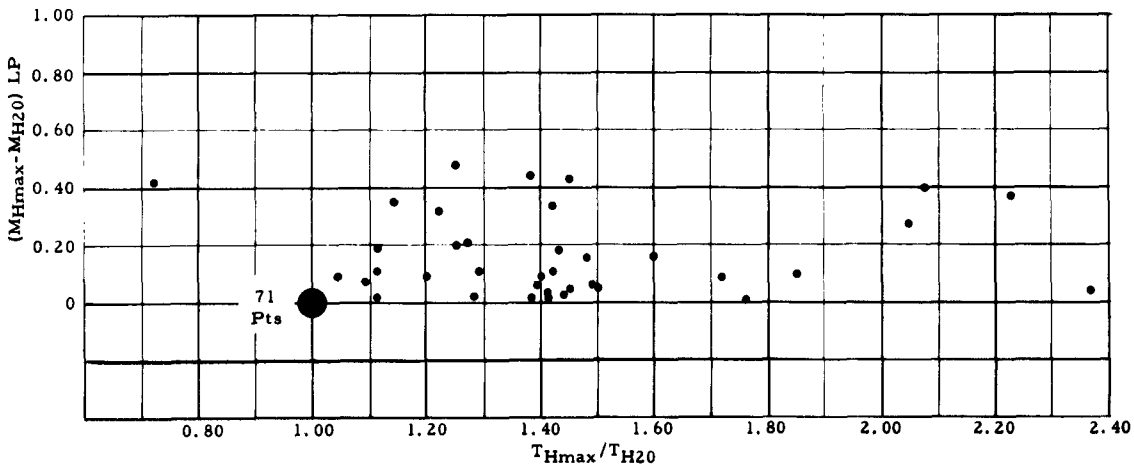


Figure 32. $M_{Hmax}$-$M_{H20}$ versus the ratio between the periods at which the measurements for each were made for 108 events recorded at WMSO 1 March-31 May 1962

Figure 33 shows the relation of the period at which the maximum amplitude-to-period ratio occurred in the horizontal component of the surface group to epicentral distance from WMSO. At distances greater than 13 degrees, there is no apparent dependence of the period at which the maximum amplitude-to-period ratio occurs on epicentral distance.

Figures 34 through 44 are comparisons of magnitudes determined from one phase or system and magnitudes determined from another phase or system. In each case, least-square analysis was applied to the data to determine the best fitting straight line. Because errors occur in both variables, deviations were measured perpendicular to the least-square line rather than parallel to one of the axes, as is usually done. The equation of the least-square line and the standard error of estimate (S) in magnitude units are given on each plot.

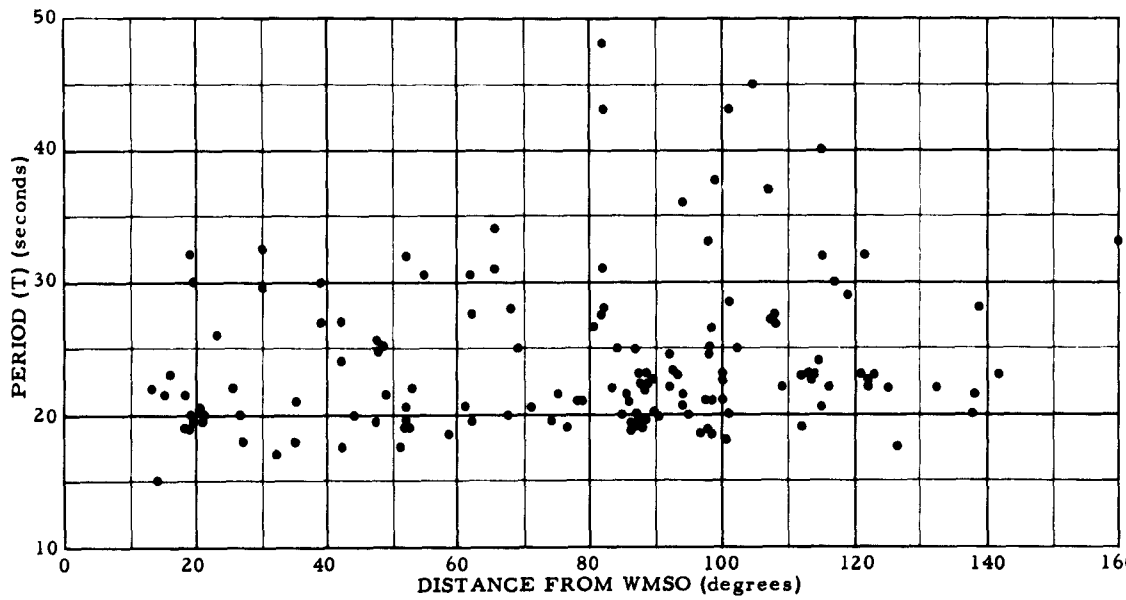


Figure 33. Plot of the period at which the maximum amplitude-to-period ratio occurred in the horizontal component of the surface group as measured on the long-period seismograms versus epicentral distance for 108 events recorded at WMSO 1 March-31 May 1962

Figure 34 shows magnitude computed from the vertical component of the surface wave ($M_{Zmax}$), assuming the same distance correction factor as is used for horizontal surface-wave magnitudes, as a function of magnitude computed from the horizontal component of the surface wave ($M_{Hmax}$). For each variable, measurement was made at the maximum amplitude-to-period ratio at whatever period the maximum ratio occurred. Measurements of the two variables were made independently; i.e., for a given point, the period at which the vertical component was measured is not necessarily the same period as that at which the horizontal component was measured.

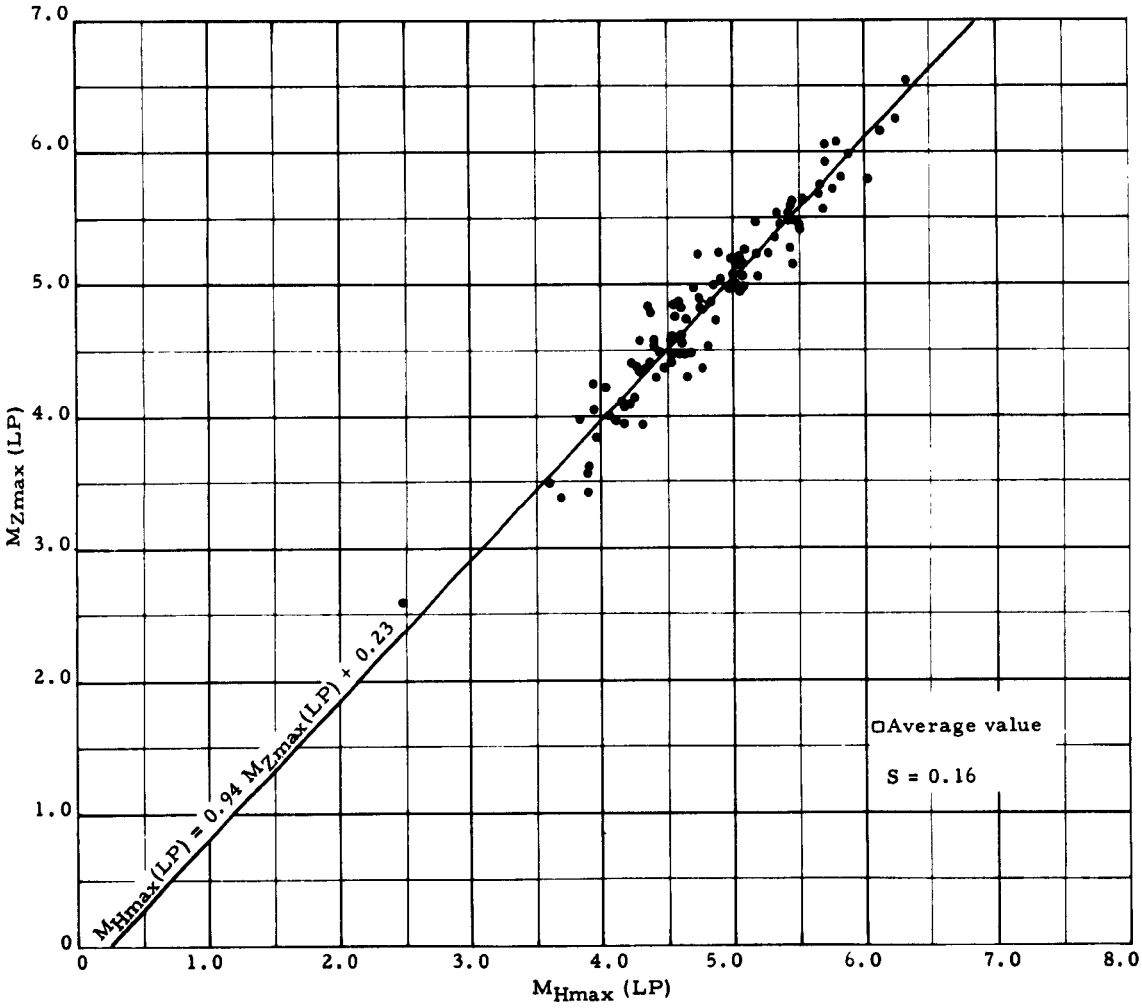


Figure 34. $M_{Zmax}$ as a function of $M_{Hmax}$ for 95 events recorded on the long-period seismograms at WMSO 1 March-31 May 1962

We conclude from these data that for the purposes of calculating magnitudes, measurements made of the vertical components of a surface wave are essentially as reliable as measurements made of the horizontal components. Use of the vertical component rather than the vector sum of the horizontal components would be advantageous in routine magnitude calculations, because measurement of only one component on the seismograms would be necessary and calculation would be simplified.

Figure 35 is a plot of P-wave magnitude ($m_p$) determined from measurements of the short-period seismographs at WMSO versus magnitude reported by the

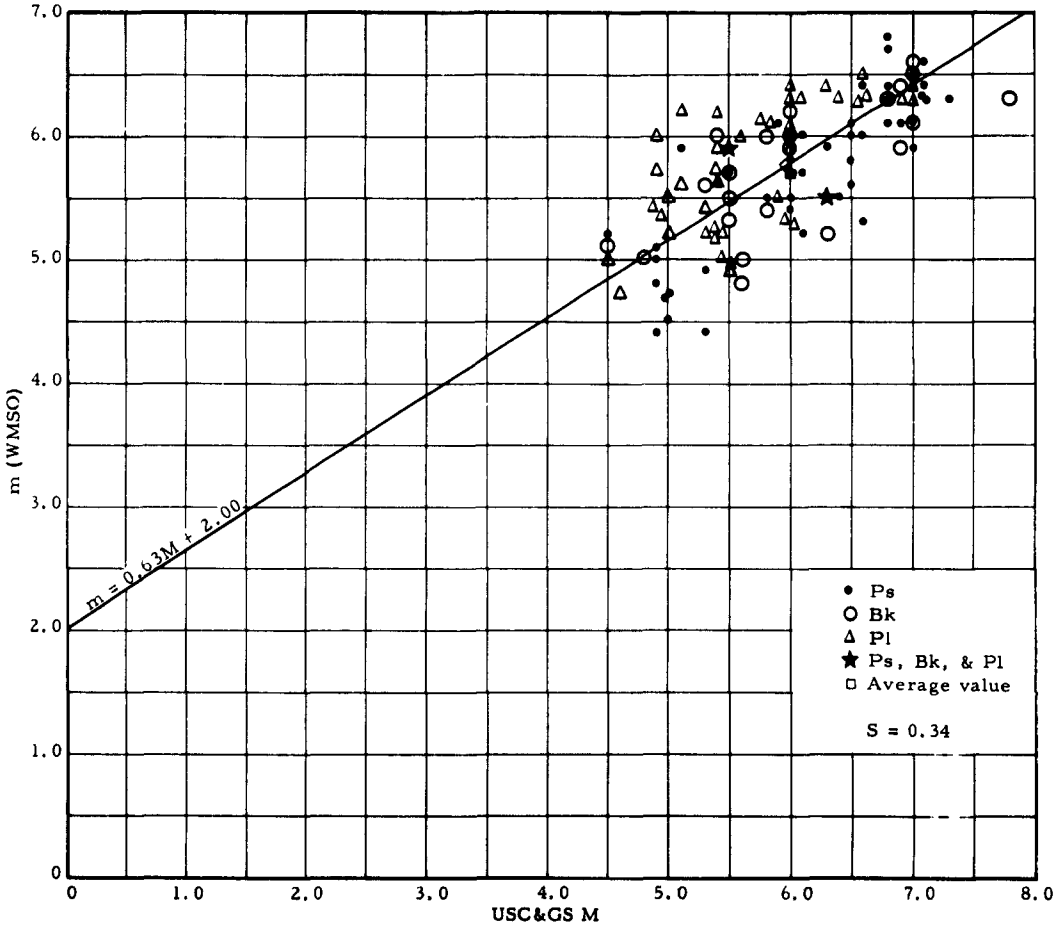


Figure 35. $m_p$ as a function of M as reported by USC&GS for events recorded at WMSO 1 March-31 October 1962

USC&GS from the stations at Pasadena (Ps), Berkeley (Bk), and Palisades (Pl). The least-square line m = 0.63M + 2.0 obtained from these data is quite close to the relation of body-wave magnitude (m) and surface-wave magnitude (M) given by Richter (1958): m = 0.63M + 2.5. However, if deviations are measured parallel to either of the axes instead of perpendicular to the least-square line, markedly different relations result due to the large scatter in the data.

Figure 36 shows the relation between $m_p$ calculated from WMSO short-period data and $M_{H20}$ calculated from WMSO long-period data. $M_{H20}$ and $m_p$ were

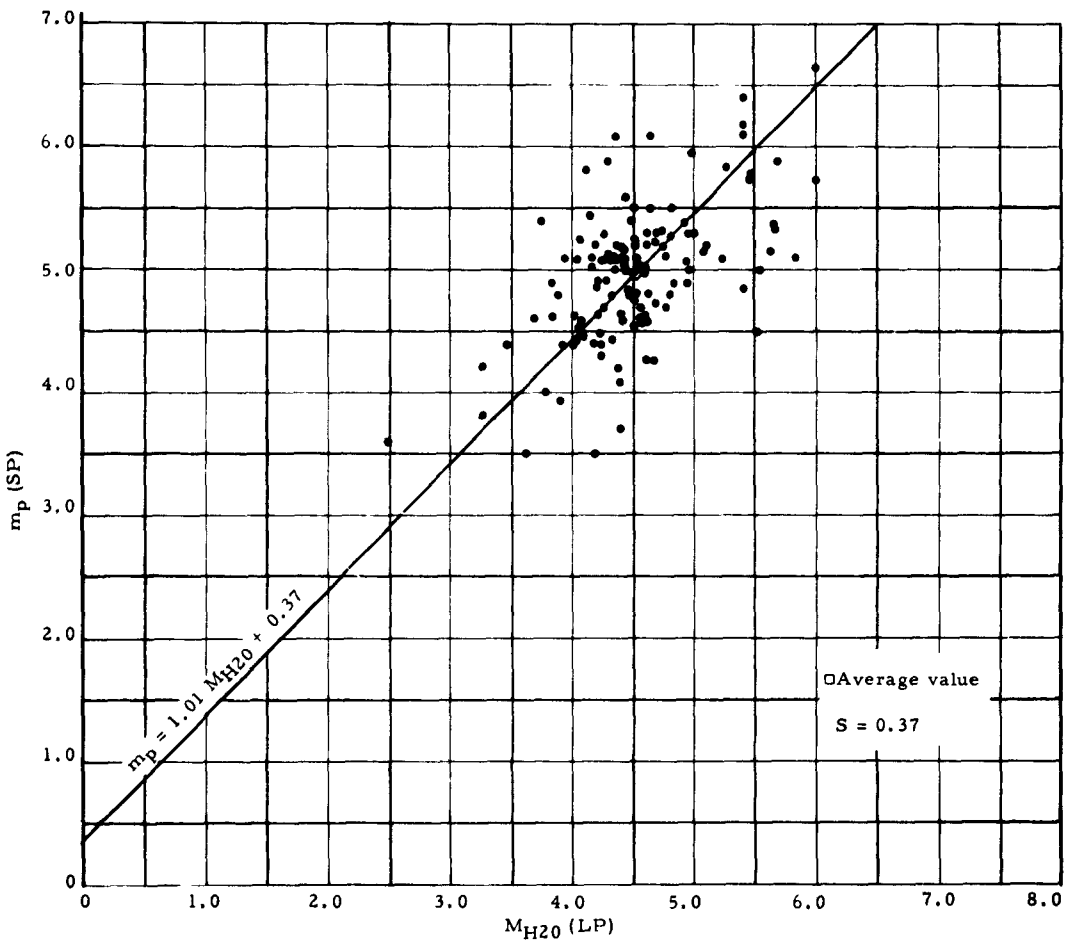


Figure 36. $m_p$ as a function of $M_{H20}$ for 124 earthquakes recorded at WMSO 1 March-31 May and 10 September-30 November 1962. Focal depths of events ≤ 80 kilometers

calculated for events recorded between 1 March and 31 May and between 10 September and 30 November 1962 with focal depth of 80 kilometers or less.

Considering the amount of scatter of the data, the least-square relation $m_p = 1.01\ M_{H20} + 0.37$ shows relatively little difference between $m_p$ and $M_{H20}$ as determined from WMSO data. Figure 37 shows the similar relation between $m_p$ and $M_{Hmax}$. No explanation can be offered at the present time

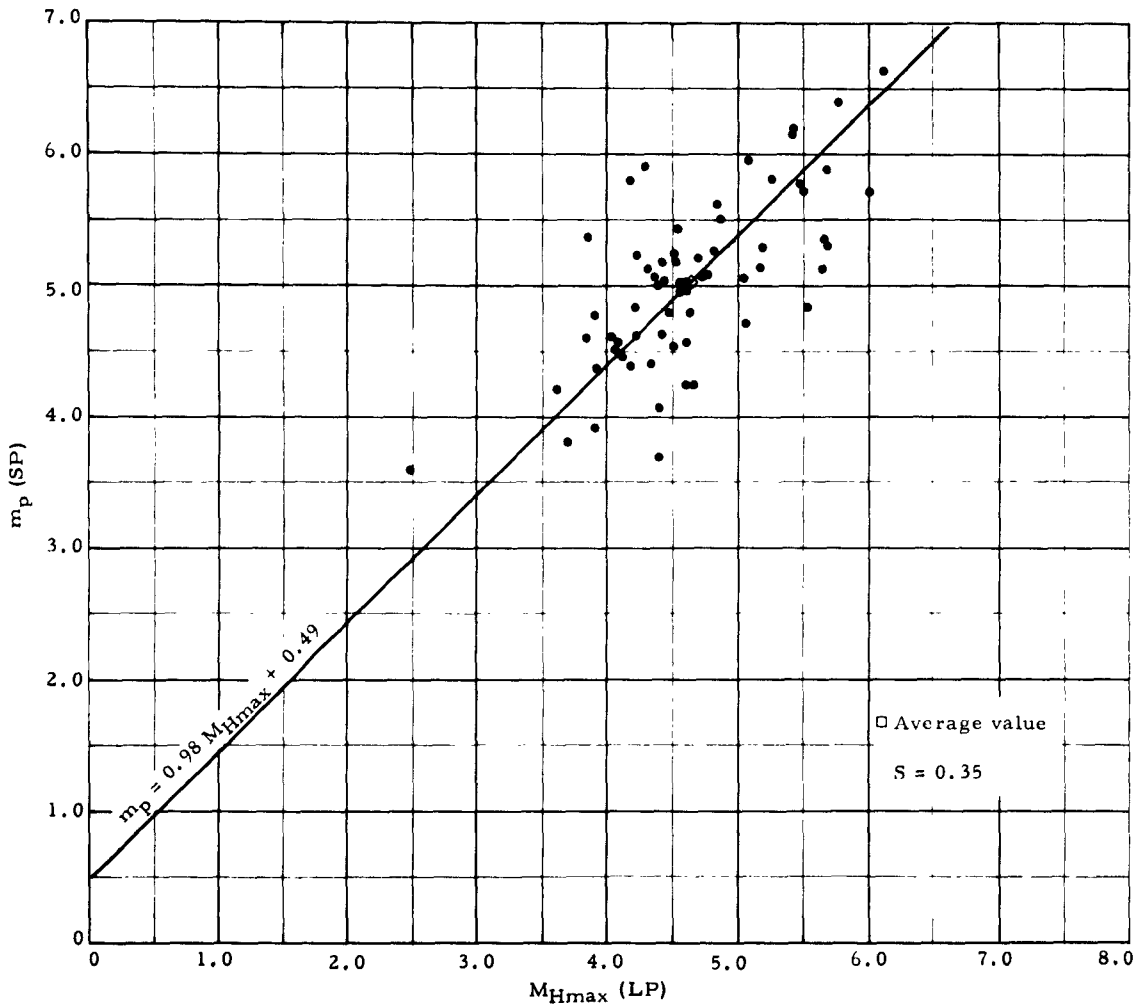


Figure 37. $m_p$ as a function of $M_{Hmax}$ for 64 earthquakes recorded at WMSO 1 March-31 May 1962. Focal depth of events ≤80 kilometers

for the difference that exists between the relationships between $m_p$ and $M_{H20}$, and $m_p$ and M as reported by the USC&GS.

Figure 38 is a plot of $m_p$ calculated from WMSO long-period data versus $M_{H20}$. Although based on a limited number of data points, the least-square line $m_p = 0.92\ M_{H20} + 0.79$ appears to be in good agreement with that

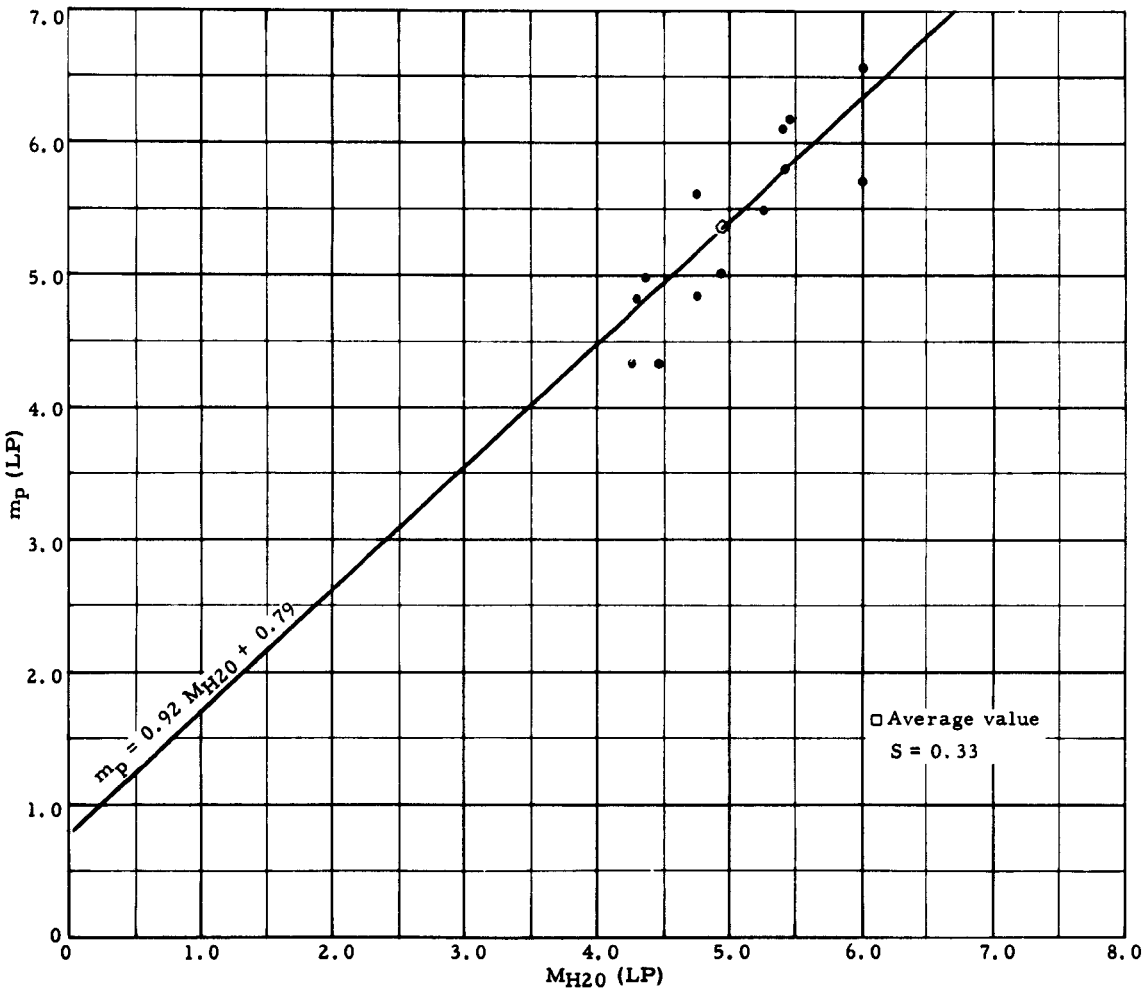


**Figure 38. $m_p$ calculated from long-period data as a function of $M_{H20}$ for 13 earthquakes recorded at WMSO 1 March-31 May and 10 September-30 November 1962**

determined for $m_p$ versus $M_{H20}$ (figure 36). In order to obtain a better comparison, $m_p$ calculated from short-period data was plotted versus $m_p$ calculated from long-period data (figure 39). Additional data were available for this comparison. The slope of the least-square line suggests the interpretation that stronger events produce relatively more compressional wave amplitude at longer periods than do weaker events. If this interpretation is

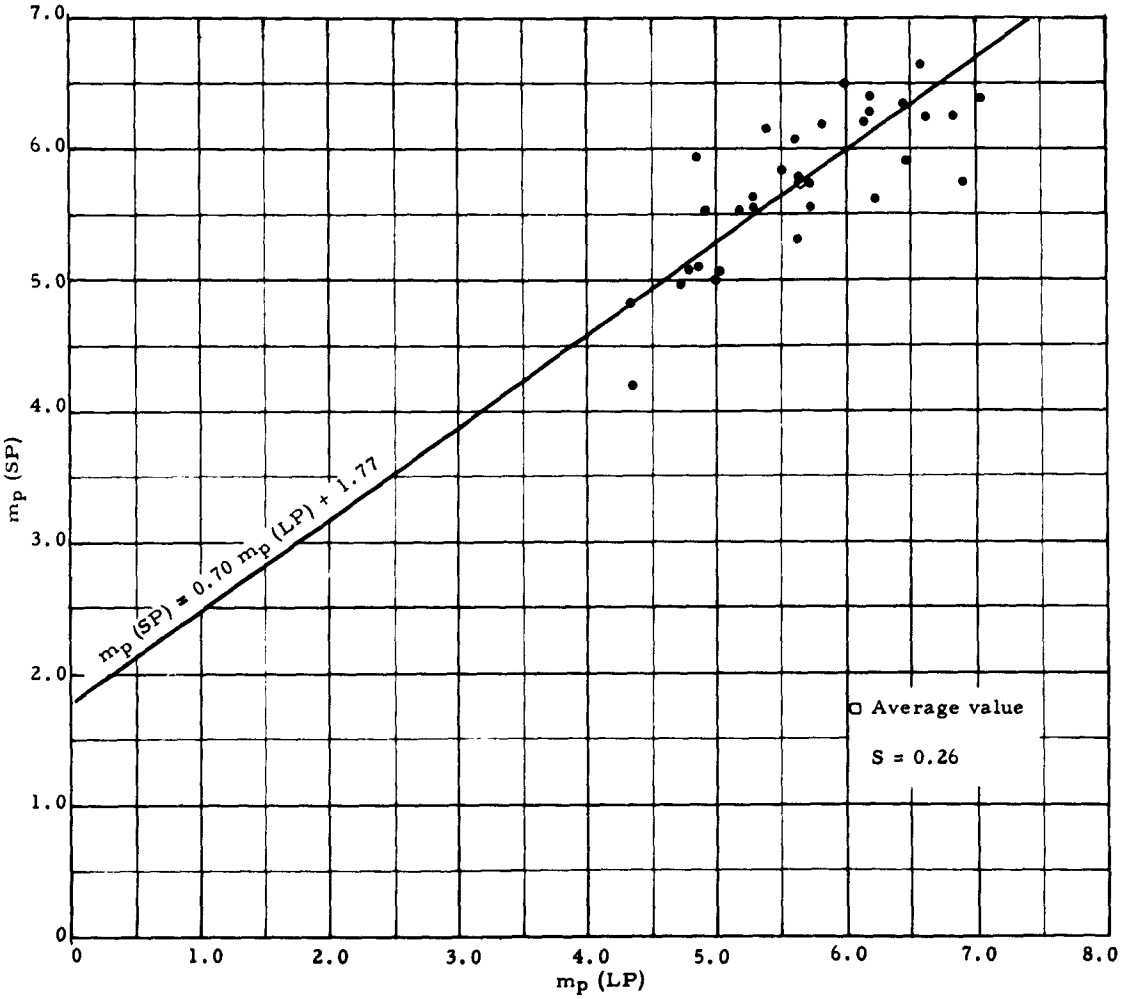


Figure 39. $m_p$ calculated from long-period data as a function of $m_p$ calculated from short-period data for 33 earthquakes recorded at WMSO 1 March-31 May and 10 September-30 November 1962

valid, frequency spectra of P waves should show a systematic shift toward lower frequencies with increasing magnitude. This will be investigated further as more data become available.

Figure 40 is a plot of $m_p$ calculated from short-period data versus $m_p$ calculated from broad-band data. These data indicate that $m_p$ calculated from

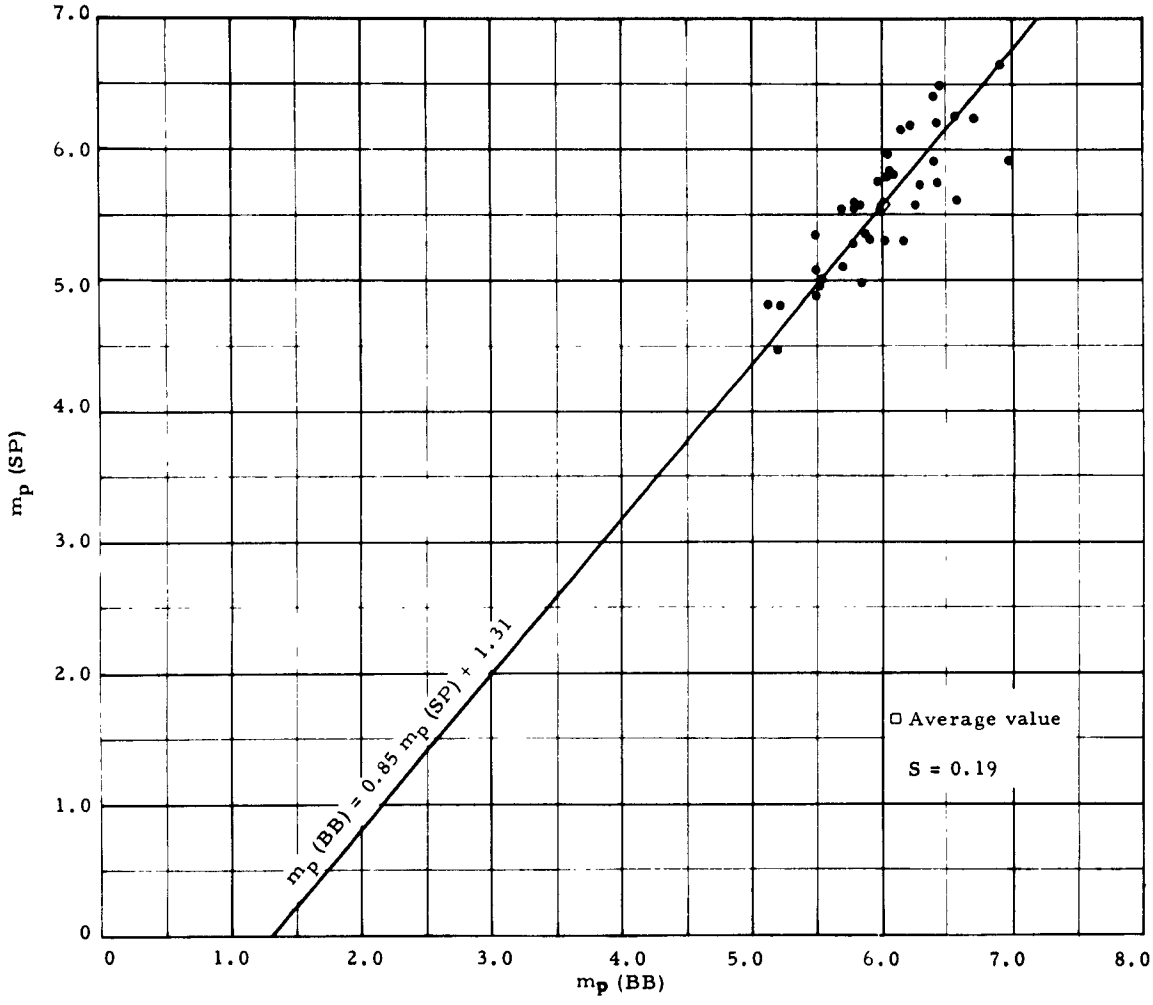


Figure 40. $m_p$ calculated from short-period data as a function of $m_p$ calculated from broad-band data for 39 earthquakes recorded at WMSO 1 March-31 May 1962

broad-band data tend to be about 0.4 magnitude unit greater than $m_p$ calculated from short-period data.

Figure 41 is a plot of $m_s$ calculated from long-period data versus $m_s$ calculated from broad-band data. This plot indicates that $m_s$ calculated from broad-band data tends to be higher than $m_s$ calculated from long-period data by an amount that increases with magnitude.

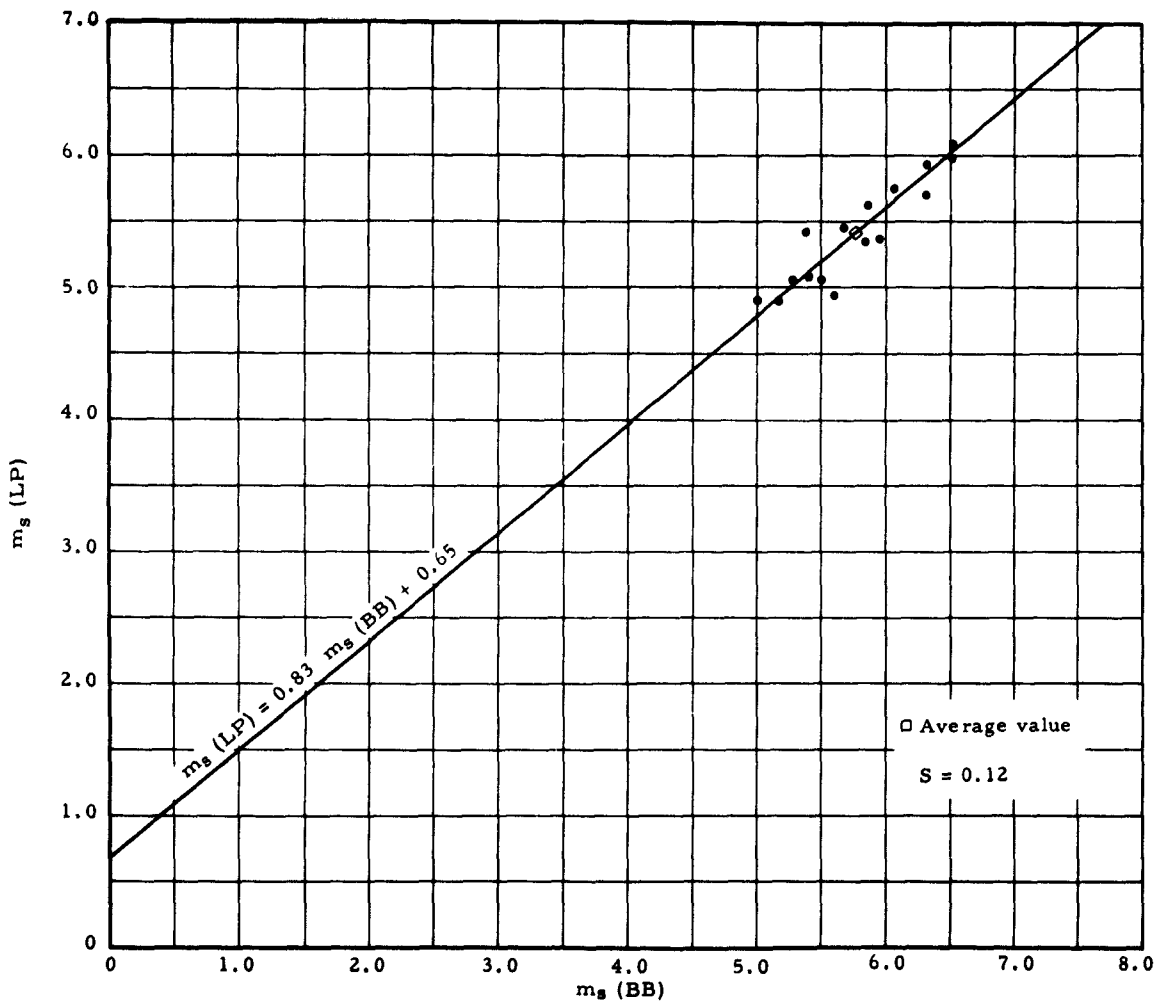


**Figure 41. $m_s$ calculated from broad-band data as a function of $m_s$ calculated from long-period data for 16 earthquakes recorded at WMSO 1 March-31 May 1962**

Figure 42 shows the relationship between $m_p$ and $m_{pp}$, both calculated from short-period data.

The least-square relation $m_p = 1.00\ m_{pp} + 0.16$ indicates that the depth-distance correction factors used for computing magnitudes from PP-phase data are consistent with those used for computing magnitudes from P-phase data.

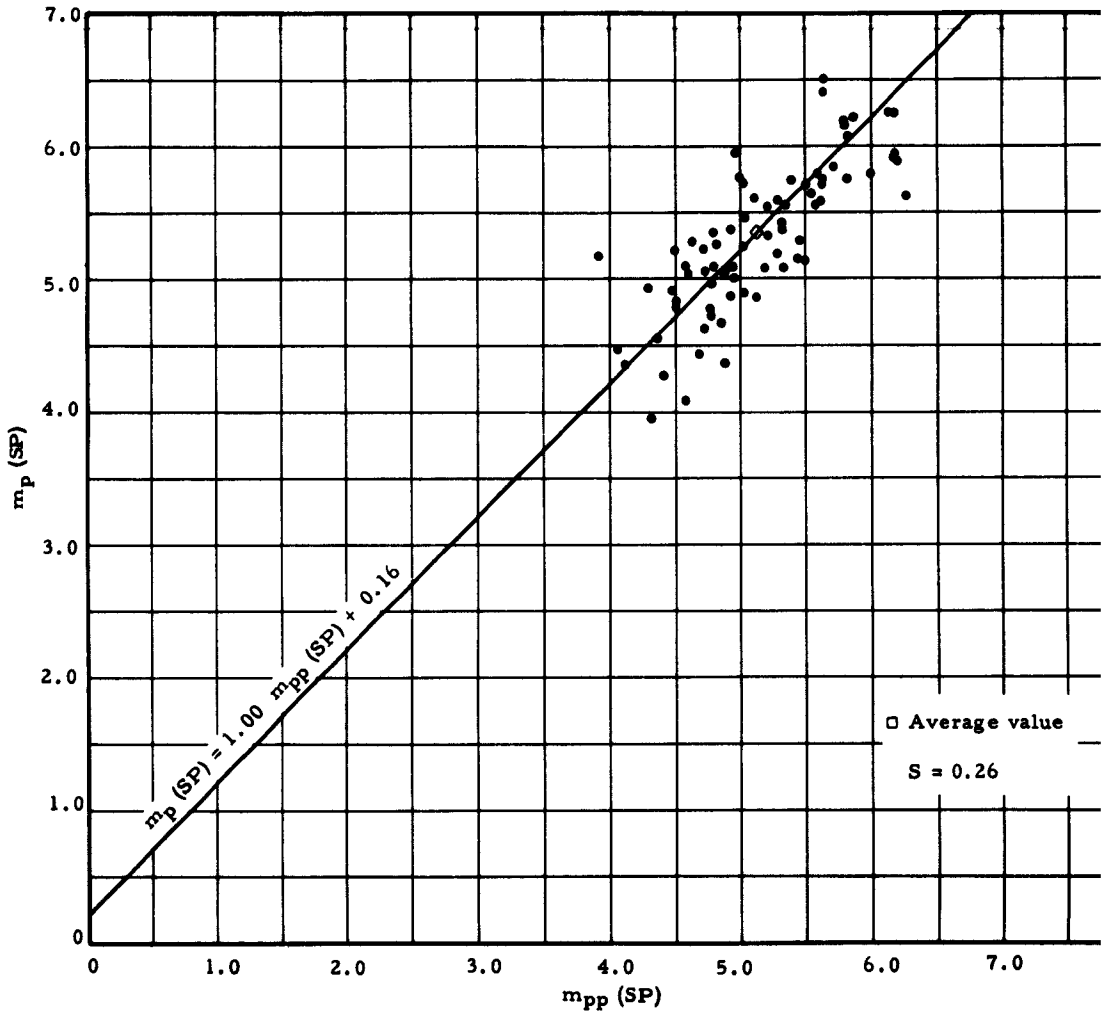


Figure 42. $m_{pp}$ as a function of $m_p$ calculated from short-period data for 73 earthquakes recorded at WMSO 1 March-31 May 1962

We conclude that body-wave magnitude determinations can be extended beyond P-phase distance by using PP-phase data.

$m_p$ calculated from short-period data was compared to $m_s$ calculated from short-period data (figure 43), and to $m_s$ calculated from long-period data

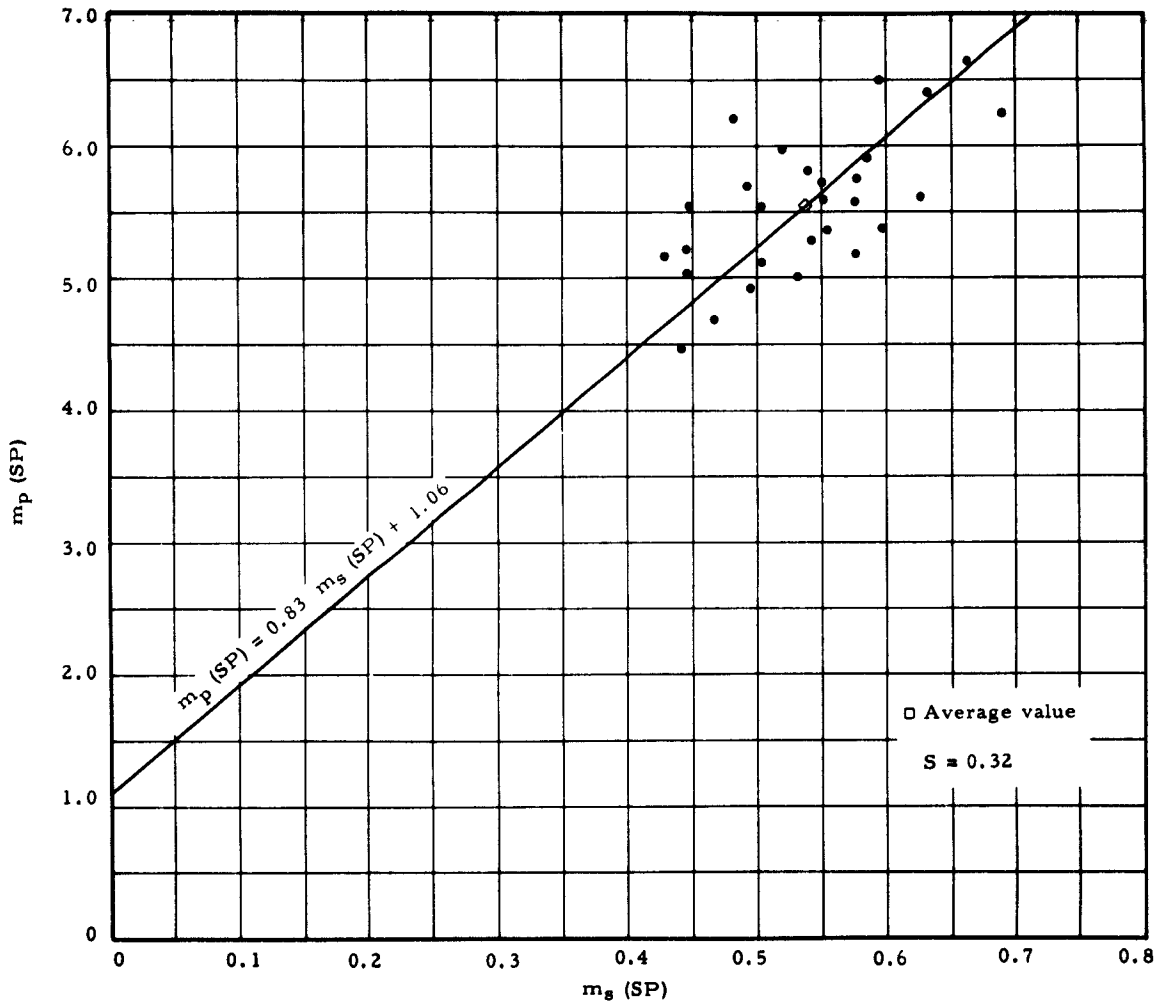


Figure 43. $m_p$ versus $m_s$, both calculated from short-period data, for 28 earthquakes recorded at WMSO 1 March-31 May 1962

(figure 44). A rather large difference exists between the slopes of the least-square lines for these 2 sets of data, but this may not be significant due to the small data samples and the relatively large scatter in the data.

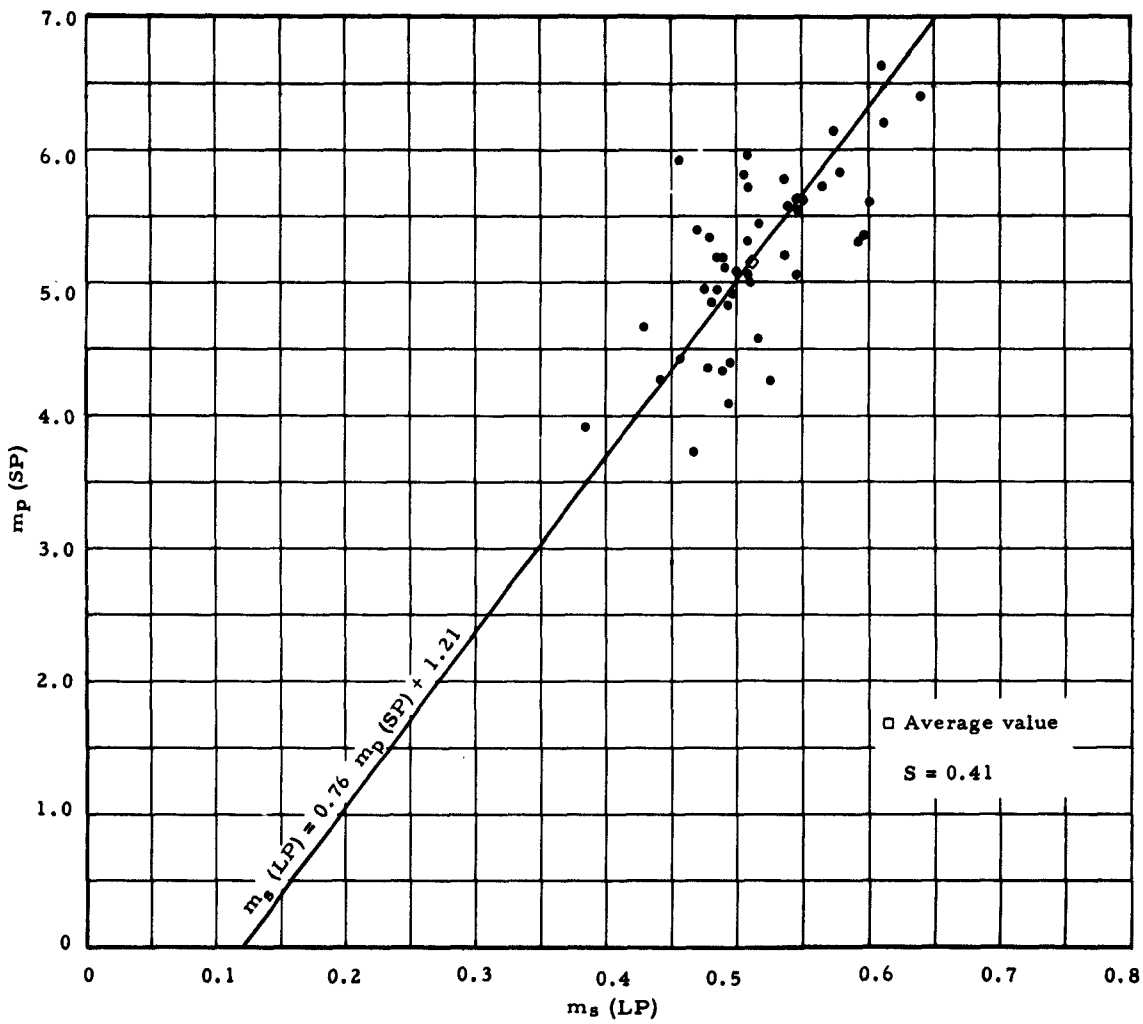


Figure 44. $m_p$ calculated from short-period data versus $m_s$ calculated from long-period data for 46 earthquakes recorded at WMSO 1 March-31 May 1962

### 6.1.3.3 Comparison of $m_p$ From Short-Period Data Measured at WMSO and LRSM Bulletin Stations

For the 8-month period 1 April to 30 November 1962, $m_p$ computed from WMSO short-period data was compared to $m_p$ computed from LRSM short-period data for each of the eleven LRSM stations for which $m_p$ was reported in the LRSM bulletin.

For each LRSM station, a plot was made of $m_p$ reported by that station versus $m_p$ reported by WMSO for all events for which both WMSO and the given LRSM station reported $m_p$.

A list of the LRSM stations and the number of events (n) for each station are given in table 7.

Linear least-square analysis was applied to the data for each comparison, measuring deviations perpendicular to the least-square line. The resulting equations of these lines expressing LRSM magnitude ($m_L$) as a function of WMSO magnitude ($m_W$) and the standard error of estimate (S) for each, in magnitude units, are also tabulated in table 7.

The slopes of the least-square lines range from 0.72 to 0.92, and the intercepts on the LRSM station axes range from + 0.05 to + 1.51.

Table 7. Comparisons of LRSM Magnitude ($m_L$) to WMSO Magnitude ($m_W$)

| Station Locations | Station Code | n | Equation of least-squares line | Std. error of estimate (S) |
|---|---|---|---|---|
| Marysville, Calif. | MV | 321 | $m_L = 0.88\ m_W + 0.34$ | 0.31 |
| Taft, Calif. | TF | 233 | $m_L = 0.83\ m_W + 0.81$ | 0.34 |
| Campo, Calif. | CP | 333 | $m_L = 0.90\ m_W + 0.33$ | 0.31 |
| Mina, Nevada | MN | 466 | $m_L = 0.95\ m_W + 0.05$ | 0.31 |
| Winnemucca, Nev. | WI | 499 | $m_L = 0.92\ m_W + 0.30$ | 0.31 |
| Fillmore, Utah | FM | 306 | $m_L = 0.82\ m_W + 0.85$ | 0.30 |
| Las Cruces, N.M. | LC | 491 | $m_L = 0.80\ m_W + 0.80$ | 0.28 |
| San Jose, Texas | SJ | 165 | $m_L = 0.78\ m_W + 1.33$ | 0.31 |
| Aurora, Wis. | AR | 93 | $m_L = 0.72\ m_W + 1.46$ | 0.29 |
| Niagara, Wis. | NG | 80 | $m_L = 0.72\ m_W + 1.47$ | 0.29 |
| Delhi, N. Y. | DH | 177 | $m_L = 0.74\ m_W + 1.51$ | 0.29 |

Figure 45 shows the geographic distribution of the slopes of the least-square lines ($P_{LW}$). There is a general decrease in the value of the slopes from west to east across the United States. The meaning of this variation of the slopes with geographic location is not clear; however, it is significant and worthy of further investigation.

Figure 46 shows the geographic distribution of the intercepts ($L_o$) of the least-square lines with the LRSM station axis. There is a clear geographic pattern here; the values of $L_o$ increase from west to east across the United States.

If the values of the slopes ($P_{LW}$) were all unity, it would be reasonable to interpret the values of the intercepts ($L_o$) as station correction factors relative to WMSO. However, the fact that the values of the slopes are not unity and are different for the different LRSM stations makes this simple interpretation invalid. It is possible to use a relative station correction factor of the form:

$$m_c = \frac{(m_L - L_o)}{P_{LW}}$$

where

$m_c$ = LRSM magnitude corrected relative to WMSO

$m_L$ = magnitude calculated from the LRSM station data

$L_o$ = intercept of the least-square line on the LRSM axis

$P_{LW}$ = slope of least-square line $\frac{\Delta m_L}{\Delta m_W}$

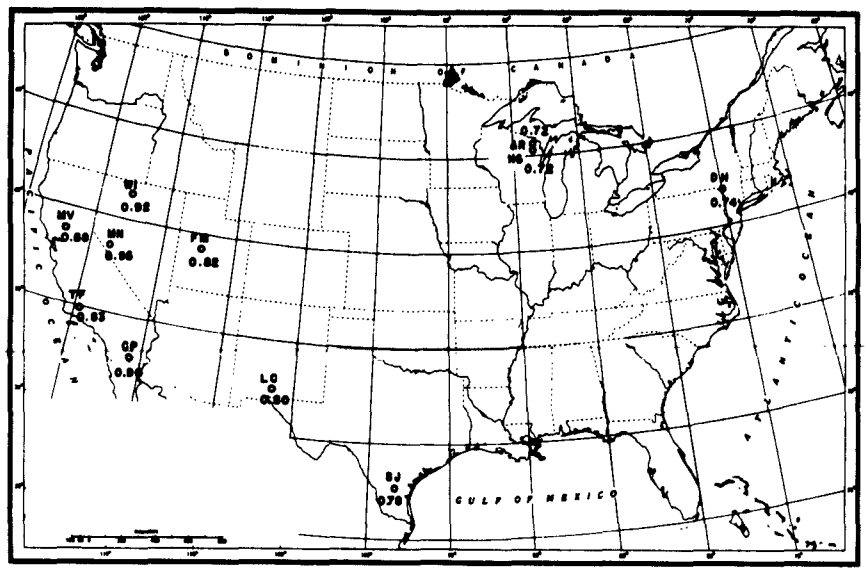


Figure 45. Geographic distribution of the slopes of the least-square lines ($P_{LW}$) obtained from the relationships between $m_p$ computed from LRSM station short-period data and $m_p$ computed from WMSO short-period data, 1 April-30 November 1962

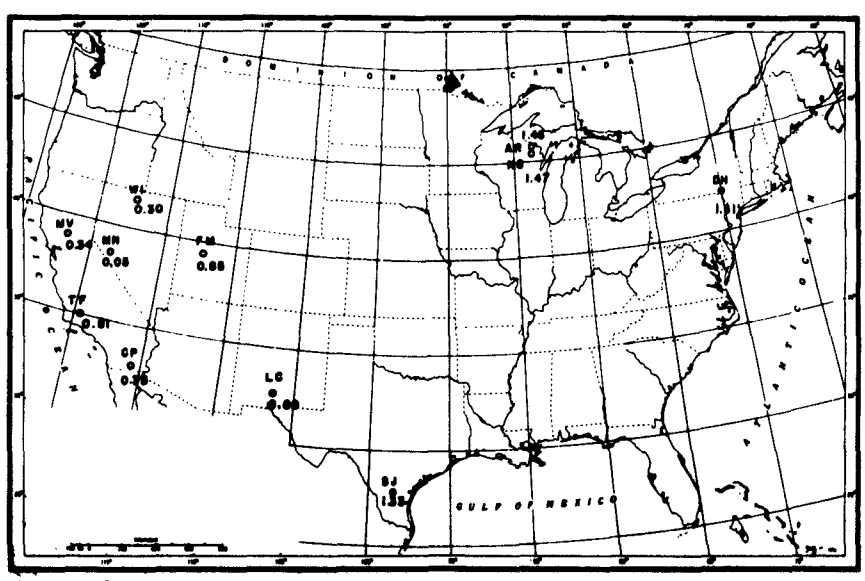


**Figure 46. Geographic distribution of the intercepts of the least-square lines on the LRSM station axes ($L_O$) obtained from the relationships between $m_p$ computed from LRSM station short-period data and WMSO short-period data, 1 April-30 November 1962**

### 6.1.4 WMSO Detection Capabilities Compared to the Detection Capabilities of Observatories With Less Extensive Instrumentation

The earthquake detection capability of WMSO, the prototype Geneva station, has been compared to the detection capabilities of other seismological observatories which are equipped with a less extensive complement of instruments than is WMSO. Seismometric data recorded at WMSO during September, October, and November 1962 were used in this comparison.

In an effort to simulate the data recorded by seismograph systems of less extensive instrumentation, portions of WMSO seismograms were masked by covering part of the viewer screen, leaving only the desired seismograms visible. The records were then analyzed, independent of all previous analysis, and each phase detected was credited to the appropriate system. Figure 47 illustrates the method of masking the seismograms used during this study.

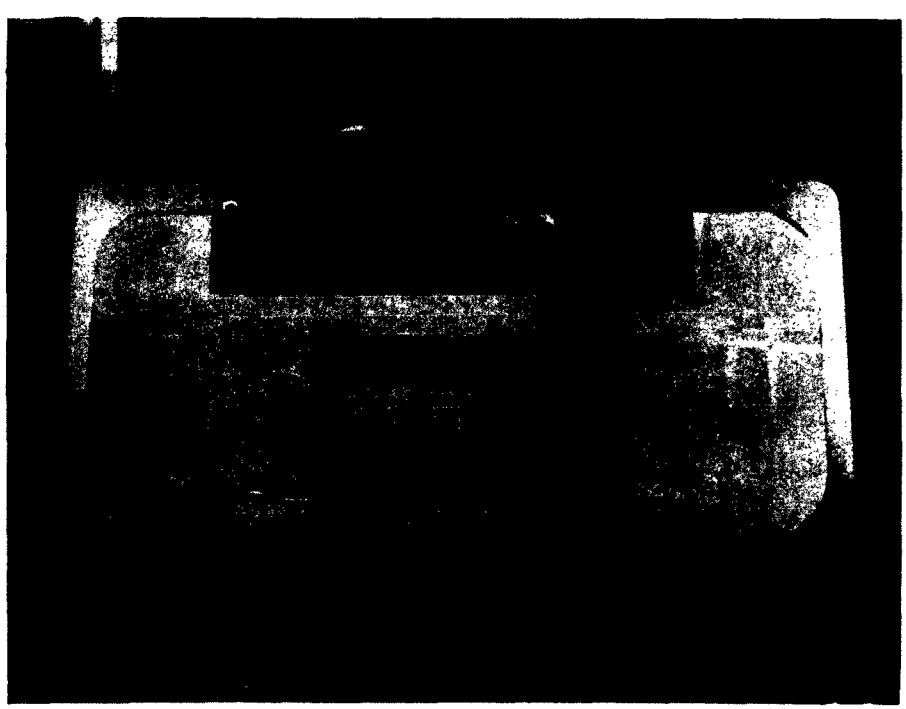

Figure 47. Method of masking WMSO seismograms to simulate the seismograms of other observatories (system A illustrated)

The data samples for this comparative study were pre-selected from the WMSO monthly earthquake bulletin, primarily for a high activity rate. In addition to a high activity rate, an effort was made to select sampling periods which contained activity of varied types and signal levels. The record samples chosen are believed to possess "normal" ratios of teleseismic events to closer events and strong to weak events.

A total of 139.6 hours of non-concurrent record time was selected for use in the evaluation, during which 1092 phases were recorded by the entire WMSO complement of seismographs.

The sampling period has an average activity rate of 7.8 phases per hour. During the entire 3-month (2184-hour) period from 1 September through 30 November 1962, from which the data were selected, approximately 3600 phases were recorded by the WMSO seismographs. The 3-month period from which the samples were chosen had an average activity rate of approximately 1.6 phases per hour; this activity rate is the same as the rate for Phase V.

The activity rate of the sampling period was 4.87 times the normal expected activity rate of Phase V, and the sampling period represents the equivalent of approximately 28.5 days at the normal rate. Because of the high activity rate and the variety of earthquake types and signal levels included in the selected sampling period, the data studied are considered to be sufficiently representative for this evaluation.

In determining the detection capabilities of the lesser systems relative to WMSO, the following assumptions have been made:

a. The lesser systems are operated at magnifications equal to the magnifications at which the respective WMSO seismograph systems are operated, as tabulated in table 3.

b. The average level of the microseismic background noise at observatories operating lesser systems is approximately the same as the average background level of the microseismic noise at WMSO.

c. Data from each of the systems are recorded at the same recording speeds and viewed at the same magnification by observatories operating lesser systems as they are for the respective systems at WMSO.

Nine different seismograph systems were simulated and evaluated, relative to each other, using WMSO data. For convenience, each of the systems evaluated was identified by a letter, as follows:

System A - A three-component short-period system (one short-period Johnson-Matheson vertical seismometer and two short-period Benioff horizontal seismometers).

System B - The three-component short-period system plus a three-component intermediate-band system (one Melton vertical seismometer and two modified Sprengnether horizontal long-period seismometers).

System C - The three-component short period system plus a three-component broad-band system (one Press-Ewing vertical seismometer and two Sprengnether horizontal long-period seismometers).

System D - The three-component short-period system, the three-component intermediate-band system, and the three-component broad-band system.

System E - The three-component short-period system plus a three-component long-period system (one long-period Sprengnether vertical and two horizontal seismometers).

System F - The three-component short-period, intermediate-band, broad-band, and long-period system.

System G - A 10-element, 3 kilometer triangular array of short-period Johnson-Matheson vertical seismometers plus two short-period Benioff horizontal seismometers and one of the vertical array elements operating at one-tenth normal gain (50K).

System H - The 10-element 3-kilometer triangular array, the summation of the 10 array elements, a filtered summation of the 10 array elements, 2 short-period Benioff horizontal seismometers, and one of the vertical array elements operating at one-tenth normal gain (50K).

System I[1] - All of the components of System H plus the three-component intermediate-band, broad-band, and long-period systems.

As the data for each of the simulated systems were analyzed, a "detection credit" was given to the appropriate system for each phase detected. In addition, Systems G, H, and I were awarded a detection credit for each instance in which a signal previously identified as a phase from the three-component short period system was shown to be noise when all ten elements of the array were utilized in analysis, and one of the detection credits previously awarded to Systems A through F was deleted. Therefore, the data tabulated in table 8 should be considered as overall detection credits for each system.

The data samples selected and the detection credits awarded each system from each data sample are tabulated in table 8.

Table 9 is a tabulation of the detection capabilities of the various simulated systems relative to System A (three-component short-period system), and the percentage of WMSO's detection capability each of the systems possesses. The increase in detection capability between System G and System H is attributed to the summing of the outputs of the 10 short-period array elements. If the summation seismographs were displayed alone, however, they would not possess 75.5 percent of the total WMSO detection capability because it would not be possible to distinguish between noise pulses on one or two of the vertical seismographs and a true seismic signal. Furthermore, local, near regional, and regional seismic events would be attenuated by the summation seismographs.

The detection capabilities of WMSO were compared to the detection capabilities of observatories with less extensive instrumentation and results were presented in the final report on Phase II (Geotech Technical Report No. 61-2).

[1] WMSO's full standard instrument complement

Based on conclusions resulting from this comparison, the rates at which the intermediate-band, broad band, and long-period data were recorded on 16-millimeter film were modified in an effort to increase the detection capabilities of each of the systems. The rates at which film records were recorded during Phase V were the modified recording speeds.

Table 8. Data Samples Selected and "Detection Credits" Awarded Each System

| Run number | Date | Time G.C.T. | Hours of data | Detection Credits A | B | C | D | E | F | G | H | I |
|---|---|---|---|---|---|---|---|---|---|---|---|---|
| 259 | 16 Sept 62 | 1900-2400 | 5:00 | 5 | 6 | 13 | 14 | 7 | 16 | 10 | 14 | 25 |
| 264 | 21 | 1800-2400 | 6:00 | 5 | 5 | 5 | 5 | 14 | 14 | 23 | 25 | 34 |
| 265 | 22 | 0500-0830 | 3:30 | 11 | 12 | 14 | 15 | 27 | 26 | 20 | 27 | 42 |
| 267 | 24 | 0920-1520 | 6:00 | 20 | 31 | 20 | 31 | 29 | 40 | 32 | 35 | 55 |
| 269 | 26 | 1000-1630 | 6:30 | 15 | 15 | 15 | 15 | 20 | 20 | 22 | 30 | 35 |
| 271 | 28 | 1840-2300 | 4:20 | 17 | 22 | 20 | 24 | 24 | 28 | 21 | 24 | 35 |
| 275-276 | 02-03 Oct | 2310-0300 | 3:50 | 20 | 26 | 21 | 27 | 29 | 34 | 29 | 34 | 48 |
| 276 | 03 | 1910-2200 | 2:50 | 14 | 14 | 14 | 14 | 16 | 16 | 20 | 24 | 26 |
| 277 | 04 | 0400-0900 | 5:00 | 11 | 11 | 11 | 11 | 16 | 16 | 15 | 22 | 27 |
| 279 | 06 | 0250-1420 | 11:30 | 28 | 30 | 49 | 51 | 78 | 80 | 33 | 54 | 106 |
| 281 | 08 | 2040-2250 | 2:10 | 18 | 18 | 22 | 22 | 24 | 26 | 20 | 21 | 29 |
| 283 | 10 | 2100-2350 | 2:50 | 12 | 14 | 12 | 14 | 15 | 17 | 19 | 19 | 24 |
| 287 | 14 | 0040-1040 | 10:00 | 12 | 13 | 12 | 13 | 19 | 20 | 15 | 22 | 30 |
| 287 | 14 | 1940-2130 | 1:50 | 3 | 6 | 3 | 6 | 4 | 7 | 5 | 6 | 10 |
| 292 | 19 | 2100-2400 | 3:00 | 17 | 17 | 18 | 18 | 18 | 18 | 22 | 23 | 24 |
| 295 | 22 | 2015-2300 | 2:45 | 13 | 14 | 13 | 14 | 13 | 14 | 16 | 18 | 19 |
| 299 | 26 | 1020-1700 | 6:40 | 6 | 8 | 6 | 8 | 23 | 25 | 11 | 14 | 33 |
| 299 | 26 | 2040-2330 | 2:50 | 14 | 14 | 14 | 14 | 14 | 14 | 27 | 30 | 30 |
| 302 | 29 | 1730-1110 | 3:40 | 9 | 9 | 9 | 9 | 12 | 12 | 14 | 24 | 27 |
| 302 | 29 | 2110-2315 | 2:05 | 23 | 23 | 24 | 24 | 29 | 29 | 22 | 26 | 32 |
| 305 | 01 Nov | 1810-2340 | 5:30 | 24 | 24 | 24 | 24 | 31 | 31 | 28 | 33 | 40 |
| 312 | 08 | 0010-0450 | 4:40 | 9 | 9 | 10 | 10 | 19 | 19 | 17 | 29 | 39 |
| 312 | 08 | 1630-2315 | 6:45 | 33 | 33 | 33 | 33 | 35 | 35 | 47 | 56 | 58 |
| 313 | 09 | 1700-2340 | 6:40 | 34 | 37 | 36 | 39 | 39 | 42 | 40 | 50 | 58 |
| 314 | 10 | 0920-1100 | 1:30 | 6 | 8 | 6 | 8 | 9 | 11 | 13 | 24 | 29 |
| 315 | 11 | 0655-1210 | 5:15 | 16 | 26 | 17 | 27 | 23 | 33 | 22 | 43 | 50 |
| 316 | 12 | 1940-2300 | 3:20 | 13 | 14 | 13 | 14 | 17 | 18 | 19 | 27 | 31 |
| 317 | 13 | 2020-2400 | 3:40 | 27 | 27 | 27 | 27 | 27 | 27 | 33 | 33 | 33 |
| 325 | 21 | 1755-2200 | 4:05 | 13 | 15 | 13 | 15 | 13 | 15 | 16 | 20 | 20 |
| 332 | 28 | 2000-2345 | 3:45 | 15 | 18 | 15 | 18 | 15 | 18 | 19 | 21 | 21 |
| 334 | 30 | 2155-2400 | 2:05 | 11 | 15 | 14 | 18 | 15 | 19 | 17 | 18 | 22 |
| TOTALS | | | 139:35 | 474 | 534 | 523 | 582 | 674 | 740 | 667 | 846 | 1092 |

Table 9. WMSO Detection Capabilities Compared to the Detection Capabilities of Observatories With Less Extensive Instrumentation

| SYSTEM | A | B | C | D | E | F | G | H | I |
|---|---|---|---|---|---|---|---|---|---|
| Instrumentation | SP-Z, N, E | SP-Z N, E & IB-Z, N, E | SP-Z, N, E & BB-Z, N, E | SP-Z, N, E; IB-Z, N, E & BB-Z, N, E | SP-Z, N, E & LP-Z N, E | SP-Z N, E; IB-Z, N, E; BB-Z, N, E & LP-Z, N, E | 10SP-Z, SPN & E | 10SP-Z, SPN & E; Σ10 SPZ Σ10 SPZ filtered | Complete complement of WMSO instruments |
| Ratio of detection capability of indicated system to detection capability of System A | 1.00 | 1.13 | 1.10 | 1.23 | 1.42 | 1.56 | 1.41 | 1.78 | 2.30 |
| Percentage of WMSO full detection capability possessed by indicated systems | 43.4% | 48.9% | 47.9% | 53.3% | 61.7% | 67.8% | 61.1% | 75.5% | 100.0% |

Table 10 lists the Phase II recording rates, the rates recommended at the end of Phase II, and recording rates during Phase V.

In comparing the results of the evaluation during Phase II with the results of the evaluation during Phase V, it should be noted that for systems whose recording rates were modified according to the recommendations made at the end of Phase II, the relative detection capabilities increased. For the broad-band system, whose recording rate was not modified according to the recommendations of Phase II, the relative detection capability decreased. See table 11.

Table 10. Past and Present Rates for Recording Seismometric Data on 16-Millimeter Develocorder Film at WMSO

| System | Recording rate used during Phase II | Recording rates recommended at the end of Phase II | Recording rates used during Phase V |
|---|---|---|---|
| Short-Period | 30 mm/min | 30 mm/min | 30 mm/min |
| Intermediate-Band | 6 mm/min | 24 mm/min | 30 mm/min |
| Broad-Band | 6 mm/min | 12 mm/min | 3 mm/min |
| Long-Period | 6 mm/min | 3 mm/min | 3 mm/min |

Table 11. WMSO's Relative Detection Capability as Determined During Phase V Compared to Phase II

| System[a] | A | B | C | D | E | F | G | H | I |
|---|---|---|---|---|---|---|---|---|---|
| Ratio of detection capability of indicated system to detection capability of system A during Phase II | 1.00 | 1.07 | 1.19 | Not evaluated during Phase II | 1.31 | Not evaluated during Phase II | Not evaluated during Phase II | 1.74 | 2.19 |
| Ratio of detection capability of indicated system to detection capability of system A during Phase V | 1.00 | 1.13 | 1.10 | 1.23 | 1.42 | 1.56 | 1.41 | 1.78 | 2.30 |
| Percentage change from Phase II to Phase V | - | 6% | -8% | - | 8.5% | - | - | 2.5% | 10% |

[a]Systems A through I are defined in section 6.2.6.

The improvement in the detection capabilities of Systems H and I during Phase V are attributed to two factors. First, a 3-kilometer triangular array was installed in place of the H array operated during Phase II; and second, the improvement in the detection capabilities of Systems B and E, as the result of modified recording rates, are reflected in the total WMSO capability (System I).

### 6.1.5 Relative Phase Detection Capability of the Individual WMSO Systems

The relative phase detection capabilities of the four standard WMSO seismograph systems (SP, IB, BB, and LP) and two test seismographs (JM 20 and SIE) were evaluated with respect to phase and earthquake type. A 3-month data sample was selected (September, October, and November), and the manner in which each phase was detected by each system during this period was evaluated. Only those events for which epicentral information was available from the USC&GS, or for which distance could be determined using S-P times, were used. The system which detected a phase "best" was awarded a one (1), second best a two (2), etc. Best, as used in this evaluation, is defined as a measure of both clarity of the phase as seen by the analyst and the signal-to-noise ratio. When a phase was recorded equally well on two or more systems, each system was awarded the same rating. If a seismograph system failed to record a given phase, no capability was indicated.

The number of times each seismograph system detected a given phase best, second best, third best, etc., are tabulated in table 12.

Table 13 shows the overall relative phase detection capability by phase and earthquake type for each of the systems evaluated.

The capability of each seismograph system to detect any part of each teleseismic earthquake in percentage of the total number recorded at WMSO during the sampling period is tabulated in table 14. Again, only earthquakes for which accurate epicentral data are available were used. The percentage of earthquakes detected by a given system is also tabulated. Accurate epicentral data were available for a total of 526 earthquakes recorded at WMSO during September, October, and November 1962.

Table 12. Number of Times the Indicated Phases Were Detected by Each Seismograph, Showing Relative Detection Capability

| System Relative Detection Capability | Phase | SP | | | | IB | | | | | BB | | | | | | LP | | | | | JM 20 | | | | | SIE | | | | | |
|---|---|---|---|---|---|---|---|---|---|---|---|---|---|---|---|---|---|---|---|---|---|---|---|---|---|---|---|---|---|---|---|---|
| | | 1 | 2 | 3 | 4 | 1 | 2 | 3 | 4 | 5 | 1 | 2 | 3 | 4 | 5 | 6 | 1 | 2 | 3 | 4 | 5 | 1 | 2 | 3 | 4 | 5 | 1 | 2 | 3 | 4 | 5 | 6 |
| Teleseisms with known epicenters | P or P' | 269 | 0 | 0 | 1 | 1 | 3 | 103 | 50 | 1 | 0 | 1 | 4 | 14 | 12 | 2 | 0 | 1 | 4 | 3 | 3 | 4 | 236 | 2 | 0 | 0 | 2 | 8 | 84 | 26 | 1 | 1 |
| | PP | 58 | 5 | 1 | 0 | 0 | 3 | 24 | 4 | 0 | 0 | 1 | 3 | 4 | 0 | 0 | 10 | 0 | 1 | 1 | 0 | 3 | 55 | 4 | 1 | 0 | 1 | 0 | 7 | 4 | 0 | 0 |
| | pP | 13 | 0 | 0 | 0 | 0 | 0 | 7 | 2 | 0 | 0 | 2 | 1 | 0 | 0 | 0 | 1 | 0 | 0 | 0 | 1 | 0 | 11 | 0 | 1 | 0 | 0 | 0 | 3 | 1 | 1 | 0 |
| | PcP | 34 | 0 | 0 | 1 | 0 | 0 | 9 | 9 | 0 | 0 | 0 | 0 | 0 | 2 | 0 | 0 | 0 | 0 | 0 | 0 | 1 | 30 | 0 | 0 | 0 | 0 | 2 | 12 | 2 | 0 | 0 |
| | PPP | 0 | 0 | 0 | 1 | 0 | 0 | 1 | 0 | 0 | 1 | 0 | 0 | 0 | 0 | 0 | 2 | 1 | 0 | 0 | 0 | 0 | 0 | 0 | 0 | 1 | 0 | 0 | 0 | 0 | 0 | 0 |
| | S | 10 | 2 | 3 | 1 | 1 | 2 | 6 | 2 | 0 | 3 | 9 | 0 | 3 | 0 | 0 | 45 | 0 | 1 | 0 | 0 | 0 | 2 | 1 | 2 | 0 | 0 | 0 | 1 | 0 | 0 | 0 |
| | PS & SP | 0 | 1 | 0 | 0 | 0 | 0 | 1 | 0 | 0 | 2 | 5 | 0 | 0 | 0 | 0 | 20 | 0 | 0 | 0 | 0 | 0 | 0 | 0 | 1 | 0 | 0 | 0 | 0 | 0 | 0 | 0 |
| | PPS & SPP | 0 | 1 | 0 | 0 | 0 | 0 | 1 | 0 | 0 | 1 | 3 | 0 | 0 | 0 | 0 | 15 | 0 | 0 | 0 | 0 | 0 | 0 | 0 | 1 | 0 | 0 | 0 | 0 | 0 | 0 | 0 |
| | SS | 0 | 0 | 0 | 0 | 0 | 0 | 0 | 0 | 0 | 0 | 6 | 0 | 0 | 0 | 0 | 27 | 0 | 0 | 0 | 0 | 0 | 0 | 0 | 0 | 0 | 0 | 0 | 0 | 0 | 0 | 0 |
| | PKKP | 46 | 1 | 0 | 0 | 0 | 1 | 13 | 2 | 0 | 0 | 0 | 0 | 0 | 0 | 0 | 0 | 0 | 0 | 0 | 0 | 12 | 29 | 0 | 0 | 0 | 1 | 1 | 3 | 0 | 0 | 0 |
| | P'P' | 11 | 0 | 0 | 0 | 0 | 0 | 2 | 0 | 0 | 0 | 0 | 0 | 0 | 0 | 0 | 0 | 0 | 0 | 0 | 0 | 0 | 9 | 0 | 0 | 0 | 0 | 0 | 0 | 0 | 0 | 0 |
| | SKP | 6 | 1 | 0 | 0 | 0 | 0 | 4 | 1 | 0 | 0 | 0 | 0 | 1 | 0 | 0 | 0 | 0 | 0 | 0 | 0 | 0 | 6 | 1 | 0 | 0 | 0 | 0 | 4 | 1 | 0 | 0 |
| | SKS | 3 | 1 | 1 | 0 | 0 | 2 | 1 | 1 | 0 | 1 | 4 | 0 | 0 | 0 | 0 | 11 | 0 | 0 | 0 | 0 | 0 | 1 | 2 | 0 | 0 | 0 | 0 | 0 | 0 | 1 | 0 |
| | SKKS | 1 | 1 | 0 | 0 | 0 | 1 | 0 | 1 | 0 | 0 | 0 | 1 | 0 | 0 | 0 | 9 | 0 | 1 | 0 | 0 | 0 | 0 | 0 | 1 | 0 | 0 | 0 | 0 | 0 | 0 | 0 |
| | L | 0 | 0 | 0 | 0 | 0 | 0 | 0 | 0 | 0 | 0 | 0 | 0 | 0 | 0 | 0 | 19 | 0 | 0 | 0 | 0 | 0 | 0 | 0 | 0 | 0 | 0 | 0 | 0 | 0 | 0 | 0 |
| | R | 10 | 3 | 0 | 0 | 1 | 4 | 5 | 2 | 0 | 2 | 48 | 5 | 3 | 0 | 0 | 33 | 1 | 1 | 0 | 0 | 2 | 2 | 1 | 0 | 0 | 1 | 4 | 1 | 2 | 1 | 0 |
| Regionals | P | 32 | 4 | 1 | 0 | 0 | 5 | 4 | 6 | 0 | 0 | 0 | 0 | 0 | 0 | 0 | 0 | 0 | 0 | 0 | 0 | 14 | 18 | 0 | 0 | 0 | 1 | 5 | 10 | 0 | 0 | 0 |
| | Lg | 35 | 1 | 1 | 0 | 0 | 5 | 10 | 6 | 0 | 0 | 0 | 2 | 2 | 0 | 0 | 1 | 0 | 1 | 0 | 1 | 5 | 26 | 2 | 0 | 0 | 1 | 5 | 10 | 3 | 0 | 0 |
| Locals and Near Regionals | P | 95 | 87 | 18 | 0 | 0 | 10 | 40 | 10 | 0 | 0 | 0 | 0 | 0 | 0 | 0 | 0 | 0 | 0 | 0 | 0 | 147 | 43 | 2 | 0 | 0 | 42 | 51 | 31 | 1 | 0 | 0 |
| | S | 183 | 13 | 2 | 0 | 0 | 53 | 65 | 33 | 0 | 0 | 0 | 0 | 0 | 0 | 0 | 0 | 0 | 0 | 0 | 0 | 84 | 100 | 2 | 0 | 0 | 46 | 41 | 49 | 2 | 0 | 0 |
| | Lg | 41 | 1 | 0 | 0 | 0 | 2 | 22 | 14 | 0 | 0 | 0 | 0 | 0 | 0 | 0 | 0 | 0 | 0 | 0 | 0 | 11 | 30 | 0 | 0 | 0 | 3 | 14 | 24 | 1 | 0 | 0 |

Table 13. Overall Relative Phase Detection Capability for Each WMSO System, by Phase

| Type of earthquake | Phase | Seismograph SP | IB | BB | LP | JM20 | SIE |
|---|---|---|---|---|---|---|---|
| Teleseism | P or P' | 1 | 3 | 5 | 6 | 2 | 4 |
| | PP | 1 | 3 | 6 | 4 | 2 | 5 |
| | pP | 1 | 3 | 4 | 6 | 2 | 5 |
| | PcP | 1 | 4 | 5 | - | 2 | 3 |
| | PPP | 4 | 3 | 2 | 1 | - | - |
| | S | 2 | 4 | 3 | 1 | - | - |
| | PS & SP | 3 | 4 | 2 | 1 | 5 | - |
| | PPS & SPP | 3 | 4 | 2 | 1 | 5 | - |
| | SS | - | - | 2 | 1 | - | - |
| | PKKP | 1 | 3 | - | - | 2 | 4 |
| | P' P' | 1 | 3 | - | - | 2 | - |
| | SKP | 1 | 3 | 5 | - | 2 | 3 |
| | SKS | 2 | 4 | 2 | 1 | 5 | - |
| | SKKS | 2 | 3 | 4 | 1 | - | - |
| | Love | - | - | - | 1 | - | - |
| | Rayleigh | 3 | 4 | 2 | 1 | 6 | 5 |
| Regional | P | 1 | 3 | 2 | 1 | 6 | 5 |
| | Lg | 1 | 3 | 5 | 5 | 2 | 3 |
| Local and near-regional | P | 2 | 4 | - | - | 1 | 3 |
| | S | 1 | 4 | - | - | 2 | 3 |
| | Lg | 1 | 4 | - | - | 2 | 3 |

(Note: 1 indicates greatest capability; 2 indicates second greatest capability, etc.)

Table 14. Individual WMSO System Capability

| | Seismograph System SP | IB | BB | LP | JM20 | SIE |
|---|---|---|---|---|---|---|
| Percentage of total earthquakes recorded at WMSO detected by the indicated seismograph | 96.5% | 66.7% | 24.3% | 29.1% | 90.5% | 54.5% |
| Percentage of total earthquakes recorded at WMSO detected solely by the indicated seismograph | 2.3% | 0 | 0 | 3.6% | 0 | 0 |

## 6.2 QUARRY BLAST STUDY

During Phase V, a mobile seismograph was developed for the purpose of determining origin times of quarry blasts which are normally recorded at WMSO. A block diagram of the seismograph and timing circuits is shown in figure 48. Information was collected on the location of major quarries in the area surrounding WMSO and owners or superintendents of the quarries were contacted for permission to record origin times at the quarry sites. All but 3 quarries (2 owned by the same company) appeared willing to cooperate.

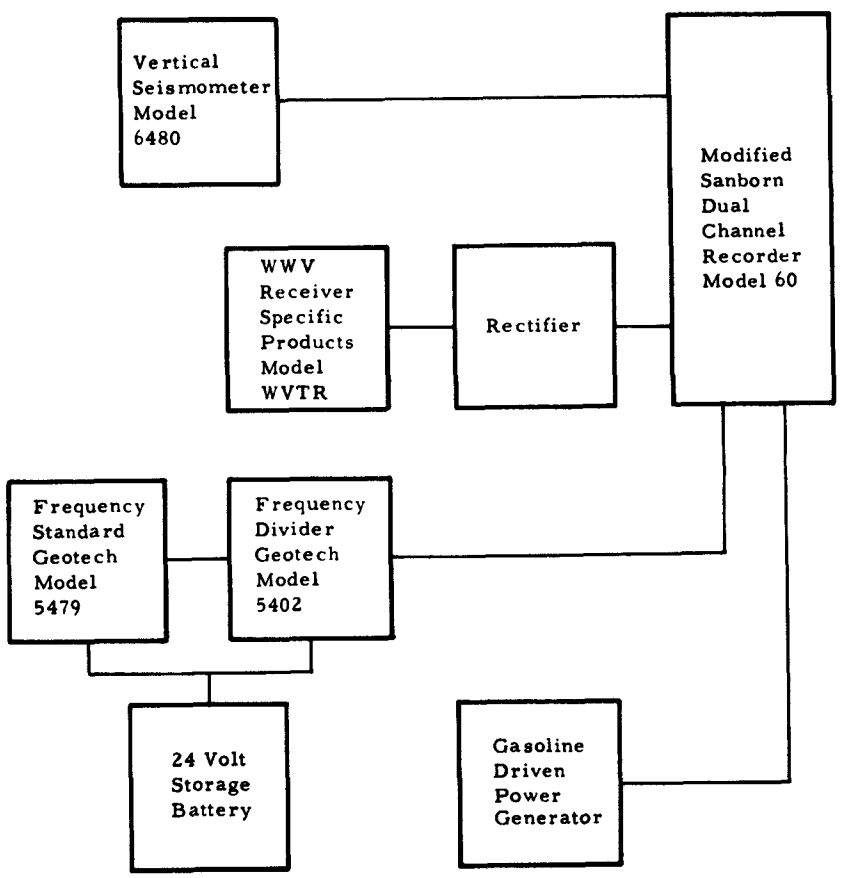


Figure 48. Block diagram of equipment used to record quarry blasts

## 6.2 QUARRY BLAST STUDY

During Phase V, a mobile seismograph was developed for the purpose of determining origin times of quarry blasts which are normally recorded at WMSO. A block diagram of the seismograph and timing circuits is shown in figure 48. Information was collected on the location of major quarries in the area surrounding WMSO and owners or superintendents of the quarries were contacted for permission to record origin times at the quarry sites. All but 3 quarries (2 owned by the same company) appeared willing to cooperate.

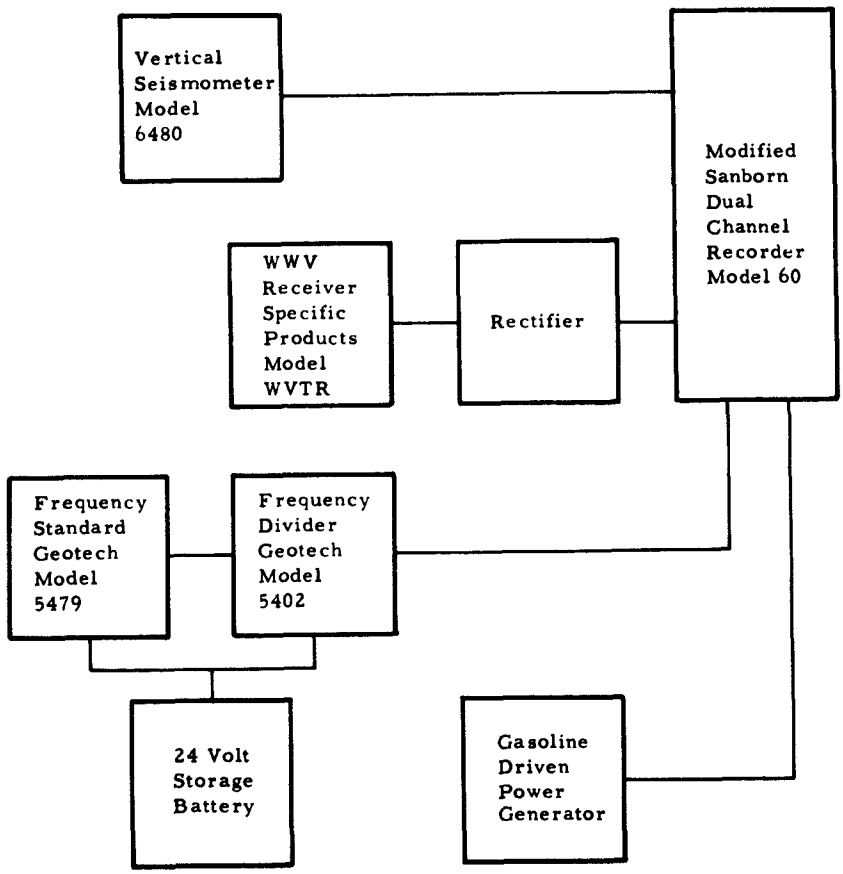


Figure 48. Block diagram of equipment used to record quarry blasts

Table 15 lists all known major quarry locations in the WMSO area and figure 49 is a plot of these quarry locations showing bearing and distance from WMSO.

Origin times were recorded for blasts at 5 different quarry locations during Phase V and the origin times of 2 blasts were recorded at 1 of the quarries. Table 16 lists the quarries, origin times, and travel times of the phases recorded at WMSO from each of these blasts.

The Gifford-Hill Co. supplied information on the amount of explosive used in 98 blasts detonated at its quarry near Chico, Texas, from May through September 1962. Of the 98 blasts detonated, 57 P phases were recorded at WMSO. Blasts from which P phases were not recorded were either stripping shots, or utilized less than 1700 pounds of explosives.

Figure 50 is a plot of the maximum ground displacement for the P phase of each blast recorded as a function of weight of explosives detonated. More than 85 percent of the P phases recorded had a period of 0.3 second and all of them were within the range 0.2 to 0.4 second. According to a least-squares fit of the data points, the ground displacement is proportional to the 0.84 power of the weight of explosives detonated according to the following relationship:

$$A = 1.2\ W^{0.84}$$

where A is the ground displacement in millimicrons and W is the weight of explosives in thousands of pounds. Four data points at 2 millimicrons were not considered in computing the least-squares fit because of the low accuracy of measurement of that amplitude from WMSO seismograms.

## 6.3 ARRAY CHARACTERISTICS

Three array configurations have been operated at WMSO and a fourth array configuration is planned. The characteristics of the individual instruments used in all of the arrays are essentially identical; however, the characteristics of the arrays are markedly different due to differences in configuration and in the number of instruments employed.

The most important characteristics associated with the arrays are noise cancellation, directional response and alteration of signal character. The study which is discussed in this section is planned to yield data on the last 2 characteristics.

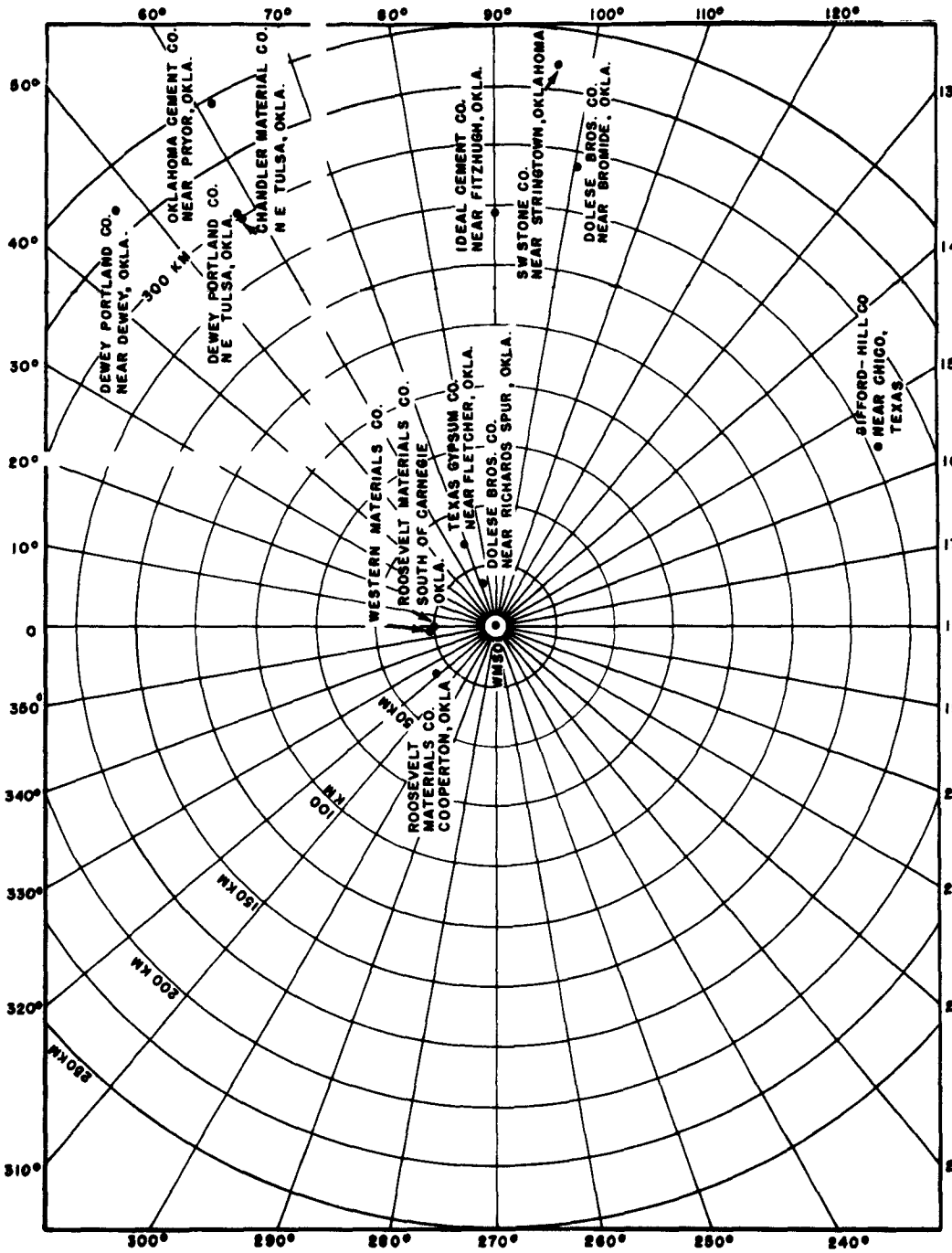


Figure 49. Polar plot showing locations of quarries relative to WMSO

Table 15. Locations of Quarries in the WMSO Area

| Quarry | Location | Latitude (N) | Longitude (W) | Bearing from WMSO (deg) | Distance from WMSO (deg) | Distance from WMSO (km) |
|---|---|---|---|---|---|---|
| Gifford-Hill Company | Chico, Texas | 33°16'10.0"[a] | 97°46'40.5" | 154.76 | 1.594 | 177.29 |
| Ideal Cement Company | Fitzhugh, Oklahoma | 34°42'00.0"[b] | 96°43'42.0" | 90.14 | 1.532 | 170.46 |
| Roosevelt Materials Company | Cooperton, Oklahoma | 34°56'39.5"[a] | 98°48'44.8" | 321.38 | 0.289 | 32.17 |
| Roosevelt Materials Company | South of Carnegie, Oklahoma | 34°57'18.0"[b] | 98°37'18.0" | 358.05 | 0.236 | 26.30 |
| Western Materials Company | South of Carnegie, Oklahoma | 34°58'06.0"[b] | 98°37'47.0" | 356.11 | 0.250 | 27.83 |
| Texas Gypsum Company | Fletcher, Oklahoma | 34°50'00.0"[a] | 98°13'47.5" | 68.57 | 0.316 | 35.16 |
| Southwest Stone Company | Stringtown, Oklahoma | 34°28'15.0"[b] | 96°03'24.0" | 96.10 | 2.103 | 233.91 |
| Dolese Brothers | Bromide, Oklahoma | 34°25'24"[b] | 96°30'54.0" | 99.16 | 1.736 | 193.09 |
| Dolese Brothers | Richards Spur, Oklahoma | 34°45'48.0"[a] | 98°23'48.0" | 73.86 | 0.163 | 18.13 |
| Chandler Materials Company | Northeast of Tulsa, Oklahoma | 36°11'12.0"[b] | 95°49'30.0" | 56.21 | 2.690 | 299.16 |
| Oklahoma Cement Company | Pryor, Oklahoma | 36°16'18.0"[b] | 95°17'30.0" | 59.11 | 3.105 | 345.26 |
| Dewey Portland Cement Co. | Dewey, Oklahoma | 36°47'54.0"[b] | 95°55'30.0" | 45.46 | 3.000 | 333.63 |
| Dewey Portland Cement Co. | Northeast of Tulsa, Oklahoma | 36°12'10.0"[b] | 95°49'25.0" | 55.93 | 2.700 | 300.23 |

[a]Coordinates - United States Department of the Interior, Geological Survey
[b]Coordinates - Mineral map of Oklahoma by John H. Warren - 1955
WMSO Z6: 34°43'05.3"N
98°35'20.7"W

Table 16. Origin Times Recorded and Travel Times Computed by WMSO from Quarry Blasts

| Quarry | Δ (km) | Bearing from WMSO (deg) | Date and time of origin (G. C. T.) | Pounds of explosives | Phase arrival times (Z6) (G. C. T.) | Phase travel time (sec) | S-P (sec) | Velocity (km/sec) | $\frac{V_P}{V_S}$ |
|---|---|---|---|---|---|---|---|---|---|
| Gifford-Hill Company | 177.29 | 154.76 | 01 Oct 1962 23:35:35.85 | 13,000 | eP 23:36:04.8 | 28.95 | | 6.12 | 1.74 |
| | | | | | e 23:36:14.8 | 38.95 | | 4.55 | |
| | | | | | eS 23:36:26.4 | 50.55 | 21.6 | 3.51 | |
| Gifford-Hill Company | 177.29 | 154.76 | 10 Jan 1963 22:58:37.82 | 4,800 | eP 22:59:07.0 | 29.18 | | 6.08 | |
| | | | | | eS 22:59:29.0 | 51.18 | 22.0 | 3.46 | 1.76 |
| Ideal Cement Company | 170.46 | 90.14 | 06 Dec 1962 20:45:30.14 | 35,000 | eP 20:45:57.8 | 27.66 | | 6.16 | |
| | | | | | e 59.1 | 28.96 | | 5.89 | |
| | | | | | e 46:06.7 | 36.56 | 20.9 | 4.66 | 1.76 |
| | | | | | e 16.7 | 46.56 | | 3.66 | |
| | | | | | eS 18.7 | 48.56 | | 3.51 | |
| Roosevelt Material Company | 32.17 | 321.38 | 23 Oct 1962 17:55:58.82 | 155,000 | eP 17:56:04.2 | 05.38 | | 5.98 | |
| | | | | | * | | | | |
| Texas Gypsum Company | 35.16 | 68.57 | 20 Sept 1962 17:27:05.09 | 3,000 | eP 17:27:11.9 | 06.81 | | 5.16 | |
| | | | | | eS 17.3 | 11.21 | 05.4 | 3.14 | 1.64 |
| | | | | | esur 22.5 | 16.91 | | 2.08 | |
| Chandler Material Company | 299.2 | 56.21 | 26 Feb 1963 21:30:01.16 | 11,100 | ** | | | | |
| | | | | | e(sur) 21:31:09.5 | 68.34 | | 4.38 | |
| | | | | | e 24.3 | 83.14 | | 3.60 | |

* "S" cannot be timed accurately due to intermingling of traces
** Initial arrival not recorded.

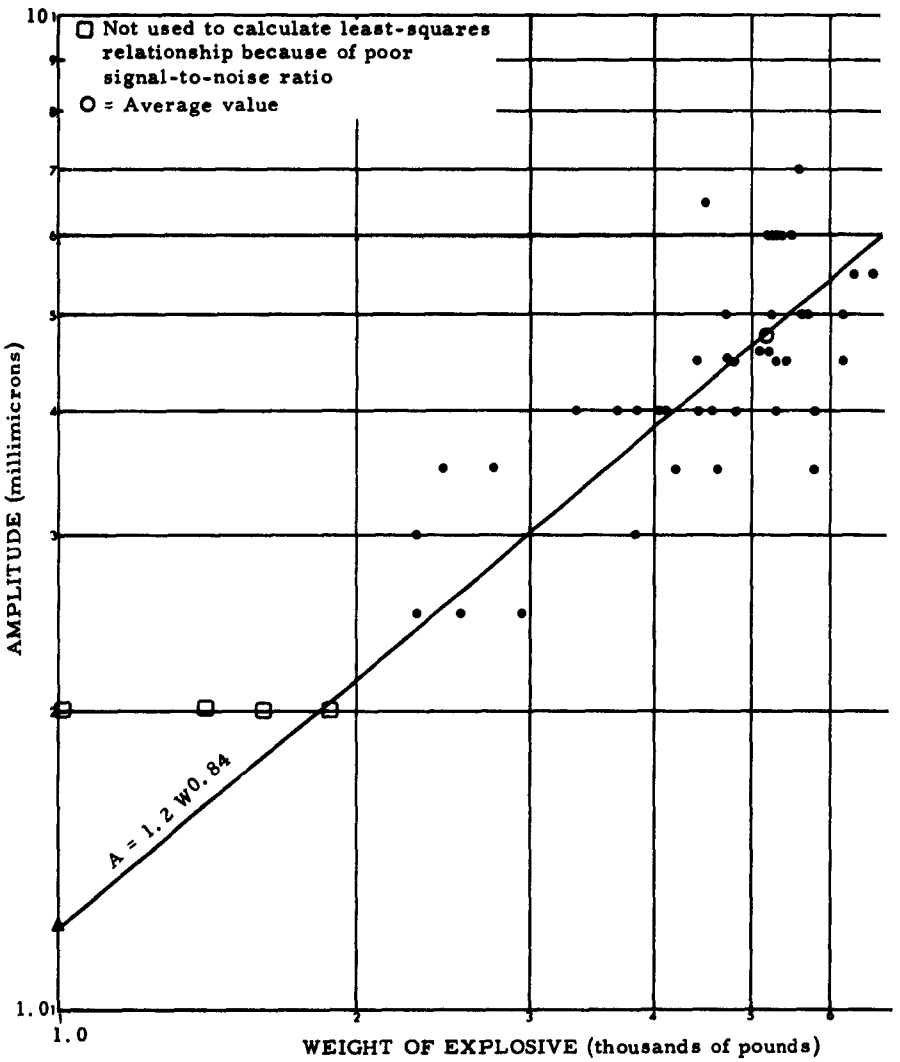


Figure 50. Ground displacement at WMSO as a function of weight of explo blasts detonated by a single quarry 177.3 kilometers from WMSO ( Chico, Texas). (A= ground amplitude in mμ, peak-to-peak; W = weight of explosives in thousands of pounds.)

The response of each array was calculated for a sinusoidal signal and for a typical signal from a teleseism with $\Delta \simeq 26$ degrees, both having a measured period of 1.0 second and an apparent surface velocity of 12 kilometers per second. Data obtained from the calculations involving the sinusoidal signal show a close correspondance to the data from the typical signal calculations except under conditions where appreciable signal cancellation occurs. The simpler method involving a sinusoidal signal may be used to obtain valid data for earthquake signals under conditions where signal cancellation is slight.

The following procedure was used in calculating the response of an array to a sinusoidal signal.

a. A relative bearing angle, $\alpha$, was chosen and the signal path plotted on a scale map of the array.

b. A wave front was established through the seismometer position selected as reference.

c. The delay times ( td ) were determined for the remaining seismometer positions.

d. The peak value S, the percentage response, was computed.

$$S = \frac{100}{n} \sum_{i=1}^{n} \sin k\,(T - td_i)$$

where

$n$ = number of seismometers

$k$ = conversion factor $\left(\frac{360^\circ}{\text{period}}\right)$

$t$ = time

$td_i$ = delay times for the individual seismometers.

The steps required for the computation of the response of an array to a typical teleseismic signal are listed below.

Steps a, b, and c are the same as for a sinusoidal signal.

d. A typical signal was selected from a Develocorder record and an amplitude time table which described the selected signal was tabulated. This tabulated function is designated A(t).

e. The percentage response (R) of the array summation to the signal for approximately 25 values of time (t) was computed by using the following formula:

$$R = \frac{100}{nA(t)} \sum_{i=1}^{n} A(t - td_i);\ n = \text{number of values of } t$$

f. R as a function of t was plotted and the maximum peak-to-peak amplitude was read from the plot.

The directional responses of the arrays are shown in figures 51, 52, 53, and 54. From these, it may be seen that the triangular array and the Star-of-David array are essentially omnidirectional for the teleseismic signal period and surface velocity. The H array response shows slight directional characteristics and the linear array response indicates that signals approaching in a direction parallel to the array axis undergo extreme cancellation.

The array summation response to a typical teleseismic signal is shown in figure 55. The summation response for the linear array with $\alpha = 0^{\circ}$ (broadside) is identical to the signal from each individual seismometer, since no cancellation occurs at this relative bearing angle. The summation signals for the linear array for other values of $\alpha$ show a reduction in amplitude, a smoothing of the curve (due to greater cancellation of the high-frequency components), and period elongation. The period elongation results from the fact that low-frequency components undergo less cancellation than the dominant frequency component.

The summation responses to the same signal for the other arrays show reduced amplitude and smoother curves, but there is no appreciable change in period.

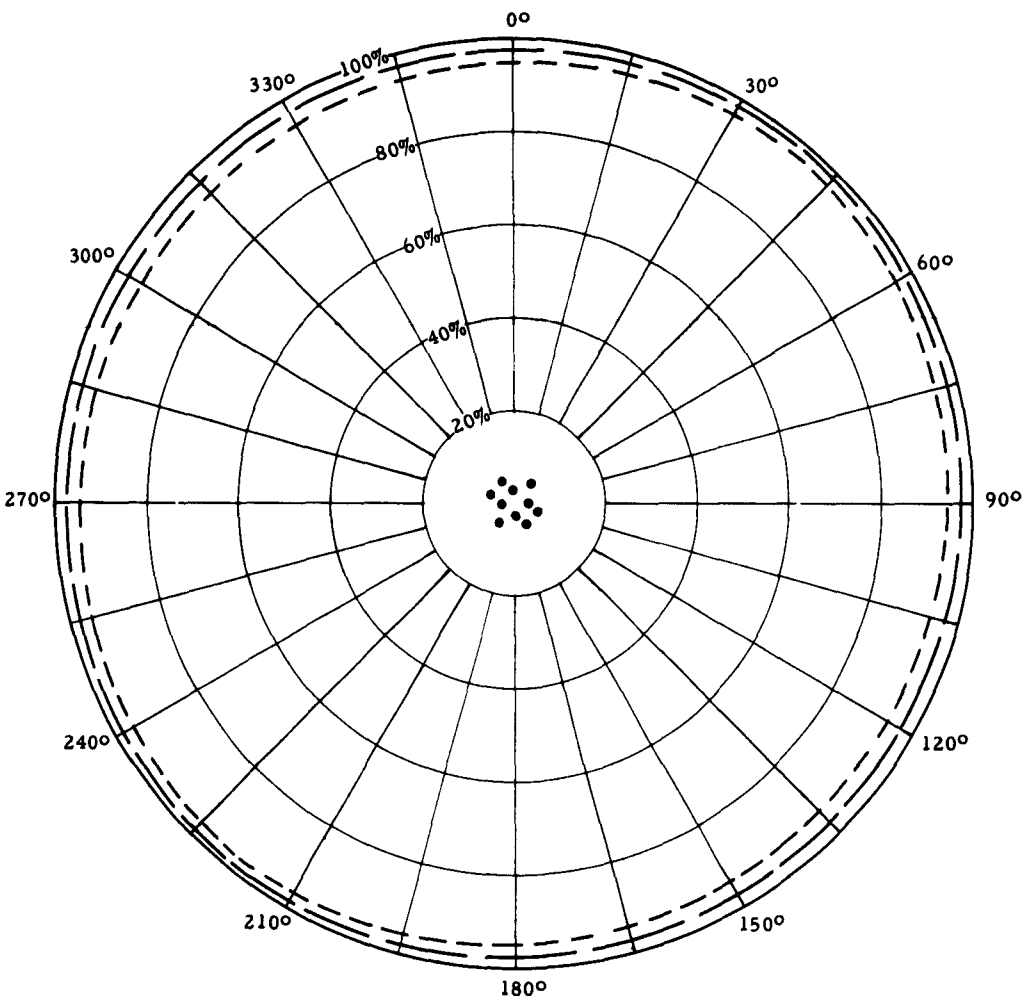


Array consists of ten seismometers with approximate 0.6 km spacing

—— —— = Response to a typical teleseismic signal with a 1-second period and 12 km/sec surface velocity (maximum deviation = 2.0%)

- - - - - - = Response to a sinosoidal signal with a 1-second period and 12 km/sec surface velocity (maximum deviation = 3.1%)

100% is considered to be the summation output with no cancellation.

Figure 51. Directional response of the H array

The steps required for the computation of the response of an array to a typical teleseismic signal are listed below.

Steps a, b, and c are the same as for a sinusoidal signal.

d. A typical signal was selected from a Develocorder record and an amplitude time table which described the selected signal was tabulated. This tabulated function is designated A(t).

e. The percentage response (R) of the array summation to the signal for approximately 25 values of time (t) was computed by using the following formula:

$$R = \frac{100}{nA(t)} \sum_{i=1}^{n} A(t - td_i);\ n = \text{number of values of } t$$

f. R as a function of t was plotted and the maximum peak-to-peak amplitude was read from the plot.

The directional responses of the arrays are shown in figures 51, 52, 53, and 54. From these, it may be seen that the triangular array and the Star-of-David array are essentially omnidirectional for the teleseismic signal period and surface velocity. The H array response shows slight directional characteristics and the linear array response indicates that signals approaching in a direction parallel to the array axis undergo extreme cancellation.

The array summation response to a typical teleseismic signal is shown in figure 55. The summation response for the linear array with $\alpha = 0^{\circ}$ (broadside) is identical to the signal from each individual seismometer, since no cancellation occurs at this relative bearing angle. The summation signals for the linear array for other values of $\alpha$ show a reduction in amplitude, a smoothing of the curve (due to greater cancellation of the high-frequency components), and period elongation. The period elongation results from the fact that low-frequency components undergo less cancellation than the dominant frequency component.

The summation responses to the same signal for the other arrays show reduced amplitude and smoother curves, but there is no appreciable change in period.

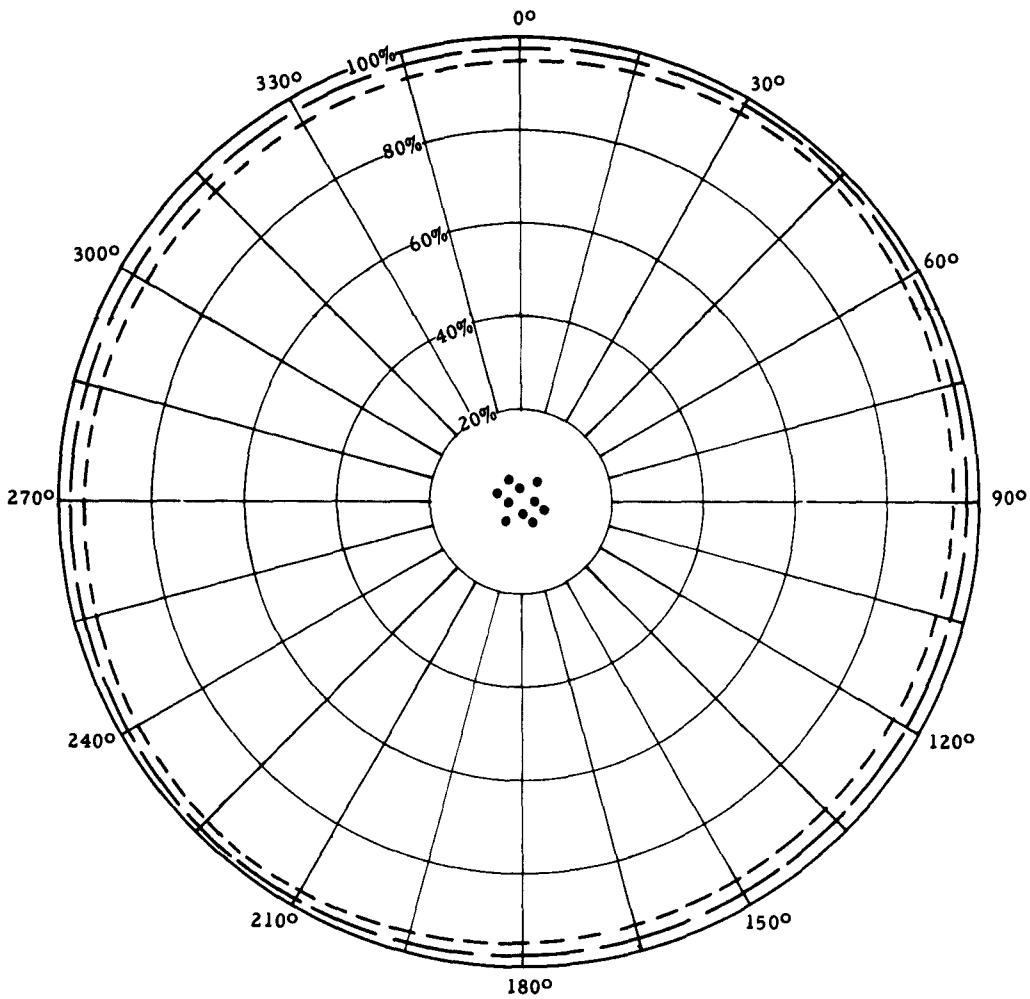


Array consists of ten seismometers with approximate 0.6 km spacing

—— —— = Response to a typical teleseismic signal with a 1-second period and 12 km/sec surface velocity (maximum deviation = 2.0%)

- - - - - - = Response to a sinosoidal signal with a 1-second period and 12 km/sec surface velocity (maximum deviation = 3.1%)

100% is considered to be the summation output with no cancellation.

Figure 51. Directional response of the H array

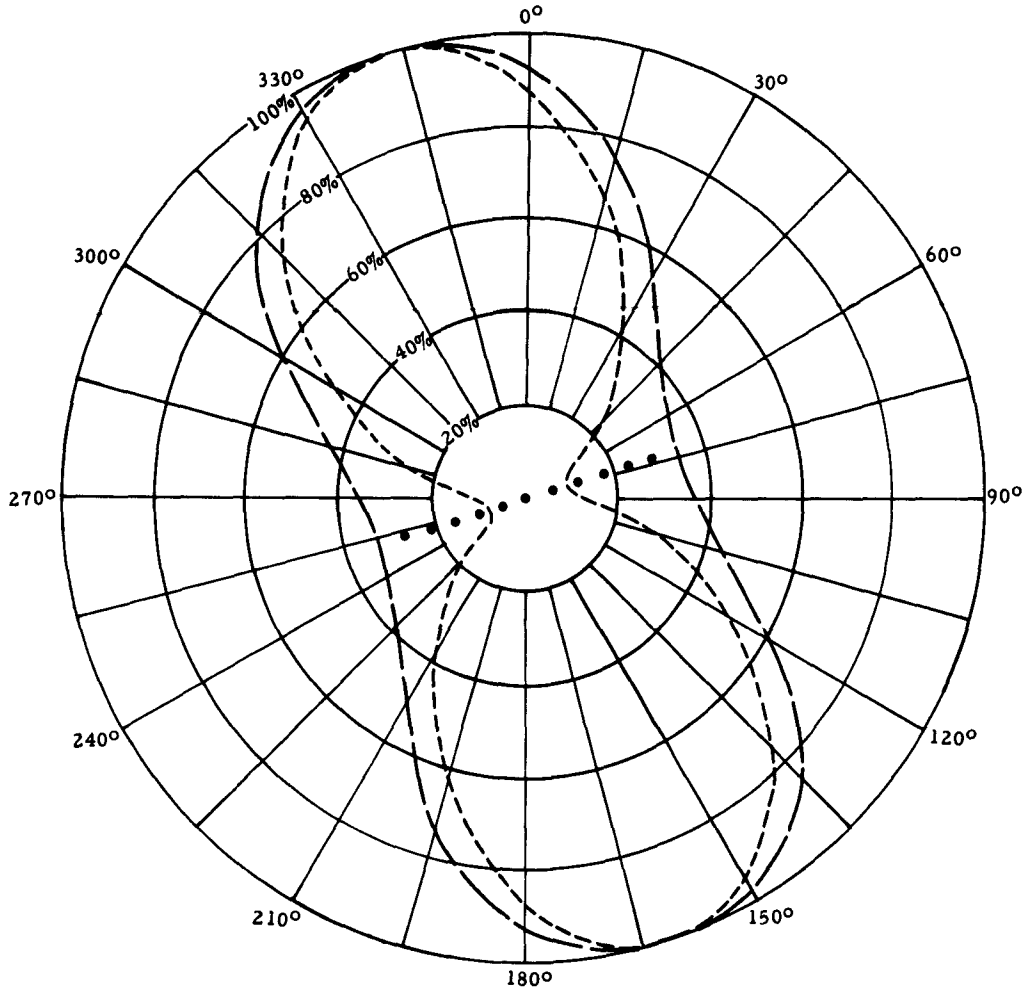


(Array consists of 11 seismometers with spacing of 1 kilometer)

—— —— = Response to a typical teleseismic signal with a 1-second period and 12 km/sec surface velocity (maximum variation = 66%)

– – – — = Response to a sinusoidal signal with a 1-second period and 12 km/sec surface velocity (maximum variation = 91%)

100% is considered to be the summation output with no signal cancellation.

Figure 53. Directional response of the linear array

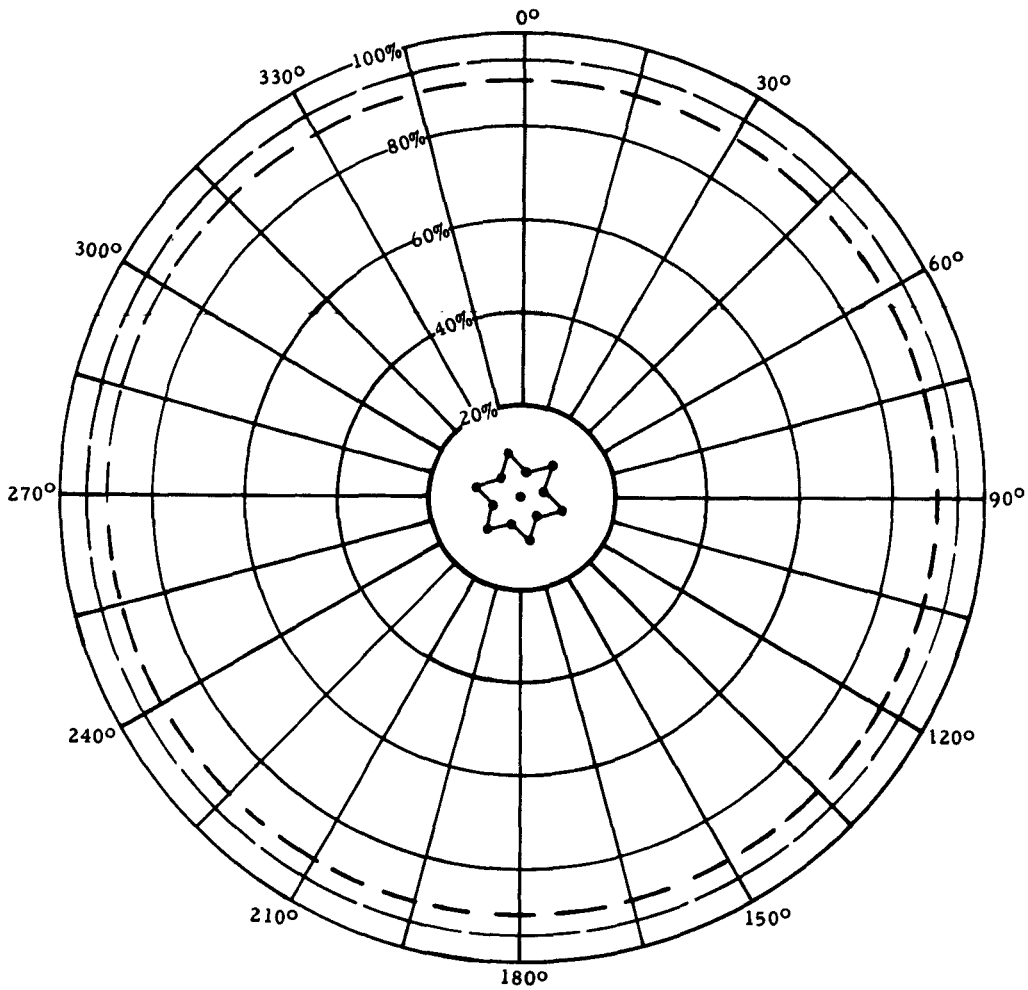


(Array consists of 13 seismometers with spacing of 1 kilometer)

—— —— = Response to a typical teleseismic signal with a 1-second period and 12 km/sec surface velocity (maximum variation = 0.02%)

– – – – – = Response to a sinusoidal signal with a 1-second period and 12 km/sec surface velocity (maximum variation = 0.02%

100% is considered to be the summation output with no cancellation.

**Figure 54. Directional response of the Star-of-David array**

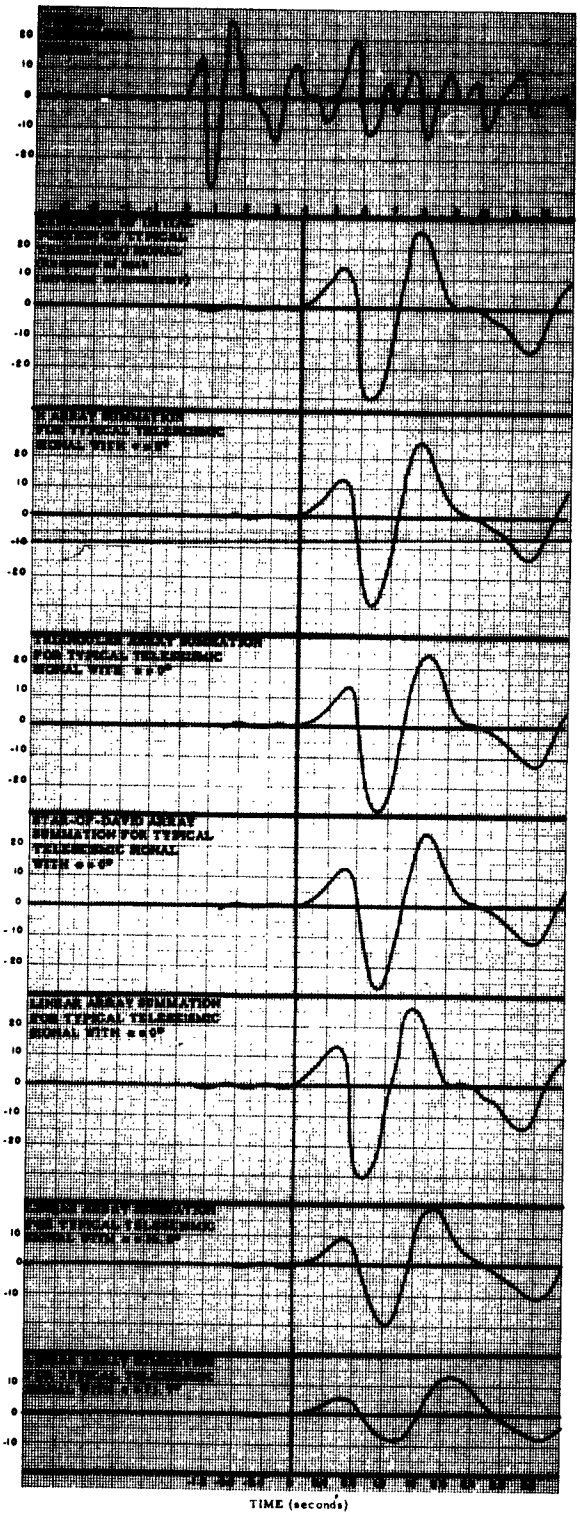


Figure 55. Observed response of a single-array element (Z6) and calculated responses of the summations of each of the four arrays to a typical teleseismic signal with a period of 1.0 second and an apparent surface velocity of 12 kilometers per second

## 6.4 COMPARISON OF THE "H" AND TRIANGULAR ARRAYS AT WMSO

Data collected during the simultaneous operation of the "H" array and triangular array between 12 October 1962 and 21 January 1963 were compared. During this period special recordings were also made at high gain through a narrow bandpass filter to determine the relative cancellation of 2-cps microseisms achieved by summing the outputs of the 10 elements of each array.

Using data from the Develocorder film recordings, 24 selected low-level teleseismic signals were observed independently for each array in a study designed to evaluate the relative detection capabilities of the arrays.

### 6.4.1 Relative Cancellation of 2-cps Microseisms

The outputs of two individual seismographs from each array (Z1 and Z6) and the outputs of the summations of the 10 seismographs of each array were recorded on the single-pen Helicorder through a narrow bandpass filter (Krohn-Hite Model 330-A) at magnifications of approximately $3 \times 10^6$ at 2 cps, and $1 \times 10^7$ at 2 cps, respectively. Prior to recording these data, the contribution of each seismograph to its respective summations was equalized and calibrated at 2 cps. The Helicorder gain was then increased by known increments until the 2-cps microseismic background level could be accurately measured. Only one filter was available for this study; therefore, data were recorded at successive time intervals based on the assumption that the distribution of the 2-cps microseismic noise was time stationary. The validity of this assumption was later confirmed by measurements made on separate days.

Summing the outputs of the 10 elements of the H array decreased the average amplitude of the 2-cps noise by a factor of 3.2. Based on the assumption that the 2-cps noise is random, summing the array elements is expected to decrease the average amplitude of the noise by a factor of 3.16. However, the results of this test on the triangular array yielded a cancellation factor of 5.1 when the 10 array elements were summed. This suggests some degree of coherence in the 2-cps noise. In an effort to further demonstrate the coherence of the 2-cps noise and to investigate the directional properties of the noise, the elements of each leg of the triangular array were summed independently. The cancellation factor of the summation of elements 1-4, 4-7, and 7-1 (figure 9) were 3.0, 1.9, and 2.4, respectively. These data suggest an approximate north-south direction of propagation of the predominant coherent components of the 2-cps noise at WMSO.

### 6.4.2 Relative Capabilities of the "H" and Triangular Arrays at WMSO to Detect Low-Level Signals

Twenty-four low-level signals that had been detected on the triangular array and reported in the daily message to USC&GS were selected for a comparative study of the detection capability of the two arrays. The detection capability of each array was evaluated, utilizing the summations alone and utilizing the summation in conjunction with the 10 elements of each array. The portions of the records containing the signals were reviewed independently by two analysts, first, with all but the summation trace masked from view and second, with the 10 elements of the array and the normal summation traces in view. For each signal detected, the corresponding system was awarded grade 1 for displaying it most clearly, 2 for second best; grade zero (0) was given when a system failed to detect a signal. In cases of equal clarity of signal, grade 1 was awarded to each. The results of this comparison are presented in table 17.

Figures 56 through 58 are typical examples of the signals considered in this study.

### 6.4.3 Conclusions

Both from the standpoint of clarity with which low-level signals are recorded and the relative 2-cps noise cancellation ability, the triangular array is superior to the "H" array.

Table 17. Relative Detection Capability of the H and Triangular Arrays for Low-Level Signals

| Array | Signals detected by Σ's | Signals detected by array | Detection grade by Σ's 1 | 2 | 0 | Detection grade by array 1 | 2 | 0 |
|---|---|---|---|---|---|---|---|---|
| Δ | 21 | 24 | 18 | 3 | 3 | 23 | 1 | 0 |
| H | 18 | 21 | 6 | 12 | 6 | 3 | 18 | 3 |

Total signals - 24

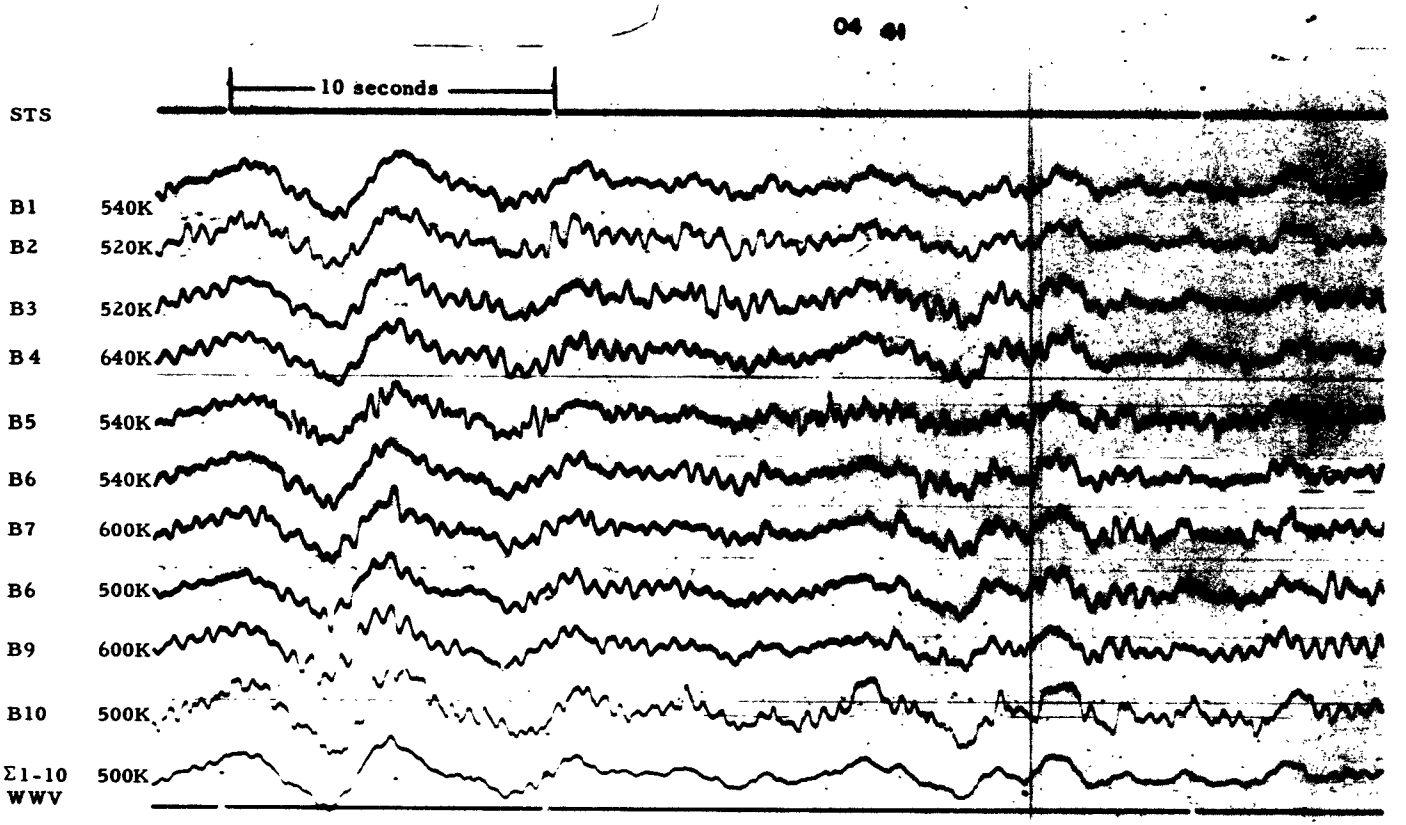
04 41
10 seconds
STS
B1 540K
B2 520K
B3 520K
B4 640K
B5 540K
B6 540K
B7 600K
B6 500K
B9 600K
B10 500K
Σ1-10 500K
WWV

Figure 56a.

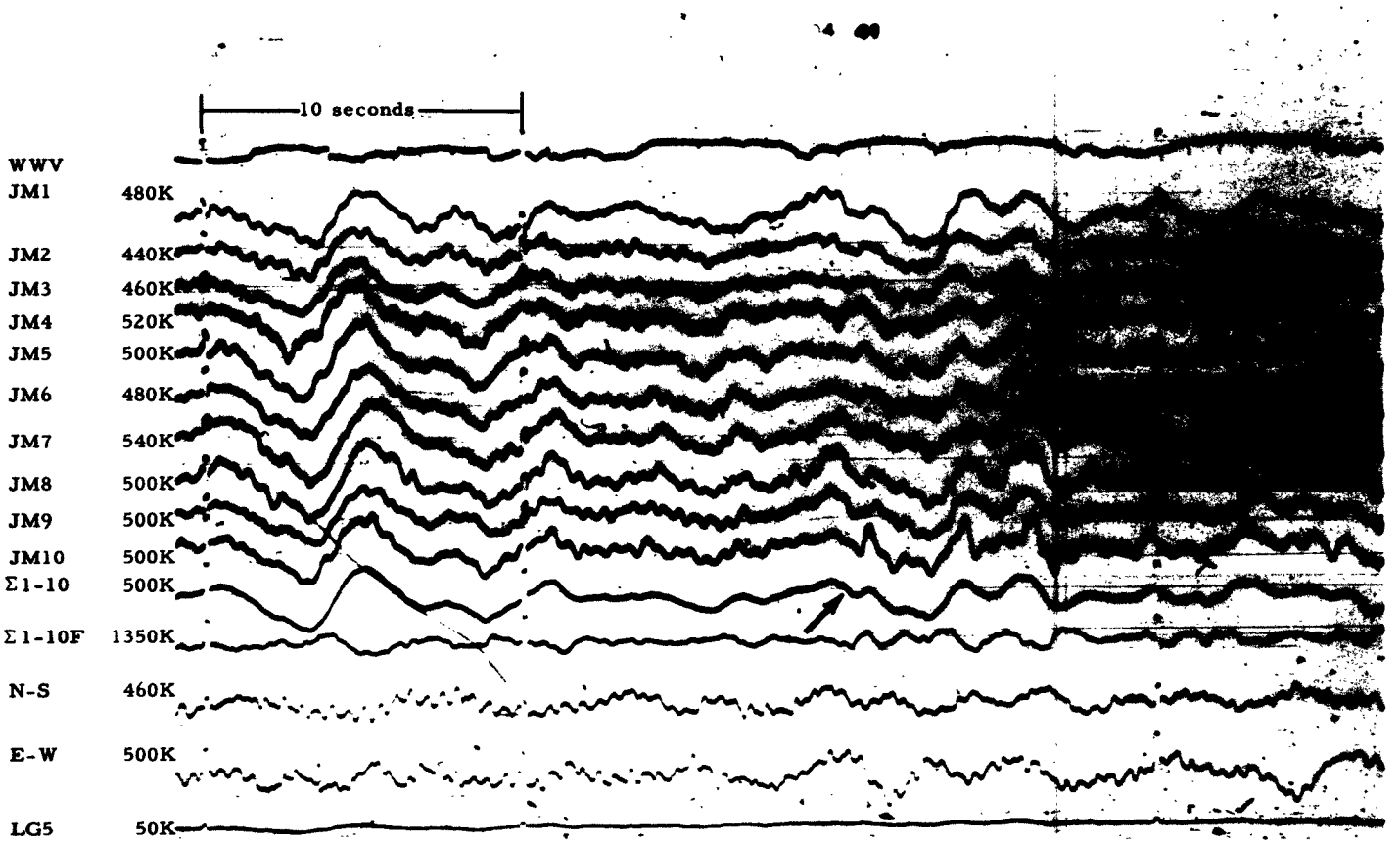


Figure 56b. Short-period Develocorder record of a typical low-level signal (arrow) detected by the analyst only on the triangular array at WMSO. Corresponding time interval for H array shown in 56a.

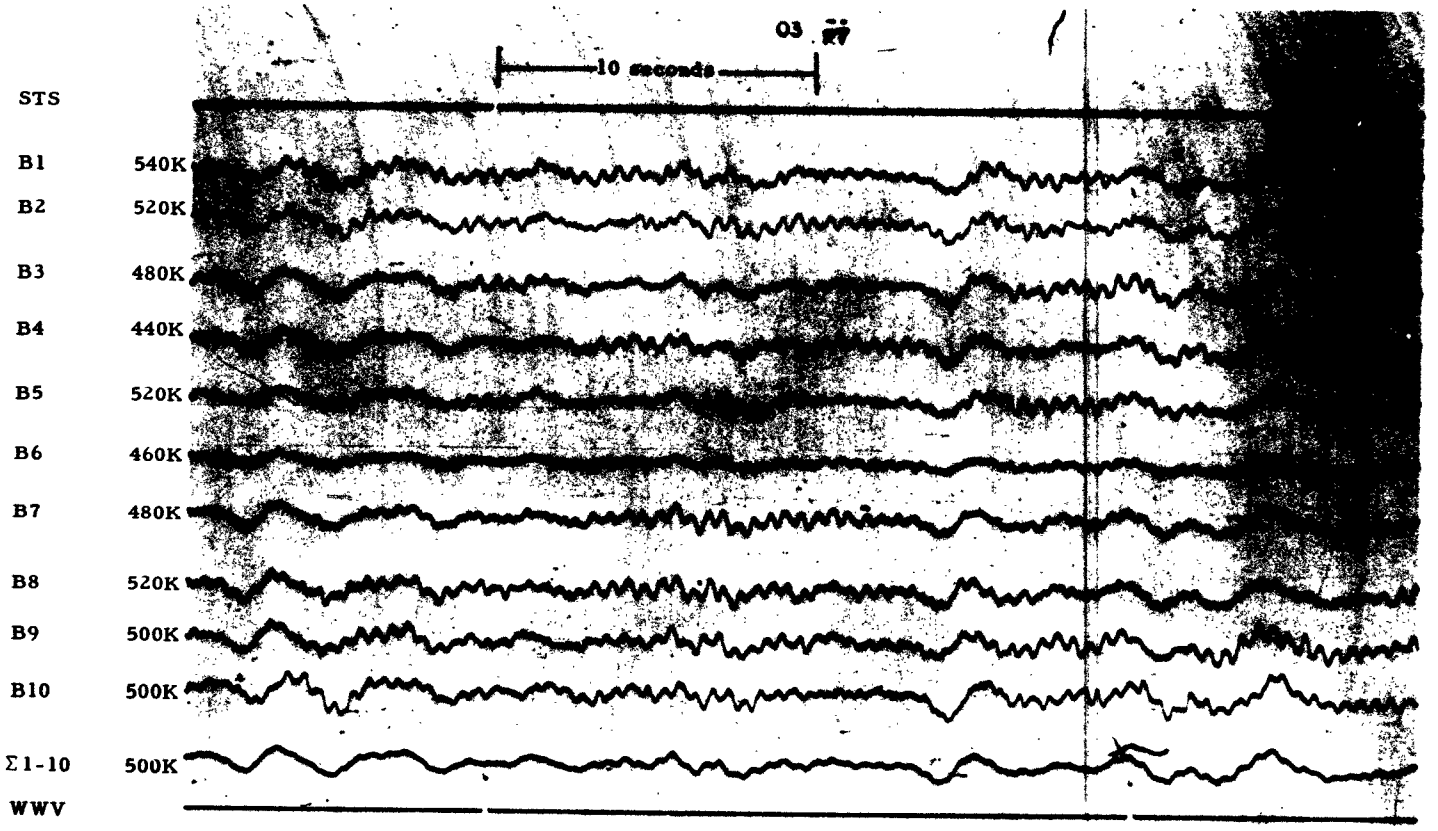
10 seconds
STS
B1 540K
B2 520K
B3 480K
B4 440K
B5 520K
B6 460K
B7 480K
B8 520K
B9 500K
B10 500K
Σ1-10 500K
WWV

Figure 57a.

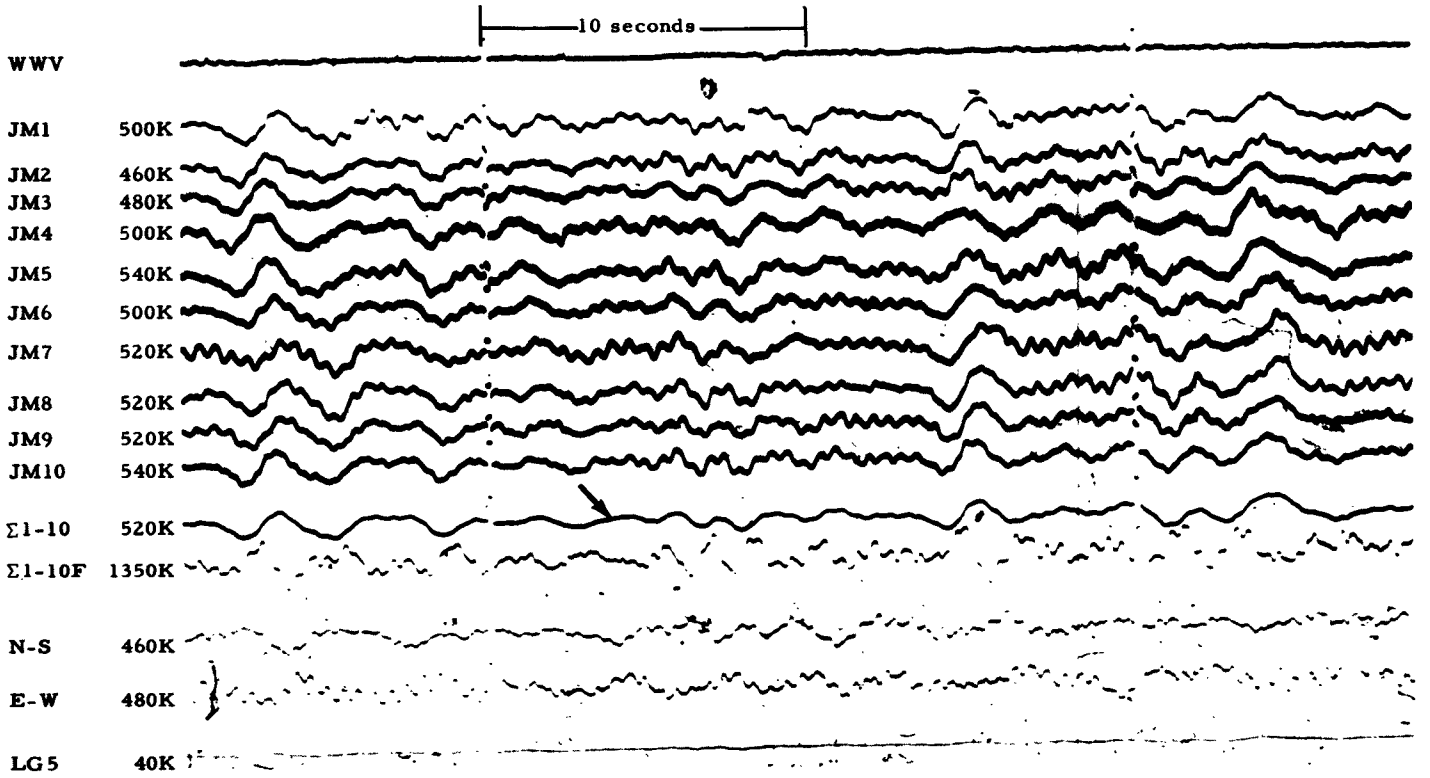


Figure 57b. Short-period Develocorder record of a typical low-level signal (arrow) detected by the analyst only on the triangular array at WMSO. Corresponding time interval for H array shown in 57a.

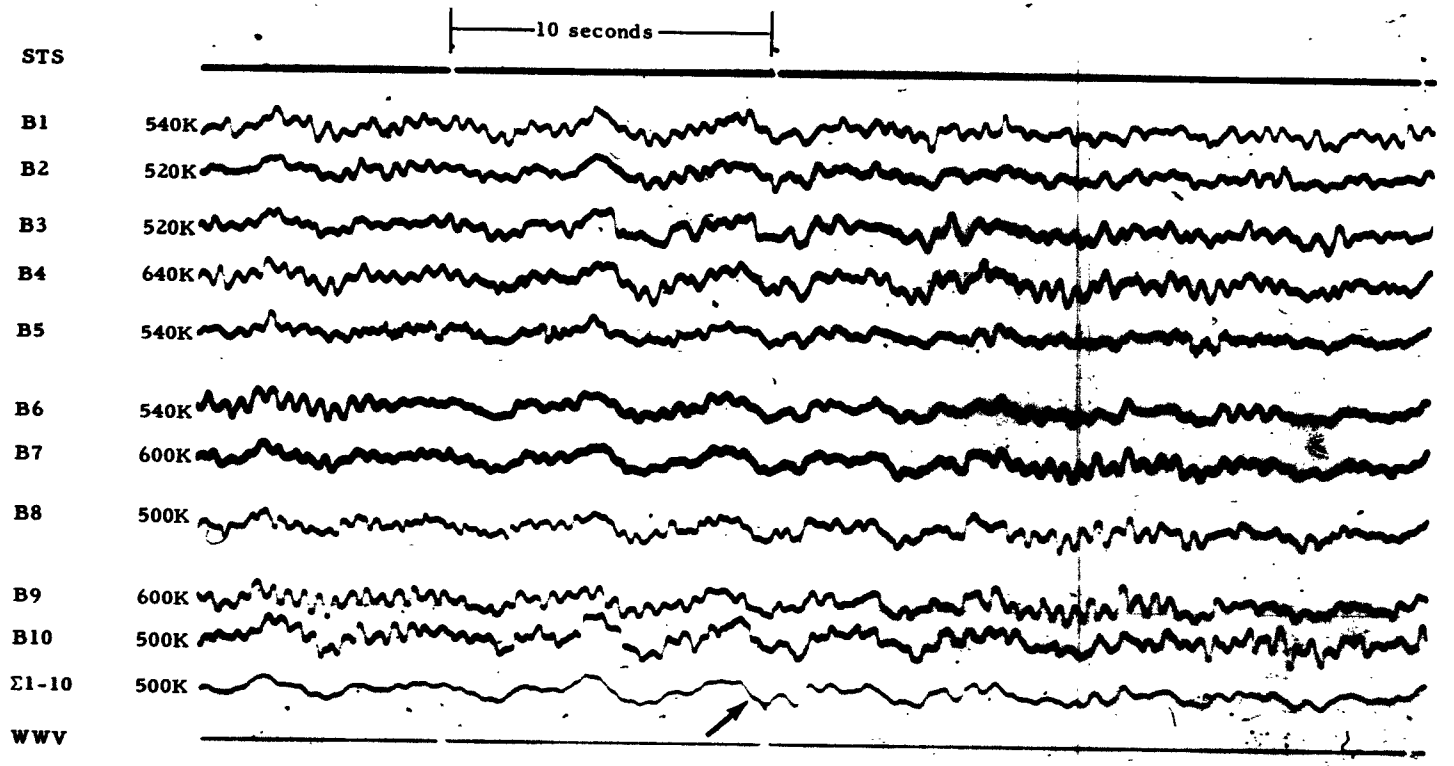
10 seconds
STS
B1
540K
B2
520K
B3
520K
B4
640K
B5
540K
B6
540K
B7
600K
B8
500K
B9
600K
B10
500K
Σ1-10
500K
WWV

Figure 58a.

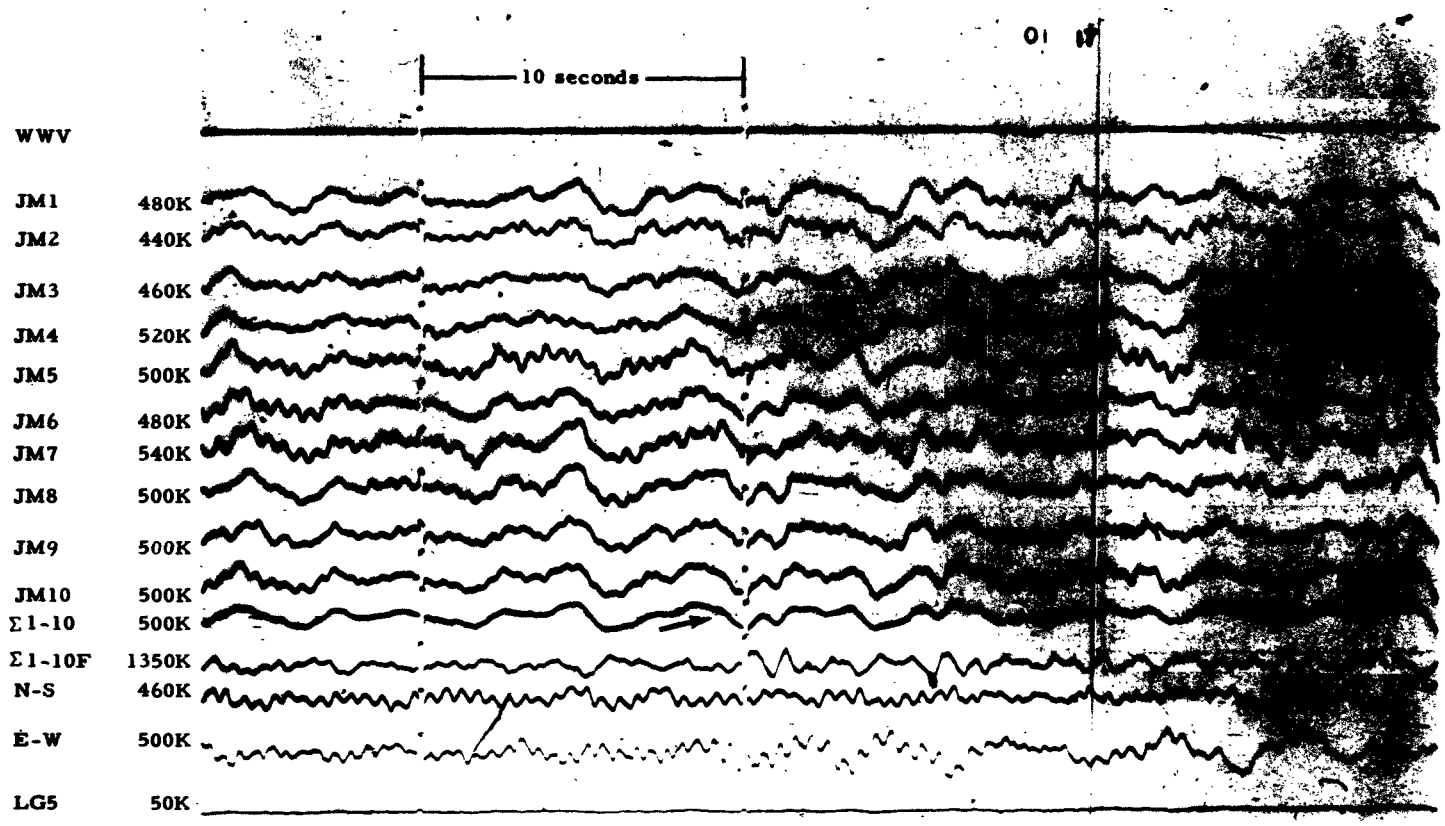


Figure 58b. Short-period Develocorder record of a typical low-level signal (arrow) detected by the analyst on both arrays but more clearly on the triangular array at WMSO. Corresponding time interval for H array shown in 58a.

## 6.5 COMPARISON OF LINEAR AND TRIANGULAR ARRAYS

Only data recorded during the second period of operation of the linear array were available for this comparison. Since reactivation of the linear array did not occur until 7 February 1963, both the available data and time for this study were limited. The characteristics of the linear array are markedly different from either of the other arrays operated at WMSO. Several general characteristics, unique to the linear array, are discussed here.

a. The array is relatively directional, even to teleseismic P signals (section 6.4).

b. Based on the 2-cps noise cancellation tests of the Σ4-7 leg of the triangular array (section 6.5), which forms part of the linear array (figure 8), cancellation of 2-cps noise expected by summing the elements of the linear array is less than that expected for the triangular array.

c. A significant degree of cancellation of the longer period microseisms (2-5 seconds) is observed on the summation of the linear array elements. The effects of this cancellation, however, would deteriorate if time delays were employed to enhance in-line signals.

Figures 59 through 61 are illustrations of typical signals from various directions and distances as recorded by the linear array.

# 7. SPECIAL TESTS

## 7.1 LONG-PERIOD TRIPARTITE

A tripartite of Geotech long-period seismographs, utilizing 100-second galvanometers in phototube amplifiers, was installed during the latter half of August 1962. The seismometers of the tripartite are located in vault 5P, in vault 8P, and at the tank farm (figure 9). In addition, an Infrasonic Microbarograph, Geotech Model 10138, was installed near the long-period seismometer at the tank farm during October 1962. Data from the three long-period seismographs and the microbarograph are being recorded on a separate Develocorder at a film speed of 3 millimeters per minute.

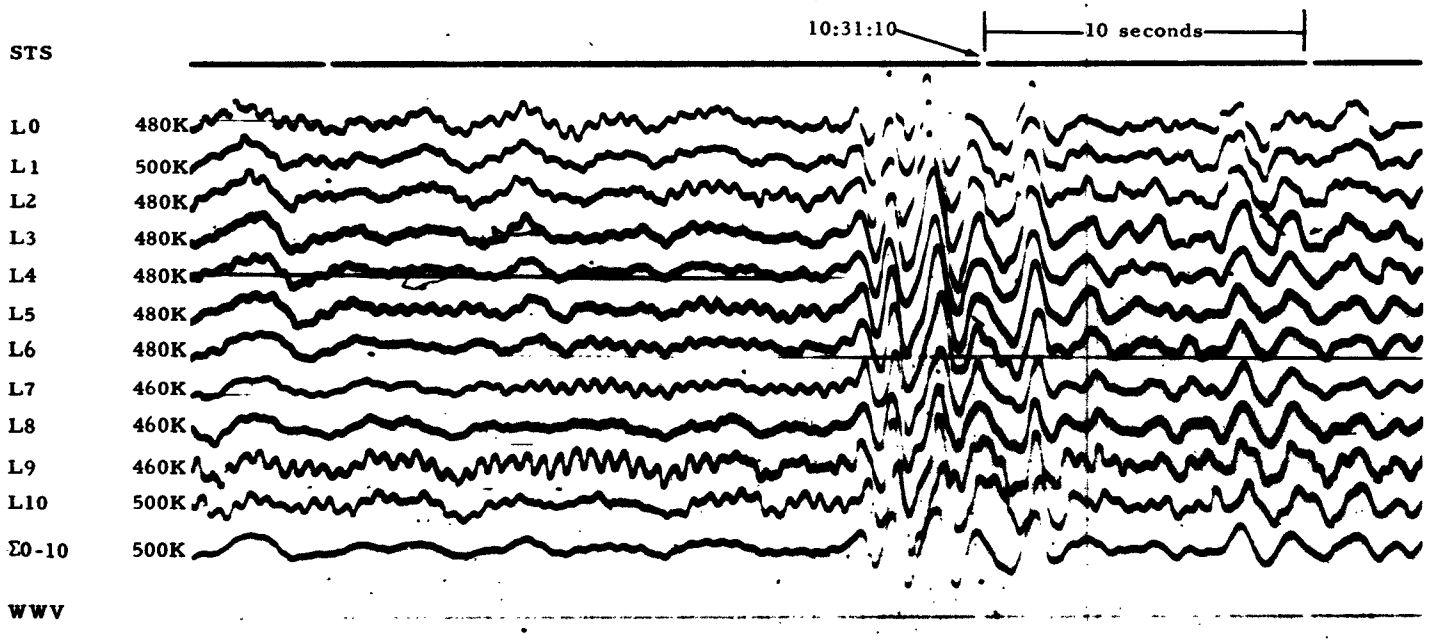


Figure 59. Short-period Develocorder record illustrating the response of the linear array to a signal that is nearly in-line with the array. Azimuth from WMSO 42°, Δ = 86°.

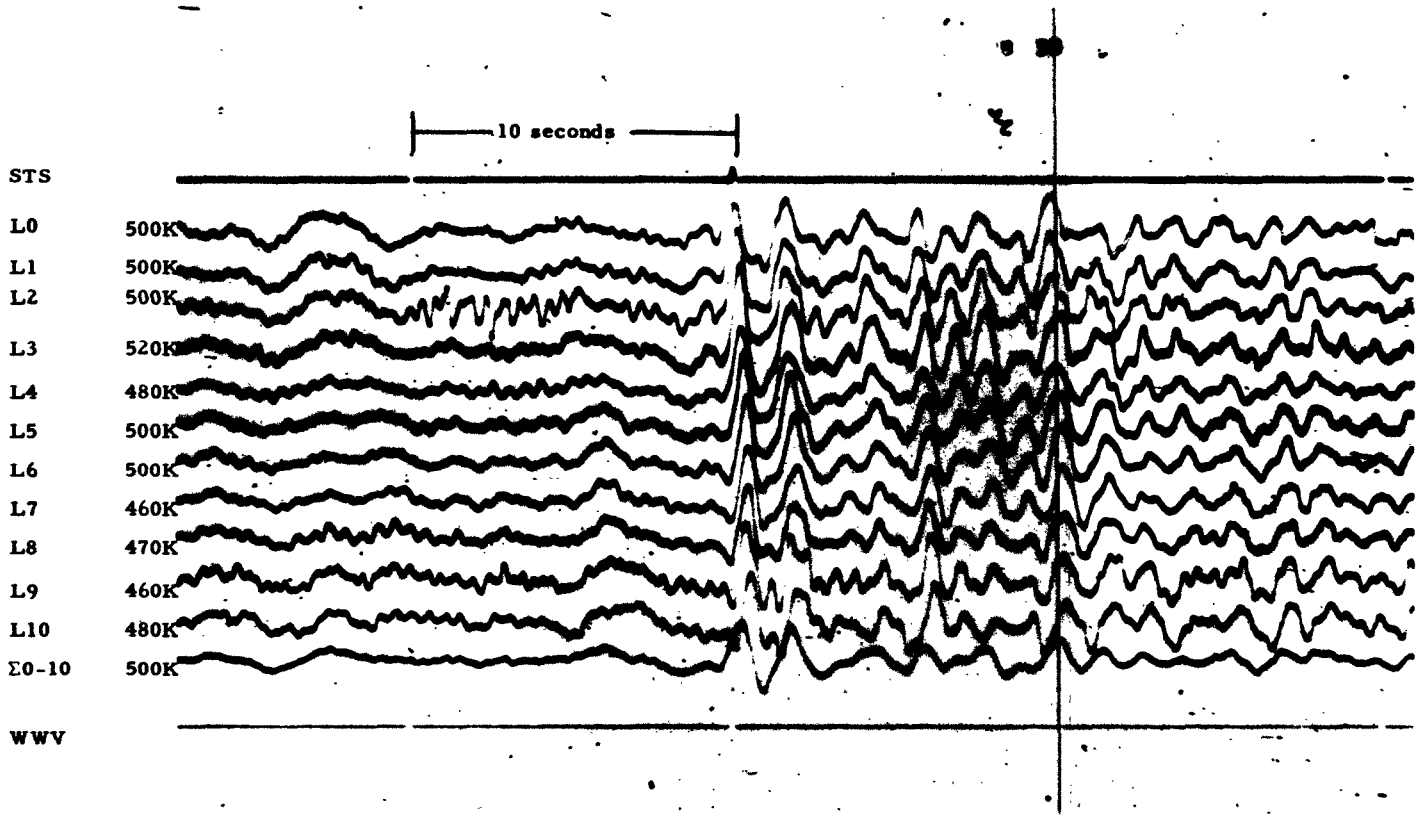


Figure 60. Short-period Develocorder record illustrating the response of the linear array to a signal that is nearly in-line with the array. Azimuth from WMSO 39°, Δ = 49°.

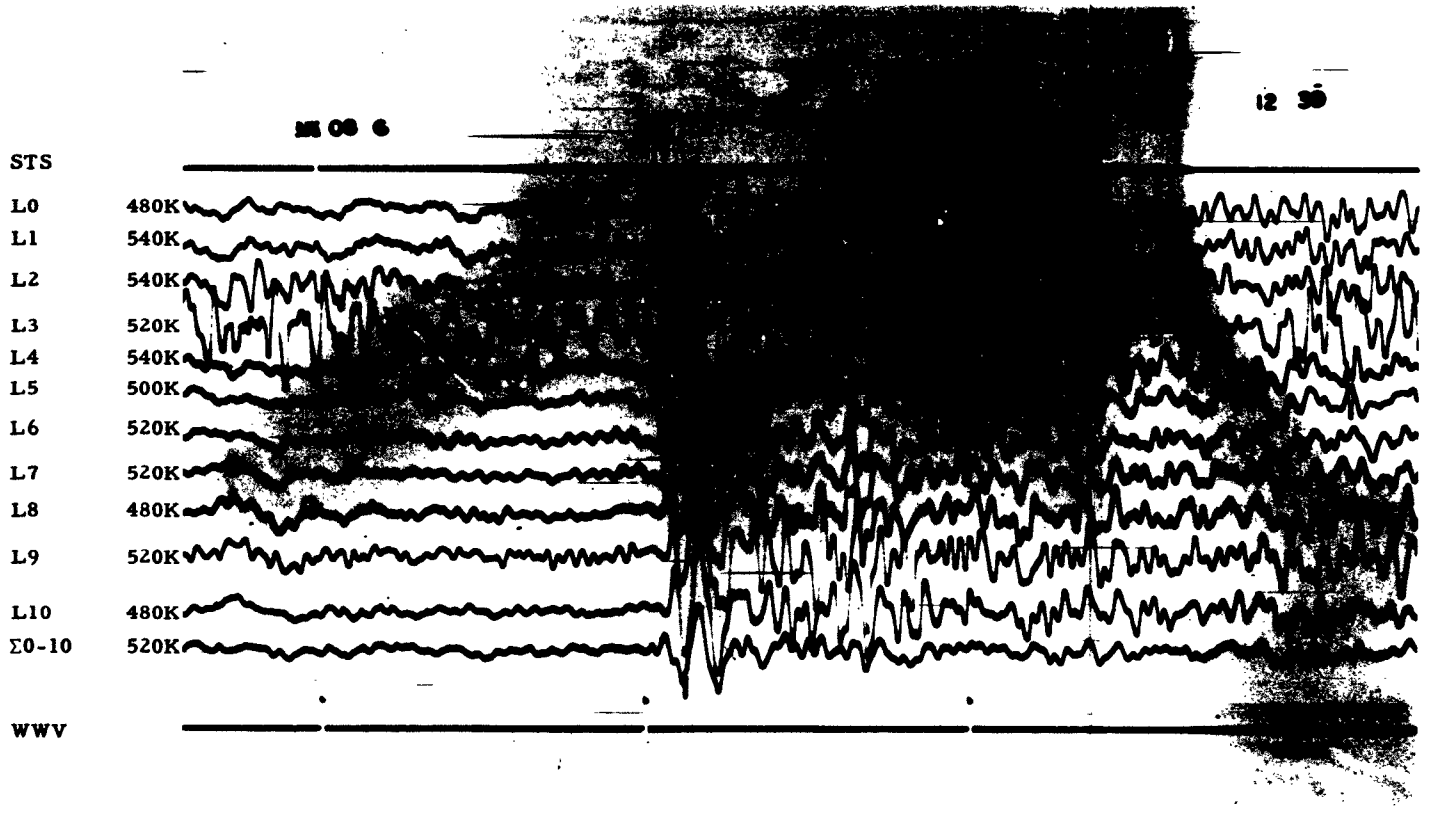


Figure 61. Short-period Develocorder record illustrating the response of the linear array to a signal that is nearly broadside to the array. Azimuth from WMSO 143°, Δ = 36.5°.

The seismometers of the long-period tripartite responded to local barometric pressure changes in the approximate period range of 30 to 150 seconds (figure 62). The response of these instruments to local pressure changes (30 to 150 seconds) was greatly reduced by sealing the seismometer cases (figure 63); however, an apparent response to long-period pressure changes in the period range of 3 to 15 minutes became evident. In December, the seal around the period-adjusting knob of the seismometers was improved, and the response of the instruments to the long period pressure changes was reduced by a factor of approximately 3.5 (see figure 64). It was discovered that the effectiveness of the seal was slightly reduced with time and variations in ambient temperature with the period-adjusting knob in place. Subsequently, the period adjusting rod was removed from the seismometer in the tank farm and the hole in the cover, through which the rod had protruded, was fitted with a pipe plug. The pipe plug provides a seal which is both more effective and more stable than the seal with the period-adjusting rod in place. Figure 65 illustrates the relative effectiveness of the two methods of sealing the period adjusting rod hole in the seismometer cover.

Additional noise which did not correlate with the microbarograph, and showed diurnal variations, was noted on the seismograms with the peak amplitudes of noise occurring during the hours of sunrise and sunset. This noise was diagnosed as thermoelectric noise, and its source traced to the fuses and fuse receptacles in the data circuit between the seismometers and their PTA's. The fuse holder clips and the data circuit wires to which they are connected are made of different metals; therefore, when the atmospheric temperature changes, a temperature differential exists between the junction points of the dissimilar metals. The temperature differential and the difference in the thermoelectric coefficients of the two metals gives rise to an unbalanced electromotive force which causes random noise on the seismograms.

A test was conducted to determine if the junctions between the fuses and the fuseholders were the primary offenders. The normal alloy of the fuses was replaced with thin copper wire. The modified fuses increased, rather than reduced, the thermoelectrically generated noise. Figure 66 illustrates the thermoelectric noise present in the seismograph systems with the normal fuse wire during a test in which the protector door at the tank farm was opened exposing the fuse assembly to direct sunlight. The effects of the thermoelectric noise were eliminated from the systems by removing the fuses and fuse receptacles from the circuits.

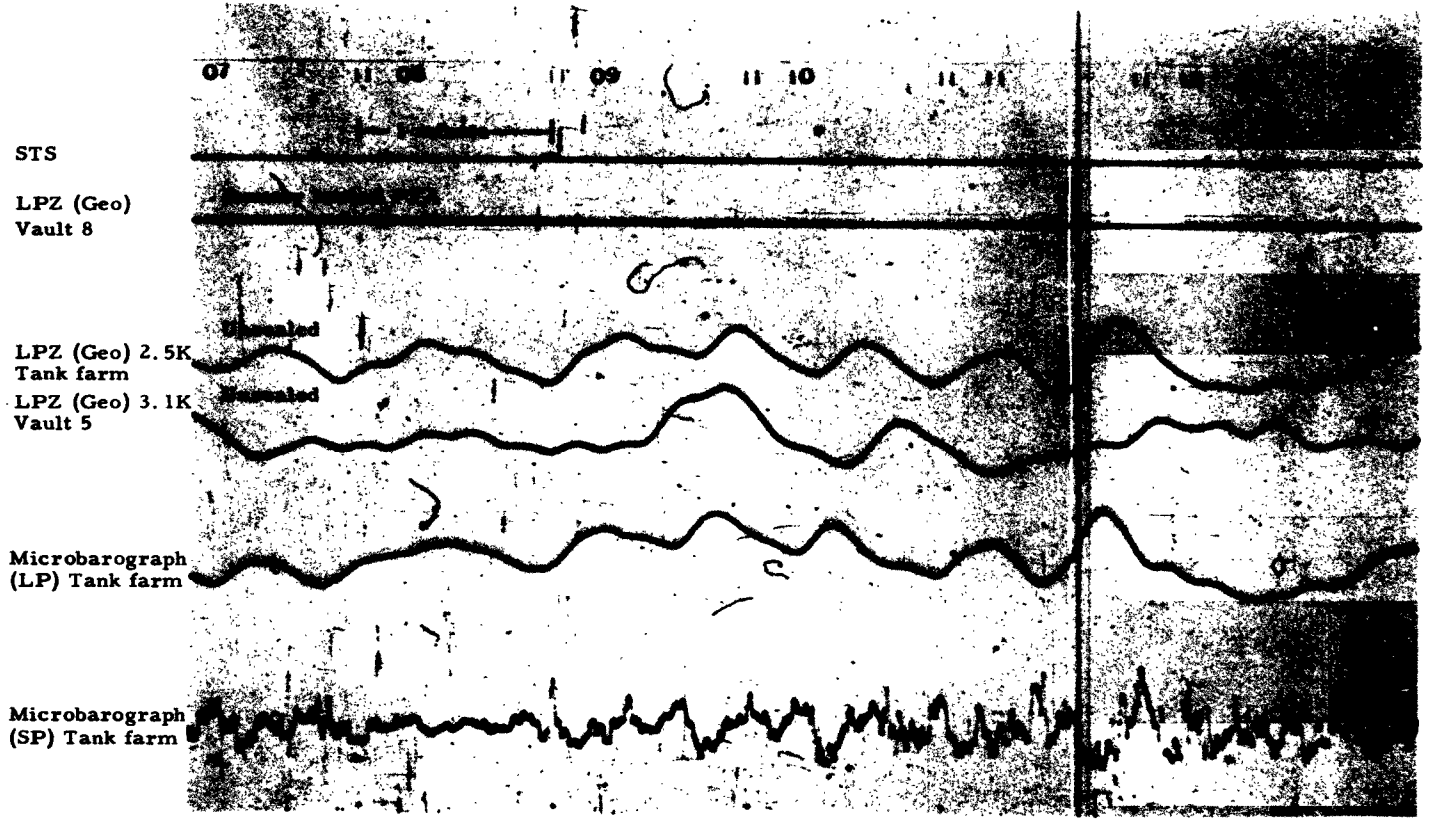


Figure 62. Record of test Develocorder recording the Geotech long-period tripartite illustrating the effects of atmospheric pressure change on the seismometers (unsealed)

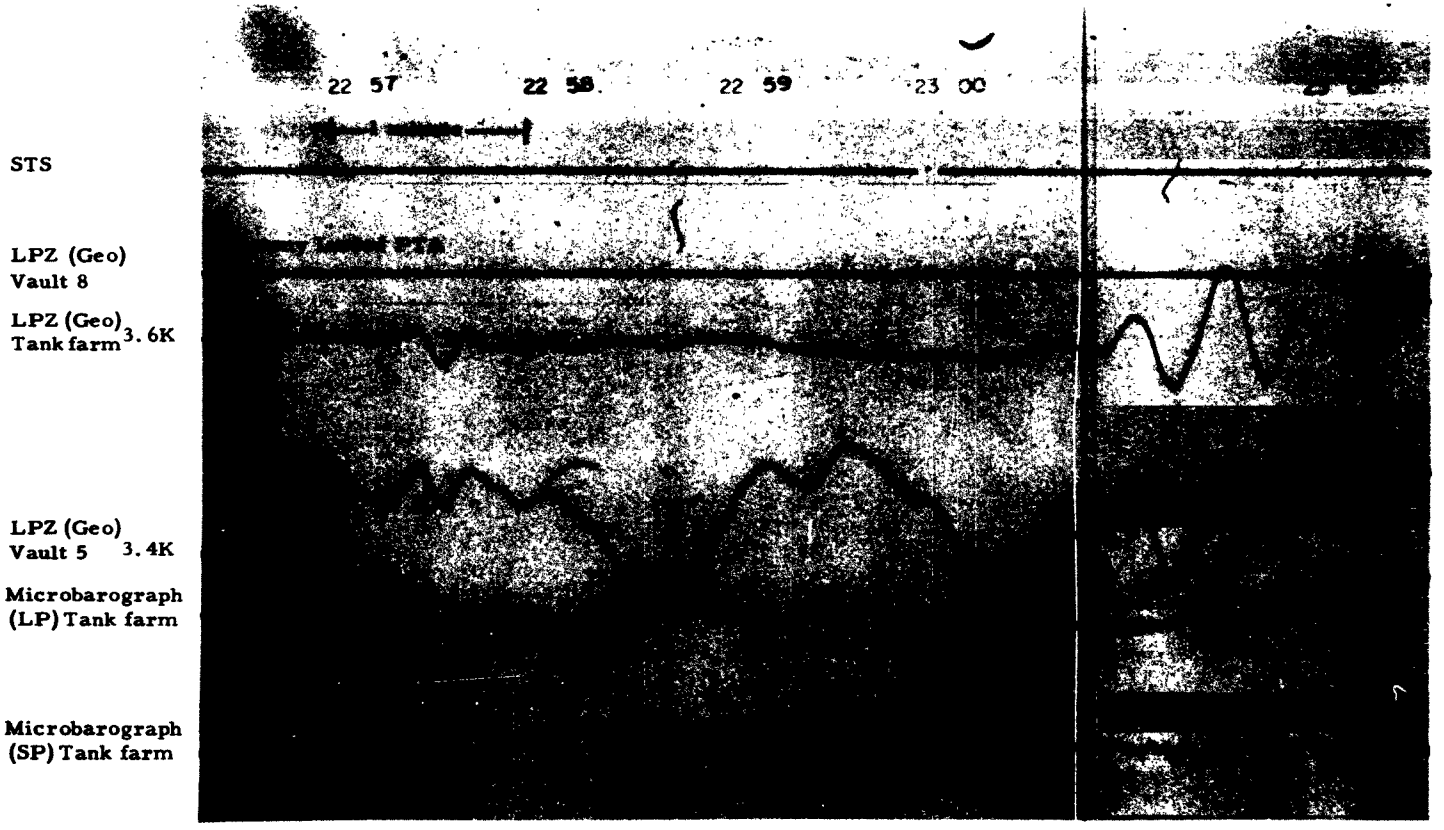


Figure 63. Test Develocorder record showing response to pressure change and P-wave signal on the Geotech long-period seismometers of the tripartite (sealed and unsealed)

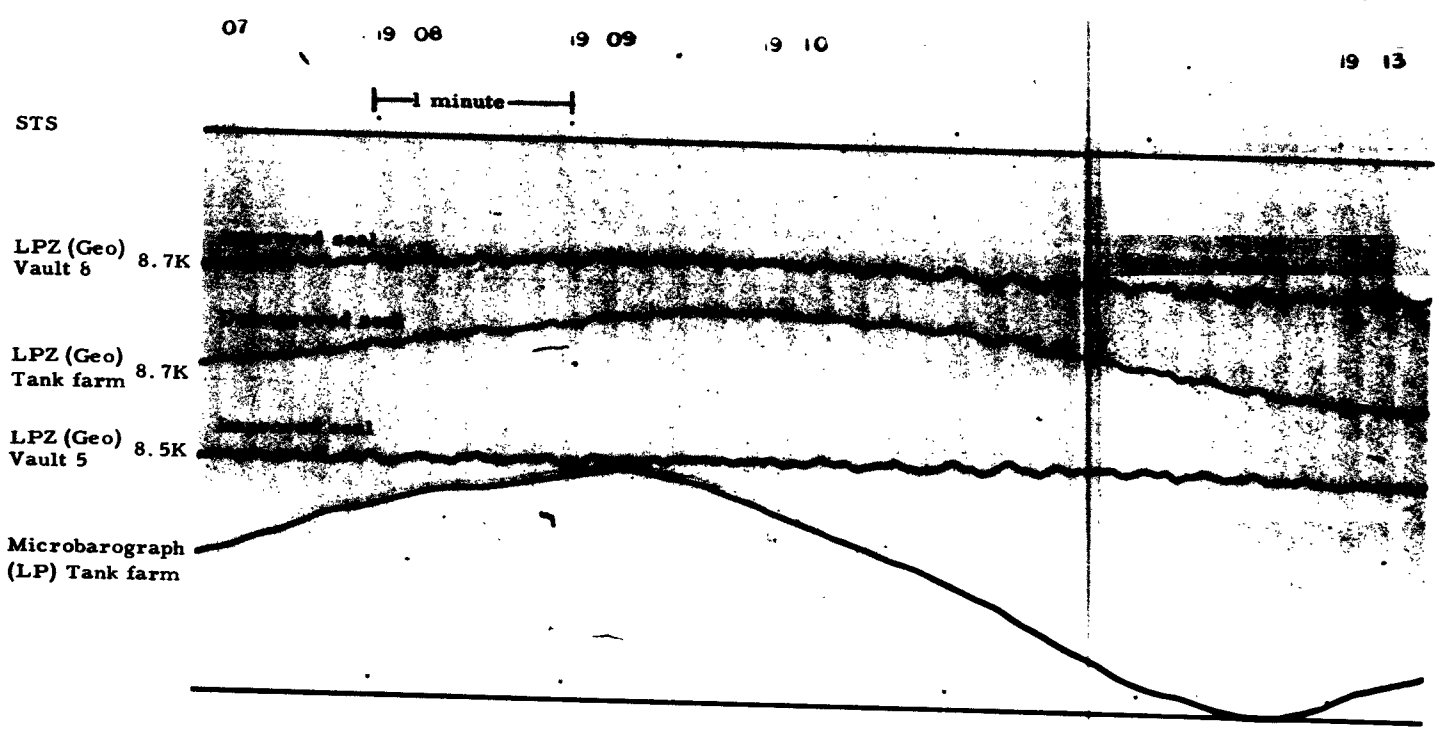


Figure 64. Record from test Develocorder recording the Geotech long-period tripartite, illustrating the response of the seismometer to atmospheric pressure change


Figure 65. Test Develocorder record illustrating the relative effectiveness of the two methods of sealing the period-adjusting rod hole in the seismometer cover

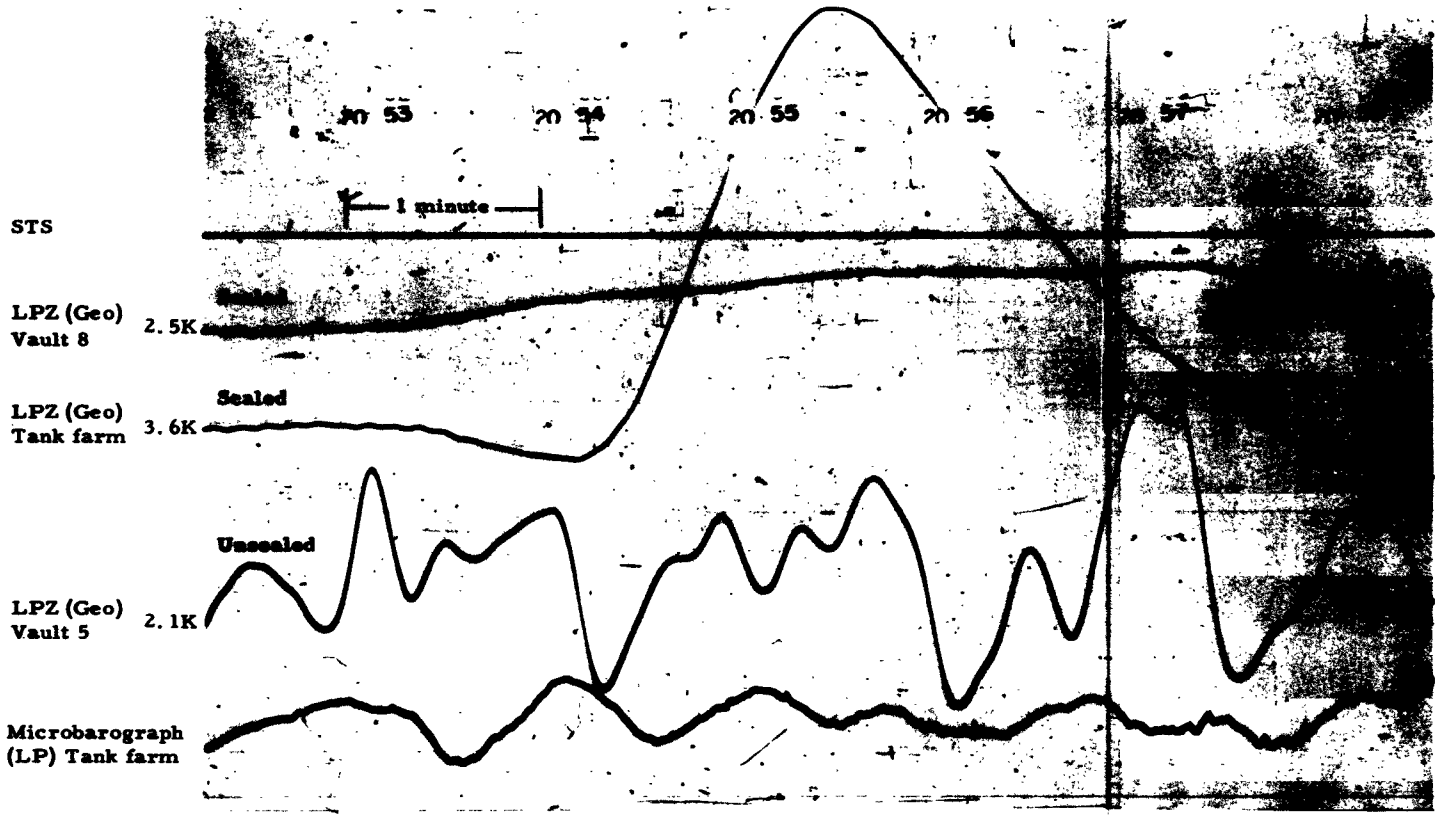


Figure 66. Test Develocorder record illustrating the effects of thermoelectric noise on the tripartite seismograms with the protector in the circuit when the protector door was opened in direct sunlight

One of the primary purposes of installing the tripartite of Geotech long-period seismographs was to study microseismic noise with periods exceeding 12 seconds. The recording of long-period microseismic noise was initially hampered by the effects of atmospheric pressure produced noise and thermoelectric noise, which limited the operating gain of the seismographs to a maximum of 2.5K to 3K at 0.04 cps. By the end of November, the effects of pressure produced noise and thermoelectric noise were sufficiently reduced to allow operation of the tripartite at a gain of 10K. When the operating gain was increased to 10K, the predominant mircoseismic noise which was apparent on the seismograms was in the 5 to 8 second period range. During limited periods of time, microseismic noise has been observed with periods up to 15 seconds, but no appreciable microseismic noise has been observed with periods greater than 15 seconds.

Six-second Notch Filters, Geotech Model 6824-9, were installed in the PTA's of two of the seismographs in the tripartite to attenuate the 6-second microseismic noise. Figure 67 illustrates the effect of the notch filter in attenuating 6-second microseisms. The third seismograph of the tripartite was operated without the notch filter to better evaluate the effectiveness of the filter. It was found that extraneous noise was more often seen on the seismographs with the 6-second notch filters. In addition, microseismic noise with periods of about 15 seconds was observed to be, in general, about as great a gain limiting factor in the seismographs with notch filters as 6-second microseismic noise was for the seismograph with no notch filter.

In order to more effectively study the longer period noise (that which correlates with the microbarograph), one of the tripartite seismometers which is not presently located at the tank farm will be relocated in a sealed tank at the tank farm. Its response to pressure changes will be compared to the sealed seismometer which is presently at the tank farm in an unsealed tank vault.

## 7.2 SEISMIC DATA FILTER, GEOTECH MODEL 11760

Evaluation of the Seismic Data Filter, Geotech Model 11760, began on 17 June 1962 at WMSO. Between 17 June and 7 August, the filter was used to filter the summation of Z1-Z10 of the triangular array within two bandpass ranges. The initial bandpass range was 0.8 cps, 18 db/octave to 3.0 cps, 18 db/octave; the second bandpass range was 0.8 cps, 24 db/octave to 2.0 cps, 24 db/octave.

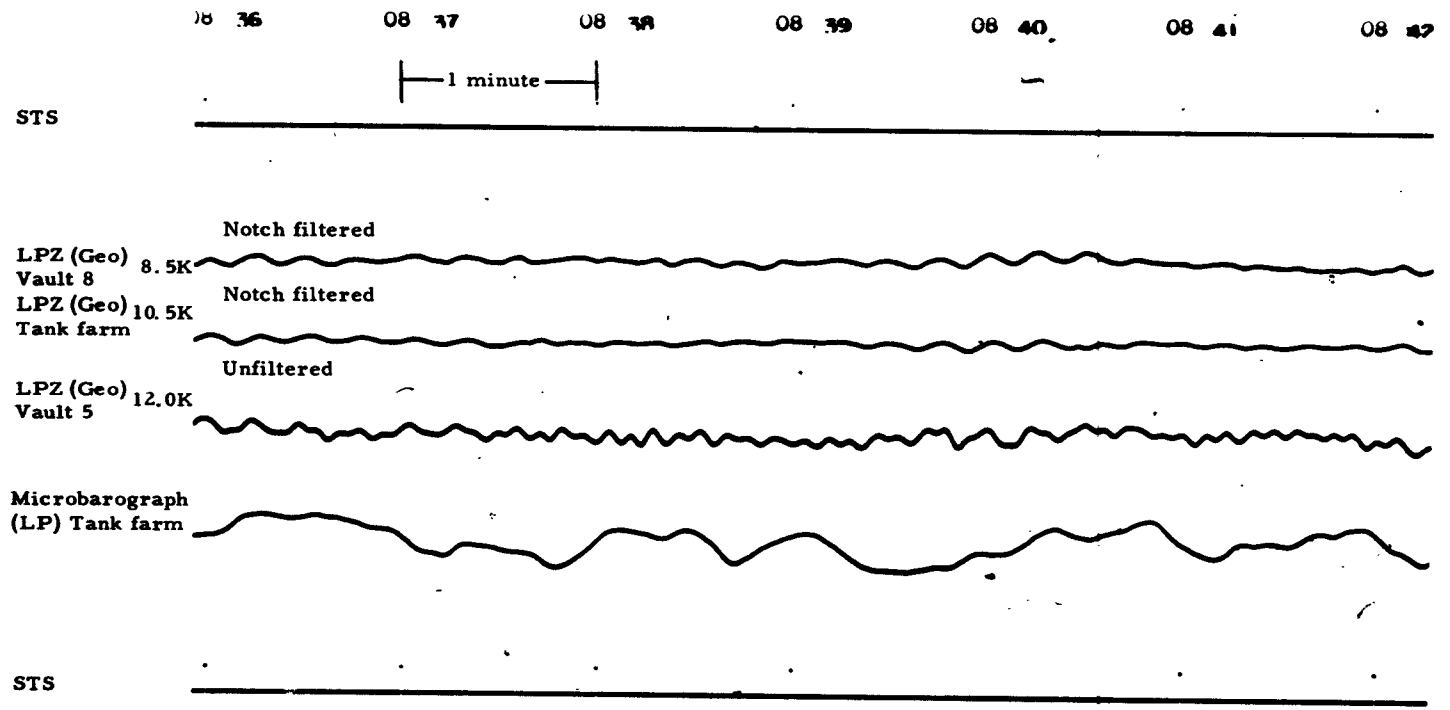


Figure 67. Test Develocorder record illustrating the effect of the notch filter in attenuating 6-second microseisms

It was difficult to attenuate adequately the low-frequency background noise with the filter, because both the maximum level of attenuation and the rate of attenuation of the low-frequency background noise that could be achieved by the filter were limited. Modifications of the filter were recommended, and the filter was returned to the lab at Garland for modification on 7 August.

While the 11760 seismic data filter was being modified, a Krohn-Hite Filter, Model 330-A, was tested. The bandpass of the Krohn-Hite filter was set at 0.8 to 2.0 cps (24 db/octave on each side). The frequency responses of the two settings at which the Geotech filter was operated and the response of the Krohn-Hite filter are shown in figure 68.

The desired results were not obtained from either the Geotech or the Krohn-Hite filter prior to 8 November. At these settings, the filters produced a slow build-up of signals because the passbands were too narrow, and because the rate of attenuation of pulses was too great. Little assistance was afforded the analyst by either of the filters with the bandpass ranges which were tested between 17 June and 8 November.

On 8 November, the operation of the Krohn-Hite filter was discontinued and the modified Geotech Seismic Data Filter, Model 11760, was reinstalled. From 8 November until 16 November, the filter was operated with a bandpass range from 0.8 cps, 18 db/octave to 5.0 cps, 24 db/octave. Figure 69 shows the frequency response of the filter while operating with this range. The capabilities of the filter, operating in this bandpass range, to function as a flag trace and to attenuate the microseism within the period range of approximately 5 to 9 seconds are illustrated in figures 70 and 71. Essentially complete attenuation of the 5- to 9-second microseisms was achieved when using the filter at this setting.

The filter settings were changed to 0.8 cps, 12 db/octave and 5.0 cps, 6 db/octave on 16 November. The frequency response of the filtered seismograph at this setting is shown in figure 72. Good attenuation of the 5- to 9-second microseisms was achieved at this setting; however, the degree of attenuation was slightly less than that accomplished at the previous setting. The attenuation and analysis enhancement capabilities of the filter operating with this bandpass range are illustrated in figures 73 and 74.

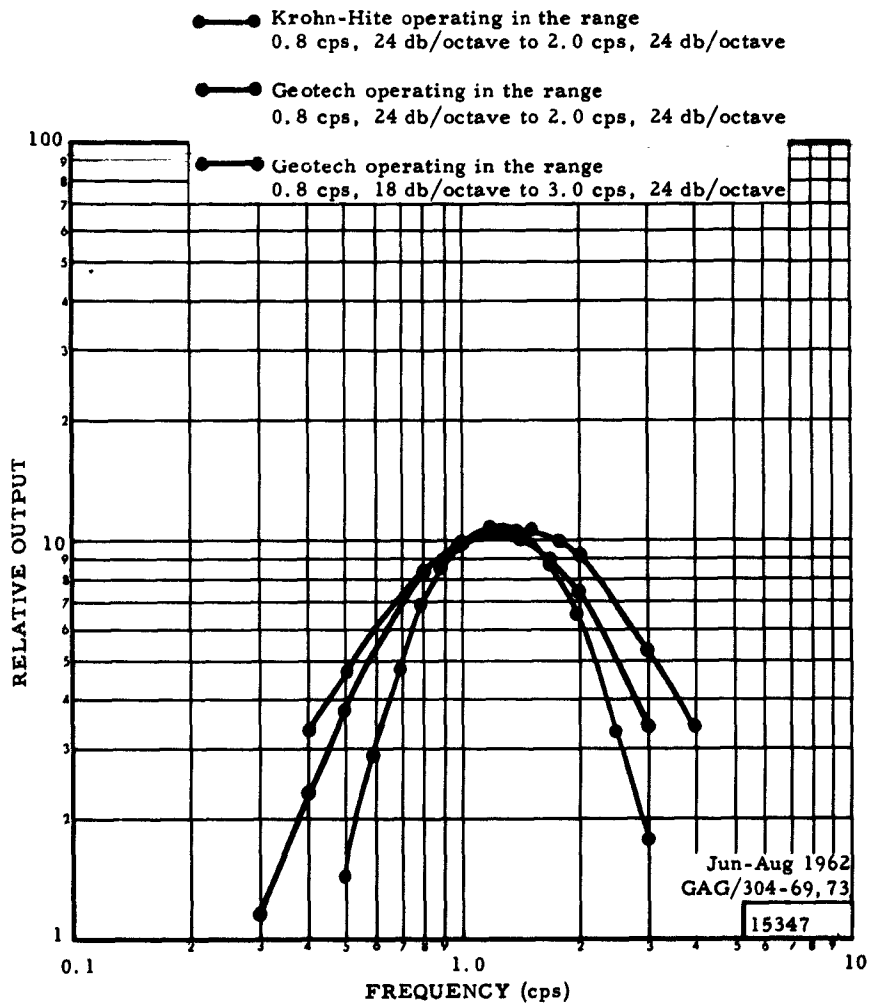


Figure 68. Comparison of the frequency response curves of the Seismic Data Filters, Geotech Model 11760 and Krohn-Hite Model 330-A, as operated at WMSO prior to 8 November 1962

A third setting of the filter was tested and evaluated beginning 11 December. Figure 75 is the frequency response of the filter with the range 0.8 cps, 12 db/octave to 3.0 cps, 6 db/octave, the third setting. Figures 76 through 78 illustrate the performance of the filter at this setting.

The 11760 seismic data filter is a valuable analysis aid for use as a flag trace. A filtered summation seismograph can be operated at higher magnifications than the normal summation seismograph because of the attenuation of the low-frequency microseisms. Frequently, earlier arrival times may

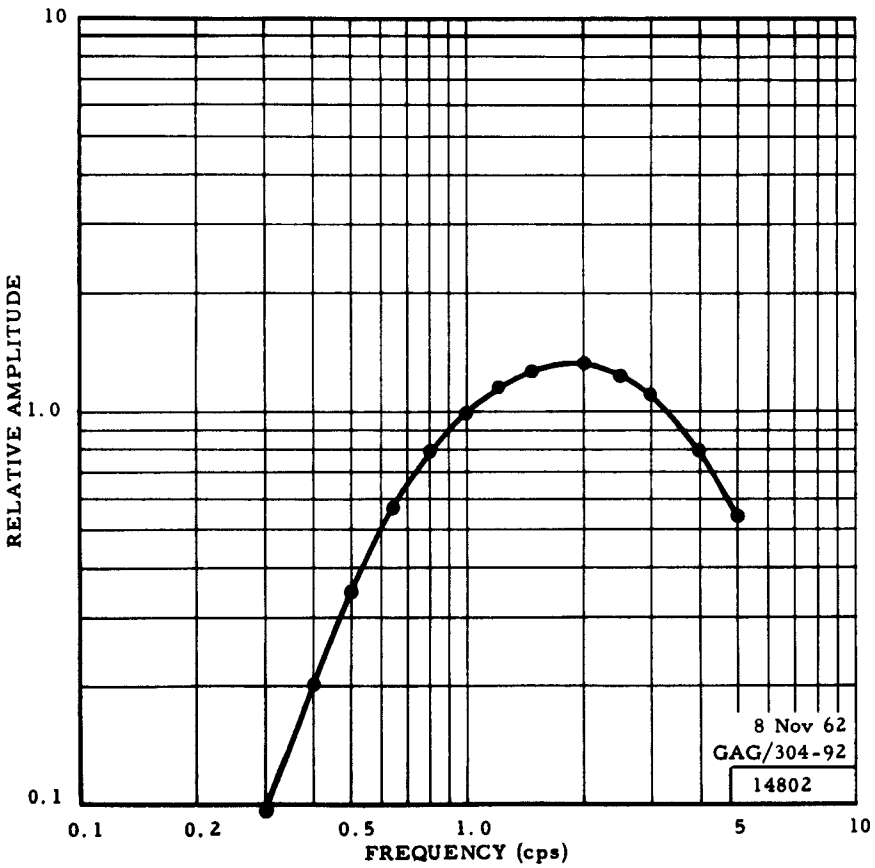


**Figure 69. Frequency response of Seismic Data Filter, Model 11760, operating in the range 0.8 cps, 18 db/octave to 5.0 cps, 24 db/octave**

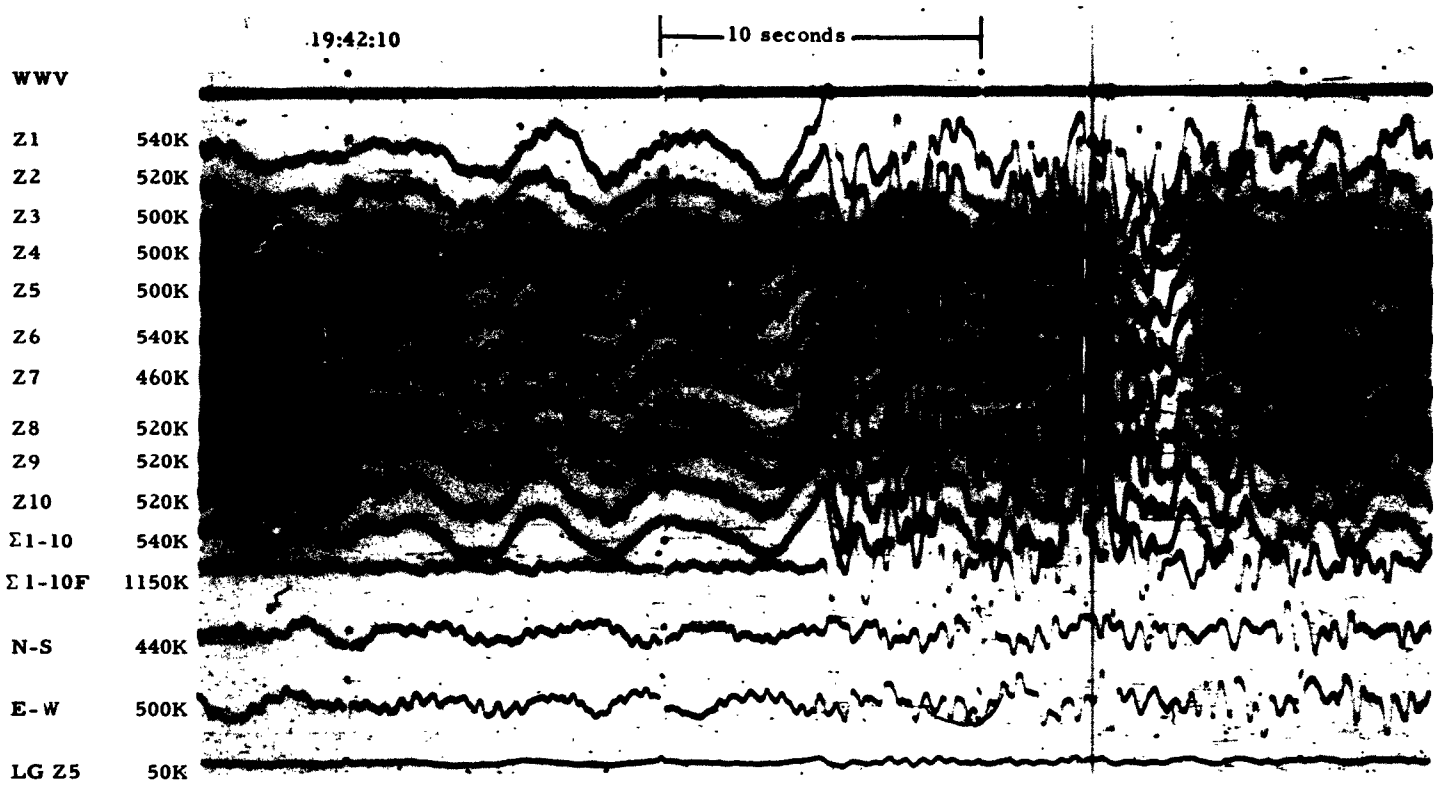


Figure 70. Short-period Develocorder record illustrating enhancement of a teleseismic signal and cancellation of microseisms in the 6-second period range by the Seismic Data Filter, Model 11760, operating in the range of 0.8 cps, 18 db/octave to 5.0 cps, 24 db/octave

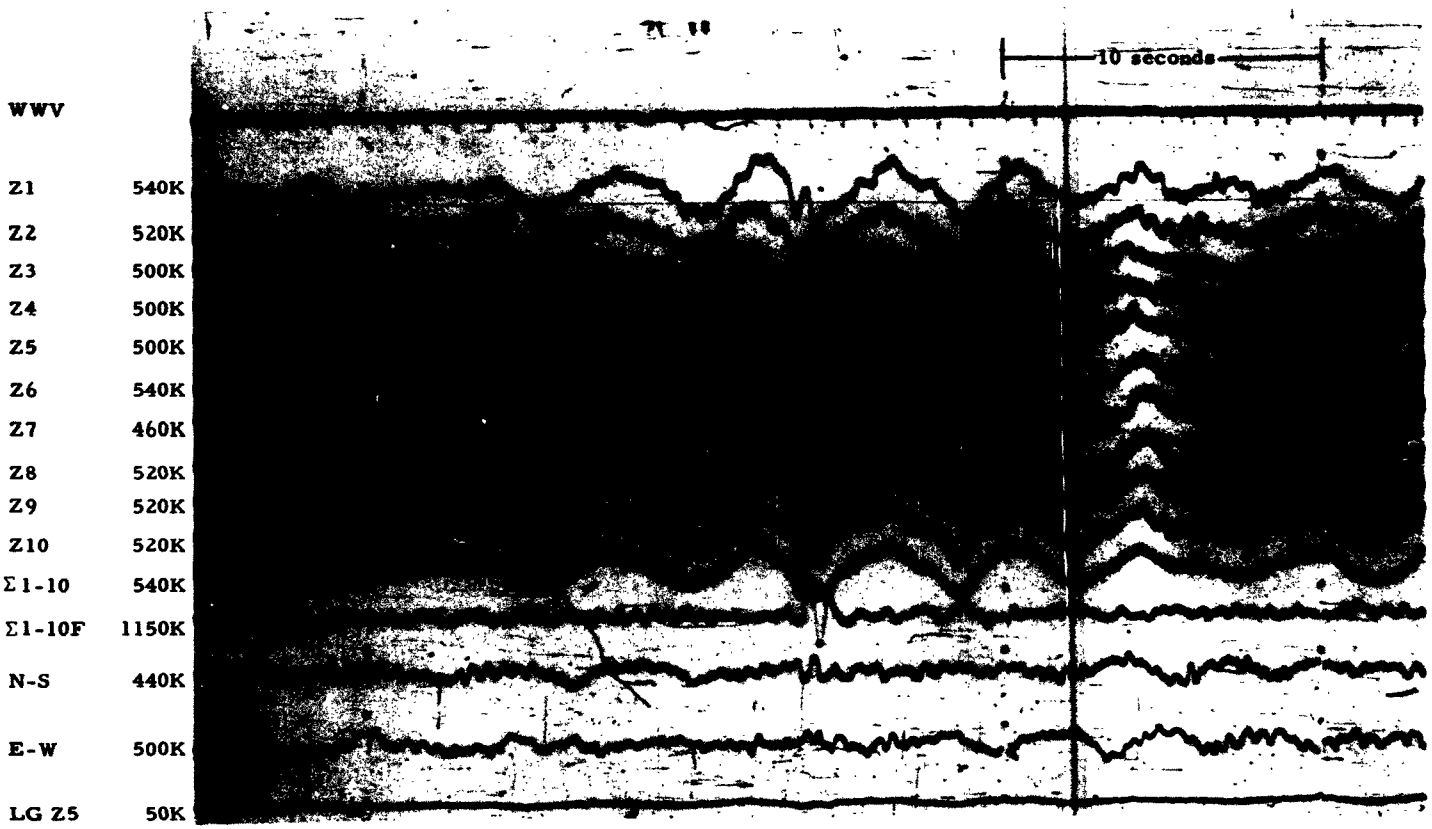


Figure 71. Short-period Develocorder record illustrating enhancement of a teleseismic signal and cancellation of microseisms in the 6-second period range by the Seismic Data Filter, Model 11760, operating in the range 0.8 cps, 18 db/octave to 5.0 cps, 24 db/octave

be indicated for events than are apparent on the individual seismograms or the normal summation seismogram, and low-level signal arrivals are enhanced by the filter, increasing the detection capabilities of the station.

The filter can be operated with many bandpass ranges. The three bandpass ranges selected for study at WMSO were chosen because of the character of the microseismic background at WMSO and because these three settings are believed to be among those that would be most valuable for use at other observatories.

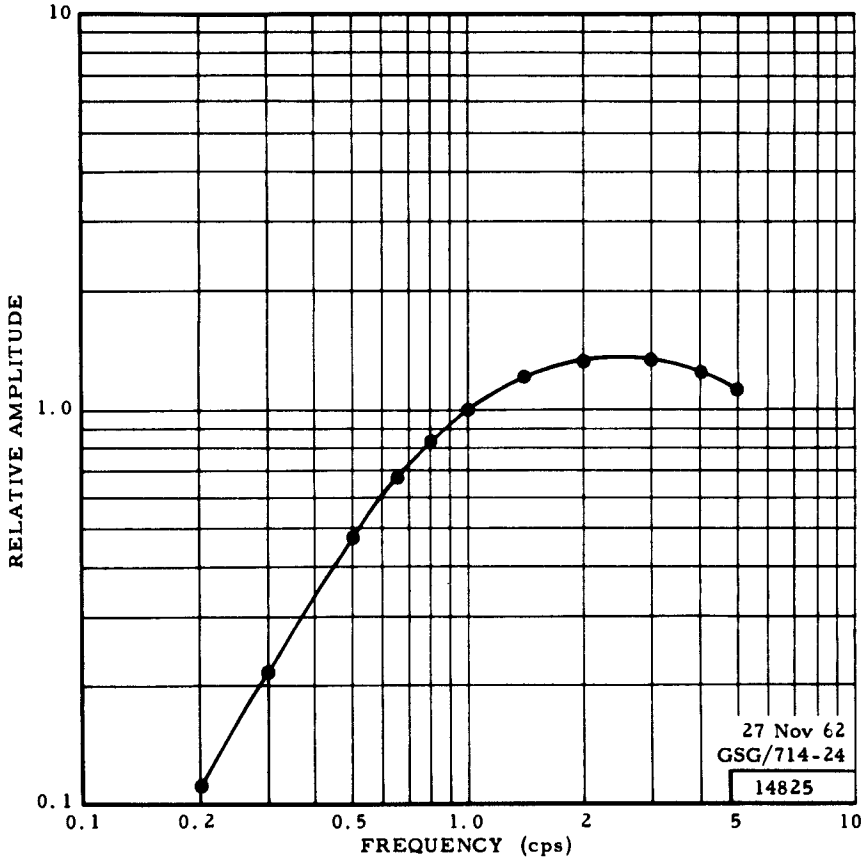


Figure 72. Frequency response of Seismic Data Filter, Model 11760, operating at a bandpass range of 0.8 cps, 12 db/octave to 5.0 cps, 6 db/octave

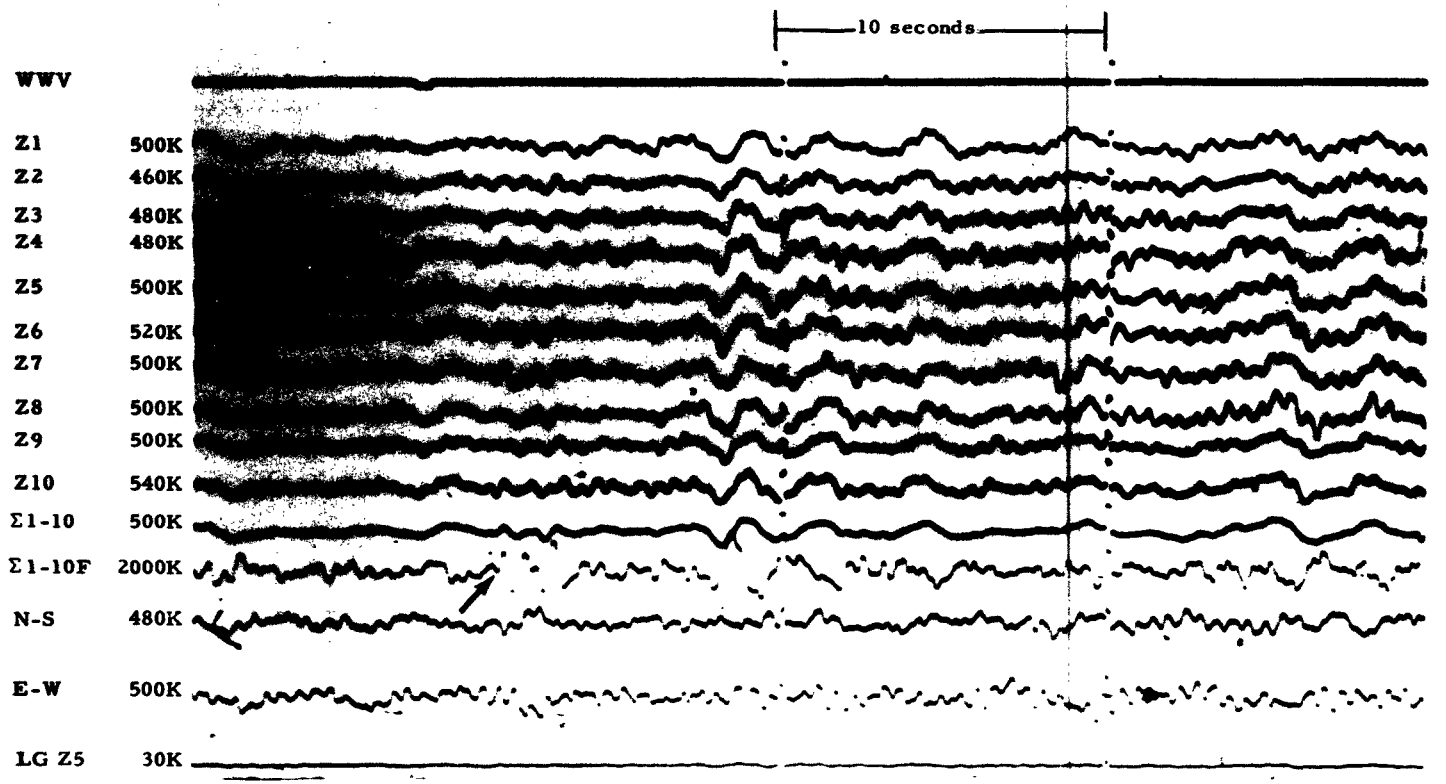


Figure 73. Short-period Develocorder record illustrating the value of the filtered Σ1-10 trace as a flag trace. Note earlier start of event (arrow) indicated by filtered trace. Seismic Data Filter, Model 11760, operating in the bandpass range 0.8 cps, 12 db/octave to 5.0 cps, 6 db/octave

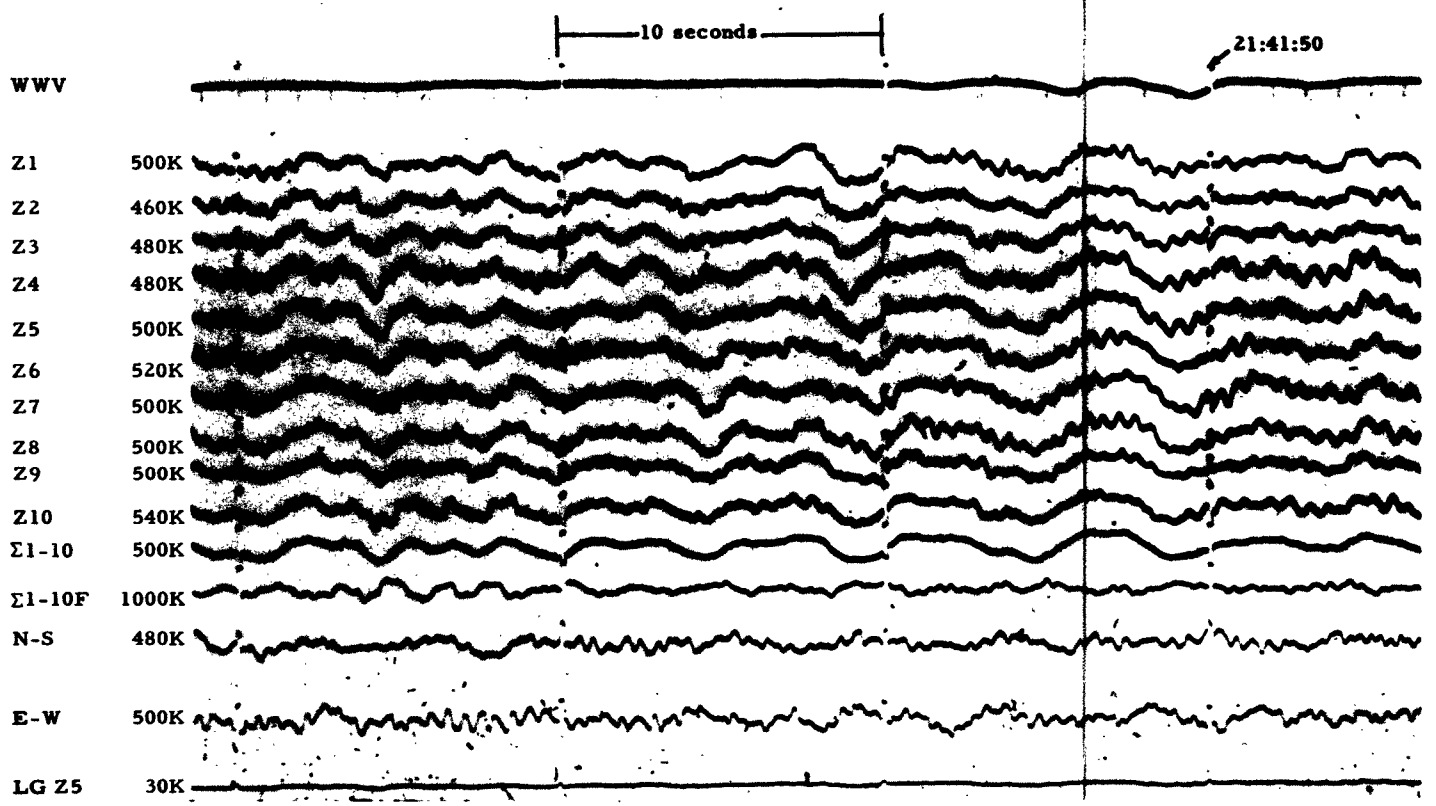


Figure 74. Short-period Develocorder record illustrating the value of the Geotech seismic data filter in the cancellation of microseisms in the 6-second period range. Seismic Data Filter, Model 11760, operating in the bandpass range 0.8 cps, 12 db/octave to 5.0 cps, 6 db/octave

No recommendation can be made for the optimum filter setting to be used at all stations. The selection of a setting for use at a given station must be based on the predominant character of the microseismic background noise at the station, and can best be determined after operating the filter at the station within several different bandpass ranges for a short time.

Each of the three bandpass ranges within which the Geotech filter was operated between 8 November and 31 December at WMSO is judged to be satisfactory. Either of the two later settings is preferable to the first setting for WMSO

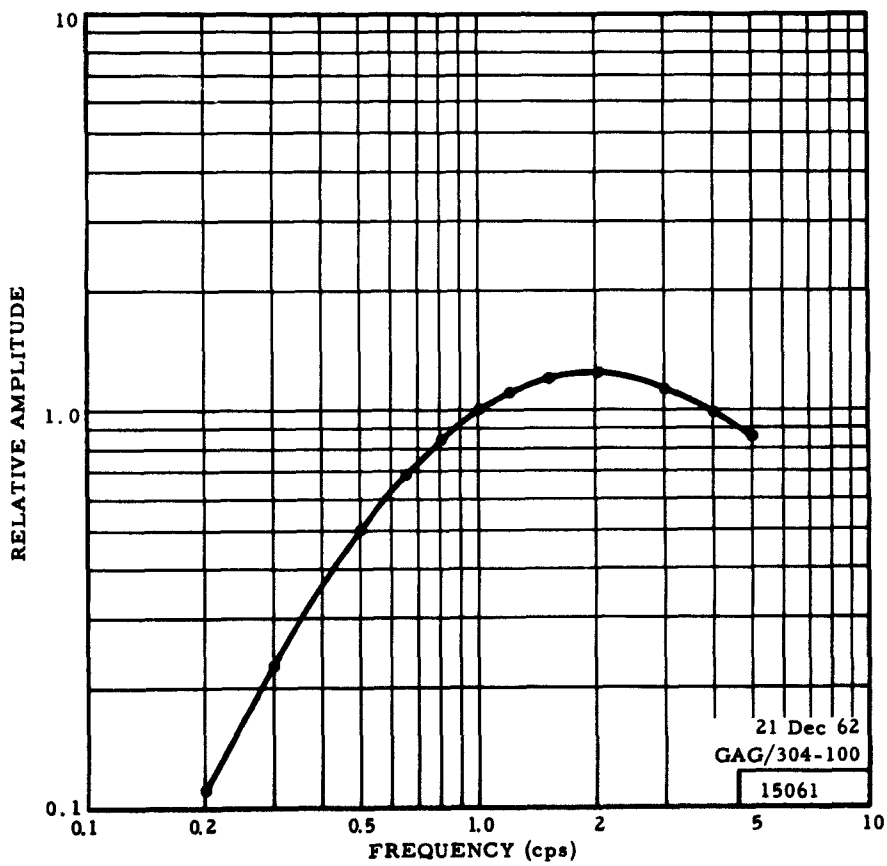


Figure 75. Frequency response of Seismic Data Filter, Model 11760, operating at a bandpass range of 0.8 cps, 12 db/octave to 3.0 cps, 6 db/octave

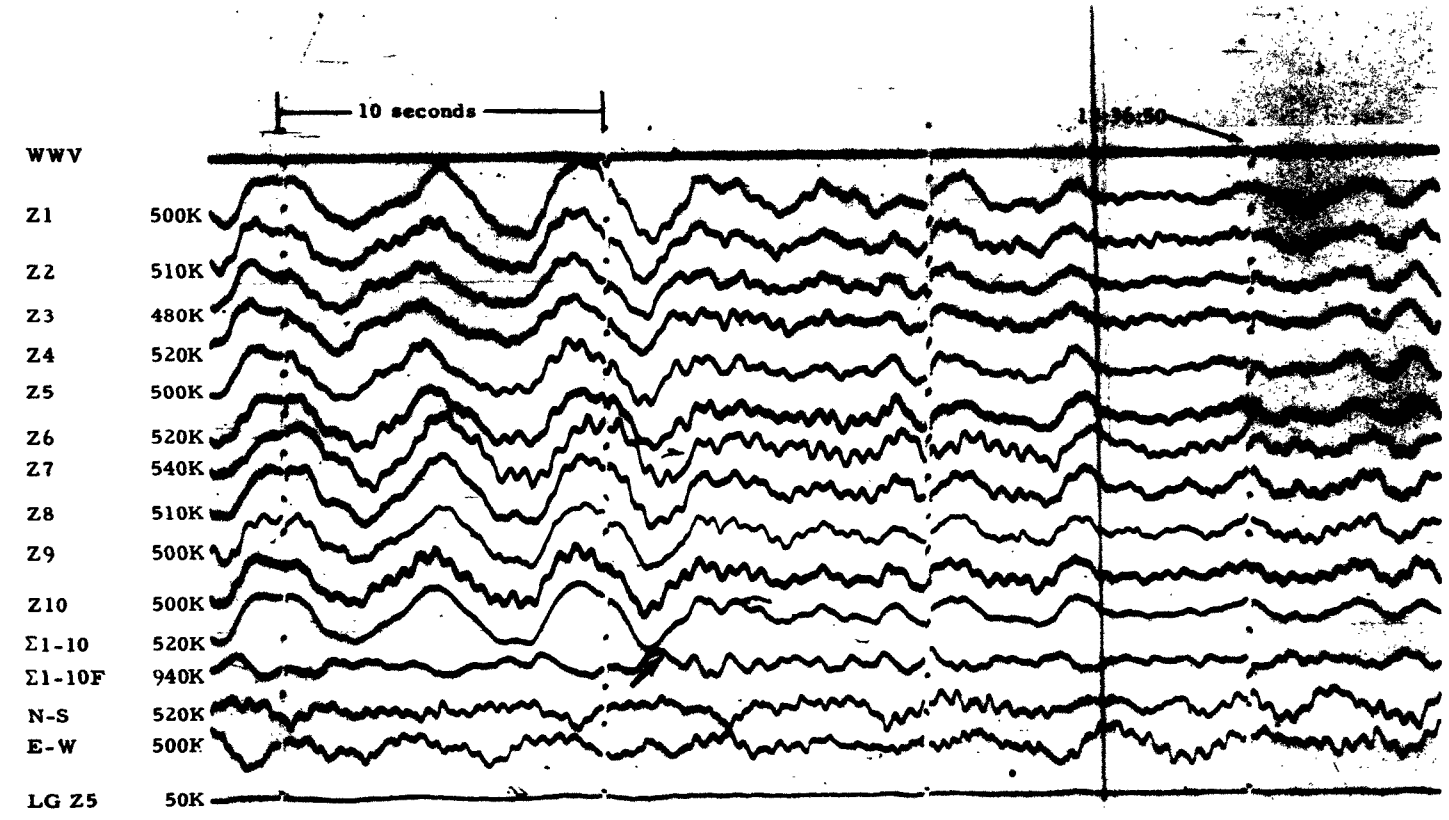


Figure 76. Short-period Develocorder record illustrating the cancellation of low-frequency microseisms and the enhancement of a low-level teleseismic signal which is partially masked by these microseisms (arrow) by the Seismic Data Filter, Model 11760, operating in the bandpass range 0.8 cps, 12 db/octave to 3.0 cps, 6 db/octave.

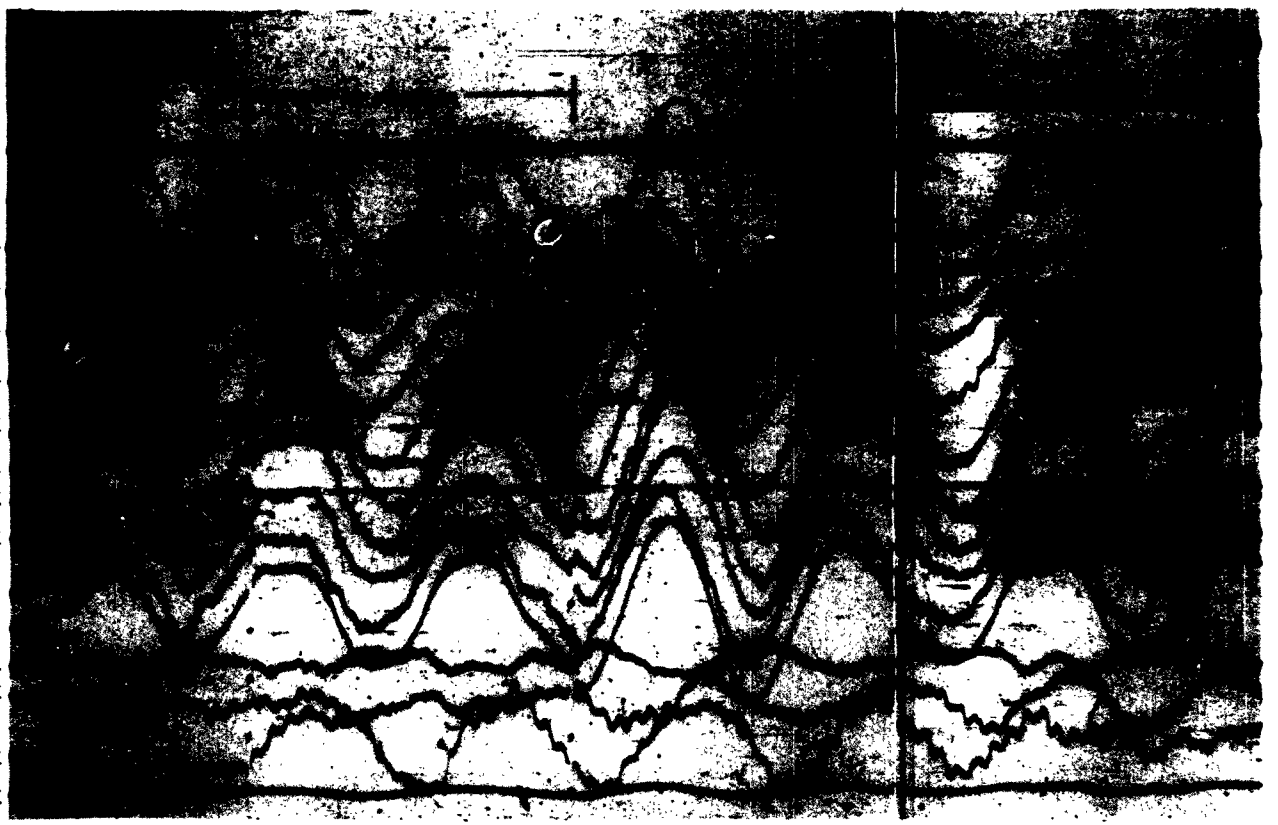


Figure 77. Short-period Develocorder record illustrating the attenuation of high-amplitude microseisms in the period range of 5 to 9 seconds by the Seismic Data Filter, Model 11760, operating in the bandpass range 0.8 cps, 12 db/octave to 3.0 cps, 6 db/octave

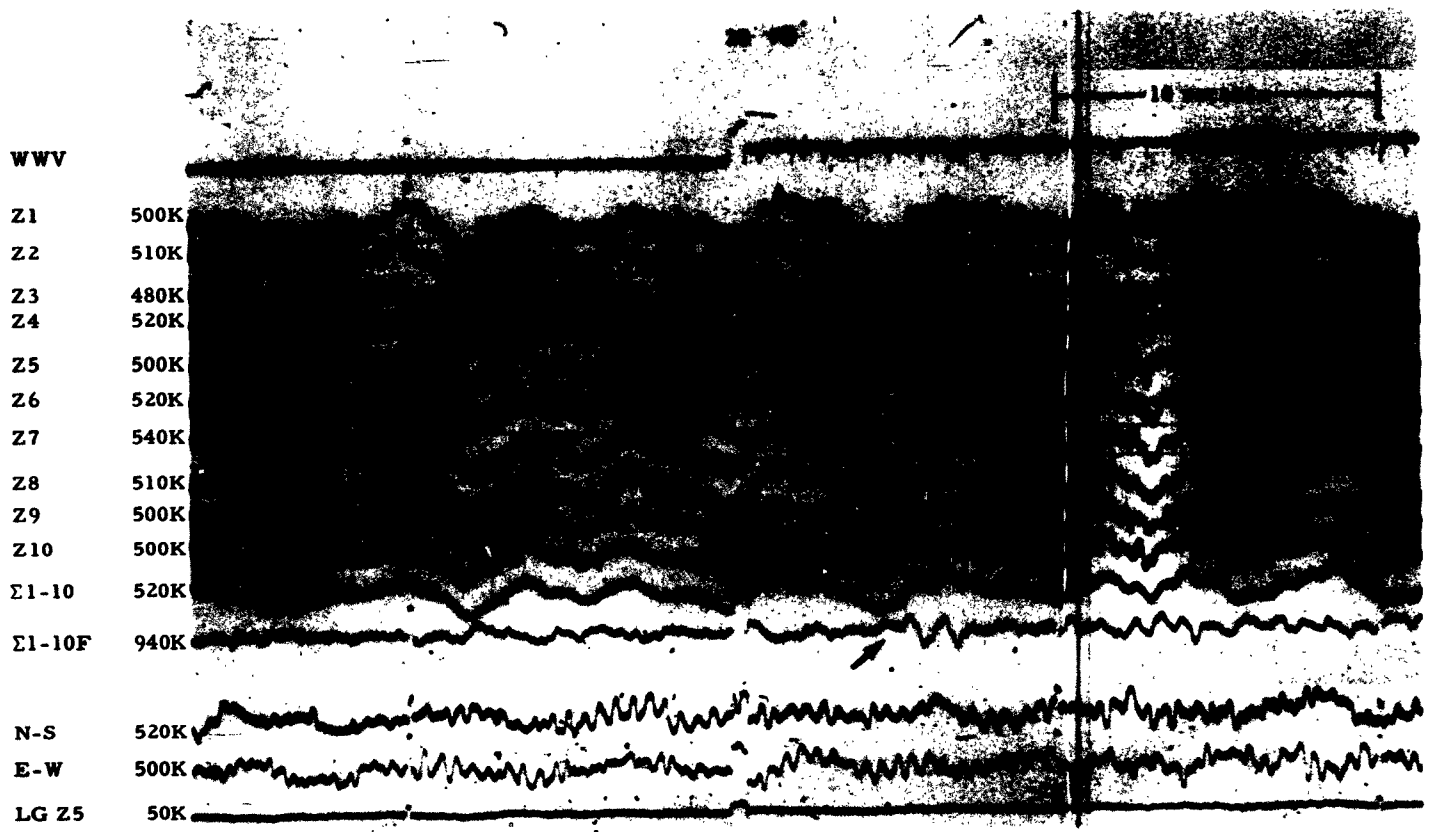


Figure 78. Short-period Develocorder record illustrating the value of the Σ1-10 filtered seismogram as a flag trace. Note the arrival of a teleseismic event well defined on the filtered trace (arrow). Seismic Data Filter, Model 11760, operating in the bandpass range 0.8 cps, 12 db/octave to 3.0 cps, 6 db/octave

operation, however, because less phase shift and signal distortion result from the action of the filter. In addition, neither of these bandpass ranges completely attenuated the microseisms within the 5- to 9-second period range, a condition which is considered useful as a check of the operation of the filter. The apparent phase shift which is evident in the illustrations of the seismograms obtained from the first setting (figures 70 and 71) is not considered to be excessive, nor are the capabilities of the filtered seismograph to function as a flag considered to be decreased; for strong signals, the same arrival time is indicated on the filtered summation seismogram as is indicated on the other seismograms.

## 7.3 BROAD-BAND FLAT VELOCITY RESPONSE

Dual recording of the output from the broad-band vertical seismometer was started on 20 November 1962. A phototube amplifier with a 5-cps galvanometer was inserted into the seismometer circuit in order to record a flat velocity response broad-band seismograph in addition to the original flat amplitude response broad-band seismograph.

During the recording of strong signals, a high-frequency "ringing" was observed on the flat-velocity seismogram. Preliminary investigations to determine the source of the ringing indicated that it could probably be attributed to vibration of the buoyancy compensator of the Press-Ewing seismometer.

During the relocation of the vertical broad-band seismometer from vault 8P to the tank farm in December 1962, the seismometer was modified by removing the buoyancy compensator. Recording of the flat velocity response seismograph was resumed, but sufficient data for an evaluation of its effectiveness have not been collected because other tests, which were assigned a higher priority, required the recording space needed for the broad-band flat-velocity response seismograph.

Data from a flat velocity response broad-band seismograph will be valuable in magnitude studies. The flat-velocity seismograms will facilitate direct measurement of ground velocity in millimicrons/second at the frequency at which maximum ground velocity occurs.

## 7.4 SIE UNMANNED SEISMOGRAPH

The SIE unmanned seismograph was installed at WMSO on 20 June 1962 by SIE personnel. Evaluation of the first five months of operation of the seismograph was presented in a report by SIE. Late in November, the unmanned seismograph became the responsibility of WMSO for long-term field evaluation. No change was made in the seismograph until 18 February 1963, when a Benioff seismometer was substituted for the EV-17 seismometer originally supplied with the system.

The SIE unmanned seismograph, as originally designed, consists of a moving-coil seismometer with a free period of 1.0 second, a transistor amplifier and FM modulator, a geophone alarm circuit, a test circuit, and a nickel-cadmium battery pack. Approximately 8 to 9 months of unattended operation is possible with fully charged batteries. The batteries had been slightly discharged due to tests made before 20 June 1962, the original installation date, and the batteries required charging about the end of the year.

The frequency response of the unmanned seismograph is similar to that of a JM seismometer with a 20-cps galvanometer (JM 20) at frequencies above approximately 2 cps. The JM 20 frequency response is shown in figure 79. At frequencies below 2 cps, the response of the unmanned seismograph drops off much more rapidly than that of the JM 20 seismograph.

Comparison of the seismograms from the unmanned seismograph, the JM 20, and the short period triangular array were made for 100 local and near-regional events (primarily quarry blasts). Four specific categories were selected for grading of the performance of each seismograph system. The four categories are:

a. Accuracy in timing first arrival;

b. Determination of direction of initial P motion;

c. Signal-to-noise ratio of all phases recorded for each event (ease with which the event as a whole can be detected);

d. Detection of phases subsequent to the initial recorded phase.

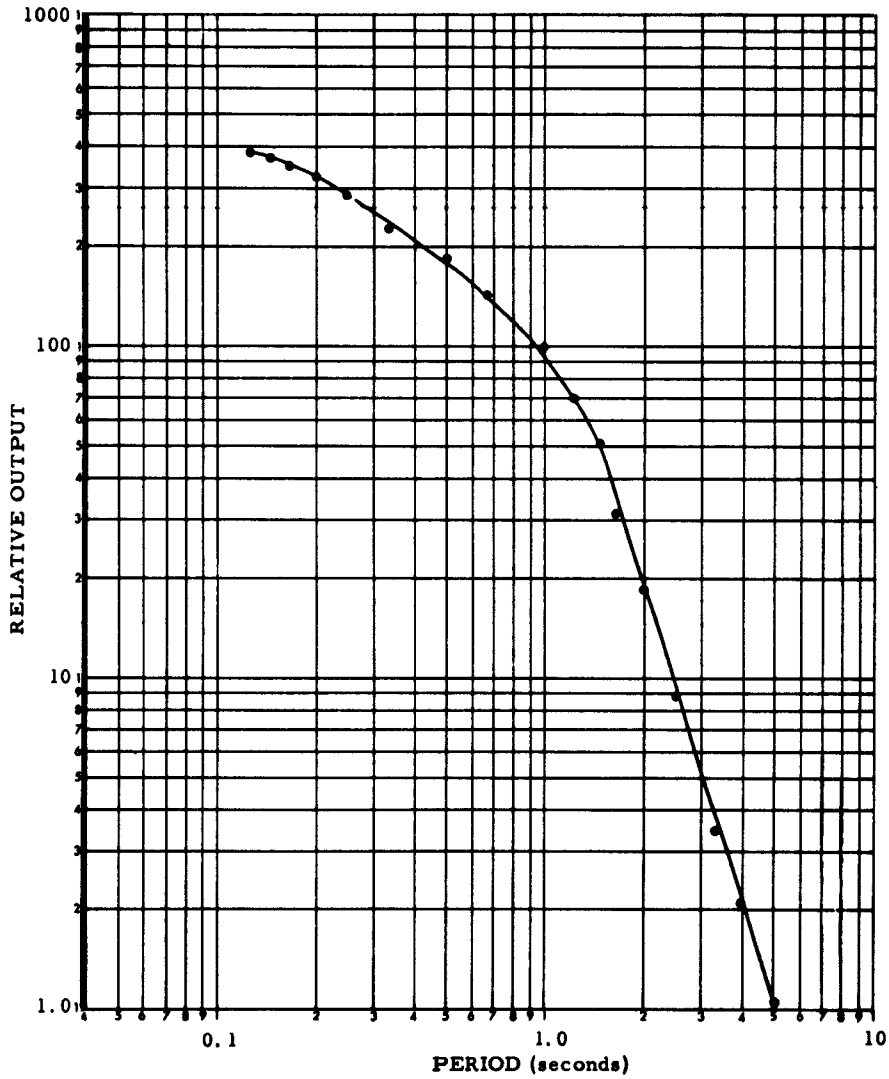


Figure 79. Frequency response of the JM 20

Each seismograph system was graded as follows: 1 - best; 2 - second best; 3 - third best; 0 - not detected. The same grade was given to more than one system for a given recorded event if the systems appeared to perform equall well. Table 18 shows the results of the comparison.

Only local and near-regional events were selected for the comparison becaus preliminary observations showed that the unmanned seismograph had very limited detection capabilities for the relatively longer periods which are predominant in the P waves from teleseismic and most regional events (figure 80). The results of the comparison indicate that the JM 20 seismograph is definitely superior to the SIE unmanned seismograph; however, the SIE unmanned seismograph detected the same number of events as the JM 20 seismograph. In general, signals were displayed more clearly on the JM 20 seismogram. Figure 81 shows the typical difference between the response of the unmanned seismograph and the JM 20 seismograph to near-regional event

Table 18. Evaluation of the Detection Capabilities of JM 20 versus SIE, JM 20 versus Triangular (△) Array, and SIE versus Triangular (△) Array

| | Grade 1 | | | Grade 2 | | | Grade 3 | | | Grade 0 | | |
|---|---|---|---|---|---|---|---|---|---|---|---|---|
| | △ | JM 20 | SIE | △ | JM 20 | SIE | △ | JM 20 | SIE | △ | JM 20 | SIE |
| Occurrence accuracy in timing | 51 | 75 | 38 | 39 | 17 | 31 | 9 | 2 | 20 | 1 | 6 | 11 |
| Occurrence direction of first motion | 10 | 22 | 16 | 3 | 0 | 1 | 0 | 0 | 0 | 87 | 78 | 83 |
| Signal-to-noise ratio as clarity of signals | 90 | 67 | 48 | 6 | 26 | 31 | 4 | 3 | 17 | 0 | 4 | 1 |
| Best phase detection | 93 | 32 | 14 | 6 | 62 | 52 | 1 | 2 | 30 | 0 | 4 | 4 |

Weight given signals:
1 Best detection
2 Second best detection
3 Third best detection
0 No detection

Note: 100 local and near-regional signals taken during the months of July, September, November, and December 1962

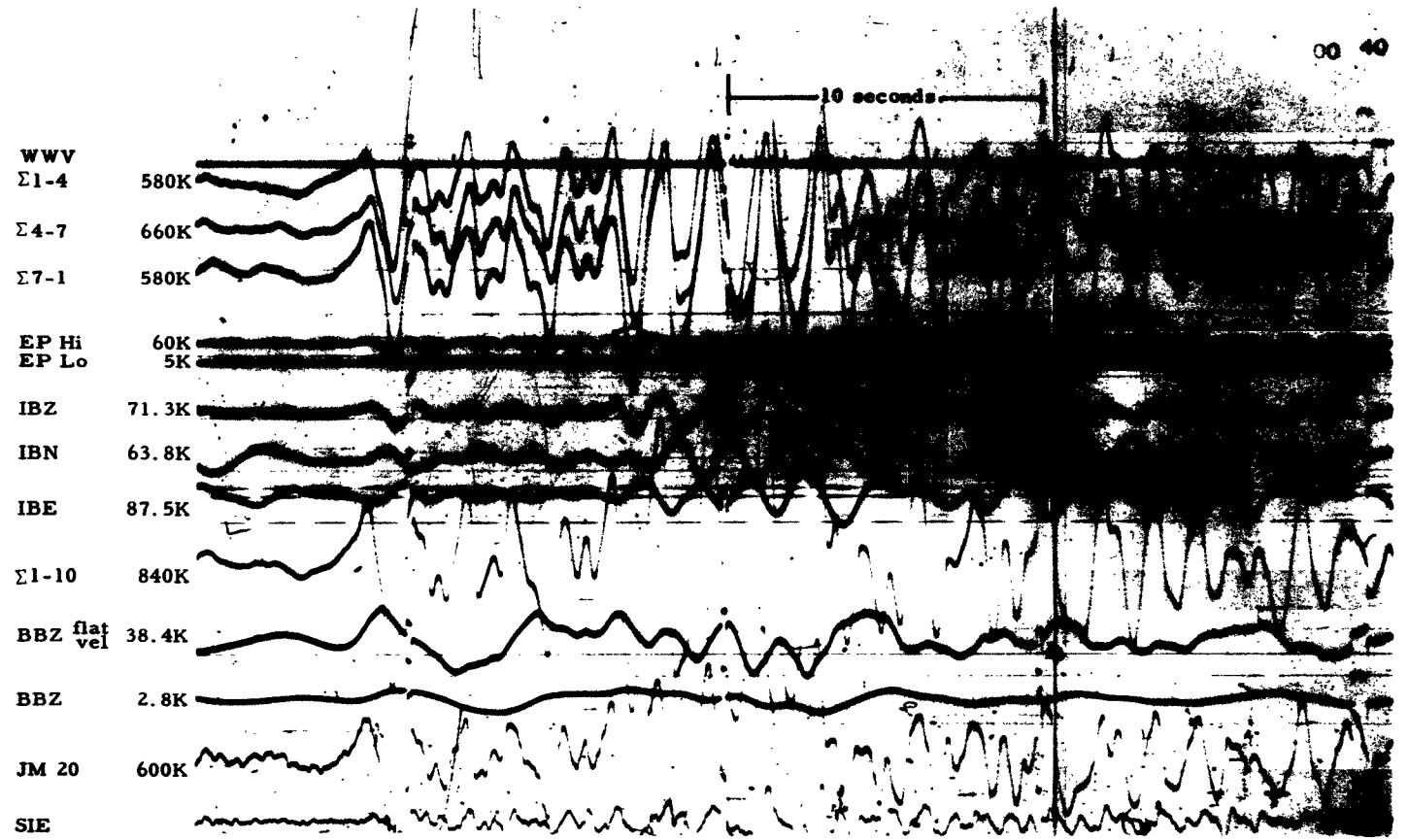


Figure 80. Test Develocorder record illustrating the limited detection capability of the SIE unmanned seismograph for relatively longer period P waves of teleseisms

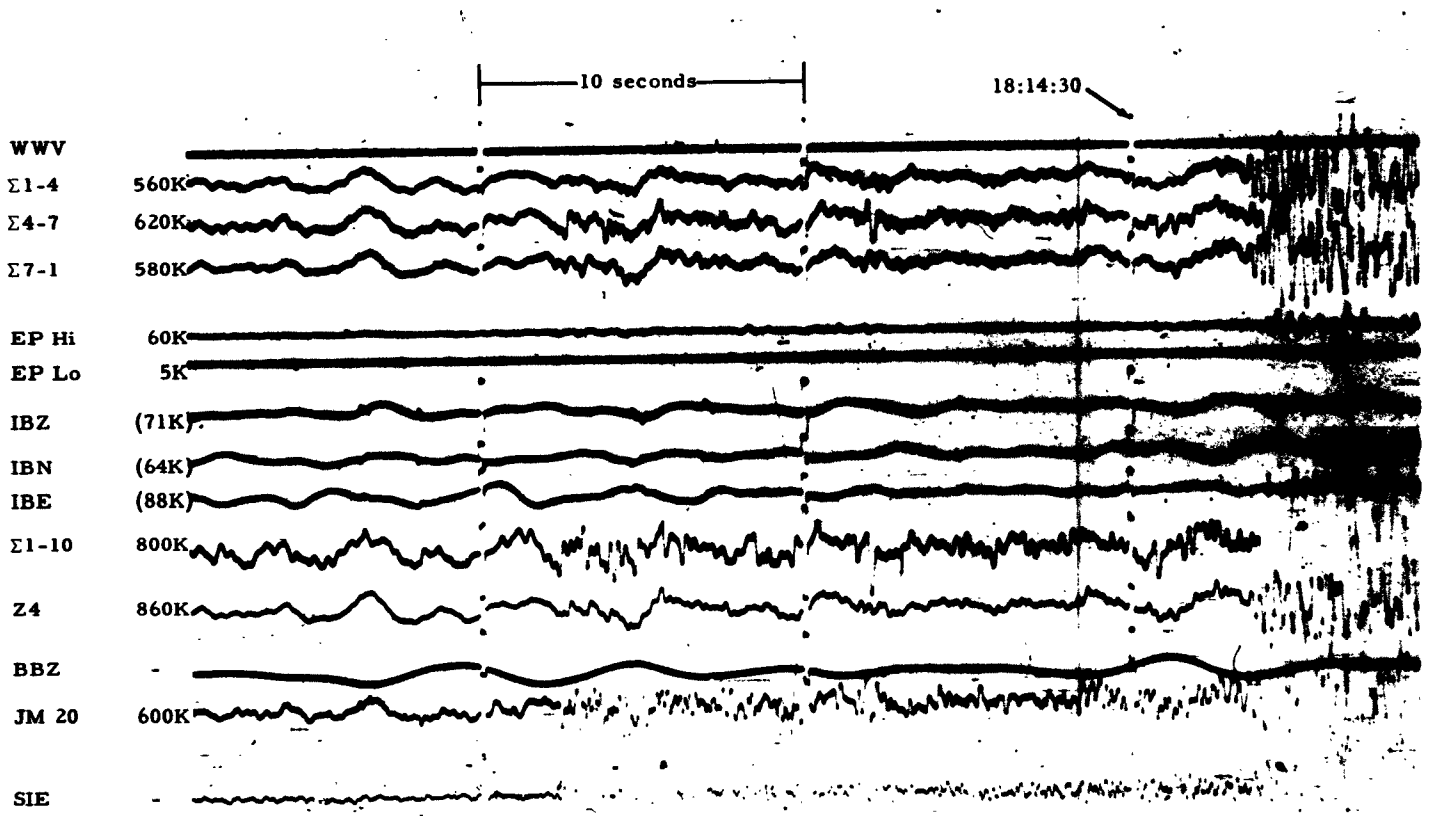


Figure 81. Test Develocorder record illustrating the difference between the response of the SIE unmanned seismograph and the JM 20 seismograph to a typical near-regional signal

## 8. VISITORS AT WMSO

During Phase V, WMSO data and facilities were available to many other participants in Project VELA-UNIFORM. Eighty-four individuals, representing 24 organizations, visited and/or used the WMSO facilities and data to train new personnel or to conduct research studies and instrument field tests. A total of 1149 man-days of training and research were conducted at WMSO, primarily by SIE, Texas Instruments, and Geotech personnel working on other VELA projects. Table 19 lists the number of man-days spent at WMSO by each organization.

In addition, magnetic-tape records and 16-mm film records of data recorded at WMSO were furnished to other VELA participants. Among those using WMSO data were Geotech under Project VT/8652 (noise study), Geotech under Project VT/1139 (deep-well seismograph), Texas Instruments, Century Geophysical Corporation, and members of the staffs of various universities.

Table 19. Man-days Spent at WMSO by Visitors

| Organization | Orientation and training of personnel by WMSO staff (man-days) | Research and special projects conducted at WMSO (man-days) | Total (man-days) |
|---|---|---|---|
| Dresser Industries (SIE) | - | 123 | 123 |
| Texas Instruments | 102 | 134 | 236 |
| Other Geotech groups | 117 | 663 | 780 |
| Others | 10 | - | 10 |
| Totals | 229 | 920 | 1149 |

## 9. BIBLIOGRAPHY

Båth, M., 1952, Earthquake magnitude determination from the vertical component of surface waves: Trans. Amer. Geophys. Union, v 33, no. 1, pp 81-89.

Gutenberg, B., 1945, Amplitudes of surface waves and magnitude of shallow earthquakes: Bull. Seis. Soc. Amer., v 35, pp 3-12.

Gutenberg, B., and Richter, C. F., 1956, Magnitude and energy of earthquakes: Annali di Geophysica, v 9, pp 1-15.

Richter, C. F., 1958, Elementary Seismology: San Francisco, Freeman Press.

# APPENDIX 1 TO TECHNICAL REPORT NO. 63-54

## STATEMENT OF WORK

## Project VELA T/036

Operation and Improvement of the Experimental Seismological Observatory Established at Fort Sill, Oklahoma under Contract AF 33(600)-41318.

1. Tasks.

a. Continue operation of the Fort Sill seismological station for a period of 12 months beginning 1 March 1962.

b. Continue the evaluation of the resulting seismometric data and conduct studies to determine optimum operation characteristics; make such changes in the operating parameters as may be required to provide the most effective station possible, subject to technical approval by the AFTAC Project Officer.

c. Simultaneously operate the new array and the old array for approximately 2 months; evaluate and compare array performance.

d. Conduct special research studies, e. g., long-period noise investigations and linear array evaluations. Additional seismic and electronics equipment may be required to supplement present station facilities for special studies. For the purpose of planning under this task, the level of effort should not exceed 24 man-months, and the total expenditure for technical equipment should not exceed $15,000. Approval of technical acceptability will be obtained from the AFTAC Project Officer for each study prior to initiation.

e. Provide minimum maintenance to maintain selected vaults of the old array in a useable condition after Task 1c has been completed.

f. Make adjustments as necessary to provide more efficient use of floor space in central recording building, e.g., expansion of useable area by removal of some partitions.

g. Use station facilities to evaluate the performance characteristics of experimental detection equipment after approval by the AFTAC Project Officer.

h. Transmit daily seismic reports to the U. S. Coast and Geodetic Survey, Washington, D. C. using established report format and detailed instructions.

i. Publish a monthly summary in 50 copies of seismological events, distribution and format as approved by the AFTAC Project Officer.

j. Provide use of station facilities, seismological data, and the technical assistance of station personnel to other participants of the VELA-UNIFORM Program. This support will not be provided without prior approval of the AFTAC Project Officer.

Letter Contract designated Supplemental Agreement No. 3 to AF 33(600)-41318.

2. Reports

a. Monthly letter-type progress reports in 12 copies, summarising work through the 25th of the month, will be dispatched to AFTAC by the end of the month.

Topics will include technical status, major accomplishments, problems encountered, future plans and any action required by AFTAC. Illustrations and photographs should be included as applicable. In addition, the monthly report submitted for the reporting period occurring six months prior to the schedule contract termination date will contain specific statements concerning requirements and justifications for extension, modification or expiration of work and changes in cost estimates which are anticipated by the contractor. The heading of each report should contain the following information:

AFTAC Project No.

Project Title

ARPA Order No. 104

ARPA Project Code No. 8100

Name of Contractor

Date of Contract

Amount of Contract

Contract Number

Contract Expiration Date

Project Scientist or Engineer's Name and Phone Number

b. A list of suggested milestones will be dispatched to AFTAC in 12 copies within 20 days following award of a definitive contract. (Milestones are defined as points of accomplishments which present significant progress when completed.) For a given milestone, the list should include the completion date and a brief description, when necessary to define specifically the accomplishment to be attained. Upon approval of milestones information, copies of SD Form 350 will be made available for use in reporting progress against the milestone schedule. The SD Form 350 will be attached to the monthly report.

c. Special reports of major events will be forwarded by telephone, telegraph, or separate letter as they occur and should be included in the following monthly reports. Specific items are to include (but are not restricted to) program delays, program breakthroughs, or new inventions or techniques.

d. A semiannual technical summary report in 20 copies, covering work performed through each 6-months period, will be submitted to AFTAC within 15 days after the close of the reporting period. This summary should be submitted as a continuation of the present sequence of similar reports. These reports will present a concise and factual discussion of the technical findings and accomplishments of the reporting period. The heading of the report will contain the heading information indicated in paragraph 2a, above.

e. A final technical report in 50 copies will be submitted within 60 days following completion of the work statement. The heading of the report will contain the information indicated in paragraph 2a, above, and the report itself will include all of the pertinent information covered in the semiannual reports described above.

f. Special reports, as requested by the AFTAC Project Officer, may be required upon completion of various portions of the work.

3. Technical Documents. The Contractor will furnish the following documents:

a. All seismograms and operating logs, to include pertinent information concerning time, date, type of instrument, magnification, etc., as requested by the AFTAC Project Officer.

b. Technical manuals on the installation, calibration, and operation of station equipment installed furing this operational period.

c. Two sets of reproducible engineering drawings and specifications for any changes or modifications in standard operational equipment and instruments and for any new equipment designed, together with one set of prints of these same drawings.

4. Miscellaneous.

a. Technical correspondence and reports, unless otherwise specified are to be submitted to:

HQ USAF (AFTAC/TD-1/Captain Clent Houston)
Washington 25, D. C.

b. DD Form 254 dated 19 Nov 1959 attached to the Basic Contract applies to this Exhibit A.

c. The following equipment under Contract AF 33(600)-43486 is authorized for use in the performance of the work hereunder:

| QTY | DESCRIPTION | MODEL # |
|---|---|---|
| 1 | Develocorder Switching Unit | 5970 |
| 1 | Develocorder Coding Unit | 6281 |
| 2 | Film Viewers | 6585 |
| 10 | Phototube Amplifiers (3-CPS Galv.) | 4300 |
| 2 | Vertical Seismometers | 7505 |
| 3 | Phototube Amplifiers | 5240 |
| 3 | Harris Galvanometers | 8530 |
| 3 | Line Termination Modules | 5874 |
| 6 | Vault Terminals | 11875 |
| 1 | Mass Position Monitor | 10073 |
| 1 | Mass Position Display | 11003 |
| 1 | Mass Position Power Supply | 110004 |
| 3 | Johnson-Matheson Seismometers | 6480 |
| 3 | Line Termination Modules | 8979A |
| 2 | Mass Position Monitors | 10074 |

APPENDIX 2 TO TECHNICAL REPORT NO. 63-54

MAILING LIST FOR WMSO EARTHQUAKE BULLETIN

APPENDIX 2 TO TECHNICAL REPORT NO. 63-54

MAILING LIST FOR WMSO EARTHQUAKE BULLETIN

HQ USAF (AFTAC, Capt. Clent Houston)
DCS/Operations
Washington 25, D. C.

HQ USAF (AFTAC, Dr. Carl Romney)
DCS/Operations
HQ USAF
Washington 25, D. C.

Dr. John H. Hodgson
Chief, Division of Seismology
Dominion Observatory
Department of Mines and Technical Surveys
Ottawa, Canada

International Seismological Summary
Kew Observatory
Richmond Surrey, England

Seismographic Station
565 Earth Sciences Building
University of California
Berkeley 4, California

Mr. Richard A. Arnett
Texas Instruments, Incorporated
Seismic Branch Division
Exchange Bank Building
Dallas 35, Texas

Dr. Hugo Benioff
Seismological Laboratory
220 North San Rafael Avenue
Pasadena, California

Mr. Leonard Murphy
Chief, Seismological Branch
U. S. Coast and Geodetic Survey
Washington 25, D. C.

Dr. Eugene Herrin
Geology Department
Southern Methodist University
Dallas, Texas

The Geotechnical Corporation
c/o Mr. J. H. Gautreaux
P. O. Box 2071
Lawton, Oklahoma

Dr. D. E. Willis
University of Michigan
Willow Run Labs
Ann Arbor, Michigan

Bureau of Ships
P. O. Lt. Commander Clark
Bell Telephone Laboratories
Whiptany, New Jersey

Father William Stauder, S. J.
Saint Louis University
Institute of Technology
3621 Olive Street
Saint Louis 8, Missouri

VESIAC
Institute of Science and Technology
The University of Michigan
Box 618
Ann Arbor, Michigan

Mr. Warren H. Westphal
Senior Geophysicist
Stanford Research Institute
Dept. of Earth Sciences
Menlo Park, California

Lamont Geological Observatory of Columbia University
Palisades, New York

Mr. D. H. Shurbet, Director
Seismological Observatory
Texas Technological College
Lubbock, Texas

Mrs. Mildred Beaman, Librarian
Dresser Electronics
P. O. Box 22187
Houston 42, Texas

Lt. Colonel Benjamin Grote
3338 49th Loop
Sandia Base
Albuquerque, New Mexico

Mrs. Mildred H. Meeder, Librarian
Natural History Museum
P. O. Box 1390
San Diego 12, California

Dr. Charles Bates
Advanced Research Projects Agency
Department of Defense
Washington 25, D. C.

Dr. Samuel Katz
Dept. of Geology
Rensselaer Polytechnic Institute
Troy, New York

Niedersächsische Staats und Universitätsbibliothek
Prinzenstrausse 1
(20b) Goettingen, West Germany

Dr. Roy E. Hanson
National Science Foundation
1951 Constitution Ave. NW
Washington 25, D. C.

Dr. Harold M. Mooney
School of Mines and Metallurgy
University of Minnesota
Minneapolis 14, Minnesota

Mr. H. I. S. Thirlaway
United Kingdom Atomic Energy Authority
Blacknest Brimpton - near Reading
Berkshire, England

Melpar, Inc.
Applied Science Division
3000 Arlington Blvd.
Falls Church, Virginia

Dr. J. P. Webb
University of Queensland
Department of Geology and Mineralogy
Brisbane, S. W. 6
Queensland, Australia

Mr. A. M. Rugg, Jr., Project Manager
Tonto Forest
Seismological Observatory
P. O. Box 337
Payson, Arizona

The Reverend J. J. Hennessey, S. J., Director
Manila Observatory
Mirador
Baguio City, Philippines

Mr. Al Sabitay
Texas Instruments, Inc.
Geosciences Department
P. O. Box 35084, Airlawn Station
Dallas 35, Texas

Dr. William Benson
National Science Foundation
Washington 25, D. C.

Mr. James I. Gimlett
Geology Department
University of Nevada
Reno, Nevada

Dr. Roy A. Savill
United Kingdom Atomic Energy Authority
Atomic Weapons Research Establishment
Foulness - Southend on Sea,
Essex, England

Dr. Glenn Werth
Lawrence Radiation Lab
Livermore, California

Dr. Sidney Kaufman
Shell Development Company
P. O. Box 481
Houston 1, Texas

Seismological Station
Department of Geology
University of Wisconsin
2544 University Avenue
Madison 5, Wisconsin

Mr. Ker C. Thompson, CRZGQ
Terrestrial Sciences Laboratory
Office of Aerospace Research
Air Force Cambridge Research Laboratories
Laurence G. Hanscom Field
Bedford, Massachusetts

Mr. Eysteinn Tryggvason
University of Tulsa
Dept. of Earth Sciences
Tulsa 4, Oklahoma

Dr. Maurice Ewing
Lamont Geological Observatory
Palisades, New York

Mr. Dan Hearn
Century Geophysical
10710 East Independence
Tulsa, Oklahoma

California Research Corporation
P. O. Box 446
La Habra, California

Mr. Rex Van Sandt
Jersey Production Research
1133 North Lewis Avenue
Tulsa 10, Oklahoma

Dr. James A. Peoples, Jr.
University of Kansas
Department of Geology
Lawrence, Kansas

Reverend Maruice Buist, S. J., Director
Observatoire de Geophysique
College Jean-de-Brebeuf
3200 Chemin Ste. Catherine
Montreal 26, Quebec, Canada

Dr. Robert W. Decker
Dartmouth College
Department of Geology
Hanover, New Hampshire

Data Analysis & Technique Center (DATC)
United ElectroDynamics
P. O. Box 334
Alexandria, Virginia

Mr. Herman J. Wirz, Jr., Technical Director
Seismological Laboratory
U. S. Coast and Geodetic Survey
Sandia Base
Albuquerque, New Mexico

Major Best, SRPG
Headquarters AFOSR
Tempo "D"
Washington 25, D. C.

Father Edward A. Bradley
Xavier University
Cincinnati 7, Ohio

Mr. Jean Lebel
ALPENS
6 Avenue Daniel-Lesueur
Paris 7'eme, France

Ceskoslovenska Akademie ved Geofysikalni Ustav
Bocni II, cp. 1401
Praha 13, Sporilov
Czechoslovakia

Mr. Frank Werner
U. S. Coast and Geodetic Survey
Seismological Laboratory, Sandia Base
Albuquerque, New Mexico

Mr. Eli Arieh
Chief, Seismological Stations
Geological Survey of Israel
30 Malkei Israel Street
Jerusalem, Israel

Dr. J. M. Bruckshaw
Geophysics Department
Imperial College
London, S. W. 7
England

Professeur J. P. Rothe
Directeur de l'Institut de Physique du Globe
38, boulevard d'Anvers
Strasbourg, France

Professor LeRoy Scharon
Geophysics Department
Washington University
St. Louis 30, Missouri

Seismological Station
Vedurstofan
Reykjavik, Iceland

# APPENDIX 3 TO TECHNICAL REPORT NO. 63-54

## MICROSEISMIC NOISE CURVES

## APPENDIX 3 TO TECHNICAL REPORT NO. 63-54

## MICROSEISMIC NOISE CURVES

Several types of microseismic noise curves were plotted for the short-period, intermediate-band, and long-period systems at WMSO. These curves include distribution of noise as a function of period and amplitude and mean peak amplitudes of noise as a function of period.

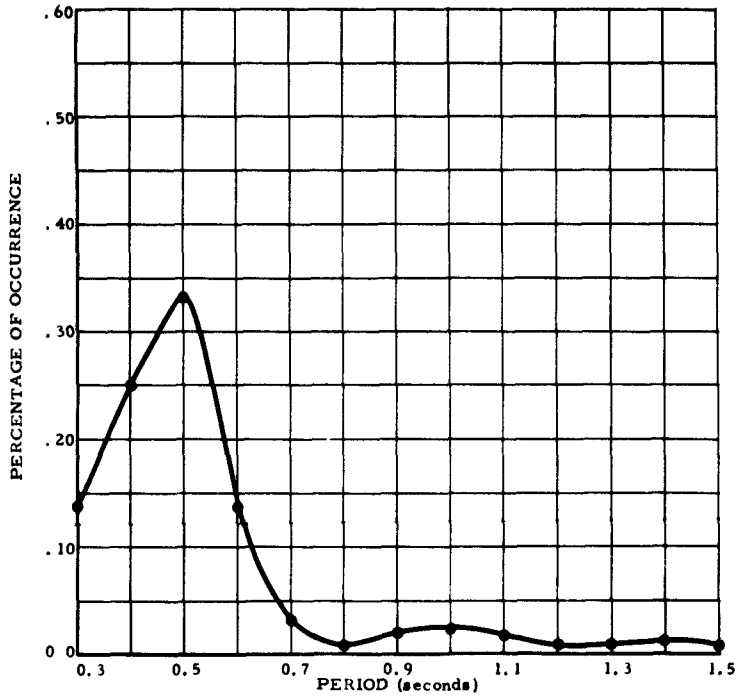


Figure 1. Probability of occurrence of microseismic background at a given period on short-period seismogram Z6 at WMSO

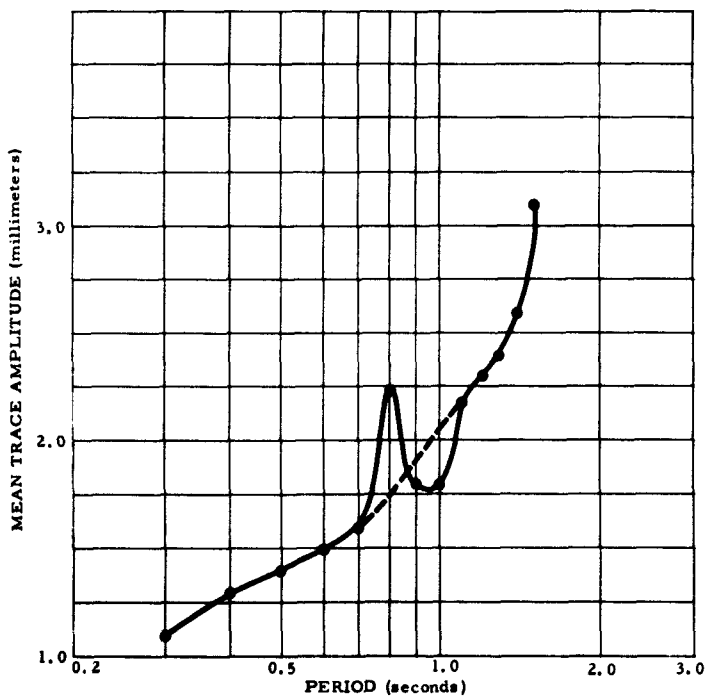


Figure 2. Mean peak trace amplitude of microseismic noise occurring at a given period versus period measured peak-to-peak on short-period seismograms Z6 at X10 view (gain 500K at 1 cps)

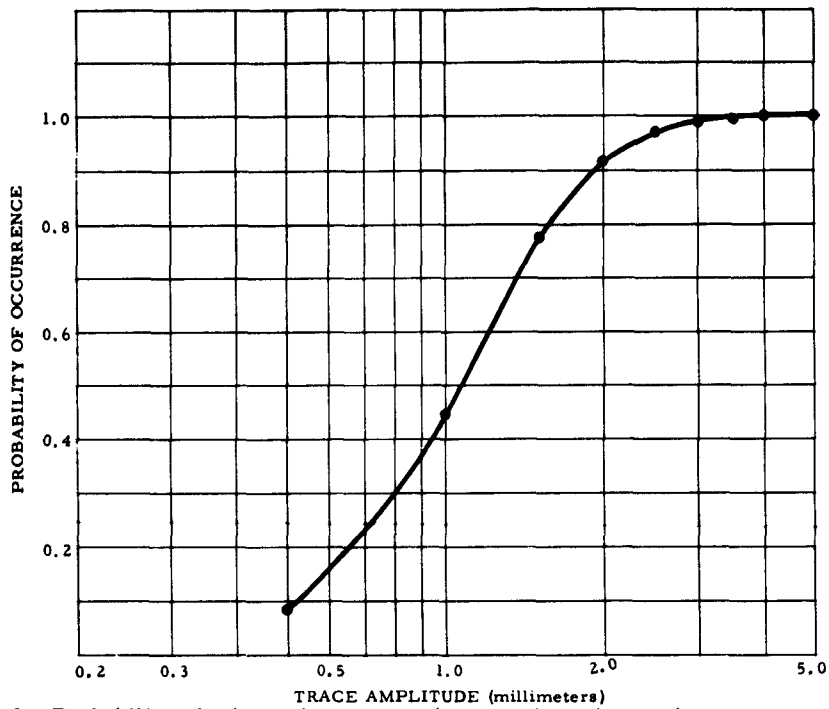


Figure 3. Probability of microseisms occurring at or less than a given trace amplitude in the period range, 0.3-1.5 seconds, measured peak-to-peak at X10 view (gain 500K at 1 cps, random data sample from 95 days throughout Phase V)

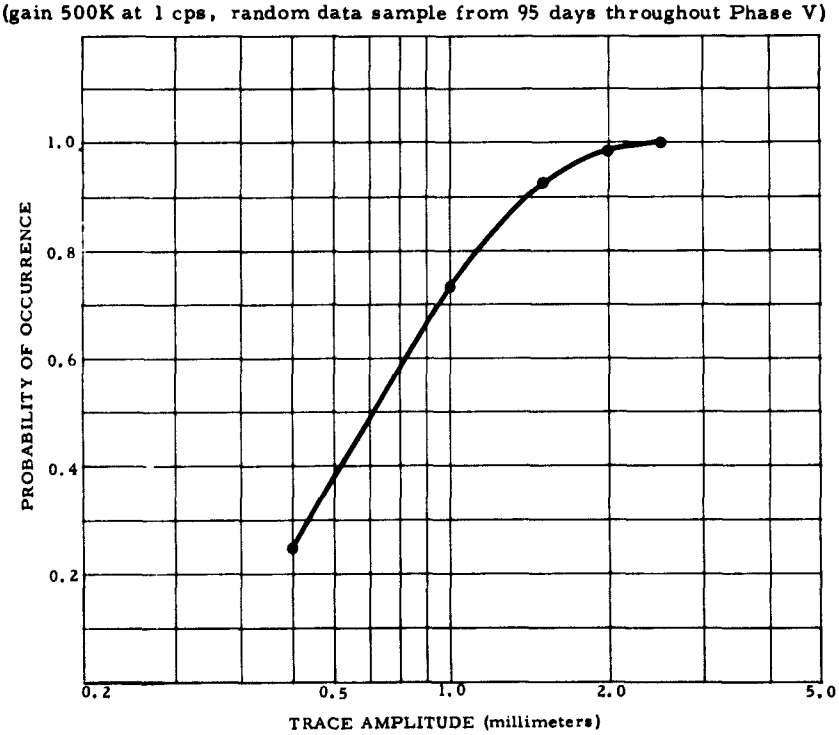


Figure 4. Probability of 0.3-second microseisms occurring at or less than a given trace amplitude, measured peak-to-peak at X10 view (gain 500K at 1 cps, random data sample from 45 days during Phase V)

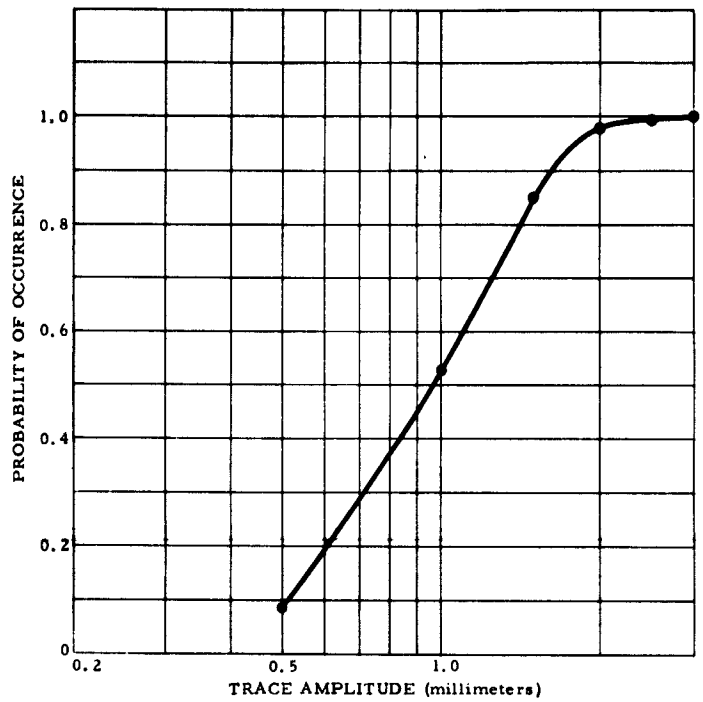


Figure 5. Probability of 0.4-second microseism occurring at or less than a given trace amplitude, measured peak-to-peak, at X10 view (gain 500K at 1 cps, random data sample from 45 days during Phase V)

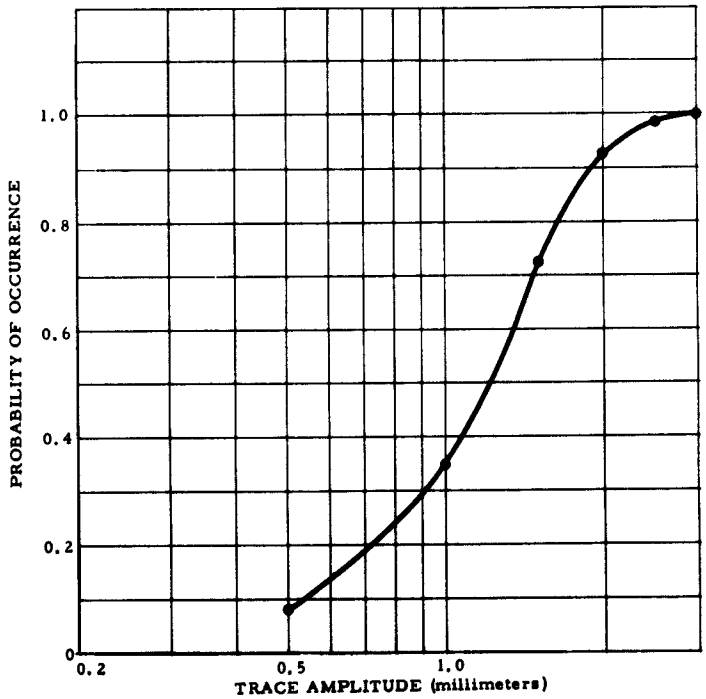


Figure 6. Probability of 0.6-second microseism occurring at or less than a given trace amplitude, measured peak-to-peak at X10 view (gain 500K at 1 cps, random data sample from 45 days during Phase V)

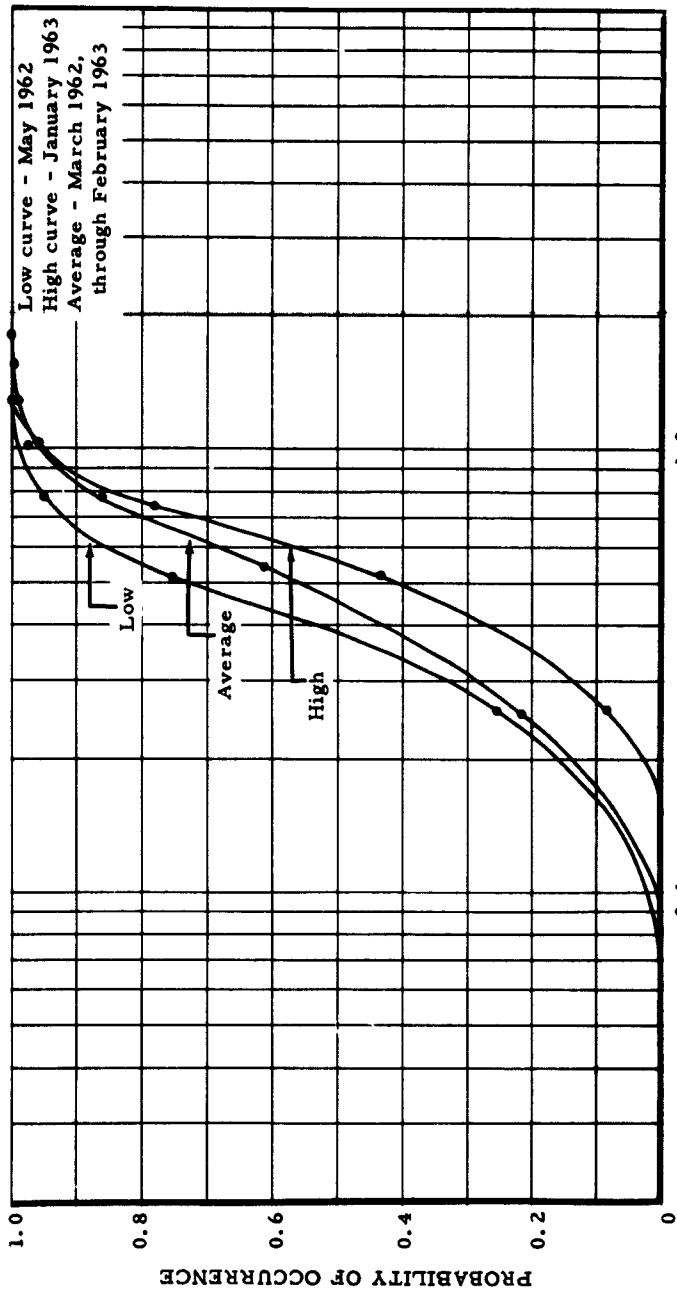


Figure 7. Probability of 0.5 second microseisms occurring at or less than a given ground amplitude (measurements made of Z6 1/2 peak-to-peak)

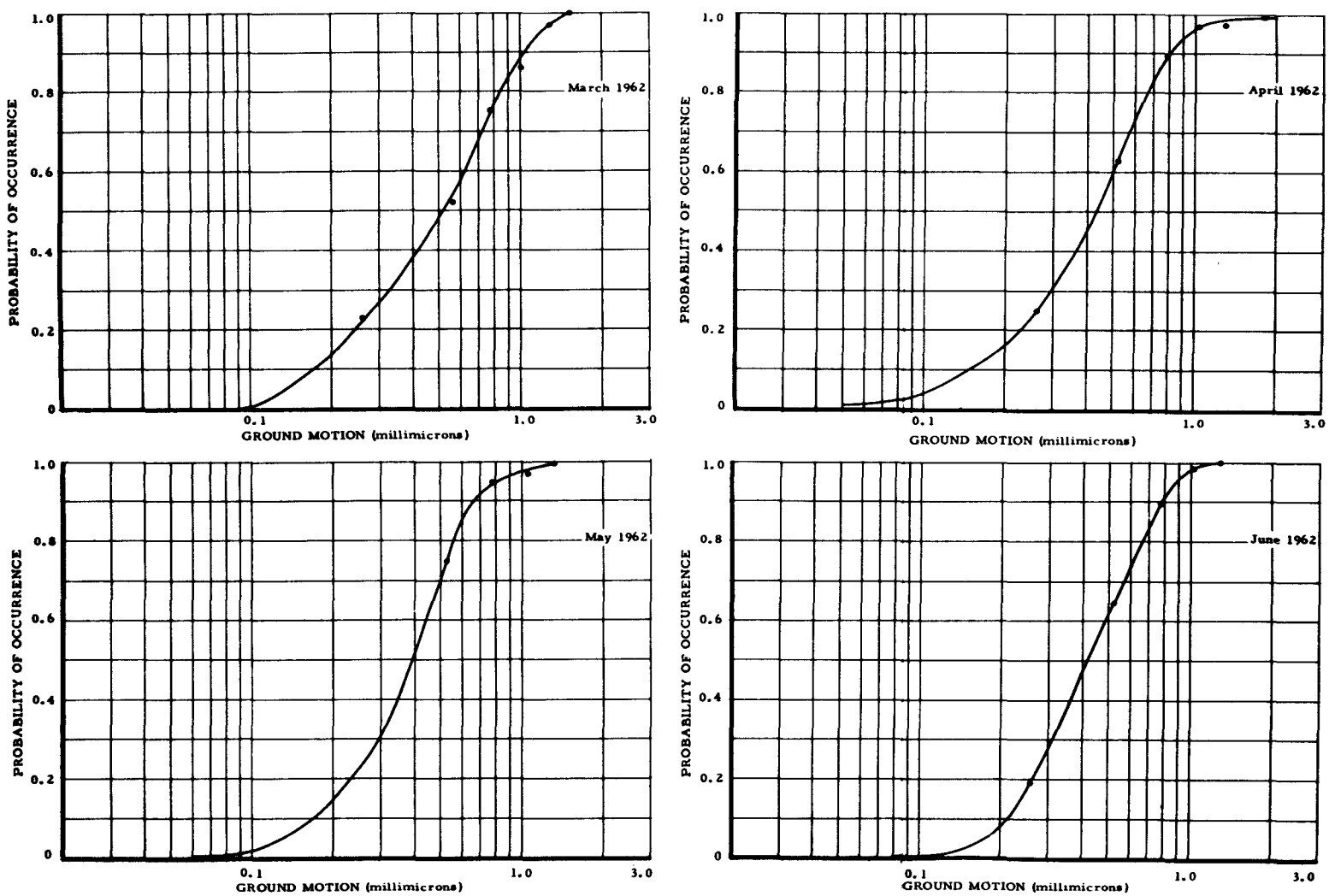


Figure 8. Probability of 0.5 second microseisms occurring at or less than a given

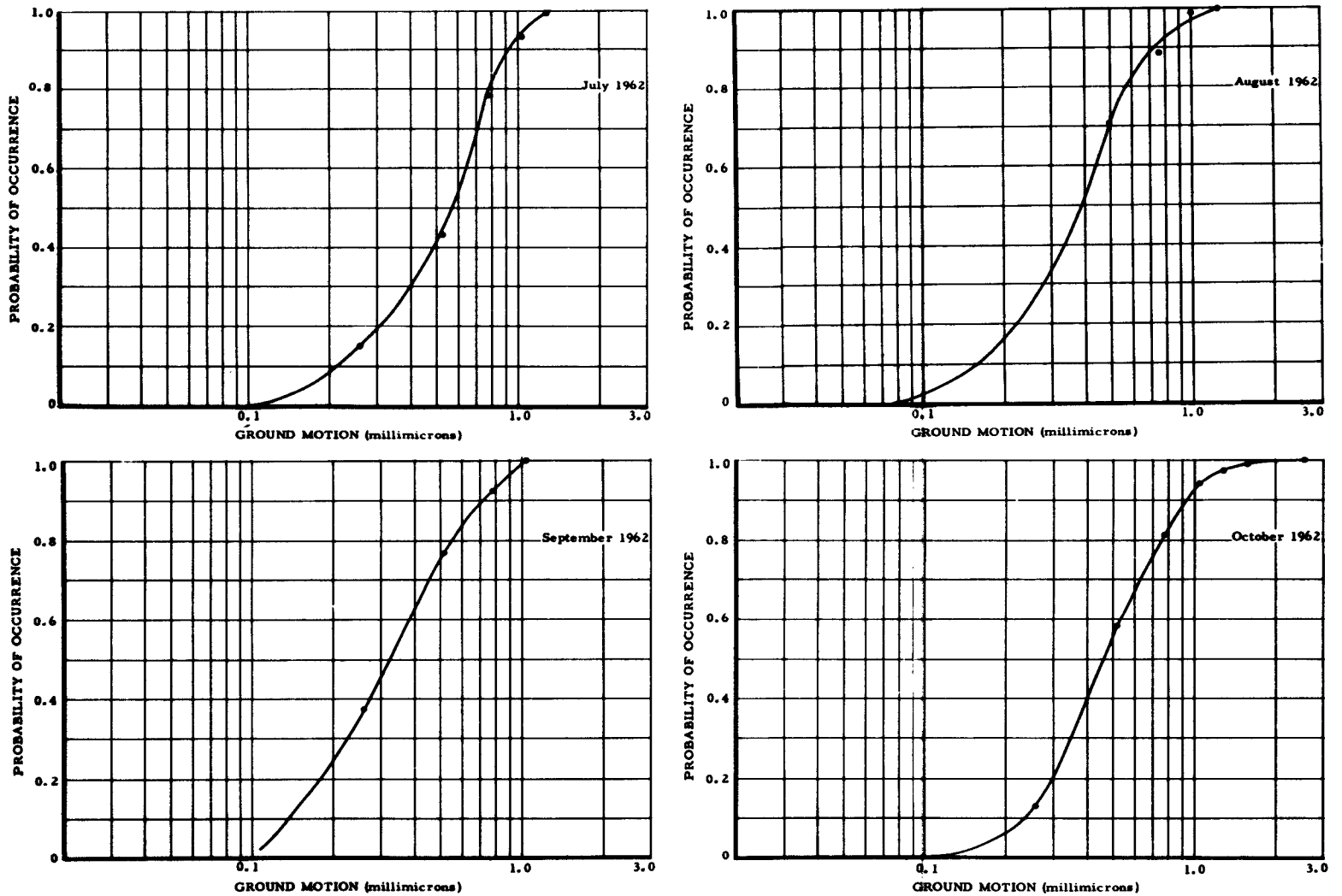


Figure 9. Probability of 0.5 second microseisms occurring at or less than a given ground amplitude (measurements made of Z6, 1/2 peak-to-peak)

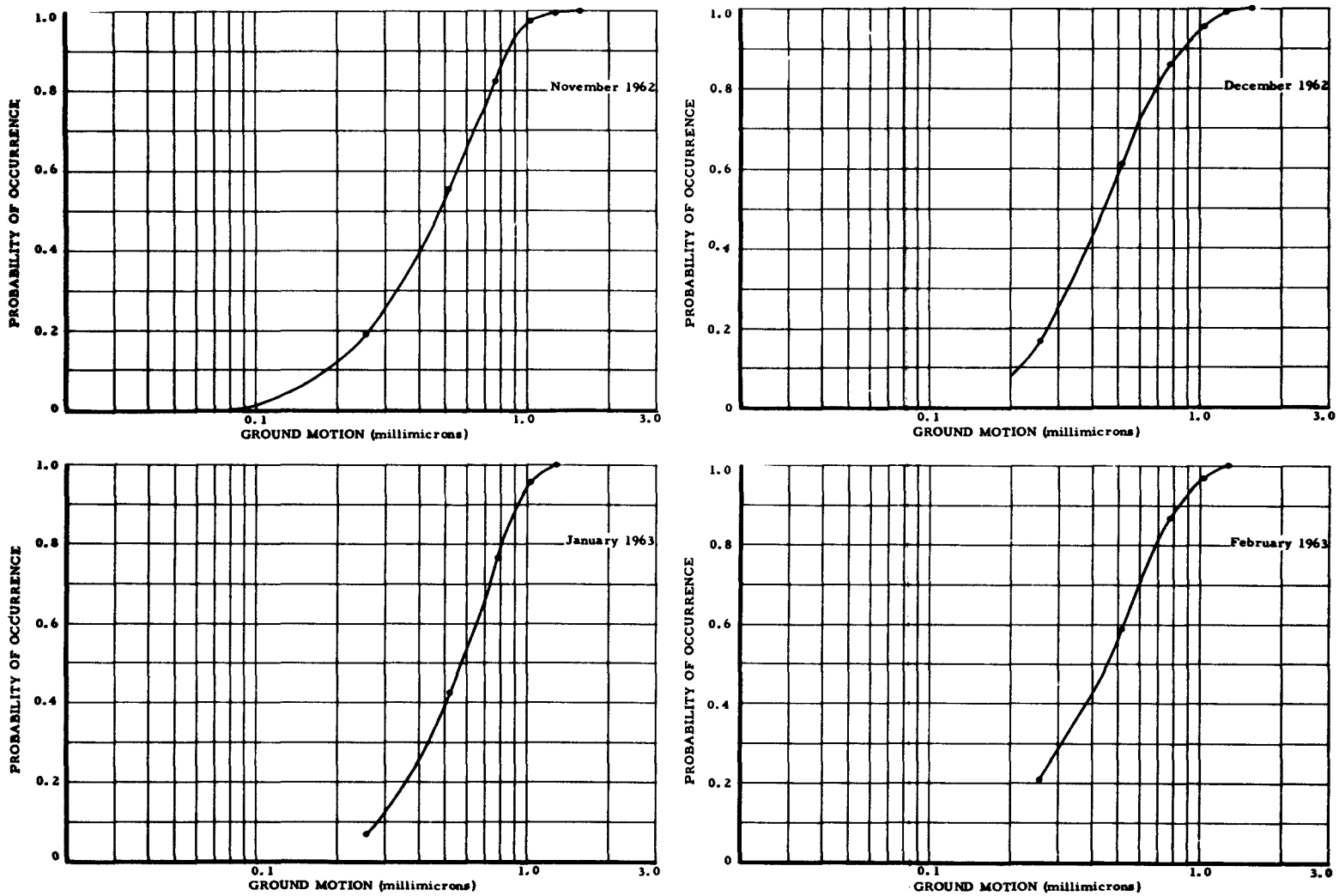


Figure 10. Probability of 0.5 second microseisms occurring at or less than a given

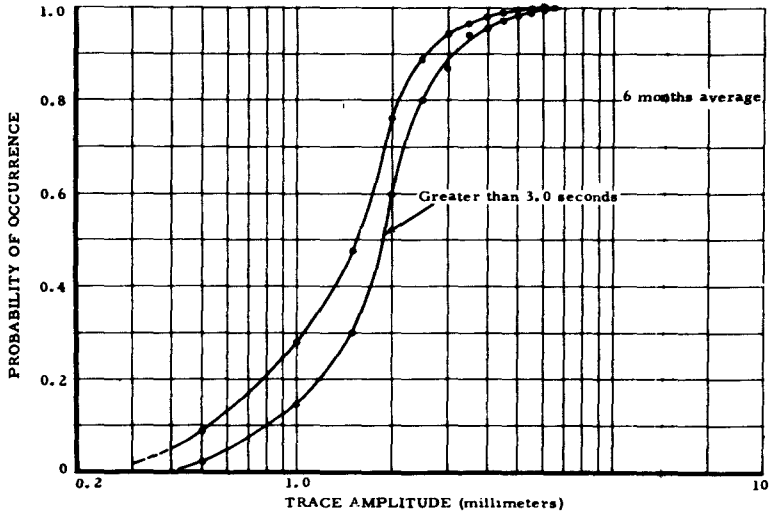
1.0
0.8
0.6
0.4
0.2
0
PROBABILITY OF OCCURRENCE
6 months average
Greater than 3.0 seconds
0.2
1.0
10
TRACE AMPLITUDE (millimeters)

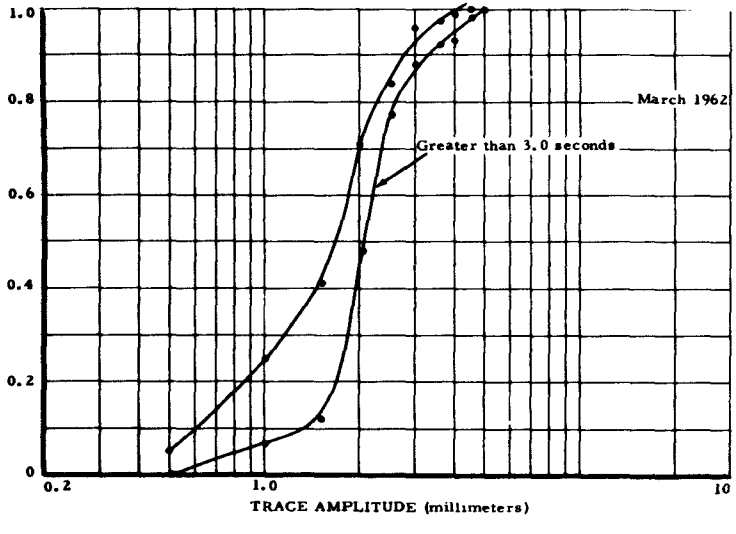
1.0
0.8
0.6
0.4
0.2
0
March 1962
Greater than 3.0 seconds
0.2
1.0
10
TRACE AMPLITUDE (millimeters)

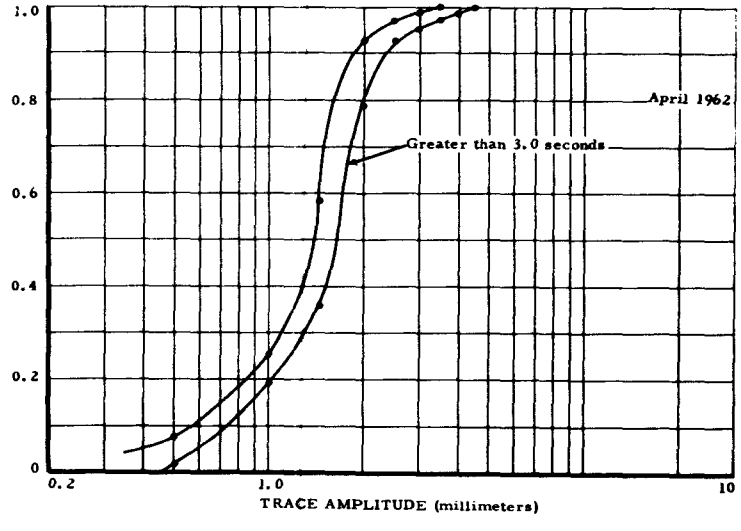
1.0
0.8
0.6
0.4
0.2
0
April 1962
Greater than 3.0 seconds
0.2
1.0
10
TRACE AMPLITUDE (millimeters)

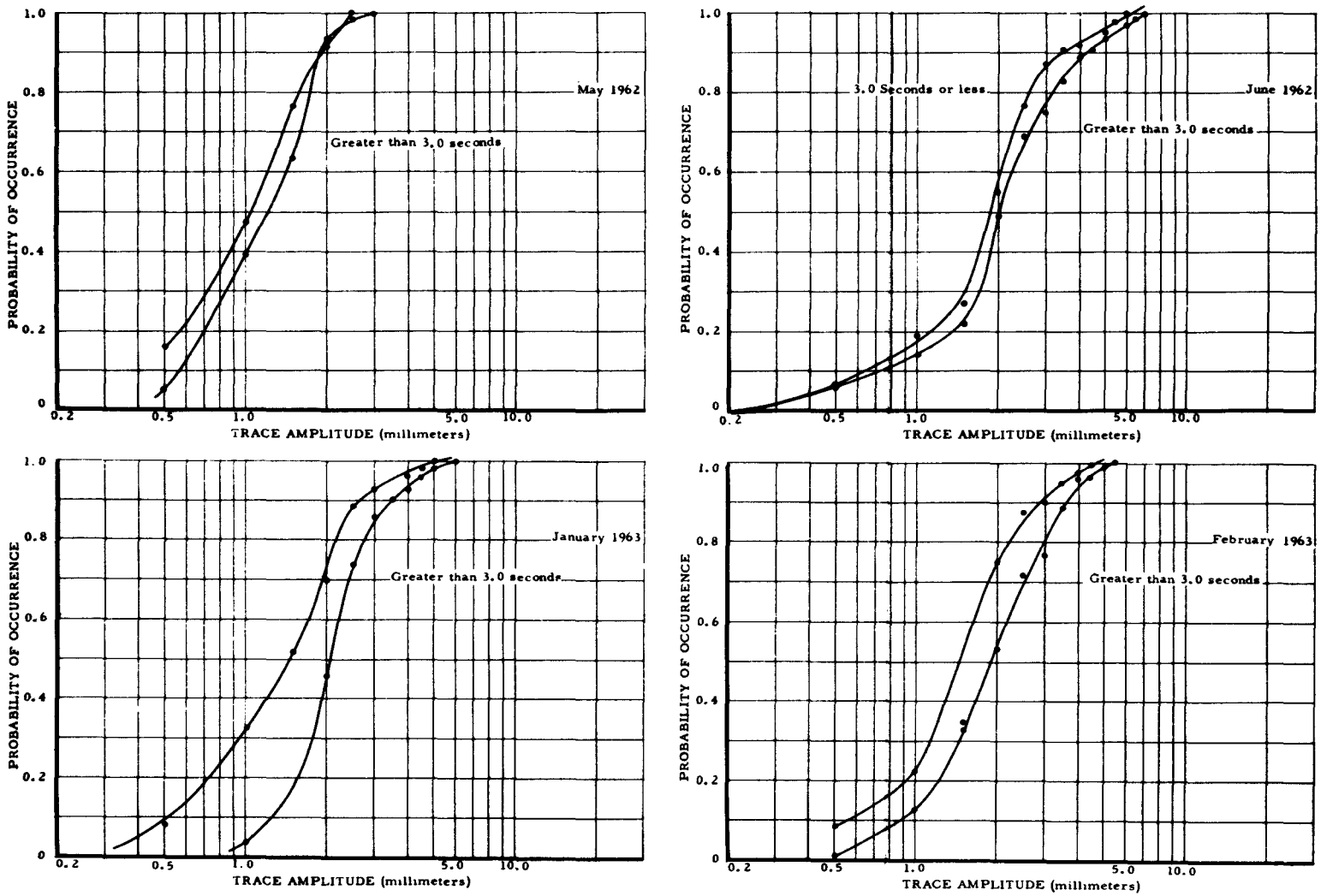


Figure 12. Probability of occurrence of predominant microseisms of 3.0-second or less period and greater than 3.0-second period on the intermediate-band seismograph

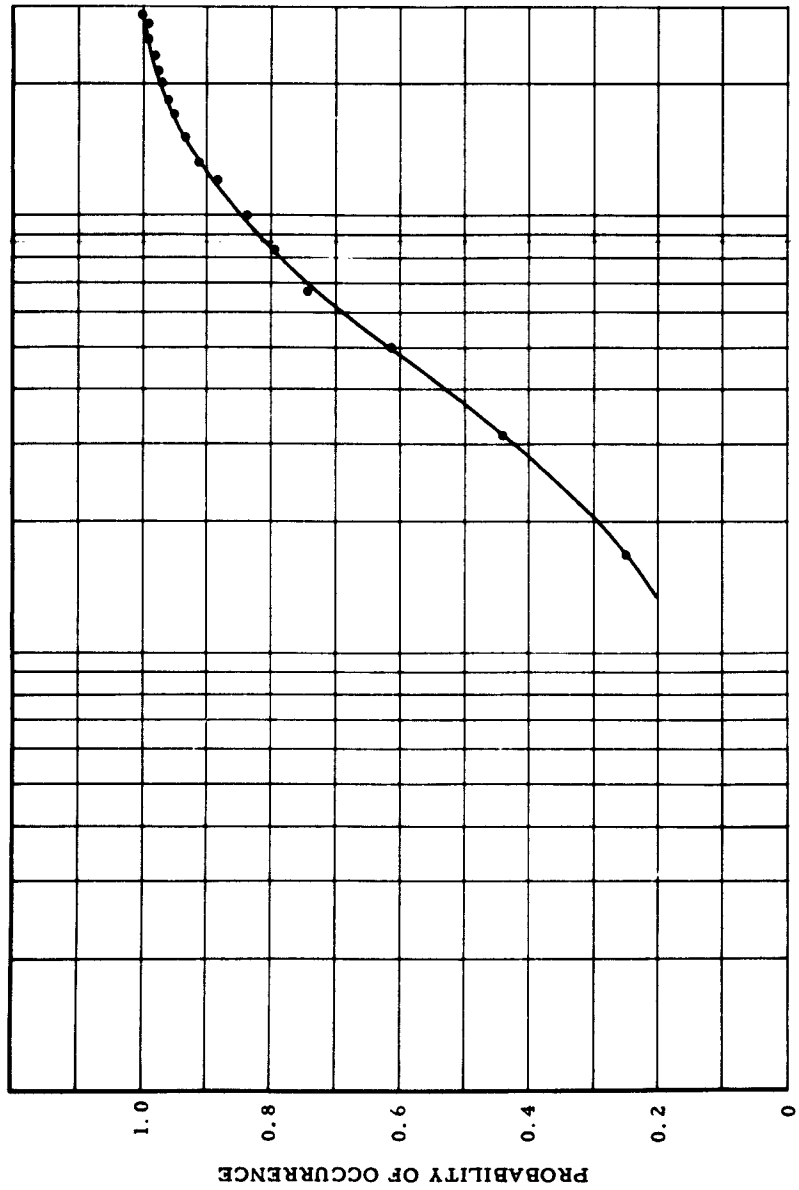


Figure 13. Probability of occurrence of predominant microseisms occurring at or less than a given ground amplitude (measurements made on the broad-band vertical, peak-to-peak)

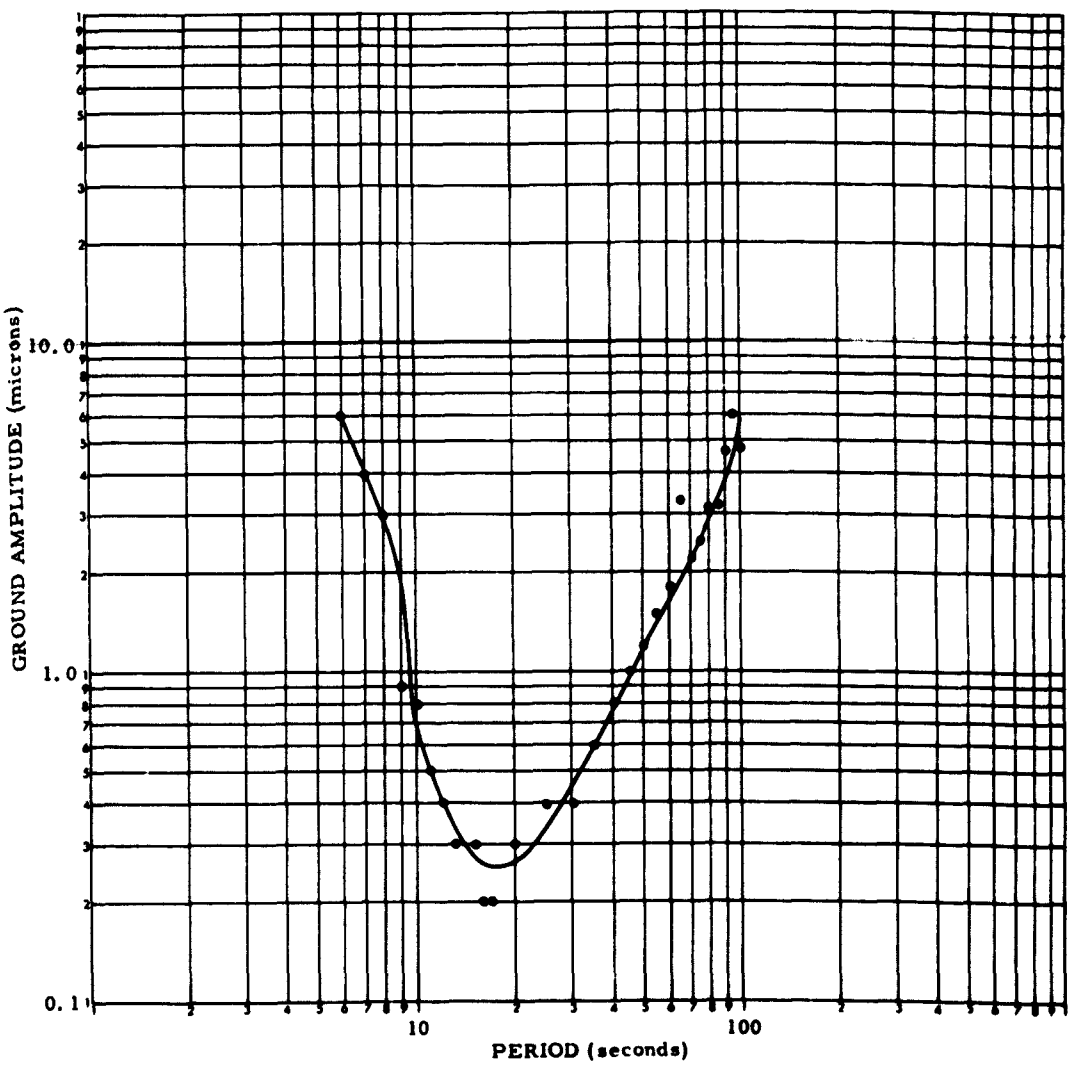


Figure 14. Average peak-to-peak background noise amplitude at a given period as a function of period, measured on WMSO long-period vertical seismograms and corrected for seismograph response